

THESIS

ATMOSPHERIC NITROGEN AND SULFUR DEPOSITION IN
ROCKY MOUNTAIN NATIONAL PARK

Submitted by

Katherine B. Beem

Department of Atmospheric Science

In partial fulfillment of the requirements

For the Degree of Master of Science

Colorado State University

Fort Collins, Colorado

Fall 2008

COLORADO STATE UNIVERSITY

September 3, 2008

WE HEREBY RECOMMEND THAT THE THESIS PREPARED UNDER OUR SUPERVISION BY KATHERINE BEEM ENTITLED ATMOSPHERIC NITROGEN AND SULFUR DEPOSITION IN ROCKY MOUNTAIN NATIONAL PARK BE ACCEPTED AS FULFILLING IN PART REQUIREMENTS FOR THE DEGREE OF MASTER OF SCIENCE.

Committee on Graduate work

Outside Committee Member, Dr. Jessica Davis

Committee Member, Dr. Sonia Kreidenweis

Advisor, Dr. Jeffrey Collett, Jr.

Department Head, Dr. Richard Johnson

ABSTRACT OF THESIS

ATMOSPHERIC NITROGEN AND SULFUR DEPOSITION IN

ROCKY MOUNTAIN NATIONAL PARK

Rocky Mountain National Park (RMNP) is experiencing a number of adverse effects due to atmospheric nitrogen (N) and sulfur (S) compounds. Airborne nitrate and sulfate particles contribute to visibility degradation in the park while nitrogen deposition is producing changes in ecosystem function and surface water chemistry. Both sulfur and nitrogen compounds are essential nutrients for life; however, some environments have naturally limited supplies of sulfur and nitrogen which restrict biological activity. Increasing the amounts of these compounds can be toxic, even life threatening, to the ecosystem. Concerns about increasing deposition are especially important in national parks where excess nitrogen and sulfur can upset the delicate balance between species of flora and fauna in prized natural ecosystems.

Measurements were made during the Rocky Mountain Airborne Nitrogen and Sulfur (RoMANS) study to quantify both N and S wet and dry deposition and to determine the most important species and pathways contributing to N deposition. Gas and particle concentrations were measured and precipitation samples were collected to gain a better understanding of nitrogen and sulfur transport to and deposition in RMNP. Samples were collected at 12 sites across the state of Colorado in March and

April 2006 and at 13 sites in north central Colorado in July and August 2006.

Historical data suggest that these are the seasons when N deposition in RMNP is greatest.

The majority of wet deposition in the spring was from a single, large upslope snowstorm, while in the summer wet deposition inputs were spread across many more events. Total wet deposition of N in the summer was larger than during spring.

Ammonium was the largest contributor to both spring and summer wet deposition in the park, followed by nitrate. Organic nitrogen, which is not routinely measured, contributed an average of 616.39 $\mu\text{g N/m}^2/\text{event}$ in the spring and 847.2 $\mu\text{g N/m}^2/\text{event}$ in the summer at the core sampling site. These deposition amounts were 22% and 16%, respectively, of total wet nitrogen deposition at this site.

Dry deposition in RMNP was dominated by gaseous species which feature higher deposition velocities than accumulation mode aerosol particles. Ammonia, which is not routinely measured, was the largest contributor to dry N deposition followed by nitric acid. Dry deposition of fine particle nitrate and ammonium made only small contributions to total N deposition.

Total N inputs were dominated by wet processes during both spring and summer.

Wet deposition of organic nitrogen and dry deposition of gaseous ammonia comprised the 3rd and 4th largest contributions to the total N deposition budget.

Together these pathways contributed nearly one-third of total measured N deposition,

suggesting they should be examined more closely in assessing nitrogen impacts on national park ecosystems.

Katherine Beem
Department of Atmospheric Science
Colorado State University
Fort Collins, CO 80523
Fall 2008

Acknowledgements

I would like to thank all of the RoMANS project participants who helped collect samples and data in the field and analyze samples in the lab. I would like to especially thank Suresh Raja and Ali Bote for chemical analysis of all precipitation and URG samples, Florian Schwander for the URG data, and Kip Carrico for the continuous gas data. The following people also contributed to the project: Courtney Taylor, Amy Sullivan, Taehyoung Lee, Derek Day, Gavin McMeeking, Bret Schichtel, Jenny Hand, Kristi Gebhart, Jeff Collett, Bill Malm, and Sonia Kreidenweis.

I am particularly grateful for the numerous insights and contributions provided by my advisor, Jeff Collett. In addition I would like to thank my entire committee, Sonia Kreidenweis, Jessica Davis, and Jeff Collett for their helpful suggestions and guidance.

I would also like to thank the entire Collett Research group for guidance and support - from introductions to equipment operation and setup and instrument repair to cake and other goodies as well as laughter and fun.

And finally I would like to thank my family and friends for their support throughout this entire process.

This project was funded by the National Park Service.

Table of Contents

Acknowledgements.....	vi
Table of Contents.....	vii
List of Figures.....	ix
List of Tables.....	xvii
1 Introduction.....	1
1.1 Motivation.....	1
1.2 Critical Loads.....	2
1.3 Ecosystem Effects.....	3
1.4 Chemistry and Sources.....	4
1.4.1 Sulfur Species and Sources.....	4
1.4.2 Nitrogen Species and Sources.....	5
1.4.3 Regional Sources.....	6
1.5 Dry Deposition.....	8
1.6 Wet Deposition.....	9
1.7 Historical Data.....	10
1.8 Meteorology in the Region Including RMNP.....	12
1.9 Objectives.....	14
2 Methods.....	16
2.1 Site Descriptions.....	16
2.2 Precipitation Collection.....	20
2.3 URG Denuder/Filter Pack Sample Collection.....	21
2.4 Sample Analysis.....	22
2.4.1 Inorganic Ions.....	22
2.4.2 Organic Nitrogen.....	23
2.5 Quality Assurance and Quality Control.....	23
2.5.1 Precision and Accuracy of Standards.....	23
2.5.2 Precipitation Blanks.....	27
2.6 Calculations.....	30
3 Results.....	32
3.1 Site Averages.....	32
3.2 Core Site.....	42
3.3 Secondary Sites.....	49
3.4 Satellite Sites.....	52
4 Wet Deposition Discussion.....	70
4.1 Precipitation Amount and Deposition Compared with Historical Data.....	70
4.2 Solute Characteristics.....	76
4.3 Seasonal and Spatial Variations of Wet Deposition.....	85
4.4 Organic Nitrogen.....	104
4.4.1 Organic Nitrogen Relationships.....	105

4.4.2	Precipitation Amount and Organic Nitrogen Deposition.....	106
4.4.3	Nitrogen Fractions of Wet Deposition for Each Campaign by Site.....	107
5	Dry Deposition.....	110
5.1	Source of Deposition Velocities	111
5.2	Variations in Deposition Velocities	116
5.3	Averaging Timescales of Concentration and Deposition Velocity.....	121
5.4	Dry Deposition.....	126
5.5	Comparison with Historical Dry Deposition Data.....	131
6	Total Fluxes	133
6.1	Wet vs. Dry	133
6.2	Core Site Nitrogen Deposition Budget	135
7	Summary and Conclusions	140
8	Future Work.....	144
	References.....	146
Appendix A	Autosampler and sub-event histograms of blanks and samples for both the spring and summer at all sites.....	151
Appendix B	Correlation Coefficient Tables.....	153
Appendix C	Slopes for the significant r-values in Appendix B.....	160
Appendix D	Core Site Sub-event Timelines	176
Appendix E	Lyons Subevent Timelines.....	182
Appendix F	Gore Pass Subevent Timelines.....	184
Appendix G	Spatial Variability charts and tables	198

List of Figures

Figure 1.1 Emission of Nitrogen (NO _x -N and NH ₃ -N).....	7
Figure 1.2 The average monthly total nitrogen and sulfur deposition budgets.	12
Figure 2.1 Map of RoMANS sites, RMNP is shaded in green in north central Colorado.19	
Figure 2.2 Nominal and measured concentration (μN) for cation Dionex check standards for all IC analysis runs.....	24
Figure 2.3 Nominal and measured concentration (μN) for anion Dionex check standards for all IC analysis runs.	24
Figure 2.4 Histograms for each ionic species measured by IC.....	29
Figure 3.1 Timelines of precipitation concentrations of sulfate (red), nitrate (blue), ammonium (green), and organic nitrogen (yellow) at the Core Site for both the spring and summer studies.....	43
Figure 3.2 Timelines of sulfate (red), nitrate (blue), ammonium (green), and organic nitrogen (yellow) wet-deposited by precipitation at the Core Site for both the spring and summer study periods.	43
Figure 3.3 Timeline of concentrations from 4/23 20:15 to 4/25 13:30 from sub event sampler at the Core Site.	44
Figure 3.4 Cumulative deposition throughout the event beginning 4/23 20:15 and ending 4/25 13:30 from the sub-event sampler at the Core Site.....	45
Figure 3.5 Timeline of concentrations from 7/7 13:00 to 7/8 08:25 from sub event sampler at the Core Site.	46
Figure 3.6 Cumulative deposition throughout the event beginning 7/7 13:00 and ending 7/8 8:25 from sub event sampler at the Core Site.....	47
Figure 3.7 Comparison of deposited amounts of ammonium, nitrate, and sulfate measured using the subevent and automated event precipitation collectors at the RoMANS Core Site.	48
Figure 3.8 Comparison of precipitation amounts measured using the subevent and automated event precipitation collectors at the RoMANS Core Site..	48
Figure 3.9 Timelines of precipitation concentrations of sulfate (red), nitrate (blue), ammonium (green), and organic nitrogen (yellow) at Lyon for both the spring and summer studies shown with amount of precipitation received.	50
Figure 3.10 Timelines of sulfate (red), nitrate (blue), ammonium (green), and organic nitrogen (yellow) wet-deposited by precipitation at Lyons for both the spring and summer study periods.	50
Figure 3.11 Timelines of precipitation concentrations of sulfate (red), nitrate (blue), ammonium (green), and organic nitrogen (yellow) at Gore Pass for both the spring and summer studies shown with amount of precipitation received....	51

Figure 3.12 Timelines of sulfate (red), nitrate (blue), ammonium (green), and organic nitrogen (yellow) wet-deposited by precipitation at Gore Pass for both the spring and summer study periods	51
Figure 3.13 Timelines of precipitation concentrations of sulfate (red), nitrate (blue), and ammonium (green) at Beaver Meadows for both the spring and summer studies.	57
Figure 3.14 Timelines of sulfate (red), nitrate (blue), and ammonium (green) wet-deposited by precipitation at Beaver Meadows for both the spring and summer study periods.	57
Figure 3.15 Timelines of precipitation concentrations of sulfate (red), nitrate (blue), and ammonium (green) Hidden Valley for both the spring and summer studies..	58
Figure 3.16. Timelines of sulfate (red), nitrate (blue), and ammonium (green) wet-deposited by precipitation at Hidden Valley during both the spring and summer study periods.	58
Figure 3.17 Timelines of precipitation concentrations of sulfate (red), nitrate (blue), and ammonium (green) at Loch Vale for both the spring and summer studies....	59
Figure 3.18 Timelines of sulfate (red), nitrate (blue), and ammonium (green) wet-deposited by precipitation at Loch Vale during both the spring and summer study periods.	59
Figure 3.19 Timelines of precipitation concentrations of sulfate (red), nitrate (blue), and ammonium (green) at Sprague Lake for both the spring and summer studies.	60
Figure 3.20 Timelines of sulfate (red), nitrate (blue), and ammonium (green) wet-deposited by precipitation at Sprague Lake during both the spring and summer study periods.	60
Figure 3.21 Timelines of precipitation concentrations of sulfate (red), nitrate (blue), and ammonium (green) at Timber Creek for both the spring and summer studies.	61
Figure 3.22 Timelines of sulfate (red), nitrate (blue), and ammonium (green) wet-deposited by precipitation at Timber Creek during both the spring and summer study periods.	61
Figure 3.23 Timelines of precipitation concentrations of sulfate (red), nitrate (blue), and ammonium (green) at Brush for the spring study.	62
Figure 3.24 Timelines of sulfate (red), nitrate (blue), and ammonium (green) wet-deposited by precipitation at Brush for the spring study period.	62
Figure 3.25 Timelines of precipitation concentrations of sulfate (red), nitrate (blue), and ammonium (green) at Dinosaur for the spring study. The amount of precipitation (mm) received and the campaign averages are also shown.....	63
Figure 3.26 Timelines of sulfate (red), nitrate (blue), and ammonium (green) wet-deposited by precipitation at Dinosaur during the spring study period.	63
Figure 3.27 Timelines of precipitation concentrations of sulfate (red), nitrate (blue), and ammonium (green) at Grant, Nebraska during the spring study.....	64
Figure 3.28 Timelines of sulfate (red), nitrate (blue), and ammonium (green) wet-deposited by precipitation at the Grant, Nebraska site during the spring study period. The amount of precipitation (mm) received and the campaign averages are also shown.....	64

Figure 3.29 Timelines of precipitation concentrations of sulfate (red), nitrate (blue), and ammonium (green) at Springfield for the spring study.....	65
Figure 3.30 Timelines of sulfate (red), nitrate (blue), and ammonium (green) wet-deposited by precipitation Springfield during the spring study period.....	65
Figure 3.31 Timelines of precipitation concentrations of sulfate (red), nitrate (blue), and ammonium (green) at the Alpine Visitors Center during the summer study..	66
Figure 3.32 Timelines of sulfate (red), nitrate (blue), and ammonium (green) wet-deposited by precipitation at Alpine Visitors Center during the summer study period.	66
Figure 3.33 Timelines of precipitation concentrations of sulfate (red), nitrate (blue), and ammonium (green) at Lake Irene during the summer study.....	67
Figure 3.34 Timelines of sulfate (red), nitrate (blue), and ammonium (green) wet-deposited by precipitation at Lake Irene during the summer study period.....	67
Figure 3.35 Timelines of precipitation concentrations of sulfate (red), nitrate (blue), and ammonium (green) at Rainbow Curve during the summer study.....	68
Figure 3.36 Timelines of sulfate (red), nitrate (blue), and ammonium (green) wet-deposited by precipitation at Rainbow Curve during the summer study period.	68
Figure 3.37 Timelines of precipitation concentrations of sulfate (red), nitrate (blue), and ammonium (green) at Rock Cut during the summer study.....	69
Figure 3.38 Timelines of sulfate (red), nitrate (blue), and ammonium (green) wet-deposited by precipitation at Rock Cut during the summer study period.....	69
Figure 4.1. Average seasonal wet deposition fluxes and precipitation from January 1998-January 2004 for the Beaver Meadows and Loch Vale NADP sites. Provided by Bret Schichtel.....	70
Figure 4.2 Yearly deposition totals for Beaver Meadows and Loch Vale for the weeks overlapping the RoMANS spring and summer study.....	73
Figure 4.3 Weekly deposition totals for the RoMANS Core Site (CS) and the collocated NADP-RoMANS sites at Beaver Meadows (BM) and Loch Vale (LV).....	75
Figure 4.4 Precipitation and deposition totals at Loch Vale (LV) and the Core Site (CS) for 7/18-8/1.	75
Figure 4.5 Precipitation amount plotted against the flux of N and S species for a)Core Site Spring and b)Core Site Summer.	80
Figure 4.6 Time evolution of precipitation solute concentrations and precipitation amount during rainfall at the RoMANS Core Site during the period 7/08-7/09/06. ...	82
Figure 4.7 Time evolution of cumulative precipitation and wet deposition of major solute species during rainfall at the RoMANS Core Site during the period 7/08-7/09/06.	82
Figure 4.8 Timeline of concentrations from 4/6 13:30 to 4/7 11:30 from sub event sampler at the Core Site.	84
Figure 4.9 Cumulative deposition throughout the event beginning 4/6 13:30 and ending 4/7 11:30 from sub event sampler at the Core Site.	85
Figure 4.10 Spatial and temporal 3-D plot of the amount of precipitation received during the spring and summer RoMANS study periods.	87
Figure 4.11 Spatial and temporal NH_4^+ deposition during the spring and summer studies of RoMANS.....	90

Figure 4.12 Spatial and temporal NO_3^- deposition during the spring and summer studies of RoMANS.....	91
Figure 4.13 Spatial and temporal SO_4^{2-} deposition during the spring and summer studies of RoMANS.....	92
Figure 4.14 Spatial profile of wet deposition from samples collected during the 4/23 event. a) Precipitation amount is shown in black, b) ammonium deposition is shown in green, c) nitrate deposition is shown in blue, and d) sulfate deposition is shown in red.	94
Figure 4.15 Profile of wet deposition from samples collected during the 7/20 event. a) Precipitation amount shown in blank, b) ammonium deposition is shown in green, c) nitrate deposition is shown in blue, and d) sulfate deposition is shown in red.....	94
Figure 4.16 Beaver Meadows comparison with the Core Site for the RoMANS spring study. a) precipitation b) concentration c) deposition.....	99
Figure 4.17 Beaver Meadows comparison with the Core Site for the RoMANS summer study. a) precipitation b) concentration c) deposition.....	99
Figure 4.18 Total spring wet deposition of SO_4^{2-} , NO_3^- , and NH_4^+ by site with total amount of precipitation. Sites are ordered by longitude.....	101
Figure 4.19 Total summer wet deposition of SO_4^{2-} , NO_3^- , and NH_4^+ by site with total amount of precipitation. Sites are order by longitude.....	102
Figure 4.20 Ratio of ammonium wet deposition flux to nitrate wet deposition flux totals by site for both the spring (orange) and summer (green striped).....	103
Figure 4.21 Total inorganic nitrogen deposition ($\mu\text{g N/m}^2$) by site and season for sites where measurements were made in both the spring and summer.....	103
Figure 4.22 Total sulfate deposition ($\mu\text{g S/m}^2$) by site and season for sites where measurements were made in both the spring and summer.	104
Figure 4.23 Relationship between inorganic N species and organic nitrogen measured during both the spring and summer a) Ammonium and organic nitrogen by site with the best-fit of all data $R^2=0.77$ b) Nitrate and organic nitrogen by site with the best-fit of all data $R^2=0.64$	106
Figure 4.24 Organic nitrogen flux vs. precipitation by site and campaign.....	107
Figure 4.25. Contribution of each N species measured to total N deposition at Lyons, the Core Site, and Gore Pass for both the spring and summer campaign sampling periods.....	109
Figure 5.1. Average diurnal variation of deposition velocities for HNO_3 , NH_3 , SO_2 , and particles from continuous gas data and CASTNet deposition velocities.....	116
Figure 5.2 Spring deposition velocities for SO_2 , HNO_3 , NH_3 and particles.	118
Figure 5.3 Summer deposition velocities for SO_2 , HNO_3 , NH_3 and particles.....	118
Figure 5.4 Histogram of daily averaged deposition velocities for SO_2 for both the spring (orange) and summer (green stripes) study periods.....	120
Figure 5.5 Histogram of HNO_3 deposition velocities for both the spring (orange) and summer (green stripes) study periods.	120
Figure 5.6 Histogram of particle deposition velocities for both the spring (orange) and summer (green stripes) study periods.	121
Figure 5.7 Comparison of the dry deposition fluxes calculated by each averaging method of NH_3	122

Figure 5.8. Average diurnal variation for each study period of NH ₃ concentration (green) and NH ₃ deposition velocity (blue).	123
Figure 5.9 Bar chart of spring dry daily deposition of each particulate species (dots) with appropriate gas (stripes) stacked for total of the species group. Red: SO ₄ ²⁻ /SO ₂ , Blue: NO ₃ ⁻ /HNO ₃ , and Green: NH ₄ ⁺ /NH ₃	127
Figure 5.10 Bar chart of summer dry daily deposition of each particulate species (dots) with appropriate gas (stripes) stacked for total of the species group. Red: SO ₄ ²⁻ /SO ₂ , Blue: NO ₃ ⁻ /HNO ₃ , and Green: NH ₄ ⁺ /NH ₃	127
Figure 5.11 Timelines of deposition flux (blue bar), deposition velocity (orange), and concentration (light blue line) for nitric acid.	129
Figure 5.12 Timelines of deposition flux (green bar), deposition velocity (orange), and concentration (light green line) for ammonia.	129
Figure 5.13 Timelines of deposition flux (red bar), deposition velocity (orange), and concentration (black line) for sulfur dioxide.	130
Figure 5.14 Timelines of deposition flux (bar), deposition velocity (orange), and concentration (blue line) for fine particle nitrate.	130
Figure 5.15 Timelines of deposition flux (bar), deposition velocity (orange), and concentration (green line) for fine particle ammonium.	130
Figure 5.16 Timelines of deposition flux (bar), deposition velocity (orange), and concentration (red) for fine particle sulfate.	130
Figure 6.1 Core Site spring deposition fluxes broken down for each species by dry gaseous, dry particle, and wet.	134
Figure 6.2 Core Site summer deposition fluxes broken down for each species by dry gaseous, dry particle, and wet.	134
Figure 6.3. Total N and S flux for the Core Site showing the amount of deposition due to each species and process.	135
Figure 6.4 Fraction of each nitrogen species that contributes to total N deposition at the Core Site during the spring RoMANS campaign.	136
Figure 6.5 Fraction of each nitrogen species that contributes to total N deposition at the Core Site during the summer RoMANS campaign.	136
Figure 6.6 Nitrogen deposition totals by species and pathway in order of contribution to total N deposition at the Core Site.	137
Figure A.1 Histograms for each ionic species measured by IC. All autosampler samples including blanks are shown in dark green with just the blanks in light green plotted on top.	151
Figure A.2 Histograms for each ionic species measured by IC. All subevent samples including blanks are shown in dark green with just the blanks in light green plotted on top.	152
Figure D.1 Concentrations of ammonium (green), nitrate (blue), and sulfate (red) in precipitation samples collected throughout the 3/26/06 event at the Core Site.	176
Figure D.2 Deposition of ammonium (green), nitrate (blue), and sulfate (red) throughout the 3/26/06 event at the Core Site.	176
Figure D.3 Cumulative deposition of ammonium (green), nitrate (blue), and sulfate (red) throughout the 3/26/06 event at the Core Site.	176

Figure D.4	Timeline of concentrations from 17:45 through 20:45 on 3/29 from sub event sampler at the Core Site.	177
Figure D.5	Deposition of ammonium (green), nitrate (blue), sulfate (red), and organic nitrogen (yellow) throughout the 3/29 event at the Core Site.....	177
Figure D.6	Cumulative deposition of ammonium (green), nitrate (blue), sulfate (red), organic nitrogen (yellow) throughout the 3/29 event at the Core Site.....	177
Figure D.7	Concentrations of ammonium (green), nitrate (blue), and sulfate (red) in precipitation samples collected throughout the 4/18 event at the Core Site.	178
Figure D.8	Deposition of ammonium (green), nitrate (blue), and sulfate (red) throughout the 4/18 event at the Core Site.	178
Figure D.9	Cumulative deposition of ammonium (green), nitrate (blue), and sulfate (red) throughout the 4/18 event at the Core Site.	178
Figure D.10	Concentrations of ammonium (green), nitrate (blue), and sulfate (red) in precipitation samples collected throughout the 4/28 event at the Core Site.	179
Figure D.11	Deposition of ammonium (green), nitrate (blue), and sulfate (red) throughout the 4/28 event at the Core Site.	179
Figure D.12	Cumulative deposition of ammonium (green), nitrate (blue), and sulfate (red) throughout the 4/28 event at the Core Site.	179
Figure D.13	Concentrations of ammonium (green), nitrate (blue), and sulfate (red) in precipitation samples collected throughout the 7/9 event at the Core Site...	180
Figure D.14	Deposition of ammonium (green), nitrate (blue), and sulfate (red) throughout the 7/9 event at the Core Site.	180
Figure D.15	Cumulative deposition of ammonium (green), nitrate (blue), and sulfate (red) throughout the 7/9 event at the Core Site.....	180
Figure D.16	Concentrations of ammonium (green), nitrate (blue), and sulfate (red) in precipitation samples collected throughout the 7/17 event at the Core Site.	181
Figure D.17	Deposition of ammonium (green), nitrate (blue), and sulfate (red) throughout the 7/17 event at the Core Site.	181
Figure D.18	Cumulative deposition of ammonium (green), nitrate (blue), and sulfate (red) throughout the 7/17 event at the Core Site.	181
Figure E.1	Timeline of concentrations from sub event sampler at the Lyons site on 4/7.	182
Figure E.2	Deposition of ammonium (green), nitrate (blue), and sulfate (red) throughout the 4/7 event at the Lyons site.	182
Figure E.3	Cumulative deposition of ammonium (green), nitrate (blue), and sulfate (red) throughout the 4/7 event at the Lyons site.....	182
Figure E.4	Timeline of concentrations from sub event sampler at the Lyons site throughout the 4/23- 4/24.	183
Figure E.5	Deposition of ammonium (green), nitrate (blue), and sulfate (red) throughout the 4/23-4/24 event at the Lyons site.	183
Figure E.6	Cumulative deposition of ammonium (green), nitrate (blue), and sulfate (red) throughout the 4/23-4/24 event at the Lyons site.	183
Figure F.1	Timeline of concentrations from sub event sampler at the Gore Pass site for 3/26.	184
Figure F.2	Deposition of ammonium (green), nitrate (blue), and sulfate (red) throughout the 3/26 event at the Gore Pass site.	184

Figure F.3 Cumulative deposition of ammonium (green), nitrate (blue), and sulfate (red) throughout the 3/26 event at the Gore Pass site.....	184
Figure F.4 Timeline of concentrations from the sub event sampler at the Gore Pass site for 3/29.....	185
Figure F.5 Deposition of ammonium (green), nitrate (blue), and sulfate (red) throughout the 3/29 event at the Gore Pass site.	185
Figure F.6 Cumulative deposition of ammonium (green), nitrate (blue), and sulfate (red) throughout the 3/29 event at the Gore Pass site.....	185
Figure F.7 Timeline of concentrations from the sub event sampler at the Gore Pass site for 3/30.....	186
Figure F.8 Deposition of ammonium (green), nitrate (blue), and sulfate (red) throughout the 3/30 event at the Gore Pass site.	186
Figure F.9 Cumulative deposition of ammonium (green), nitrate (blue), and sulfate (red) throughout the 3/30 event at the Gore Pass site.....	186
Figure F.10 Timeline of concentrations from the sub event sampler at the Gore Pass site for 4/1.....	187
Figure F.11 Deposition of ammonium (green), nitrate (blue), and sulfate (red) throughout the 4/1 event at the Gore Pass site.	187
Figure F.12 Cumulative deposition of ammonium (green), nitrate (blue), and sulfate (red) throughout the 4/1 event at the Gore Pass site.....	187
Figure F.13 Timeline of concentrations from the sub event sampler at the Gore Pass site for 4/6.....	188
Figure F.14 Deposition of ammonium (green), nitrate (blue), and sulfate (red) throughout the 4/6 event at the Gore Pass site.	188
Figure F.15 Cumulative deposition of ammonium (green), nitrate (blue), and sulfate (red) throughout the 4/6 event at the Gore Pass site.....	188
Figure F.16 Timeline of concentrations from the sub event sampler at the Gore Pass site for 4/15.....	189
Figure F.17 Deposition of ammonium (green), nitrate (blue), and sulfate (red) throughout the 4/15 event at the Gore Pass site.	189
Figure F.18 Cumulative deposition of ammonium (green), nitrate (blue), and sulfate (red) throughout the 4/15 event at the Gore Pass site.....	189
Figure F.19 Timeline of concentrations from the sub event sampler at the Gore Pass site for 4/18.....	190
Figure F.20 Deposition of ammonium (green), nitrate (blue), and sulfate (red) throughout the 4/18 event at the Gore Pass site.	190
Figure F.21 Cumulative deposition of ammonium (green), nitrate (blue), and sulfate (red) throughout the 4/18 event at the Gore Pass site.....	190
Figure F.22 Timeline of concentrations from the sub event sampler at the Gore Pass site for 4/24.....	191
Figure F.23 Deposition of ammonium (green), nitrate (blue), and sulfate (red) throughout the 4/24 event at the Gore Pass site.	191
Figure F.24 Cumulative deposition of ammonium (green), nitrate (blue), and sulfate (red) throughout the 4/24 event at the Gore Pass site.....	191
Figure F.25 Timeline of concentrations from the sub event sampler at the Gore Pass site on 7/7.	192

Figure F.26 Deposition of ammonium (green), nitrate (blue), and sulfate (red) throughout the 7/7 event at the Gore Pass site.	192
Figure F.27 Cumulative deposition of ammonium (green), nitrate (blue), and sulfate (red) throughout the 7/7 event at the Gore Pass site.	192
Figure F.28 Timeline of concentrations from the sub event sampler at Gore Pass site for 7/8.	193
Figure F.29 Deposition of ammonium (green), nitrate (blue), and sulfate (red) throughout the 7/8 event at the Gore Pass site.	193
Figure F.30 Cumulative deposition of ammonium (green), nitrate (blue), and sulfate (red) throughout the 7/8 event at the Gore Pass site.	193
Figure F.31 Timeline of concentrations from the sub event sampler at the Gore Pass site for 7/9.	194
Figure F.32 Deposition of ammonium (green), nitrate (blue), and sulfate (red) throughout the 7/9 event at the Gore Pass site.	194
Figure F.33 Cumulative deposition of ammonium (green), nitrate (blue), and sulfate (red) throughout the 7/9 event at the Gore Pass site.	194
Figure F.34 Timeline of concentrations from the sub event sampler at the Gore Pass site for 7/31.	195
Figure F.35 Deposition of ammonium (green), nitrate (blue), and sulfate (red) throughout the 7/31 event at the Gore Pass site.	195
Figure F.36 Cumulative deposition of ammonium (green), nitrate (blue), and sulfate (red) throughout the 7/31 event at the Gore Pass site.	195
Figure F.37 Timeline of concentrations from the sub event sampler at the Gore Pass site for 8/1.	196
Figure F.38 Deposition of ammonium (green), nitrate (blue), and sulfate (red) throughout the 8/1 event at the Gore Pass site.	196
Figure F.39 Cumulative deposition of ammonium (green), nitrate (blue), and sulfate (red) throughout the 8/1 event at the Gore Pass site.	196
Figure F.40 Timeline of concentrations from the sub event sampler at the Gore Pass site for 8/4.	197
Figure F.41 Deposition of ammonium (green), nitrate (blue), and sulfate (red) throughout the 8/4 event at the Gore Pass site.	197
Figure F.42 Cumulative deposition of ammonium (green), nitrate (blue), and sulfate (red) throughout the 8/4 event at the Gore Pass site.	197
Figure G.1 Wet deposition of NH_4^+ at all sites during the spring study period.	202
Figure G.2 Wet deposition of NO_3^- at all sites during the spring study period.	203
Figure G.3 Wet deposition of SO_4^{2-} at all sites during the spring study period.	204
Figure G.4 Wet deposition of NH_4^+ at all sites during the summer study period.	205
Figure G.5 Wet deposition of NO_3^- at all sites during the summer study period.	206
Figure G.6 Wet deposition of SO_4^{2-} at all sites during the summer study period.	207

List of Tables

Table 2.1 Locations of monitoring sites during spring and summer campaigns of RoMANS	17
Table 2.2 Accuracy and precision of standard analysis	26
Table 2.3 Precision of sample replicates.....	27
Table 3.1 Spring average precipitation amount and pH for each event by site.	33
Table 3.2 Summer average precipitation amount and pH for each event by site.	33
Table 3.3. Spring site average concentrations in precipitation for all ions measured.	35
Table 3.4. Summer average concentrations in precipitation for all ions measured in $\mu\text{g/L}$	36
Table 3.5. Spring average event daily wet deposition fluxes for all ions	38
Table 3.6. Summer average event daily wet deposition fluxes for all ions	39
Table 3.7. Spring average concentrations ($\mu\text{g N or S/L}$) and daily fluxes ($\mu\text{g N or S/m}^2$) of key N and S species.....	40
Table 3.8. Summer average concentrations ($\mu\text{g N or S/L}$) and daily fluxes ($\mu\text{g N or S/m}^2$) of key N and S species.....	41
Table 4.1. Total precipitation for the RoMANS campaign compared with historical data. Historical averages were calculated with NADP data from 1983 - 2004 for the time period overlapping RoMANS.....	71
Table 4.2 Comparison of historical wet deposition totals to RoMANS measurements at Beaver Meadows. Units are $\mu\text{g of N or S/m}^2$	72
Table 4.3 Comparison of historical wet deposition totals to RoMANS measurements at Loch Vale. Units are $\mu\text{g of N or S/m}^2$	72
Table 4.4 Comparison with measurements made by the NADP during the same weeks RoMANS took place. Total deposition values have units of $\mu\text{g of N (or S)/m}^2$	74
Table 4.5. Correlation table of Pearson's r-values for concentrations during the spring campaign measured at the Core Site for samples collected with the autosampler.....	78
Table 4.6. Correlation table for fluxes during the spring campaign measured at the Core Site for samples collected with the autosampler.....	78
Table 4.7. Correlation table for concentrations during the summer campaign measured at the Core Site for samples collected with the autosampler.....	79
Table 4.8. Correlation table for fluxes during the summer campaign measured at the Core Site for samples collected with the autosampler.....	79
Table 4.9 Correlation (r) between sites for precipitation amount (mm) during the RoMANS spring study period.	88
Table 4.10 Correlation (r) between sites for precipitation amount (mm) during the RoMANS summer study period.	88

Table 4.11 Correlation coefficient between sites for ammonium deposition during the RoMANS summer study period.	96
Table 4.12 Correlation coefficient between sites for nitrate deposition during the RoMANS summer study period.	96
Table 4.13 Correlation coefficient between sites for sulfate deposition during the RoMANS summer study period.	97
Table 5.1 Deposition velocities of nitric acid and ammonia from a number of studies. Studies where both species were measured are shaded.	114
Table 5.2 Influence of averaging timescale on total deposition. Column titles correspond to the timescale over which averages of deposition velocity and concentration were taken.	125
Table 5.3 Dry deposition totals by species for both the summer and spring campaigns at the Core Site. Units are $\mu\text{g N}$ or S/m^2	129
Table 5.4 Comparison of dry deposition during RoMANS with historical CASTNet data average from 1995-2005 for the same periods as RoMANS as well as measurements made by CASTNet during the period overlapping RoMANS in 2006. Units are in μg of N (or S)/ m^2	132
Table B.1 Correlation coefficients for concentrations from the spring campaign at Gore Pass for precipitation collected with a bucket.	154
Table B.2. Correlation coefficients for fluxes from the spring campaign at Gore Pass for precipitation collected with a bucket.	154
Table B.3. Correlation coefficients for concentrations from the summer campaign at Gore Pass for precipitation collected with the autosampler.	155
Table B.4. Correlation coefficients for fluxes from the summer campaign at Gore Pass for precipitation collected with the autosampler.	155
Table B.5. Correlation coefficients for concentrations from the summer campaign at Gore Pass for precipitation collected with a bucket.	156
Table B.6. Correlation coefficients for fluxes from the summer campaign at Gore Pass for precipitation collected with a bucket.	156
Table B.7. Correlation coefficients for concentrations from the spring campaign at Lyons for precipitation collected with the autosampler.	157
Table B.8. Correlation coefficients for fluxes from the spring campaign at Lyons for precipitation collected with the autosampler.	157
Table B.9. Correlation table for concentrations during the summer campaign measured at Lyons for samples collected with the bucket.	158
Table B.10. Correlation table for fluxes during the summer campaign measured at Lyons for samples collected with the bucket.	158
Table B.11. Correlation coefficients for concentrations from the spring campaign at the Core Site for precipitation collected with a bucket.	159
Table B.12. Correlation coefficients for fluxes from the spring campaign at the Core Site for precipitation collected with a bucket.	159
Table C.1 Significant slopes for concentrations from the Core Site during the summer campaign for samples collected with the autosampler. Slopes were calculated with the rows as y values and columns as x values.	161

Table C.2 Significant slopes for fluxes from the Core Site during the summer campaign for samples collected with the autosampler. Slopes were calculated with the rows as y values and columns as x values.	161
Table C.3 Significant slopes for concentrations from the Core Site during the spring campaign for samples collected with the autosampler. Slopes were calculated with the rows as y values and columns as x values.	162
Table C.4 Significant slopes for fluxes from the Core Site during the spring campaign for samples collected with the autosampler. Slopes were calculated with the rows as y values and columns as x values.	162
Table C.5 Significant slopes for concentrations from the Core Site during the spring campaign for samples collected with the bucket. Slopes were calculated with the rows as y values and columns as x values.	163
Table C.6 Significant slopes for fluxes from the Core Site during the spring campaign for samples collected with the bucket. Slopes were calculated with the rows as y values and columns as x values.	163
Table C.7 Significant slopes for concentrations from the Gore Pass during the spring campaign for samples collected with the bucket. Slopes were calculated with the rows as y values and columns as x values.	164
Table C.8 Significant slopes for fluxes from the Gore Pass during the spring campaign for samples collected with the bucket. Slopes were calculated with the rows as y values and columns as x values.	164
Table C.9 Significant slopes for concentrations from the Gore Pass during the summer campaign for samples collected with the autosampler. Slopes were calculated with the rows as y values and columns as x values.	165
Table C.10 Significant slopes for fluxes from the Gore Pass during the summer campaign for samples collected with the autosampler. Slopes were calculated with the rows as y values and columns as x values.	165
Table C.11 Significant slopes for concentrations from the Gore Pass during the summer campaign for samples collected with the bucket. Slopes were calculated with the rows as y values and columns as x values.	166
Table C.12 Significant slopes for fluxes from the Gore Pass during the summer campaign for samples collected with the bucket. Slopes were calculated with the rows as y values and columns as x values.	166
Table C.13 Significant slopes for concentrations from the Lyons during the spring campaign for samples collected with the autosampler. Slopes were calculated with the rows as y values and columns as x values.	167
Table C.14 Significant slopes for fluxes from the Lyons during the spring campaign for samples collected with the autosampler. Slopes were calculated with the rows as y values and columns as x values.	167
Table C.15 Significant slopes for concentrations from the Lyons during the summer campaign for samples collected with the bucket. Slopes were calculated with the rows as y values and columns as x values.	168
Table C.16 Significant slopes for fluxes from the Lyons during the summer campaign for samples collected with the bucket. Slopes were calculated with the rows as y values and columns as x values.	168

Table C.17 Significant slopes for spring sulfate concentrations by site. Slopes were calculated with the rows as y values and columns as x values.	169
Table C.18 Significant slopes for spring sulfate fluxes by site. Slopes were calculated with the rows as y values and columns as x values.	169
Table C.19 Significant slopes for spring nitrate concentrations by site. Slopes were calculated with the rows as y values and columns as x values.	170
Table C.20 Significant slopes for spring nitrate fluxes by site. Slopes were calculated with the rows as y values and columns as x values.	170
Table C.21 Significant slopes for spring ammonium concentrations by site. Slopes were calculated with the rows as y values and columns as x values.	171
Table C.22 Significant slopes for spring ammonium fluxes by site. Slopes were calculated with the rows as y values and columns as x values.	171
Table C.23 Significant slopes for spring precipitation amounts by site. Slopes were calculated with the rows as y values and columns as x values.	172
Table C.24 Significant slopes for summer sulfate concentrations by site. Slopes were calculated with the rows as y values and columns as x values.	172
Table C.25 Significant slopes for summer fluxes by site. Slopes were calculated with the rows as y values and columns as x values.	173
Table C.26 Significant slopes for summer nitrate concentrations by site. Slopes were calculated with the rows as y values and columns as x values.	173
Table C.27 Significant slopes for summer nitrate fluxes by site. Slopes were calculated with the rows as y values and columns as x values.	174
Table C.28 Significant slopes for summer ammonium concentrations by site. Slopes were calculated with the rows as y values and columns as x values.	174
Table C.29 Significant slopes for summer ammonium fluxes by site. Slopes were calculated with the rows as y values and columns as x values.	175
Table C.30 Significant slopes for summer precipitation amounts by site. Slopes were calculated with the rows as y values and columns as x values.	175
Table G.1 Correlation coefficient between sites for ammonium deposition during the RoMANS spring study period	199
Table G.2 Correlation coefficient between sites for nitrate deposition during the RoMANS spring study period	199
Table G.3 Correlation coefficient between sites for sulfate deposition during the RoMANS spring study period	200
Table G.4 Correlation between sites for ammonium concentration during the RoMANS spring study period	200
Table G.5 Correlation between sites for nitrate concentration during the RoMANS spring study period	201
Table G.6 Correlation between sites for sulfate concentration during the RoMANS spring study period	201

1 Introduction

The Rocky Mountain Airborne Nitrogen and Sulfur Study (RoMANS) was conducted during two campaigns in the spring and summer of 2006 to provide a more comprehensive data set for Rocky Mountain National Park (RMNP) regarding nitrogen (N) and sulfur (S) deposition.

1.1 Motivation

RMNP is experiencing a number of adverse effects due to atmospheric N and S compounds. Airborne nitrate and sulfate particles contribute to visibility degradation in the park, while nitrogen deposition is producing changes in ecosystem function and surface water chemistry. Both sulfur and nitrogen compounds are essential nutrients for life; however, some environments have naturally limited supplies of sulfur and nitrogen which restrict biological activity. Increasing the amounts of these compounds can be toxic, even life threatening to the ecosystem. Concerns about increasing deposition are especially important in national parks where excess nitrogen and sulfur can upset the delicate balance between species of flora and fauna in natural ecosystems.

RMNP serves as an indicator of future environmental issues for the surrounding area. High elevation ecosystems are more sensitive to changes because of extensive areas of exposed and unreactive bed rock, rapid hydrologic flush rates during snowmelt,

limited extents of vegetation and soils, and a short growing season (Williams et al., 1993).

Analysis of N deposition patterns at 217 sites nationally demonstrated that 45 sites had an increasing trend in N deposition; more than half of these sites were in remote areas previously thought to be relatively pristine, including RMNP, Bryce Canyon National Park in Utah, and Sequoia National Park in California (Williams and Tonnessen, 2000). Nitrogen saturation of forested catchments has contributed to environmental problems including reduced drinking-water quality, nitrate induced toxic effects on freshwater biota, disruption of nutrient cycling, increased soil acidification, and aluminum mobility (Fenn et al., 1998). Identification of changes to biological systems that have occurred as a result of nitrogen deposition include changes in diatom speciation and abundance (Baron et al., 2000), changes in zooplankton (Williams and Tonnessen, 2000), and effects on trees (Craig and Friedland, 1991; Williams et al., 1996). The increased N deposition in RMNP is of particular importance since it is classified as a Class 1 area by the Clean Air Act of 1977, which mandates remediation of environmental issues that are causing the park to no longer be in its original condition and to prevent further degradation of the area.

1.2 Critical Loads

A critical load is defined as a deposition amount above which natural resources can be negatively affected (Williams and Tonnessen, 2000). Changes in diatom assemblages in alpine lakes in RMNP led to the establishment of a critical load for N deposition of

1.5 kg N ha⁻¹ yr⁻¹ (Baron, 2006). Diatom assemblages changed from predominantly ultra-oligotrophic to predominately meso-trophic between 1950 and 1964, defining the level at which a negative change occurred to the ecosystem (Baron, 2006). There has been continued increasing N deposition at high elevation sites (Burns, 2003) since the critical load was reached; background levels of nitrogen deposition at the park are estimated to be 0.5 kg N ha⁻¹ yr⁻¹. As much as 7.5 kg ha⁻¹ yr⁻¹ of nitrogen is deposited in the Rocky Mountain region of Colorado and Wyoming (Burns, 2003). It is important to identify sources of pollutants that contribute to deposition and to understand processes associated with nitrogen and sulfur deposition in order to identify changes that could be made to reduce the levels of pollutants that are deposited.

1.3 Ecosystem Effects

Increasing nitrogen deposition contributes to the degradation of terrestrial and aquatic resources. Biotic response to increased N deposition includes a positive feedback mechanism that may further contribute to N saturation (Bowman and Steltzer 1998). Craig and Friedland (1991) found that high elevation red spruce showed high levels of mortality because of reduced cold tolerance caused by increased amounts of atmospheric pollutants; however, there is uncertainty about the relative importance of sulfur, nitrogen, and acidity in the decline in cold tolerance. In addition, increasing deposition of pollutants can cause acidification of surface waters which results in changes in aquatic resources. An example of this is the restructuring of assemblages for some zooplankton species when exposed to acidic waters (Williams and

Tonnessen, 2000). Fish species can also be affected by changes in water chemistry. Cutthroat trout and rainbow trout are two examples of fish that are sensitive to acidic waters, with the sensitivity depending on the life stage at which exposure occurs.

Acidity of surface water is dependent upon the pathways by which deposited pollutants enter bodies of water. As mentioned previously, high elevation ecosystems have a limited extent of vegetation and soil with abundant exposed bedrock, creating a situation where deposited N and S can easily enter surface waters. In the Colorado Front Range about 50% of nitrate loading from annual wet deposition is exported in stream waters (Williams et al., 1996).

1.4 Chemistry and Sources

1.4.1 Sulfur Species and Sources

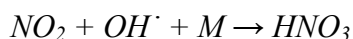
Sulfur dioxide (SO₂) has been the main sulfur species of interest due to formation of particulate sulfate resulting from atmospheric oxidation of SO₂ and the effects of acid rain. Anthropogenic sources of SO₂ include fossil fuel combustion (the most important source in the U.S.), chemical manufacturing, and mineral ore processing. SO₂ can also be produced by the oxidation of naturally occurring sulfur species like dimethylsulfide and hydrogen sulfide. These and other gaseous sulfur species are less abundant in the free troposphere and are only high in concentration near sources. SO₂ can react through both dry and aqueous pathways to produce sulfuric acid which exhibits a strong tendency to form aerosols.

1.4.2 Nitrogen Species and Sources

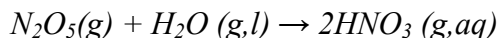
Atmospheric nitrogen species of interest have several sources including combustion processes and agriculture. Combustion sources include power plants, vehicles, and fires where N_2 and O_2 combine at high temperatures to produce nitrogen oxides (NO_x). NO_x can also be emitted through the combustion of fuels containing N compounds. Both of these processes occur simultaneously; the relative amount of emission from each process is dependent on fuel type and combustion temperature.

NO_x can react in the atmosphere to form other species including gaseous nitric acid, which is the major component in the dry deposition of N to tundra plants (Sievering et al., 1996). The nitrate radical (NO_3^{\cdot}) is an important precursor to the formation of HNO_3 but as it rapidly photolyzes in the daylight, reactions involving it will only be important at night. Listed below are several formation pathways for HNO_3 :

- Oxidation of NO/ NO_2 :

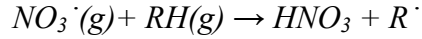


- N_2O_5 is an important nighttime source of HNO_3 , thought to account for one half to one third of HNO_3 produced:

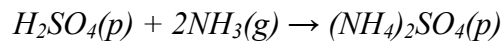
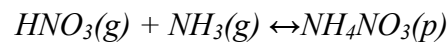


- The nitrate radical (NO_3^{\cdot}), formed from reaction of NO_2 with ozone, can also react to form N_2O_5 or HNO_3 :





Animal waste and fertilizers are agricultural sources that directly emit ammonia (NH₃) as the N main pollutant. Although NH₃ is stable with respect to reaction during its typical atmospheric residence time, both NH₃ and reaction products of NO_x can enter aerosol particles. This phase change is important to consider due to the different atmospheric behaviors of gases and particles. Important reactions include:



Particles formed by these and other reactions contribute to haze formation and visibility degradation. They are also important contributors to atmospheric cloud condensation nuclei (CCN). The dry removal of particles and gases takes place at different rates; particle phase nitrogen survives longer in the atmosphere and can be transported further. Particles and gases are also scavenged during precipitation by different mechanisms. Thus the phase of the pollutant species is important to consider when identifying both atmospheric effects and, most relevant here, removal processes.

1.4.3 Regional Sources

The Colorado Front Range is a densely populated urban corridor that forms a boundary between the mountains and plains. The Denver-Colorado Springs-Fort Collins, metropolitan areas are the major sources of anthropogenic emissions including NO_x and SO₂.

Point source emissions are one of the largest contributors to N emission, followed by highway mobile emissions and off-road (trains, construction, machinery) emissions in the Front Range (Baron et al., 2004; Williams and Tonnessen, 2000). Point sources include large electrical generating facilities and other industrial manufacturing and processing plants. Denver has an emission rate greater than 5 Mg/yr of NO_x (Williams and Tonnessen, 2000). Mobile sources accounted for 46% (or 0.4 Mg/day) of NO_x emitted throughout the state in 1990. Baron et al. (2004) examined emissions inventories and land use changes between 1985 and 1995 and found that counties just to the east of the mountains, Weld, Denver, and Adams, emitted greater than 8000 Mg N in 1995, the highest N emissions found in the South Platte Valley Basin (Figure 1.1a).

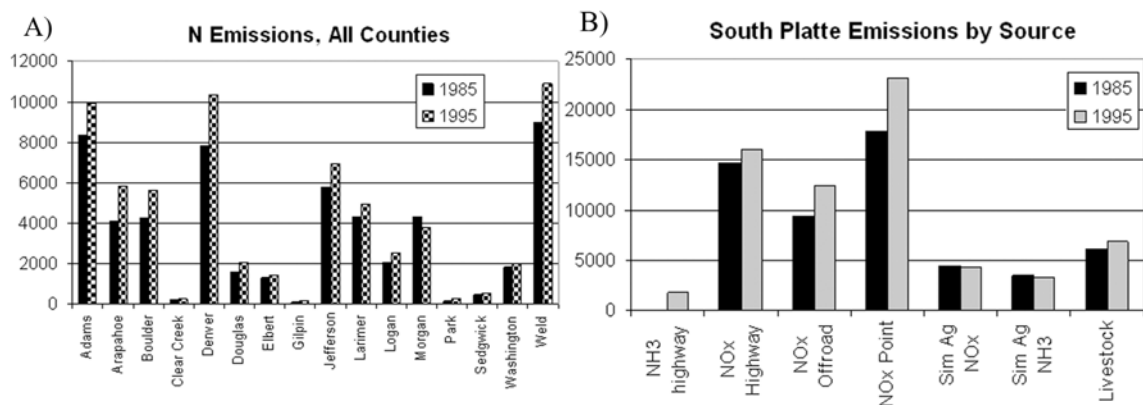


Figure 1.1 Emission of Nitrogen (NO_x-N and NH₃-N) by A) county and B) by source for 1985 and 1995 for the South Platte Basin, Colorado. From Baron et al (2004).

A comparison of NO_x and NH₃ sources in Figure 1.1b indicates that emissions of ammonia are much smaller than NO_x. However, county emissions vary by land use. For example, in Weld County, emissions are dominated by agriculture, not point or mobile sources (Baron et al., 2004). The same point sources that emit NO_x will also

contribute to SO₂ emissions, adding to the SO₂ emitted from the combustion of fossil fuels in mobile sources.

1.5 Dry Deposition

The removal of pollutant species from the atmosphere to the ground is referred to as deposition. There are two main types of deposition, wet and dry, to consider when determining fluxes in RMNP. The rate of dry deposition, where particles and gases are directly deposited, is dependent upon the deposition velocity of the species and its concentration. Deposition velocities vary with the chemical species, the surface to which deposition is occurring, and the atmospheric concentration of the species. Environmental conditions (*i.e.*, relative humidity, temperature, boundary layer thickness) are also important for determining dry deposition rates.

Dry deposition velocities (V_d) of HNO₃ have been measured in a number of studies in different forest environments for HNO₃ (Meyers et al., 1989; Pryor et al., 2001; Pryor and Klemm, 2004; Sievering et al., 1994; Sievering et al., 2001) and NH₃ (Andersen et al., 1993; Andersen and Hovmand, 1999; Duyzer et al., 1994; Wyers et al., 1992) while far fewer studies have measured the deposition velocities of both ammonia and nitric acid in the same study (Andersen and Hovmand, 1995; Janson and Granat, 1999; Zimmermann et al., 2006). There is a wide range of measured deposition velocities for HNO₃ as shown in Sievering et al. (2001), where $V_d(\text{HNO}_3)$ ranged from 0.8 cm·s⁻¹ to 20 cm·s⁻¹ over the course of the study period. There is, however, generally good agreement between studies for an average HNO₃ deposition velocity

between 4 and 8 $\text{cm}\cdot\text{s}^{-1}$. Measured deposition velocities for NH_3 span a smaller range and are typically slightly lower, ranging from 3 to 4.5 $\text{cm}\cdot\text{s}^{-1}$.

There is poor agreement between studies when both nitric acid and ammonia were measured at the same time. Ammonia V_d was measured to be twice $V_d(\text{HNO}_3)$ in one study (Andersen and Hovmand, 1995), while the opposite was found in a different study where $V_d(\text{HNO}_3)$ was twice $V_d(\text{NH}_3)$ (Zimmermann et al., 2006). In a third case the results matched well with the studies where only one species was measured. The deposition velocities were fairly similar with nitric acid having a slightly higher velocity: $V_d(\text{HNO}_3) = 4.2 \text{ cm}\cdot\text{s}^{-1}$ and $V_d(\text{NH}_3) = 3.2 \pm 4.8 \text{ cm}\cdot\text{s}^{-1}$ (Namiesnik et al., 2003).

Particles have smaller deposition velocities than gases. Fine particles ($\leq 2 \mu\text{m}$) have typical deposition velocities $< 0.5 \text{ cm s}^{-1}$, while larger particles have deposition velocities up to $2 \text{ cm}\cdot\text{s}^{-1}$ (Lovett, 1994).

1.6 Wet Deposition

Wet deposition occurs when particles and gases are scavenged and deposited by precipitation. There are several processes by which this can occur. Soluble gases can enter rain or snow via below-cloud or in-cloud scavenging. Aerosols can enter by similar means. In-cloud scavenging mechanisms include nucleation, impaction, and diffusion. Gas scavenging depends on the aqueous solubility of the species of interest. In addition, chemical reactions (acid-base reactions or complexation) occur

in the aqueous phase, which provide another aqueous phase sink for the gas species and enhance the overall solubility. While gas phase scavenging is governed by an equilibrium process, equilibration times may not be sufficient to actually achieve equilibrium for scavenging of very soluble species or scavenging by large drops (*e.g.*, rain drops).

Historically, in RMNP, the largest contribution to total N and S deposition is by wet processes followed by dry deposition of gases. These historical observations, and their limitations, are reviewed next.

1.7 Historical Data

Several monitoring networks, the Interagency Monitoring of Protected Visual Environments (IMPROVE) network, the Clean Air Status and Trends Network (CASTNet), and the National Atmospheric Deposition Program/National Trends Network (NADP/NTN), collect data in or near RMNP. Records from these monitoring networks will allow for comparison with the data collected during RoMANS. They also provided insight into important factors useful in designing RoMANS measurement plans. The IMPROVE, CASTNet, and NADP data from 2000-2004 were combined and analyzed to examine the seasonal variation in concentrations and deposition of the measured nitrogen and sulfur species.

The nitrogen (from NH_4^+ , NO_3^- , and HNO_3) and sulfur (from SO_2 and SO_4^{2-}), measured by CASTNet and IMPROVE have similar monthly mean concentrations.

Concentrations peak during the warm months (May through August) at about $0.5 \mu\text{g}\cdot\text{m}^{-3}$ and are the lowest during the colder months (November through January), with concentrations typically between 0.2 to $0.3 \mu\text{g}\cdot\text{m}^{-3}$. During the winter months, sulfate accounts for 35% to 50% of the total sulfur, but a higher fraction, 55%-62%, of total sulfur is sulfate during the spring and summer. Ammonium contributes the most to total measured nitrogen, accounting for about half during all months, while gaseous nitric acid accounts for 25 to 40% of the measured nitrogen, and particulate nitrate contributes only 10 to 25%. The contribution of gaseous ammonia to total nitrogen is unknown since it is not measured.

Ambient concentrations peak in warmer months driving dry deposition rates up during summer. Ambient concentrations of nitrogen and sulfur species are similar but nitrogen dry deposition rates are 2 to 3 times larger than sulfur dry deposition rates. Nitric acid has a higher deposition velocity relative to the other species, so that nitric acid accounts for 75 to 85% of the calculated nitrogen deposition while comprising only 25-40% of the measured nitrogen species. The NH_4^+ dry deposition rate in the historical record is less than nitrate deposition except during the peak months of March-April and July.

During most months, measured nitrogen and sulfur wet deposition rates are greater than dry deposition rates (Figure 1.2), and from March through August wet deposition accounts for 65% to 80% of the total measured deposition. Wet deposition has two peak periods: March, when precipitation is high, and July, when concentrations and

precipitation rates are large. The dry deposition rates are greatest during the summer months, peaking in June, when the concentrations measured by CASTNet are highest. July, August, and March have the highest total deposition of nitrogen and sulfur, in that order.

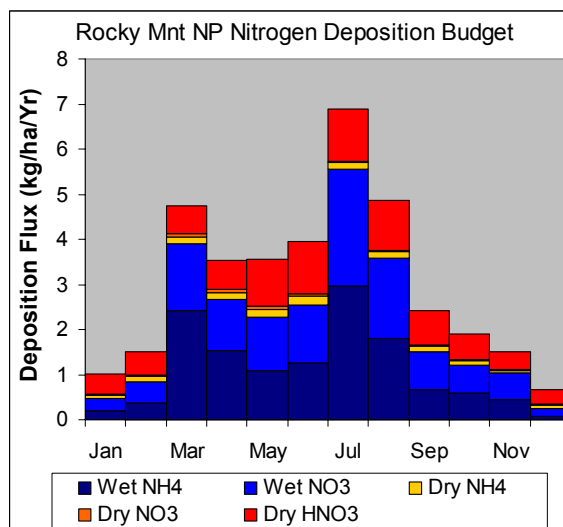


Figure 1.2 The average monthly total nitrogen and sulfur deposition budgets. Beaver Meadows NADP data and Rocky Mountain NP CASTNet data from 2000-2004 were used.

1.8 Meteorology in the Region Including RMNP

Prevailing winds across Colorado are westerly. Downslope winds in the park expose the region to relatively clean continental air containing background levels of nitrogen compounds (Langford and Fehsenfeld, 1992). Storms from the west generally lose much of their Pacific moisture on mountaintops. Areas to the east and very near the mountains are subject to periodic severe, turbulent winds from the effects of high-speed westerly winds over the mountain barrier. Strong winds are common at elevations above tree-line (approximately 11,500 feet) throughout the winter months and can exceed 50 to 100 mph in exposed locations.

Wind patterns at RMNP show typical mountain upslope/downslope flows, both at a local scale in the valleys and canyons within the park, as well as at a mesoscale level as influenced by the Front Range. Upslope flow is induced by heating of the mountain surface, especially during summer months, causing a late morning to mid-afternoon counterclockwise shift from westerly to southerly to easterly flow (Brazel and Brazel, 1983).

Upslope flow can also result from synoptic weather patterns. For example, the circulation around a low pressure system located in the southeast Colorado plains can result in easterlies throughout the Front Range. This type of forcing is more common in the winter, which is especially important due to the periodic influx of moist air during this season.

Front Range upslope winds may be particularly significant in bringing pollutants into the park area from the large urbanized and agricultural areas from Fort Collins to Pueblo. Emissions and pollutants are highly subject to trapping by inversions in the valleys and basins of RMNP. Higher elevations will typically be above trapped local haze and may also be above regional haze trapped below large-scale subsidence inversions.

Precipitation increases with elevation during both winter and summer, but the elevation effect is greatest in mid-winter. Outbreaks of polar air are responsible for sudden drops in temperature accompanied by strong northerly winds (mentioned

previously) which come in contact with moist air from the south to cause heavy snowfall. During the spring, easterlies induced by midlatitude cyclones combined with the effects of orographic forcing frequently lead to snowstorms. As a result, the high peaks generally receive the majority of their precipitation during the winter and spring. During the summer, daytime heating of the higher terrain combined with relatively moist air along the eastern slopes produces thunderstorms and associated upslope flow. It is not unusual to have thunderstorms every afternoon from the end of July through August. The western slope receives more precipitation than the eastern slope, which is in the rain shadow of a predominantly westerly flow.

Most of Colorado's heaviest precipitation events occur during either late-May through early June or late July through early September (Petersen et al., 1999). The peak in precipitation in late-May is associated with quasi-stationary storms bringing moisture from the Gulf of Mexico westward to the Front Range. The increase in storm activity from the end of July through September has a pronounced maximum from the last week of July to the first week in August. These convective storms often cover a small area but have occurred in nearly all parts of Colorado. The greatest of these storms have occurred east of the mountains and often near the eastern foothills of the Rockies.

1.9 Objectives

Gas and particle concentrations were measured and precipitation samples were collected to gain a better understanding of nitrogen and sulfur deposition in and

around Rocky Mountain National Park. Samples were collected in March and April 2006 for five weeks and in July and August 2006 for five weeks. Historically these months have high deposition and will have different meteorological influences due to differences in the seasons. The goals of this work are to identify the important processes and components of N deposition and to quantify the deposition of N and S in the RMNP region.

This thesis presents the methods used to collect and analyze precipitation samples during RoMANS. The results of chemical analysis of the precipitation samples are presented for all sites in addition to site averages of concentrations and deposition. The wet deposition data are compared with historical data and examined for temporal and spatial variability. The dry deposition data are also compared with historical data and temporal variability is examined. In addition, factors influencing the dry deposition are investigated, including the averaging timescales of concentration and deposition velocity. Deposition totals are presented for the core sampling site and the main contributors to N deposition are identified.

2 Methods

The RoMANS study was conducted over five weeks in March and April 2006 and five weeks in July and August 2006. These months have a historically high period of nitrogen deposition in the park and, in order to aid in the understanding of important processes and to identify the major components of deposition, samples were collected during these time periods.

2.1 Site Descriptions

Sampling sites were located at various locations within the park and across Colorado (Table 2.1). The most comprehensive set of measurements was made at the Core Site which was co-located with the IMPROVE and CASTNet monitoring sites. This allowed for comparison with the data collected from each of these monitoring networks. The Core Site also featured sufficient power to operate the large suite of instruments planned for operation. A wide variety of measurements was made at the Core Site. The instruments of interest to this work included continuous gas measurements of SO₂, O₃, and NH₃, 24-hour integrated URG annular denuder/filter pack measurements of SO₂, HNO₃, and NH₃ and PM_{2.5} for inorganic chemical speciation, and several types of precipitation measurements. Other instruments in operation included an Optec nephelometer, a Particle Into Liquid Sampler (PILS) coupled to two ion chromatographs for inorganic cation and anion fine particle speciation, a Micro-Orifice Uniform Deposit Impactor (MOUDI), a Sunset OC/EC Analyzer, and a suite of aerosol particle sizing instruments.

Table 2.1 Locations of monitoring sites during spring and summer campaigns of RoMANS

Spring							
ID	Site Name	Site Type	In Park	URG	Latitude	Longitude	Elevation (m)
BM	Beaver Meadows	Satellite	X	X	40.356	-105.581	2509
BR	Brush	Satellite		X	40.3138	-103.6022	333
DI	Dinosaur	Satellite		X	40.4372	-109.305	1463
GP	Gore Pass	Secondary		X	40.1172	-106.532	2641
HV	Hidden Valley	Satellite	X		40.394	-105.656	2879
LV	Loch Vale	Satellite	X		40.2878	-105.663	3170
LY	Lyons	Secondary		X	40.2273	-105.275	1684
CS	Core Site	Core Site	X	X	40.2783	-105.546	2784
NE	Grant, Nebraska	Satellite		X	40.8696	-101.731	317
SF	Springfield	Satellite		X	37.369	-102.743	405
SL	Sprague Lake	Satellite	X		40.32167	-105.607	2656
TC	Timber Creek	Satellite	X	X	40.38	-105.85	2767
Summer							
ID	Site Name	Site Type	In Park	URG	Latitude	Longitude	Elevation (m)
AL	Alpine VC	Satellite	X	X	40.442	-105.754	3599
BM	Beaver Meadows	Satellite	X	X	40.356	-105.581	2509
BR	Brush	Satellite		X	40.3138	-103.6022	333
GP	Gore Pass	Secondary		X	40.1172	-106.5317	2641
HV	Hidden Valley	Satellite	X		40.394	-105.656	2879
LI	Lake Irene	Satellite	X		40.413	-105.819	3260
LV	Loch Vale	Satellite	X		40.2878	-105.6628	3170
LY	Lyons	Secondary		X	40.2273	-105.2751	1684
CS	Core Site	Core Site	X	X	40.2783	-105.5457	2760
RB	Rainbow Curve	Satellite	X		40.3998	-105.663	3271
RC	Rock Cut	Satellite	X		40.392	-105.72	3664
SL	Sprague Lake	Satellite	X		40.32167	-105.6071	2656
TC	Timber Creek	Satellite	X	X	40.38	-105.85	2767

Two secondary sites, Lyons and Gore Pass (located east and west of the park, respectively) were chosen to identify the properties of air masses moving into the park. Secondary sites had far fewer measurements than the Core Site. At these sites URG annular denuder/filter-pack samplers were operated, and precipitation samples were also collected. A MOUDI was operated at Lyons and off-line PILS were

operated at both sites. Meteorological parameters were measured at the Core Site and at both secondary sites.

As the third main type of site in the RoMANS study, satellite sites had the fewest measurements. At satellite sites precipitation samples were collected; a subset of these sites also had denuder/filter-pack measurements. The satellite sites changed from spring to summer as a result of budget constraints and accessibility. The extreme eastern and western sites were eliminated in the summer when several sites were added within the park. During the summer, Brush was the only satellite site where precipitation was not collected.

Figure 2.1 shows the locations of most of the RoMANS sampling sites. Sites within the park not presented in Figure 2.1 can be found in Figure 2.2 which is a zoomed-in view of the park (located within the green boundary). Most of the sites within the park were operated only during summer due to limited accessibility during the spring. Figure 2.1 also shows locations of weekly passive ammonia monitoring sites operated by volunteers. These sites and the associated measurements are not discussed in this thesis.

Figure 2.1 Map of RoMANS sites, RMNP is shaded in green in north central Colorado.

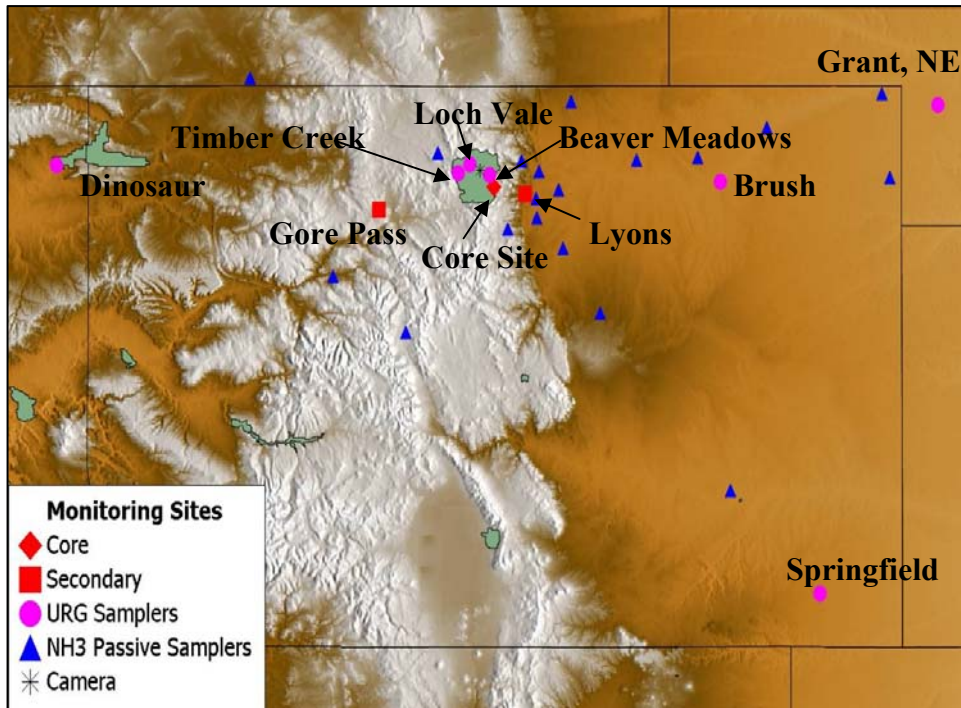
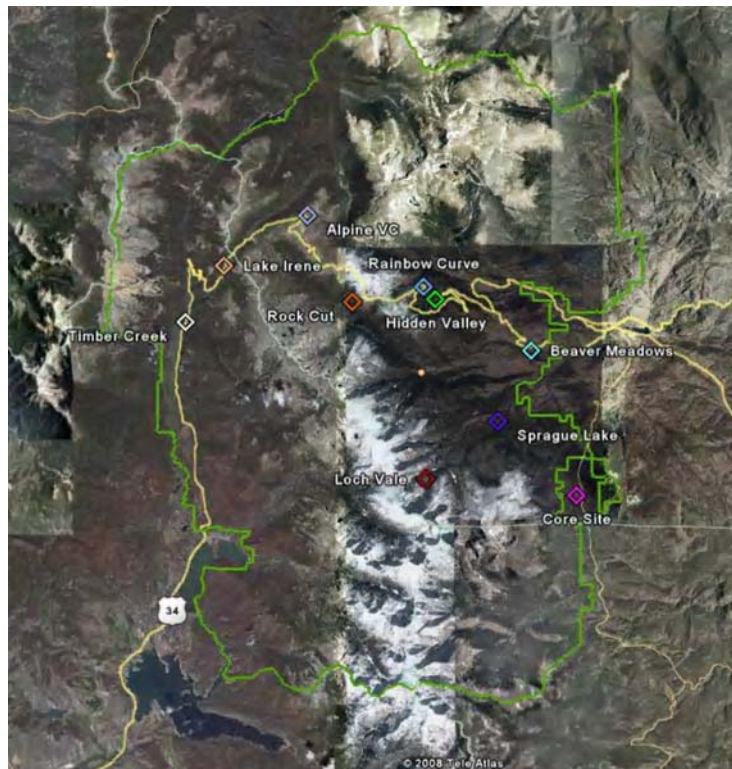


Figure 2.2 RoMANS sampling sites within Rocky Mountain National Park. The green border is the park boundary. From Google Maps



2.2 *Precipitation Collection*

Three different methods were used to collect precipitation (rain or snow) during the RoMANS study. The type of sampler at each location was dependent on site operator duties and the other types of measurements taking place site. An open bucket sampling system consisted of an open bucket, 23.02 cm in diameter, placed inside a second bucket with a weight between the buckets to anchor it down. The bucket collected sample for 24 hours (approx. 8 am to 8 am). At the end of the sampling period it was exchanged for a clean bucket, and the sample was processed. The automatic precipitation sampling system, a TPC-3000 (Yankee Environmental Systems, Inc., Turners Fall, MA), has a combination optical/resistance grid precipitation sensor that opens a lid to a bucket (diameter = 25.2575 cm) when precipitation is sensed; an internal data logger records when the lid to the bucket is opened and closed. This system is similar to those used by the NADP network for wet-only sampling. The sample was typically collected every morning at 8 am, for a 24 hour sample, and a clean bucket was placed in the auto-sampler. A sub-event sampling system collected precipitation with a large funnel (diameter = 52.705 cm) which drained into a collection bottle or bucket. The bottle (or bucket) was changed periodically, approximately hourly, throughout a precipitation event. The collection time for the sub-event samples changed with site and event. A log book was kept for each site to record stop and start times of sample collection and blank collection. The collection funnel was gently heated to melt the snow during the spring.

At the Core Site all three types of precipitation samplers were used. At Lyons an open bucket was used during both campaigns with the auto-sampler and the sub-event sampler only in the spring. At Gore Pass a bucket and sub-event sampler were used during both campaigns and an auto-sampler was used only during the summer. At the satellites sites only an open bucket was used.

Precipitation collectors were rinsed thoroughly with deionized (DI) water prior to each sample collection period. Blanks were collected periodically by pouring approximately 500 mL of DI water into the collector and collecting as a sample would have been. Empty bottles were weighed prior to sample collection and then after to determine the total volume of sample collected. pH measurements were completed after weighing. Two aliquots of 650 μ L were taken for ion chromatography analysis. In some cases an aliquot of approximately 10 mL was placed into an amber nalgene bottle and immediately frozen for organic nitrogen (ON) analysis. ON samples were taken only at the Core and secondary sites and then only if enough sample was collected.

2.3 URG Denuder/Filter Pack Sample Collection

24-hr URG denuder/filter-pack samples were collected at several sites during RoMANS, but only data from the Core Site are analyzed and presented in this thesis to determine dry deposition contributions of various gases and particles at that location. The URG denuder/filter pack (URG-3000C University Research Glassware Inc., Chapel Hill, NC) sampling train at the Core Site consisted of a PM_{2.5} cyclone

followed by two denuders in series, the first coated with phosphorous acid solution for collection of NH_3 and the second coated with a carbonate solution for collection of HNO_3 and SO_2 . Airflow exiting these first two denuders passed through a Nylon filter (Nylasorb, pore size 1.0 μm , Pall Corporation) for collection of fine particles and subsequently a second phosphorous acid-coated denuder to collect any ammonia volatilized from collected particles on the filter. Volatilized nitric acid has been demonstrated to be retained by the Nylasorb filter (Yu et al., 2005). Denuder samples were extracted with 10 mL deionized water, and filter samples were extracted with 5 mL deionized water in an ultrasonic bath. Extracts were analyzed by the procedures outlined below for inorganic ions.

2.4 Sample Analysis

2.4.1 Inorganic Ions

Filter extracts and precipitation samples were analyzed for both cations (Na^+ , NH_4^+ , K^+ , Mg^{2+} , and Ca^{2+}) and anions (Cl^- , NO_3^- , NO_2^- , and SO_4^{2-}) by ion chromatography. Denuder extracts were analyzed either for ammonium (phosphorous acid-coated denuders) or for sulfate and nitrate (carbonate-coated denuders). Cations were separated with a Dionex CS12A column followed by a CSRS ULTRA II suppressor and a Dionex CD-20 conductivity detector. Anions were separated with a Dionex AS14A column followed by an ASRS ULTRA II suppressor and a Dionex CD-20 conductivity detector. Each instrument was calibrated daily using standards prepared from analytical grade salts. Periodic standard and replicate sample analyses were used to monitor calibration stability and analytical precision. In addition, Dionex

NIST traceable check standards were analyzed during each run to independently check the accuracy and precision of analysis.

2.4.2 Organic Nitrogen

Samples were thawed completely immediately before ON analysis. The nitrogen species analyzed during inorganic ion analysis provided the sum of inorganic nitrogen before ON analysis. After thawing, samples were acidified to a pH of approximately 3 using concentrated H₂SO₄ (5% (v/v)). Using a carousel photolysis chamber, acidified samples were exposed to UV radiation for 24 hrs. Samples were reanalyzed by ion chromatography after sample photo-oxidation and the organic nitrogen concentration was determined as the difference between the sum of inorganic N species before and after 24 hour photo-oxidation. Variations of the photo oxidation method have been used to determine dissolved organic nitrogen for many studies (Cornell and Jickells, 1999; Cornell et al., 2003; Russell et al., 1998; Scudlark et al., 1998). Advantages of the UV photo oxidation method include reduced sample handling and reagent addition during analysis (Cornell et al., 2003). However, the efficiency of this method is uncertain and the chemistry of photolysis is complex and not well understood (Scudlark et al., 1998)

2.5 Quality Assurance and Quality Control

2.5.1 Precision and Accuracy of Standards

Measured ion concentrations were compared to the nominal values of the Dionex NIST-traceable check standards for each cation IC run, in Figure 2.2, and each anion

run, in Figure 2.3, during analysis of samples following both campaigns. Some variability is seen throughout the analysis period for both the spring and summer.

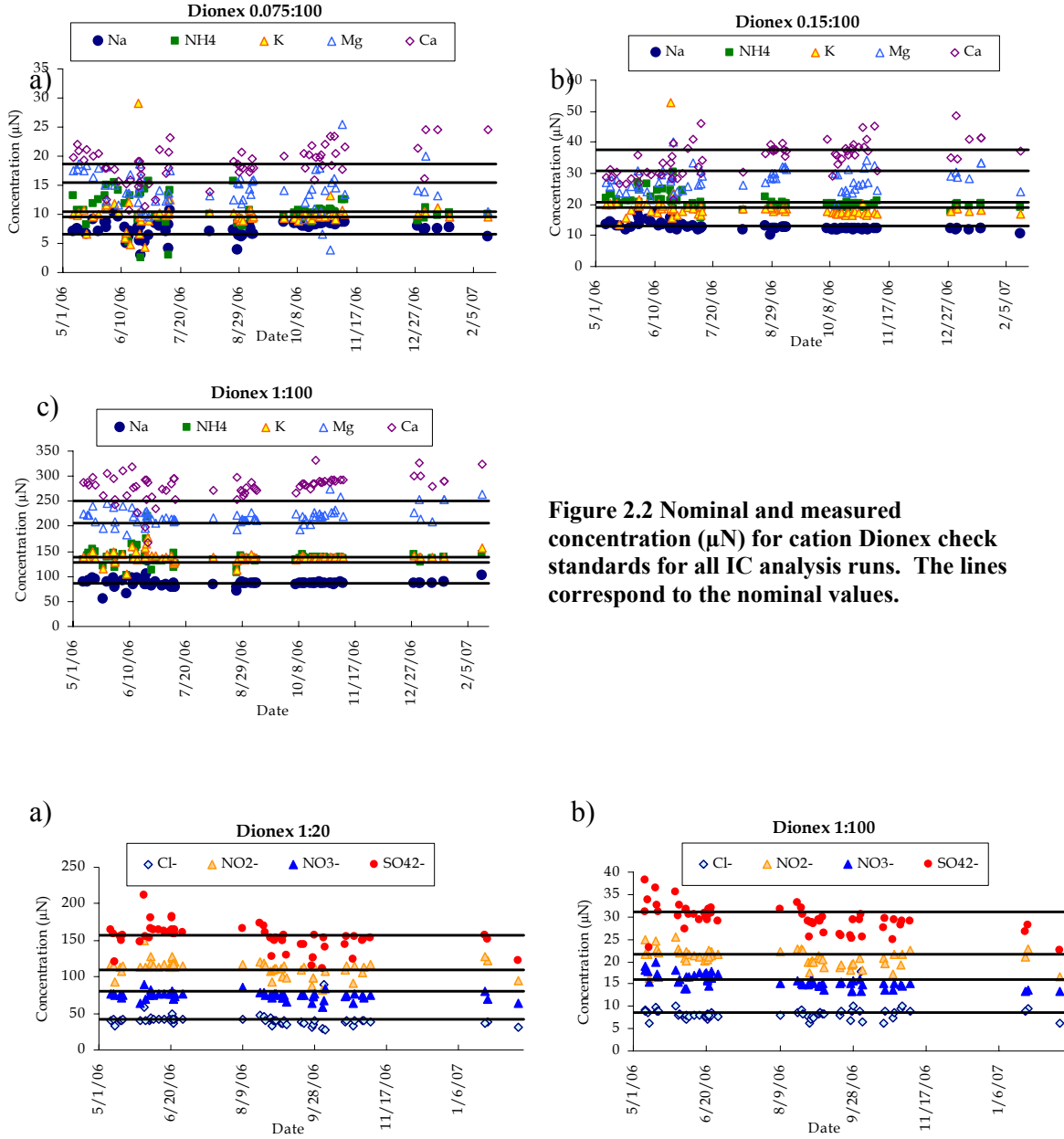


Figure 2.2 Nominal and measured concentration (µN) for cation Dionex check standards for all IC analysis runs. The lines correspond to the nominal values.

Figure 2.3 Nominal and measured concentration (µN) for anion Dionex check standards for all IC analysis runs. The lines correspond to the nominal values.

Two Dionex NIST traceable standards were diluted (1:100 and 1:20 for anions and 0.075:100, 0.15:100, and 1:100 for cations). These diluted Dionex standards were used

as accuracy check standards at the beginning of each daily IC run. Information about the accuracy and precision of IC analyses from the Dionex check standards is presented in Table 2.2. Measurement precision and accuracy, based on results from these standard analyses, were somewhat poorer than seen in many previous studies in our laboratory. The overall accuracies of the main species of interest for RoMANS (nitrate, sulfate, and ammonium), however, were good with deviations of only 0.3-7.8% from nominal values.

To determine the precision of the chemical analysis, replicate measurements were made every tenth sample during IC analysis. The replicate measurement was followed by injection of a standard and DI water. Table 2.3 shows a summary of the results of these replicates, including the pooled standard and relative standard deviation (RSD). The RSDs were lowest for nitrate (0.58%) and sulfate (2.26%). The precision of the ammonia measurement is among the highest of all species with an RSD of 5.5%.

Table 2.2 Accuracy and precision of standard analysis

	Standard	Nominal (μN)	Average (μN)	Absolute Error $ \text{X}_i - \text{X}_t $	Relative Error $((\text{X}_i - \text{X}_t) / \text{X}_t) * 100$	Std. Dev.	Precision CV (%)	n
Na ⁺	Dionex 0.075:100 check	6.52	7.51	0.99	15.26	1.35	17.94	68
	Dionex 0.15:100 check	13.05	12.78	0.27	2.05	1.27	9.94	67
	Dionex 1:100 check	86.99	86.67	0.32	0.37	8.96	10.34	68
	Standard 3	10	10.30	0.30	2.99	0.17	1.61	66
	Standard 4	20	21.56	1.56	7.78	2.74	12.71	39
NH ₄ ⁺	Dionex 0.075:100 check	10.39	10.51	0.12	1.14	2.52	24.00	68
	Dionex 0.15:100 check	20.79	20.86	0.07	0.32	2.40	11.48	67
	Dionex 1:100 check	138.59	137.60	0.99	0.72	15.27	11.10	68
	Standard 3	20	20.69	0.69	3.44	0.27	1.30	66
	Standard 4	40	39.16	0.84	2.10	2.81	7.17	36
K ⁺	Dionex 0.075:100 check	9.59	9.94	0.35	3.70	2.80	28.11	68
	Dionex 0.15:100 check	19.16	18.63	0.53	2.78	4.48	24.04	67
	Dionex 1:100 check	127.88	138.17	10.29	8.05	10.09	7.31	68
	Standard 3	10	10.10	0.10	0.98	0.14	1.38	66
	Standard 4	20	39.16	19.16	95.80	0.79	2.01	38
Mg ²⁺	Dionex 0.075:100 check	15.43	14.28	1.15	7.44	3.33	23.29	62
	Dionex 0.15:100 check	30.86	27.94	2.92	9.45	3.55	12.69	64
	Dionex 1:100 check	205.72	220.73	15.02	7.30	16.85	7.63	68
	Standard 3	10	10.45	0.45	4.47	0.57	5.41	64
	Standard 4	20	17.39	2.61	13.07	1.29	7.43	36
Ca ²⁺	Dionex 0.075:100 check	18.71	18.72	0.01	0.04	3.09	16.52	62
	Dionex 0.15:100 check	37.43	35.02	2.41	6.44	5.37	15.32	66
	Dionex 1:100 check	249.50	279.25	29.75	11.92	25.71	9.21	68
	Standard 3	10	11.61	1.61	16.06	0.68	5.85	64
	Standard 4	20	17.47	2.53	12.67	1.65	9.46	36
Cl ⁻	Dionex 1:100 check	8.46	8.35	0.11	1.33	1.57	18.74	59
	Dionex 1:20 check	42.31	40.39	1.92	4.53	8.17	20.23	58
	Standard 3	10	12.62	2.62	26.20	2.33	18.45	106
	Standard 4	20	17.14	2.86	14.28	0.59	3.46	28
NO ₂ ⁻	Dionex 1:100 check	21.74	20.85	0.89	4.10	1.87	8.99	59
	Dionex 1:20 check	108.68	111.78	3.09	2.85	10.88	9.73	58
	Standard 3	10	11.81	1.81	18.14	2.61	22.08	105
	Standard 4	20	18.56	1.44	7.18	1.79	9.66	28
NO ₃ ⁻	Dionex 1:100 check	16.13	15.55	0.57	3.56	1.52	9.77	59
	Dionex 1:20 check	80.64	74.32	6.32	7.84	5.46	7.34	58
	Standard 3	20	19.62	0.38	1.88	0.71	3.60	106
	Standard 4	40	36.21	3.79	9.47	1.13	3.12	28
SO ₄ ²⁻	Dionex 1:100 check	31.23	29.51	1.72	5.52	2.98	10.09	59
	Dionex 1:20 check	156.15	153.39	2.76	1.77	54.13	35.29	58
	Standard 3	20	23.57	3.57	17.83	4.71	20.00	106
	Standard 4	40	34.62	5.38	13.44	1.16	3.35	28

Table 2.3 Precision of sample replicates.

	Average (μN)	Pooled Standard Deviation (μN)	# of sets	# of samples	RSD (%)
Na^+	12.50	0.44	65	136	3.51
NH_4^+	34.79	1.91	61	127	5.49
K^+	22.63	5.72	62	121	25.30
Mg^{2+}	13.67	0.89	61	121	6.50
Ca^{2+}	48.54	2.11	65	133	4.35
Cl^-	24.90	1.15	101	206	4.60
NO_2^-	1.75	0.25	12	22	14.24
NO_3^-	36.38	0.21	105	219	0.58
SO_4^{2-}	28.79	0.65	107	222	2.26

2.5.2 Precipitation Blanks

Rinsing of precipitation collector surfaces with deionized water is a common way to collect a precipitation “blank.” However, there are several complicating issues, however, associated with blank correction of precipitation data. Blank contamination can occur from absorption of soluble gases or particle scavenging from the air when taking a blank by spraying or pouring water into the bucket. In this case, contributions of analytes taken up from the air may not be representative of blank contamination caused by contact with the collector itself. The clean deionized water can absorb atmospheric gases and particles not associated with the clean collection device, which is not representative of a blank. In addition dry deposition can occur on the collection surface, especially in the case of the open bucket and sub-event samplers, which would not be represented by a blank. Also, blanks were not consistently taken at all RoMANS sites, especially during the spring campaign period.

No blank corrections were made to the precipitation data. After reviewing the blank and sample concentrations for both the spring and summer it was determined that most contamination (from collection surfaces or from airborne scavenging) was

minor. In addition, comparison between the different types of co-located samplers showed fairly good agreement. Good agreement between co-located samplers occurred without including the blanks, indicating that contamination was minor and blank correction was unnecessary. The histograms of each species measured are shown below in Figure 2.4 for the bucket samples at all sites for both campaigns. The histograms for the auto-sampler and sub-event sampler can be found in Appendix A. The histograms show the blanks in light green laid over the top of all samples, including blanks. The difference between the top of the light green bar and the dark green bar is the number of samples of that concentration. The blanks are relatively low compared with the sample concentrations.

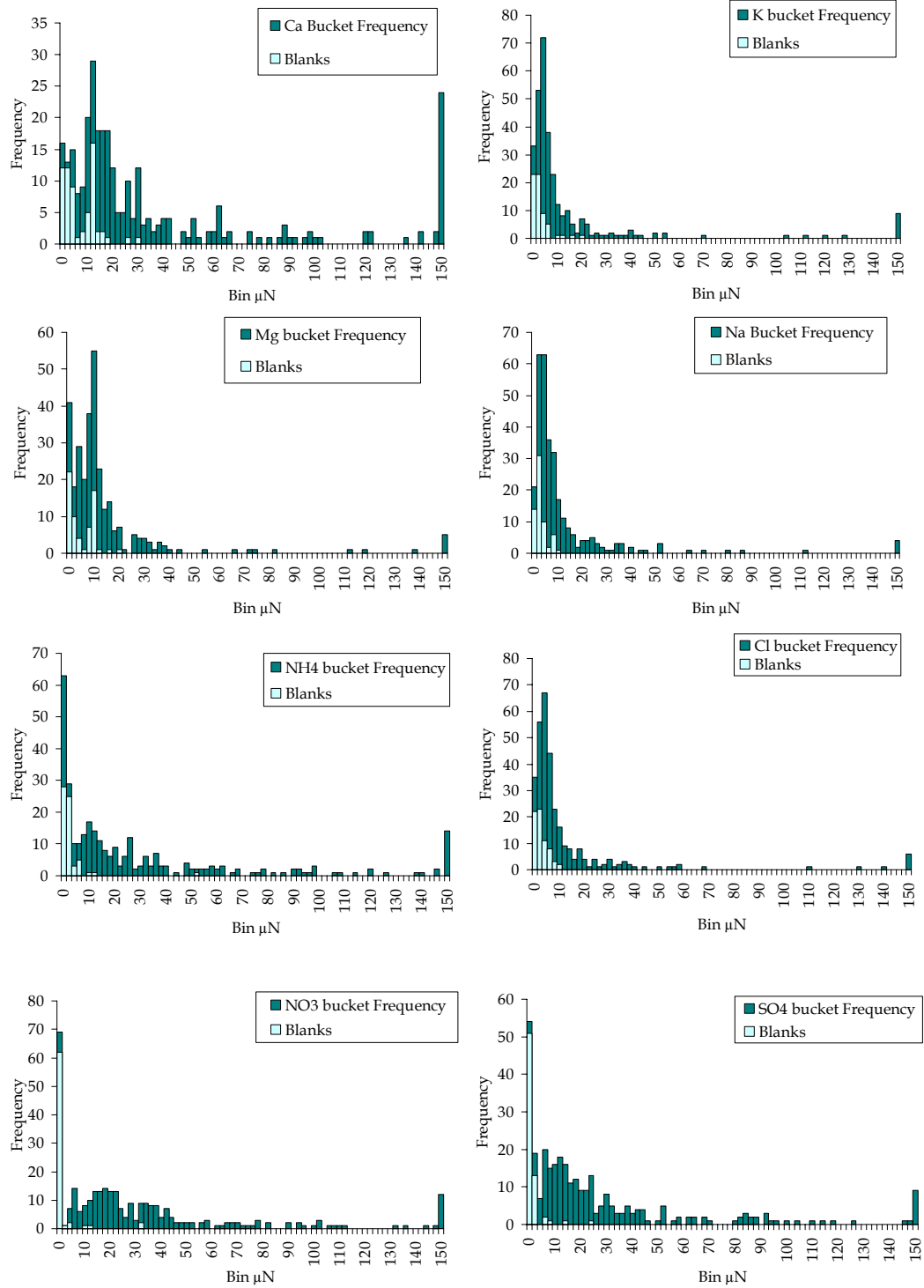


Figure 2.4 Histograms for each ionic species measured by IC. All bucket samples including blanks are shown in dark green with just the blanks in light green plotted on top. The difference between the two bars is the number of samples with concentrations in that bin.

2.6 Calculations

Methods used to calculate several key quantities reported in this thesis are outlined here.

Concentration (converting μN measured by IC to $\mu\text{g/L}$)

X is ionic species of interest (Na^+ , NH_4^+ , K^+ , Mg^{2+} , Ca^{2+} , Cl^- , NO_2^- , NO_3^- , SO_4^{2-})

$$\left[\mu\text{N or } \frac{\mu\text{eq of } X}{L} \right] * \left| \frac{1}{\text{charge of } X} \right| * \text{MW of } X = \frac{\mu\text{g of } X}{L}$$

To get $\mu\text{g N/L}$ or $\mu\text{g S/L}$ the atomic weight of N or S is used instead of the molecular weight (MW) of X.

Time-integrated Precipitation Solute Flux ($\mu\text{g/m}^2$)

v = volume of sample (L)

A = cross-sectional area sampling bucket (m^2)

$$\frac{\mu\text{g of } X}{L} * \frac{v(L)}{A(\text{m}^2)} = \frac{\mu\text{g of } X}{\text{m}^2}$$

Amount of precipitation in millimeters

v = volume of sample (L)

A = cross-sectional area of sampling bucket (m^2)

$$\frac{v(L)}{A(\text{m}^2)} * \frac{0.001\text{m}^3}{1\text{L}} * \left(\frac{1000\text{mm}}{1\text{m}} \right) = \text{mm of precipitation}$$

Correlations

A correlation coefficient is used to indicate the strength of the linear relationship between two variables.

$$\text{Correlation Coefficient} = \frac{\sum (x - \bar{x})(y - \bar{y})}{\sqrt{\sum (x - \bar{x})^2 \sum (y - \bar{y})^2}}$$

The significance of the correlation was determined by a two-tailed t-test at the 95% confidence level. A two-tailed test was chosen because a general idea of the relationships between the correlation pairs was unknown and it is more stringent than a one-tailed test.

The t-value was calculated with the following equation:

$$t = \frac{r\sqrt{N-2}}{\sqrt{1-r^2}}$$

where N is the number of independent data points and r is the correlation coefficient. In order to get more information about the relationship, the slope was calculated using the following equation:

$$slope = \frac{\sum (x - \bar{x})(y - \bar{y})}{\sum (x - \bar{x})^2}$$

The slopes for all significant r-values can be found in Appendix C.

3 Results

3.1 Site Averages

At the RoMANS Core Site in the spring, there were only eleven days with measurable precipitation. The amount of precipitation per event was generally very small; there were only two days (4/23 & 4/24) where considerable snow fell. The spring daily average precipitation was 0.88 mm, and the average per event was 2.44 mm. A total of 29.33 mm fell during the spring study period at the Core Site. The site with the smallest event average volume of precipitation was Lyons (1.81 mm), and the site with the highest event average volume of precipitation was Loch Vale (6.04 mm). All averages (here and below) are arithmetically averaged (not volume weighted).

At the Core Site in the summer, there were twenty days with precipitation. The amount of precipitation per event was more variable than during the spring events. There were several events in the summer with larger volumes than any event in the spring; a larger total volume also fell over the summer study period. The summer daily average was 2.6 mm at the Core Site and the average precipitation per event was 4.8 mm. A total of 96.03 mm fell during the summer study period at the Core Site. Timber Creek had the lowest event average volume of precipitation during the study (2.87 mm), and Lyons had the largest event average, with 8.54 mm of precipitation.

In the spring, the sites farthest from the park (Brush, Nebraska, Springfield, and Dinosaur) had the most basic precipitation pH and were the only sites with an average

pH above 6 (Table 3.1). Average pH was calculated by calculating the H^+ concentration and arithmetically averaging it before recalculating the pH. Within and close to the park, the average pH varied from 5.21 to 5.71. In the summer the pH was lower at all sites with no site having an average pH above 5.16 (Table 3.2). Lyons and Hidden Valley had the least acidic summer precipitation as the only sites with a pH average above 5. The smallest change between seasons was at Hidden Valley. At all other sites sampled during both campaigns the drop in pH was much larger. It is important to note that three of the four sites with the most basic pH in the spring were not active during the summer campaign period.

Table 3.1 Spring average precipitation amount and pH for each event by site.

	Precip. (mm)	pH
Core Site	2.44	5.43
Gore Pass	2.39	5.21
Lyons	1.81	5.71
Beaver Meadows	2.72	5.35
Hidden Valley	3.44	5.43
Loch Vale	6.04	5.42
Sprague Lake	2.46	5.46
Timber Creek	2.02	5.42
Brush	2.49	7.11
Dinosaur	2.42	6.20
Grant, Nebraska	2.59	6.43
Springfield	1.96	6.69

Table 3.2 Summer average precipitation amount and pH for each event by site.

	Precip. (mm)	pH
Core Site	4.80	4.52
Gore Pass	4.62	4.40
Lyons	8.54	5.16
Beaver Meadows	2.99	4.24
Hidden Valley	3.88	5.07
Loch Vale	3.29	4.45
Sprague Lake	3.32	4.56
Timber Creek	2.87	4.50
Alpine VC	5.45	4.65
Lake Irene	3.45	4.52
Rainbow Curve	3.85	4.56
Rock Cut	5.44	4.48

Spring site event concentration averages for each ionic species, measured in the collected precipitation samples, are shown in Table 3.3. During the spring, concentrations varied widely from site to site for each species measured. Overall, nitrate had the highest concentrations of any species with the maximum average concentration of 5512.34 $\mu\text{g/L}$

occurring at Brush and the minimum average concentration of 1151.45 $\mu\text{g/L}$ occurring at the Core Site. The lowest ammonium concentration for the site spring averages occurred in the park at Loch Vale (234.12 $\mu\text{g/L}$) and the maximum occurred outside the park at Brush (2468.98 $\mu\text{g/L}$). Sulfate also had high average concentrations; the maximum average concentration occurred at Nebraska (4122.93 $\mu\text{g/L}$) while the minimum average concentration occurred at the Core Site (1051.50 $\mu\text{g/L}$). The maximum average concentration of calcium, 5110.66 $\mu\text{g/L}$, occurred at Loch Vale while the minimum, 312.19 $\mu\text{g/L}$, occurred at Gore Pass. The maximum average concentration of potassium during the spring occurred at Grant, Nebraska, while the minimum occurred at Sprague Lake. Average concentrations of magnesium didn't vary as widely as other species; the maximum occurred in Nebraska (440.88 $\mu\text{g/L}$) and the minimum at Gore Pass (92.66 $\mu\text{g/L}$). Average sodium concentrations reached a maximum of 818.78 $\mu\text{g/L}$ at Dinosaur and a minimum of 110.31 $\mu\text{g/L}$ at Gore Pass. The spring average chloride concentration was lowest at Gore Pass (87.57 $\mu\text{g/L}$) and highest in Grant, Nebraska (2345.94 $\mu\text{g/L}$). At several sites nitrite was not detected, while Nebraska had the maximum concentration (280.74 $\mu\text{g/L}$).

Table 3.3. Spring site average concentrations in precipitation for all ions measured.

	Ca ²⁺ µg/L	K ⁺ µg/L	Mg ²⁺ µg/L	Na ⁺ µg/L	NH ₄ ⁺ µg/L	Cl ⁻ µg/L	NO ₂ ⁻ µg/L	NO ₃ ⁻ µg/L	SO ₄ ²⁻ µg/L
Core Site	386.51	156.72	113.06	137.48	317.46	116.38	0.00	1151.45	1051.50
Gore Pass	312.19	107.54	92.66	110.31	420.57	87.57	0.00	1289.33	1203.90
Lyons	547.76	169.07	96.67	168.38	1263.18	145.72	31.37	2959.93	1985.58
Beaver Meadows	2513.08	525.10	301.14	507.90	1094.95	682.74	3.61	3141.13	3474.55
Hidden Valley	1186.53	147.57	159.13	273.19	284.42	155.68	0.00	1658.49	1727.41
Loch Vale	5110.66	159.90	322.76	243.59	234.12	153.02	0.00	1460.39	1688.63
Sprague Lake	405.94	96.25	293.00	225.95	317.95	142.84	22.44	1992.61	1794.09
Timber Creek	792.11	171.40	147.24	151.97	469.79	112.89	0.00	1457.88	1366.99
Brush	834.21	494.80	157.65	251.09	2468.98	293.81	68.99	5512.34	2908.51
Dinosaur	3409.77	757.45	334.01	977.78	1663.72	1095.49	47.84	4235.36	3752.01
Grant, Nebraska	1843.58	5639.01	440.88	494.96	2345.94	2004.94	280.74	1344.46	4122.93
Springfield	2631.57	471.30	223.05	370.33	918.80	400.76	31.03	1976.14	1596.84

During the summer, concentrations were generally higher than the spring, but this was not always true. Summer site event averages for each ionic species measured in the collected precipitation samples are shown in Table 3.4. The minimum average nitrate concentration (1933.86 µg/L) occurred at Gore Pass while the maximum (5381.33 µg/L) occurred at Lyons. The minimum average concentration of ammonium of 313.84 µg/L occurred at Hidden Valley while the maximum concentration of 2424.47 µg/L occurred at Lyons. The average sulfate concentration was lowest (811.86 µg/L) at Gore Pass and highest (5297.92 µg/L) at Loch Vale. The average minimum concentration of calcium occurred at Timber Creek (587.51 µg/L) and the maximum concentration of 2236.66 µg/L occurred at Hidden Valley. The average minimum concentration of potassium occurred at Gore Pass (112.63 µg/L) while the maximum occurred at Hidden Valley (3644.57 µg/L). Magnesium concentrations were again not as widely variable; the minimum average concentration was below detection at Lyons, and the maximum

concentration of 302.63 µg/L occurred at Beaver Meadows. Average concentrations of sodium were lowest at Gore Pass (73.52 µg/L) and highest at Rainbow Curve (737.24 µg/L). The average summer chloride minimum concentration occurred at Gore Pass (131.18 µg/L) while the maximum occurred at Beaver Meadows (1492.76 µg/L). Minimum nitrite concentrations were below detection at the majority of sites, and the maximum nitrite concentration of 44.32 µg/L occurred at Lyons.

Table 3.4. Summer average concentrations in precipitation for all ions measured in µg/L.

	Ca ²⁺ µg/L	K ⁺ µg/L	Mg ²⁺ µg/L	Na ⁺ µg/L	NH ₄ ⁺ µg/L	Cl ⁻ µg/L	NO ₂ ⁻ µg/L	NO ₃ ⁻ µg/L	SO ₄ ²⁻ µg/L
Core Site	650.51	117.38	136.25	540.75	759.50	951.85	9.45	3158.03	1757.79
Gore Pass	382.77	112.63	58.88	73.52	545.67	131.18	0.00	1933.86	811.86
Lyons	1107.66	159.87	0.00	142.48	2424.47	195.62	44.32	5381.33	1206.40
Beaver Meadows	2170.55	1251.13	302.63	676.28	2769.04	1492.76	4.12	2248.41	4125.69
Hidden Valley	2236.66	3644.57	295.11	442.77	313.84	1066.17	3.07	3305.06	1899.25
Loch Vale	1996.05	504.86	236.03	679.50	3185.77	1383.56	3.84	5187.16	5297.92
Sprague Lake	1094.14	966.39	168.94	225.55	728.23	531.39	0.00	3316.58	1732.03
Timber Creek	587.51	404.53	111.75	188.06	325.12	291.31	0.00	1958.59	939.64
Alpine VC	801.82	859.43	121.47	251.51	439.24	764.24	0.00	2421.17	1389.19
Lake Irene	756.19	525.66	117.86	217.97	435.20	424.98	0.00	2478.24	1108.49
Rainbow Curve	1733.74	1358.43	189.59	737.24	1423.42	1289.13	1.61	3876.72	2478.84
Rock Cut	666.36	196.35	79.23	169.17	533.31	298.38	0.00	2320.10	1049.93

Flux is related to concentration and the amount of precipitation during the event. A deposition flux represents the input of material per unit area per unit time. These are derived for a given species as the product of the measured precipitation solute concentration of that species and the precipitation volume, divided by the cross-sectional area of the collector and the collection period (here taken as one day). Implicit in the deposition flux calculations is an assumption that the precipitation collector samples a representative amount of precipitation.

The spring average event fluxes for each ionic species measured in the collected precipitation samples are shown in Table 3.5. A high concentration does not necessarily mean a large flux; the amount of precipitation that fell during the event is also a very important factor. The amount of each species deposited varied, in some cases, significantly, by site. The sites with study minimum and maximum average fluxes were more consistent between campaigns and species compared to the sites with study maximum and minimum average concentrations. The Grant, Nebraska site had the maximum average flux for calcium ($7634.57 \mu\text{g}/\text{m}^2$), potassium ($3312.26 \mu\text{g}/\text{m}^2$), magnesium ($1032.48 \mu\text{g}/\text{m}^2$), sodium ($1467.45 \mu\text{g}/\text{m}^2$), ammonium ($11582.42 \mu\text{g}/\text{m}^2$), and chloride ($953.55 \mu\text{g}/\text{m}^2$) while Brush had the maximum average flux for the three remaining species, nitrite ($171.82 \mu\text{g}/\text{m}^2$), nitrate ($13729.39 \mu\text{g}/\text{m}^2$), and sulfate ($7244.12 \mu\text{g}/\text{m}^2$). Gore Pass had many of the lowest fluxes, with minimum event average fluxes for sodium ($150.66 \mu\text{g}/\text{m}^2$), ammonium ($326.78 \mu\text{g}/\text{m}^2$), chloride ($164.13 \mu\text{g}/\text{m}^2$), nitrate ($1780.73 \mu\text{g}/\text{m}^2$), and sulfate ($1345.29 \mu\text{g}/\text{m}^2$) all having the lowest average flux for the spring. The calcium flux was lowest at Sprague Lake, with an average of $848.35 \mu\text{g}/\text{m}^2$ deposited per event. The Core Site had the lowest average potassium deposition ($126.24 \mu\text{g}/\text{m}^2$), while Lyons had the lowest average magnesium deposition ($171.23 \mu\text{g}/\text{m}^2$).

Table 3.5. Spring average event daily wet deposition fluxes for all ions

	Ca ²⁺ μg/m ²	K ⁺ μg/m ²	Mg ²⁺ μg/m ²	Na ⁺ μg/m ²	NH ₄ ⁺ μg/m ²	Cl ⁻ μg/m ²	NO ₂ ⁻ μg/m ²	NO ₃ ⁻ μg/m ²	SO ₄ ²⁻ μg/m ²
Core Site	917.85	126.24	301.89	208.75	1623.52	237.43	0.00	3895.28	2725.10
Gore Pass	507.36	170.43	190.51	150.66	326.78	164.13	0.00	1780.73	1345.29
Lyons	880.20	315.14	171.23	256.47	2254.09	242.30	60.84	5146.37	3215.09
Beaver Meadows	5125.16	647.65	524.62	479.22	3221.92	604.85	2.29	5727.18	4076.58
Hidden Valley	3038.10	378.03	356.96	433.66	1783.37	604.18	0.00	5148.02	4256.70
Loch Vale	6058.30	580.92	646.65	721.36	1578.01	823.99	0.00	8352.46	5732.29
Sprague Lake	848.35	135.73	495.62	278.87	799.50	222.32	5.23	3565.04	2780.83
Timber Creek	2216.68	310.44	317.83	357.07	830.10	223.53	0.00	2440.71	2178.81
Brush	2077.74	1232.38	392.66	625.39	6149.41	731.79	171.82	13729.39	7244.12
Dinosaur	2411.14	1123.06	380.73	1100.70	1282.54	859.86	7.26	4053.93	3392.45
Grant, Nebraska	7634.57	3312.26	1032.48	1467.45	11528.42	953.55	30.69	3955.57	2599.62
Springfield	2353.92	443.81	274.82	459.98	2078.80	537.82	25.35	2949.01	2266.74

The summer average event fluxes for each ionic species measured in the collected precipitation samples are shown in Table 3.6. During the summer, Hidden Valley had the highest average fluxes for calcium (5689.35 μg/m²), potassium (38294.12 μg/m²), magnesium (729.71 μg/m²), sodium (1143.32 μg/m²), and chloride (3686.26 μg/m²), while Lyons had the highest average event fluxes for ammonium (6473.18 μgN/m²), nitrite (60.82 μgN/m²), nitrate (16823.64 μgN/m²), and sulfate (5218.99 μgS/m²). Minimum average event fluxes occurred at Gore Pass for potassium (231.81 μg/m²), sodium (179.56 μg/m²), and chloride (239.27 μg/m²). The minimum average calcium flux of 837.72 μg/m² occurred at Beaver Meadows, while the minimum average ammonium flux (739.16 μgN/m²) occurred at Lake Irene and the minimum average nitrate flux (2708.17 μgN/m²) occurred at Hidden Valley. Sulfate had a minimum average flux for the summer of 1904.85 μg/m² at Lyons. The flux of magnesium at Lyons for the summer

was below detection as was the nitrite minimum for both the spring and summer since the concentrations were below detection limits.

Table 3.6. Summer average event daily wet deposition fluxes for all ions

	Ca ²⁺ µg/m ²	K ⁺ µg/m ²	Mg ²⁺ µg/m ²	Na ⁺ µg/m ²	NH ₄ ⁺ µg/m ²	Cl ⁻ µg/m ²	NO ₂ ⁻ µg/m ²	NO ₃ ⁻ µg/m ²	SO ₄ ²⁻ µg/m ²
Core Site	1004.75	375.28	155.06	716.97	1966.86	1055.62	10.22	5506.32	2643.10
Gore Pass	875.35	231.81	141.21	179.56	1279.28	239.27	0.00	4630.17	1904.85
Lyons	3265.74	583.21	0.00	1101.70	6473.18	816.55	60.82	16823.64	5218.99
Beaver Meadows	837.72	388.47	91.59	485.52	1414.65	930.51	0.44	4785.36	2246.40
Hidden Valley	5689.35	38294.12	729.71	1143.32	132.51	3686.26	3.45	2708.17	2667.67
Loch Vale	1524.40	517.77	251.01	539.94	2041.22	847.25	0.34	6994.33	3005.73
Sprague Lake	1590.72	1821.43	216.90	508.38	1445.26	1195.96	0.00	6096.40	2793.00
Timber Creek	1340.50	968.85	275.06	402.24	794.99	624.21	0.00	4918.29	2304.99
Alpine VC	2969.18	1269.93	412.24	718.59	1569.01	1485.75	0.00	9020.89	4618.51
Lake Irene	1734.00	1387.11	229.08	473.11	739.16	907.38	0.00	5809.88	2569.26
Rainbow Curve	2102.05	1414.36	160.25	444.98	980.12	693.07	0.26	6005.33	2903.90
Rock Cut	1910.71	563.08	234.25	437.57	1687.95	795.92	0.00	7121.52	3273.90

Since a critical load of nitrogen is determined in units related to the number of grams of nitrogen deposited, it is useful to present precipitation concentrations and wet deposition fluxes of all nitrogen species in terms of the mass of nitrogen. This also facilitates comparison between N inputs from different nitrogen species. Table 3.7 (spring) and Table 3.8 (summer) present the average concentrations and fluxes for the key nitrogen and sulfur species in micrograms of nitrogen or sulfur (µg N or S). These tables also include averages of concentrations and fluxes for organic nitrogen which were not provided above. Because the organic nitrogen analysis measures the amount of nitrogen in organic form, and not the total mass of N-containing organic molecules, only masses (or moles) of organic N can be directly determined from the measurements.

During the spring, ammonium had the largest average concentration and flux of the nitrogen species. The highest concentration, 1917.22 $\mu\text{g N/L}$, occurred at Brush while the largest flux, 8952.07 $\mu\text{g N/m}^2$, occurred at the Nebraska site. Nitrate fluxes were highest at Brush, followed by Nebraska. Organic nitrogen had both the smallest average nitrogen concentration and flux during the spring. These minima occurred at Lyons where the average flux was 191.97 $\mu\text{g N/m}^2$ and the average concentration was 419.28 $\mu\text{g/L}$. The average sulfur concentration was greatest at Nebraska (1376.31 $\mu\text{g S/L}$) which is where the greatest sulfur flux also occurred (2535.74 $\mu\text{g S/L}$).

Table 3.7. Spring average concentrations ($\mu\text{g N or S/L}$) and daily fluxes ($\mu\text{g N or S/m}^2$) of key N and S species.

	NH_4^+ $\mu\text{g N/L}$	NO_3^- $\mu\text{g N/L}$	SO_4^{2-} $\mu\text{g S/L}$	ON $\mu\text{g N/L}$	NH_4^+ $\mu\text{g N/ m}^2$	NO_3^- $\mu\text{g N/ m}^2$	SO_4^{2-} $\mu\text{g S/ m}^2$	ON $\mu\text{g N/ m}^2$
Core Site	246.92	259.96	350.50	115.83	1262.74	879.44	908.37	616.39
Gore Pass	326.58	291.30	401.88	149.94	253.75	426.52	469.60	191.97
Lyons	980.89	668.74	662.83	419.28	1750.35	1162.73	1073.26	604.70
Beaver Meadows	850.25	709.68	1159.87	n.m.	2501.89	1777.19	1832.78	n.m.
Hidden Valley	220.86	374.71	576.64	n.m.	1384.82	1164.10	1421.77	n.m.
Loch Vale	181.80	329.95	563.70	n.m.	1225.36	1887.08	1913.55	n.m.
Sprague Lake	246.90	450.19	598.90	n.m.	620.83	805.45	928.29	n.m.
Timber Creek	364.80	329.38	456.33	n.m.	644.59	568.28	726.30	n.m.
Brush	1917.22	1245.41	970.92	n.m.	4775.15	3101.90	2418.22	n.m.
Dinosaur	1291.91	956.90	1252.49	n.m.	995.92	992.11	1279.24	n.m.
Grant, Nebraska	1821.68	303.76	1376.31	n.m.	8952.07	2832.50	2535.74	n.m.
Springfield	713.47	446.47	533.06	n.m.	1614.23	666.27	756.68	n.m.

n.m = not measured

During the summer, the largest concentrations and fluxes were again of ammonium. At Loch Vale the maximum average concentration seen in the sampling network was 2473.81 $\mu\text{g/L}$, while the maximum average flux of 5026.56 $\mu\text{g/m}^2$ occurred at Lyons. Summer nitrate concentrations and fluxes were both highest at Lyons. The minimum

average nitrogen species concentration was once again organic nitrogen (222.71 $\mu\text{g/L}$) occurring this time at Gore Pass. The minimum average nitrogen species flux measured was 102.89 $\mu\text{g N/m}^2$ of ammonium at Hidden Valley. Differences in precipitation chemistry and fluxes at Hidden Valley (higher pH, lower N species content) suggest that precipitation sampled at this site may have interacted with canopy foliage before reaching the sampling bucket. This is not surprising given the extensive forest canopy at this site and the difficulty locating the bucket away from areas of possible canopy influence. For this reason, we will exclude data from the Hidden Valley site from future data analyses. The average sulfur concentration was greatest at Loch Vale (1768.55 $\mu\text{g S/L}$) while the greatest average sulfur flux occurred at Lyons (1742.20 $\mu\text{g S/m}^2$).

Table 3.8. Summer average concentrations ($\mu\text{g N}$ or S/L) and daily fluxes ($\mu\text{g N}$ or S/m^2) of key N and S species.

	NH_4^+ $\mu\text{g N/L}$	NO_3^- $\mu\text{g N/L}$	SO_4^{2-} $\mu\text{g S/L}$	ON $\mu\text{g N/L}$	NH_4^+ $\mu\text{g N/ m}^2$	NO_3^- $\mu\text{g N/ m}^2$	SO_4^{2-} $\mu\text{g S/ m}^2$	ON $\mu\text{g N/ m}^2$
Core Site	590.72	712.99	585.93	585.83	1491.29	1243.16	881.03	847.27
Gore Pass	423.73	436.92	271.01	222.71	993.39	1046.10	635.88	1087.12
Lyons	1882.66	1215.81	402.72	525.52	5026.56	3800.99	1742.20	1657.72
Beaver Meadows	2150.22	507.99	1377.23	n.m.	1098.50	1081.16	749.89	n.m.
Hidden Valley	243.70	746.72	634.01	n.m.	102.89	611.86	890.52	n.m.
Loch Vale	2473.81	1171.94	1768.55	n.m.	1585.05	1580.24	1003.37	n.m.
Sprague Lake	565.49	749.32	578.18	n.m.	1122.28	1377.37	932.36	n.m.
Timber Creek	252.46	442.51	313.67	n.m.	617.32	1111.20	769.45	n.m.
Alpine VC	341.08	547.02	463.74	n.m.	1218.37	2038.10	1541.75	n.m.
Lake Irene	337.94	559.91	370.03	n.m.	573.98	1312.63	857.67	n.m.
Rainbow Curve	1105.31	875.87	827.48	n.m.	761.08	1356.79	969.38	n.m.
Rock Cut	414.12	524.18	350.49	n.m.	1310.73	1608.98	1092.89	n.m.

n.m = not measured

3.2 *Core Site*

Timelines of Core Site precipitation solute concentrations and wet deposition fluxes are presented in Figure 3.1 and Figure 3.2, respectively. The spring and summer campaigns are plotted together to facilitate comparison. Considerable variability is observed between events, with concentrations during summer typically exceeding those during spring. Particularly noticeable are the differences between the spring and summer wet deposition fluxes.

The spring flux was dominated by one large event over two days, 4/23/06 and 4/24/06, but the average concentrations were not markedly different during this event than in previous events. These two samples came from a single snow event that began late on April 23rd and continued until early on April 25th. The sample labeled April 23rd actually ran through approximately noon on April 24th; the April 24th sample was collected from 12:15 PM on the 24th until 1:30 PM on the 25th. This single period of precipitation contributed 79.1%, 80.0%, 84.4 % and 90.7% of the total spring wet deposition fluxes of sulfate, nitrate, ammonium, and organic nitrogen, respectively. The high deposition fluxes during this storm are the result of both the large precipitation amount associated with this event combined with reasonably high average precipitation solute concentrations.

The total flux for all species was greater during the summer than during spring. The total wet deposition of major species was also more evenly spread across numerous precipitation episodes during the summer campaign than was observed during spring.

The bulk of the summer campaign wet deposition was observed during July, with smaller deposition fluxes measured in August. In general, the larger summer deposition fluxes result from a combination of greater precipitation amounts and higher average precipitation solute concentrations. None of the summer episodes, however, individually contributed as much to wet deposition as the late April snowfall discussed above.

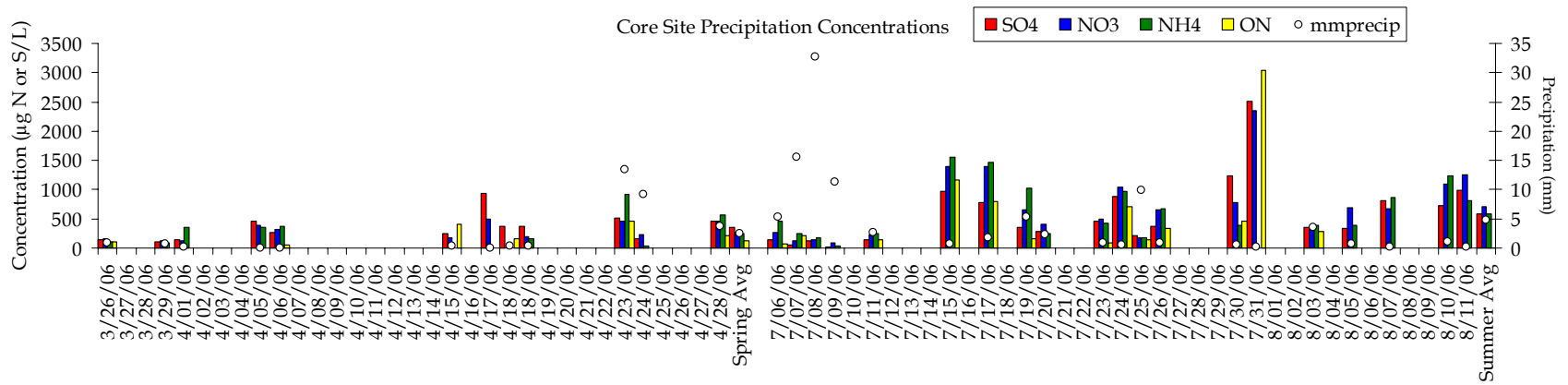


Figure 3.1 Timelines of precipitation concentrations of sulfate (red), nitrate (blue), ammonium (green), and organic nitrogen (yellow) at the Core Site for both the spring and summer studies, shown with amount of precipitation received. Campaign averages are also shown.

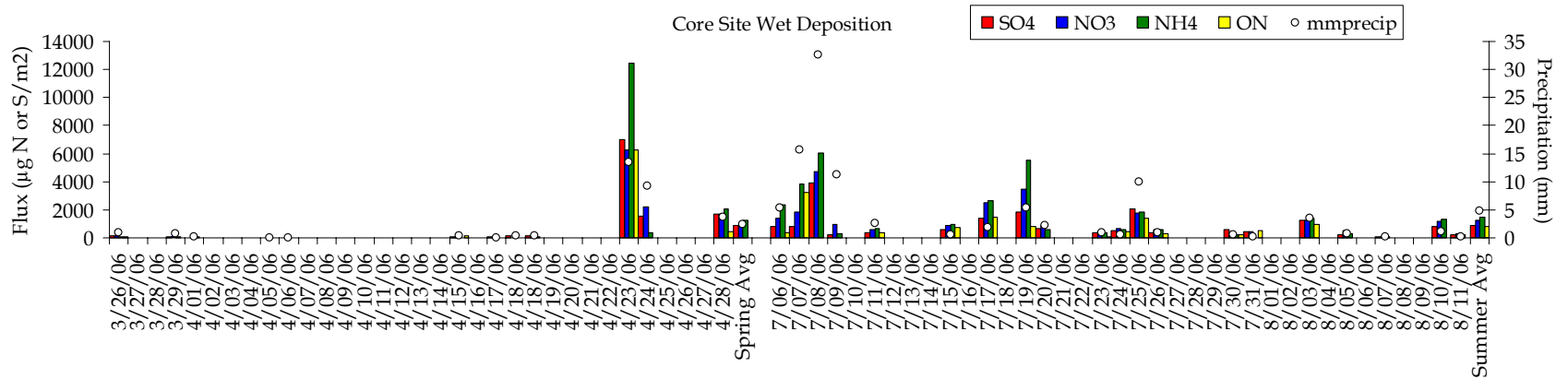


Figure 3.2 Timelines of sulfate (red), nitrate (blue), ammonium (green), and organic nitrogen (yellow) wet-deposited by precipitation at the Core Site for both the spring and summer study periods. Campaign averages are also shown.

To better understand the factors influencing the amount of deposition occurring during a precipitation event, we can look at the time evolution of solutes in samples collected from the sub-event sampler (Figure 3.3). Samples were taken throughout the April 24th event at the Core Site with a sub-event precipitation collector. The concentrations of NH_4^+ , NO_3^- , SO_4^{2-} , and ON all followed the same pattern: higher initial concentrations that decreased as the event continued. Even as precipitation intensity picked up around midnight, the solute concentrations remained low. Interestingly, the highest initial concentrations of nitrogen species during this event were seen for ammonium followed by ON.

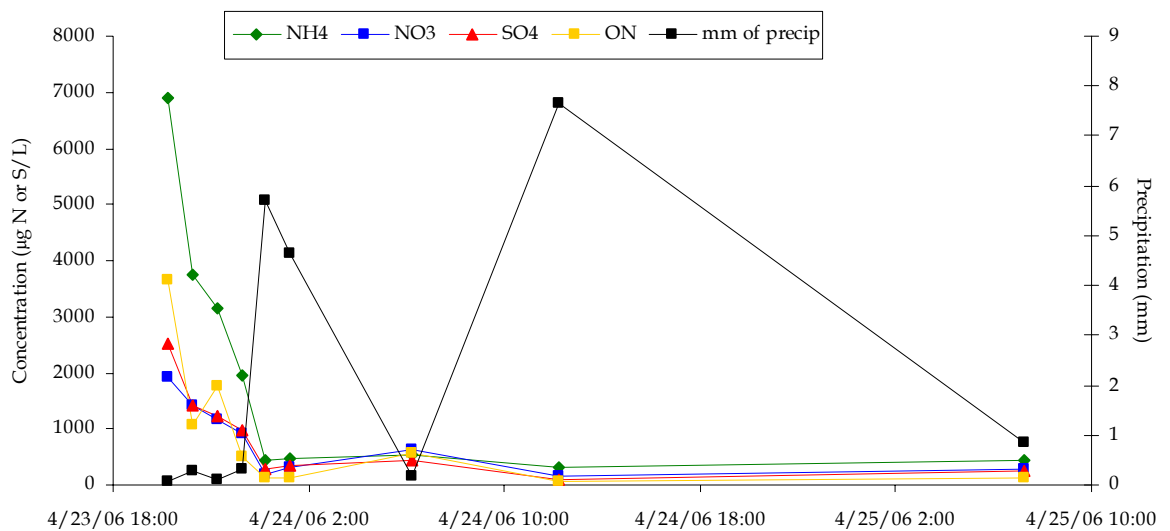


Figure 3.3 Timeline of concentrations from 4/23 20:15 to 4/25 13:30 from sub event sampler at the Core Site.

The time-resolved deposition flux for the April 23rd-25th episode is shown in Figure 3.4. Here we see a steady climb in deposited N and S during the first several hours of the event. The steady increase was followed by a more gradual increase later. During this particular episode, ammonium was the main species contributing to total N deposition,

followed by nitrate and ON. Note that the cumulative deposition fluxes of individual species during this event differ somewhat between the sub-event and daily precipitation samples, with the daily sample fluxes exceeding those from the sub-event sampler. The greater deposition in the daily precipitation sampler was at least partly due to greater precipitation collection by this sampler (almost 24 mm) compared to the sub-event sampler (approximately 20 mm). These modest differences may be due to some periods of missed precipitation in the manually deployed sub-event sampler and/or differences in snowfall collection efficiency by the two collector geometries.

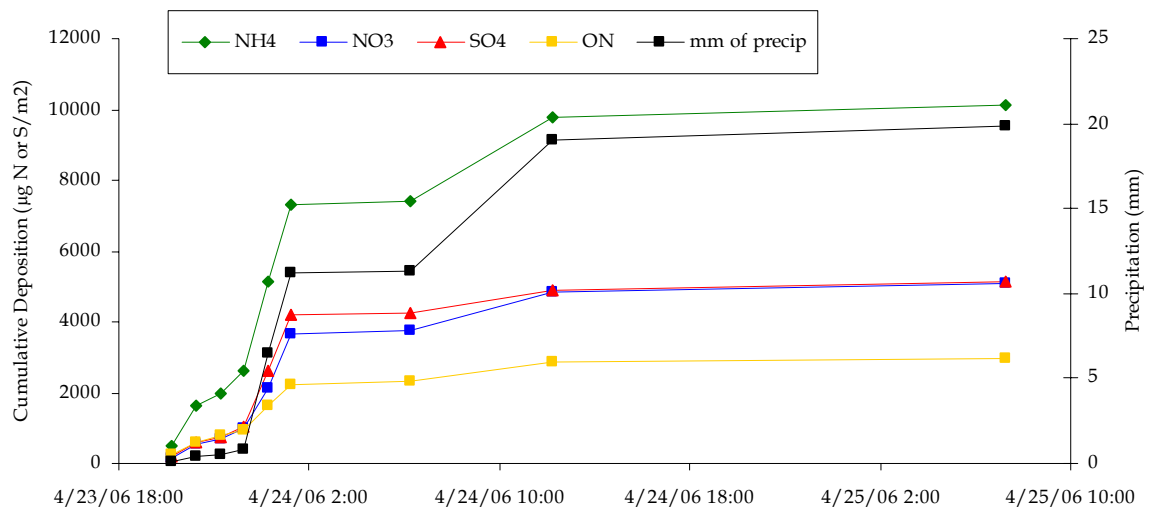


Figure 3.4 Cumulative deposition throughout the event beginning 4/23 20:15 and ending 4/25 13:30 from the sub-event sampler at the Core Site.

The time evolution of precipitation solute concentrations (and associated wet deposition fluxes) can vary from one precipitation event to another. As an example, in contrast to the 4/23-4/25 episode described above, precipitation solute concentrations during the 7/7-7/8 event do not show a rapid decline with time (Figure 3.5). In fact, even with substantial precipitation rates at the start of the episode, concentrations of ammonium climbed while nitrate and sulfate concentrations remain steady. When heavier precipitation begins in the

evening, concentrations declined. Like the April event described earlier, nitrogen from ammonium was a more important contributor to nitrogen deposition in this episode than nitrogen from nitrate. ON was not measured in sub-event samples during this precipitation episode.

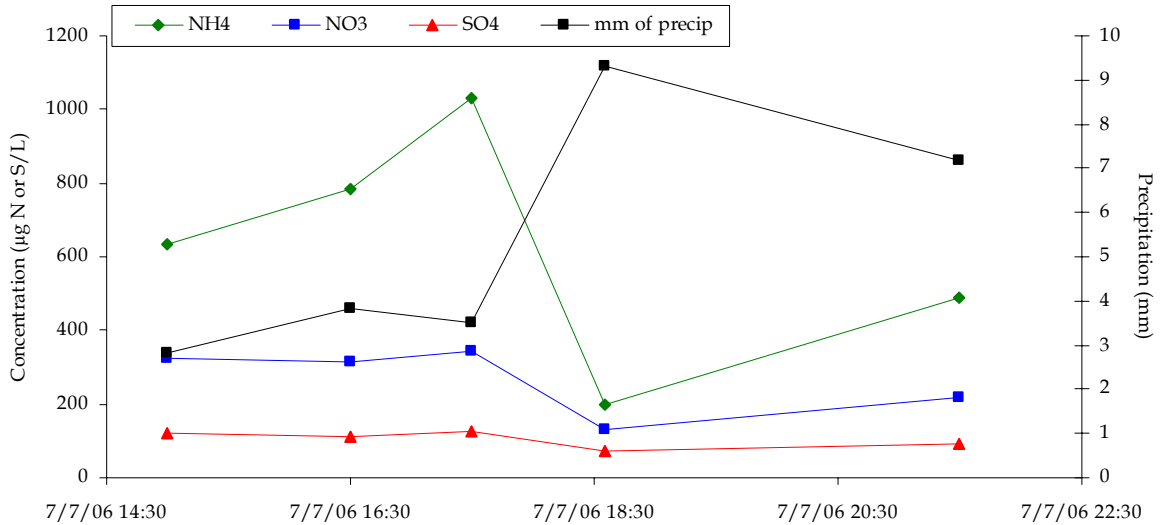


Figure 3.5 Timeline of concentrations from 7/7 13:00 to 7/8 08:25 from sub event sampler at the Core Site.

The cumulative deposition timelines for this event (Figure 3.6) reveal a steady climb in the deposition of nitrate, ammonium, and sulfate. Wet deposition of N from ammonium was more than double wet N deposition in the form of nitrate during this event. A comparison of precipitation amount and wet deposition solute fluxes for this event between the sub-event sampler and the automated precipitation collector reveals a discrepancy. In contrast to the April 23-25 event, both precipitation amount and solute deposition were substantially higher in this case for the sub-event sampler. Approximately 27 mm of rainfall was measured by the sub-event sampler during the period ending at approximately 08:30 on July 8. This contrasts with approximately 16 mm of rainfall measured over the same period with the wet-

only automated precipitation sampler. A check of an independent rain gauge at the site, as observed by a meteorological measurement station, reveals precipitation for this period of approximately 23 mm, consistent with the value measured using the sub-event sampler. The low bias in precipitation collected for this event by the automated precipitation collector suggests a malfunction in instrument operation or some event-specific bias in precipitation collection efficiency.

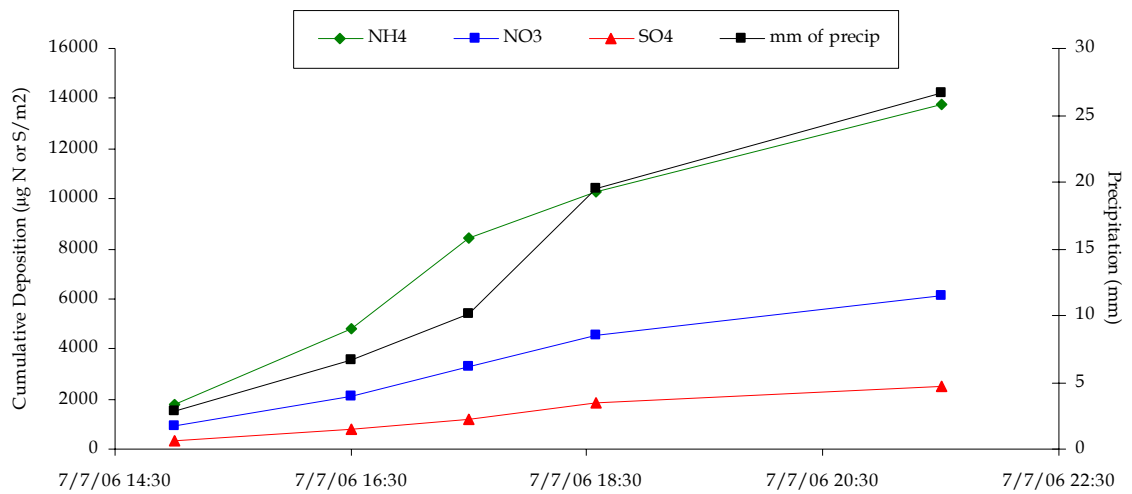


Figure 3.6 Cumulative deposition throughout the event beginning 7/7 13:00 and ending 7/8 8:25 from sub event sampler at the Core Site.

A comparison of precipitation amounts and deposition fluxes between these samplers was made to check the accuracy of measurements from the automated event precipitation collector and the manually operated sub-event sampling system across the RoMANS study. As illustrated in Figure 3.7, deposited amounts of nitrate, sulfate, and ammonium generally show reasonable agreement between the two sampling approaches. Figure 3.8 reveals a similar relationship for sampled precipitation amounts. A tendency of the sub-event sampler to sometimes underestimate deposition fluxes is expected, since it is manually deployed and relies on site operators watching for the onset of precipitation to deploy it. Clearly, though,

the strong negative bias in precipitation amount and solute deposition recorded by the automated collector on July 7-8 was an outlier. Timelines of sub-event precipitation chemistry and deposition for other summer episodes measured at the Core Site are included in Appendix C.

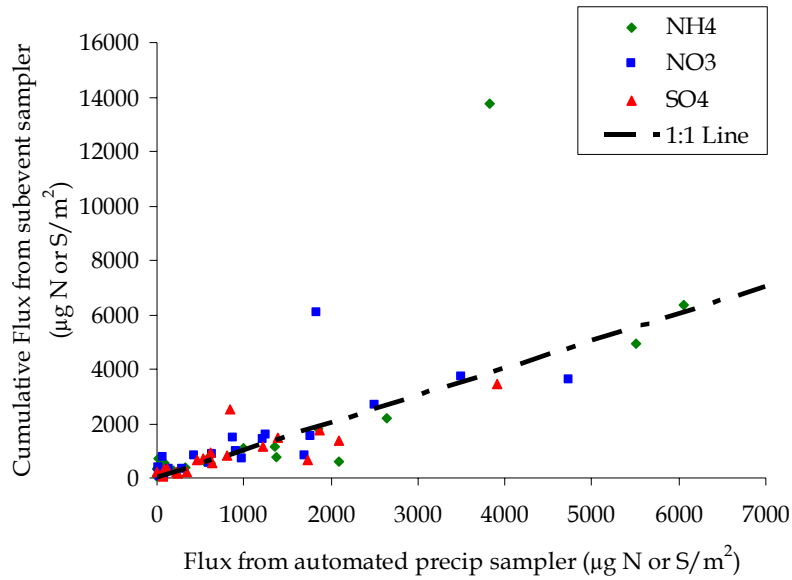


Figure 3.7 Comparison of deposited amounts of ammonium, nitrate, and sulfate measured using the subevent and automated event precipitation collectors at the RoMANS Core Site. A 1:1 line is shown for comparison. The 3 high outlier points correspond to the July 7th precipitation episode described above.

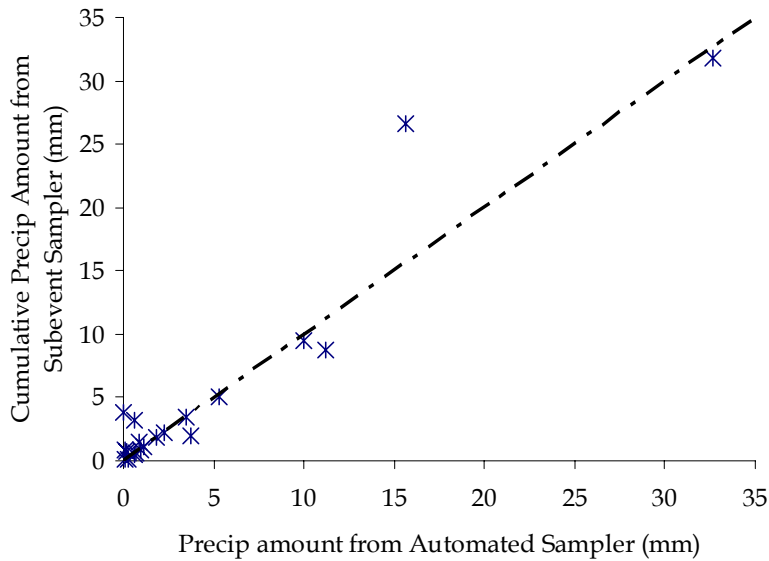


Figure 3.8 Comparison of precipitation amounts measured using the subevent and automated event precipitation collectors at the RoMANS Core Site. A 1:1 line is shown for comparison. The outlier point in the upper middle part of the figure corresponds to the July 7th episode discussed above.

3.3 *Secondary Sites*

Figure 3.9 presents the timelines of precipitation solute concentrations at Lyons during both campaigns. There were only four precipitation days during the spring, all with similar concentrations and amounts of precipitation. In the summer there were several more days with measurable precipitation. Concentrations on 8/03 were the highest for either sampling period. A large flux (Figure 3.10) was also observed on this day, even though the amount of precipitation was small. Daily spring fluxes were generally smaller than those in the summer at Lyons. Ammonium concentrations and wet deposition fluxes were always greater than nitrate or organic nitrogen at this site.

Measured precipitation solute concentrations at Gore Pass for both the spring and summer are presented in Figure 3.11. Wet deposition by day for Gore Pass is presented in Figure 3.12. Numerous precipitation days were observed at Gore Pass during both the spring and summer campaigns. Fluxes of organic nitrogen were higher than ammonium and nitrate wet deposition fluxes for the majority of the events at Gore Pass during the summer, compared to the spring when there were several events where organic nitrogen concentrations were below detection.

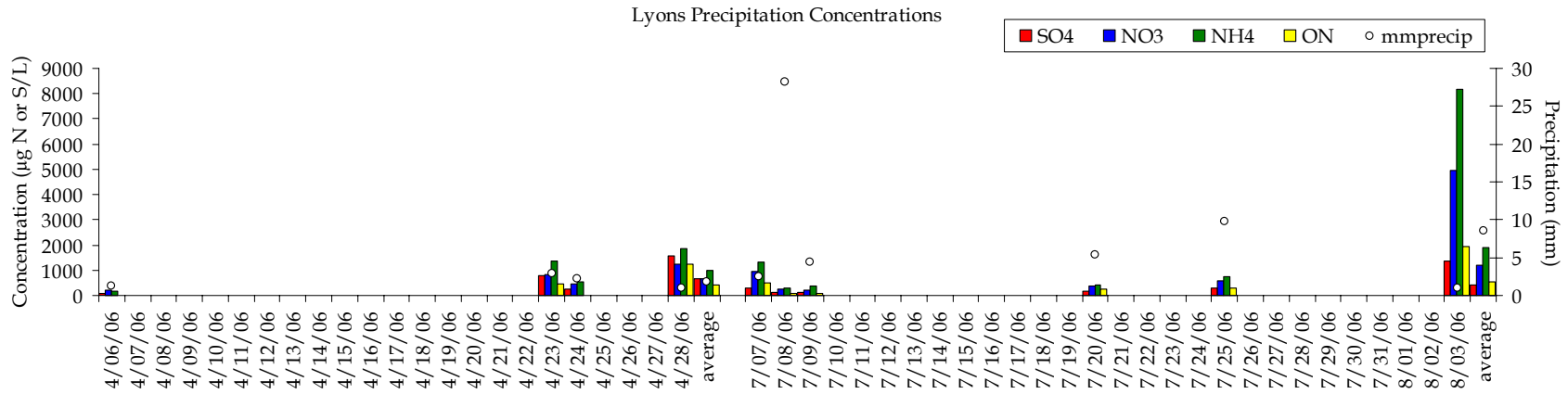


Figure 3.9 Timelines of precipitation concentrations of sulfate (red), nitrate (blue), ammonium (green), and organic nitrogen (yellow) at Lyon for both the spring and summer studies shown with amount of precipitation received. Campaign averages are also shown.

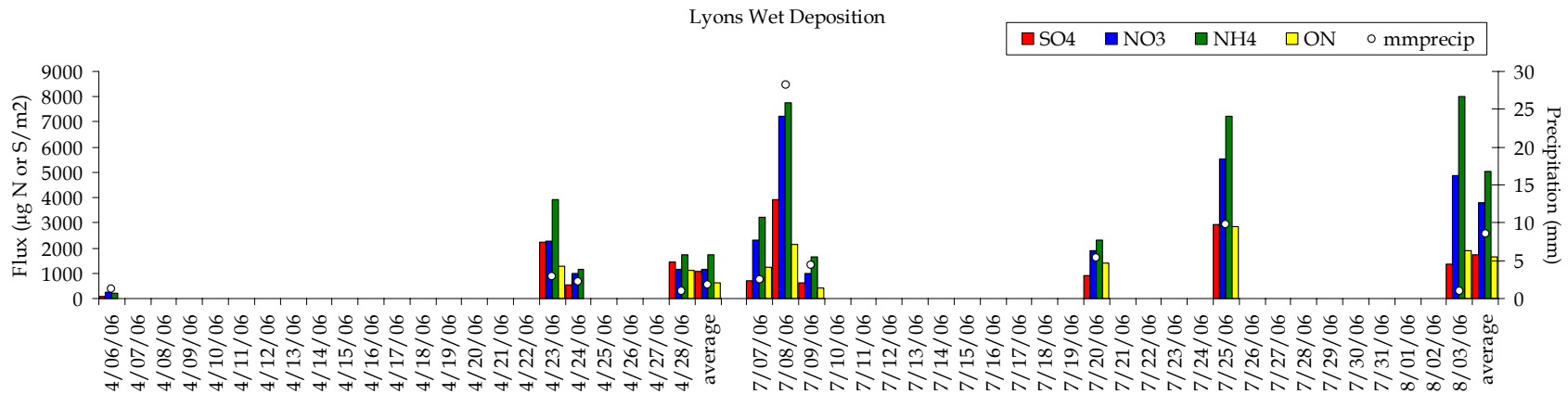


Figure 3.10 Timelines of sulfate (red), nitrate (blue), ammonium (green), and organic nitrogen (yellow) wet-deposited by precipitation at Lyons for both the spring and summer study periods. Campaign averages are also shown.

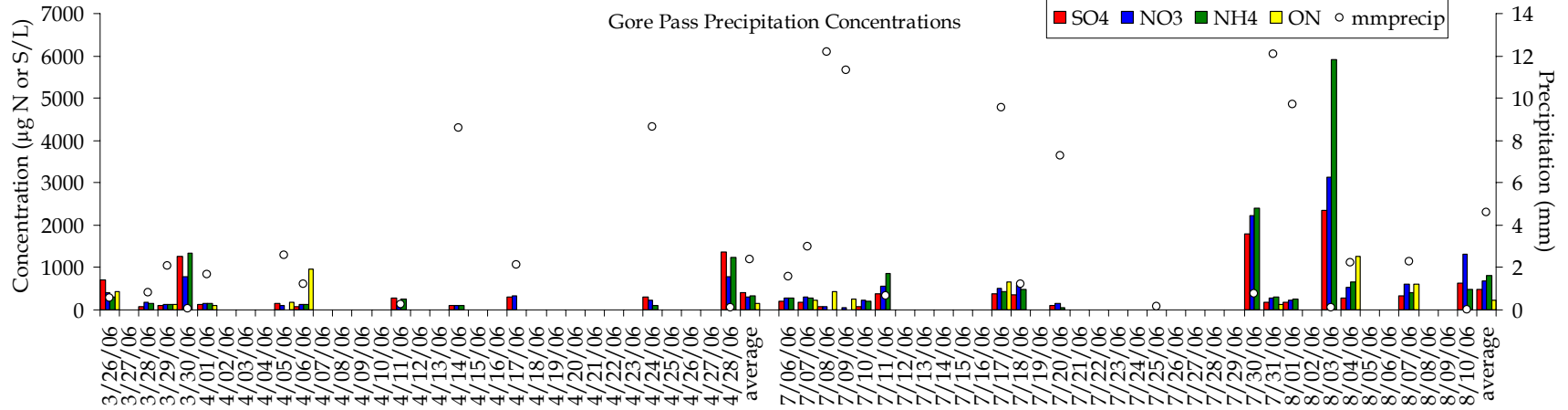


Figure 3.11 Timelines of precipitation concentrations of sulfate (red), nitrate (blue), ammonium (green), and organic nitrogen (yellow) at Gore Pass for both the spring and summer studies shown with amount of precipitation received. Campaign averages are also shown.

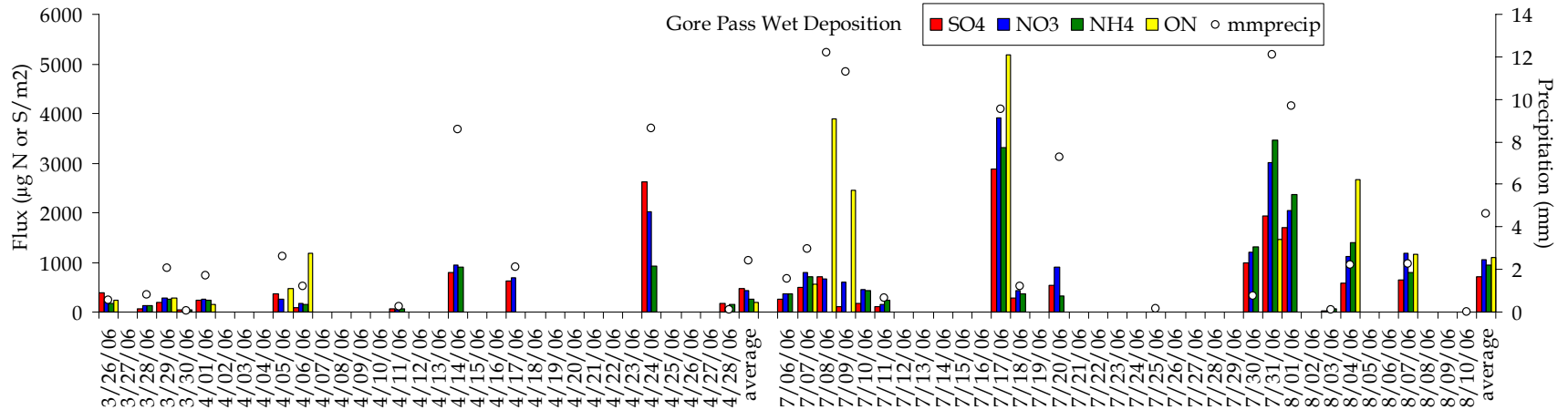


Figure 3.12 Timelines of sulfate (red), nitrate (blue), ammonium (green), and organic nitrogen (yellow) wet-deposited by precipitation at Gore Pass for both the spring and summer study periods. Campaign averages are also shown.

3.4 *Satellite Sites*

Timelines of precipitation solute concentrations and wet deposition fluxes for each of the satellite sites are presented below. Only species important to nitrogen and sulfur deposition are plotted: ammonium, nitrate, and sulfate. Organic nitrogen was not measured at the satellite sites.

Concentrations of ammonium, nitrate, and sulfate at Beaver Meadows were generally low throughout both campaigns with only two events (one in each campaign) having concentrations that were much larger than all others (Figure 3.13). In the spring the majority of N and S was deposited during one large event on 4/23/06 while wet deposition was spread out more in the summer (Figure 3.14). The sample from 7/17 was contaminated and is not included here or in the analysis of total deposition.

There were more days with precipitation at Hidden Valley than at most of the other sites. Spring concentrations (Figure 3.15) were generally lower than those in the summer, and nitrate concentrations were larger than ammonium for both sampling periods. The 4/23/06 event dominates the deposition of all species during the spring. In the summer, deposition fluxes were well-distributed between events, with similar fluxes per event (Figure 3.16). In addition, the average flux for ammonium, nitrate, and sulfate was smaller in the summer than in the spring. As mentioned above, assumed precipitation interactions with the forest canopy at this site limit the usefulness of this set of observations.

At Loch Vale, concentrations in the spring were much lower than those in the later part of the summer campaign (Figure 3.17). There were many more events in the summer which contributed to a higher total flux even though the spring event average fluxes for nitrate and sulfate were larger (Figure 3.18). In the spring, nitrate contributed more than ammonium to nitrogen deposition, while in the summer the largest contributor to N deposition changed with event. The sample from 7/26 was contaminated and is not included here or in the analysis of total deposition.

In the spring, precipitation sulfate concentrations at Sprague Lake were the highest of the three key species, while concentrations of nitrate were larger in the summer (Figure 3.19). Concentrations of sulfate in precipitation at Sprague Lake were fairly consistent between the spring and summer. Concentrations of ammonium and nitrate appear to increase from spring to summer. The greatest wet deposition flux for the entire sampling period of all key species occurred on 4/23/06 (Figure 3.20).

Figure 3.21 presents the timelines of concentrations of sulfate, nitrate, and ammonium measured at Timber Creek in precipitation during the spring and summer campaigns. The corresponding timelines of wet deposition fluxes of the same species are presented in Figure 3.22. Fluxes were higher in the summer than in spring with the exception of the 4/23/06 event. Concentrations of sulfate were higher than either nitrate or ammonium in precipitation composition in the spring, with nitrate concentrations generally highest in the summer.

There was only one precipitation event measured at Brush during the spring campaign. A second sample was compromised by strong winds that blew the buckets over. The concentrations of ammonium, nitrate, and sulfate are shown in Figure 3.23 while the fluxes are shown in Figure 3.24. Precipitation was not collected during the summer at the Brush site.

Concentrations of ammonium, nitrate, and sulfate in precipitation collected at Dinosaur are presented in Figure 3.25. Nitrate was the highest nitrogen species measured for all except two events. Sulfate dominated deposition for several events at Dinosaur (Figure 3.26).

At the Grant, Nebraska site precipitation concentrations of ammonium were generally largest; only the event on 4/26/06 had a larger sulfate flux (Figure 3.27). There were six days with precipitation at this site during the spring (this site was not operated during summer) but only two events, 4/14/06 and 4/22/06, contributed significantly to wet deposition fluxes of the major species (Figure 3.28). The sample from 4/26 was contaminated and is not included here or in the analysis of total deposition.

Springfield only received enough precipitation to analyze during the last two days of the spring campaign. Concentrations of nitrate and sulfate were lower by more than 50% on the second day (4/28/06) while the concentration of ammonium did not decrease as much (Figure 3.29). The fluxes of sulfate, nitrate, and ammonium were

similar on the first day, while the flux of ammonium was much higher than sulfate or nitrate fluxes on the second day of the event (Figure 3.30).

Samples were only collected in the summer at the Alpine Visitors Center site, which is inaccessible during much of the year. The same is true for other high altitude RMNP sites, including Lake Irene, Rock Cut and Rainbow Curve.

Figure 3.31 shows the timeline of samples collected at Alpine Visitor Center and the concentrations of sulfate, nitrate, and ammonium for each sample. Fluxes of the same species from each event are shown in Figure 3.32. Concentrations of nitrate were greater than ammonium for all events while nitrate and sulfate dominance varied by date. The largest flux for all three species occurred on 7/12/06, despite the fact that total precipitation on this date was only a few mm.

At Lake Irene, concentrations of nitrate were greater than sulfate and ammonium for most samples (Figure 3.33). Concentrations were much higher in the sample collected on 7/24/06. Fluxes on 7/24/06, however, were the lowest for all days with measurable precipitation (Figure 3.34) due to the small amount of precipitation on this date. The highest fluxes of the major N and S species were measured a week later during a 7/31/06 event which featured much more precipitation.

The timelines of concentrations of precipitation ammonium, nitrate, and sulfate at Rainbow Curve are presented in Figure 3.35. Concentrations were highest on 7/17/06

and 7/18/06 while all other samples contained much lower concentrations of these three species. No individual species concentration was consistently higher than any other; the species contributing the most to deposition changed with the sample. Wet deposition fluxes for Rainbow Curve are presented in Figure 3.36. The amount of day-to-day precipitation received at Rainbow Curve during the summer was quite variable, causing the amount of N and S deposited during each event to vary. Even though concentrations were greatest on 7/17/06 and 7/18/06, the wet deposition flux on 7/18/06 was one of the smallest due to low rainfall. Deposition was high on 7/08/06 for sulfate and on 7/19/06 for nitrate and ammonium. The sample from 8/1 was not analyzed and is not included in the analysis presented here.

Precipitation major ion concentrations at Rock Cut were greatest on 7/17/06 (Figure 3.37), similar to observations from the nearby Rainbow Curve site. Wet deposition was greatest on 7/31/06 (Figure 3.38) for the three key species, similar to the high wet deposition fluxes observed on this date at other RMNP satellite sites including Timber Creek, Lake Irene, Alpine Visitor Center, and Rainbow Curve. Wet deposition fluxes were fairly consistent across summer precipitation days at this site, with only a few days receiving less than 1000 $\mu\text{g N or S/m}^2/\text{species}$.

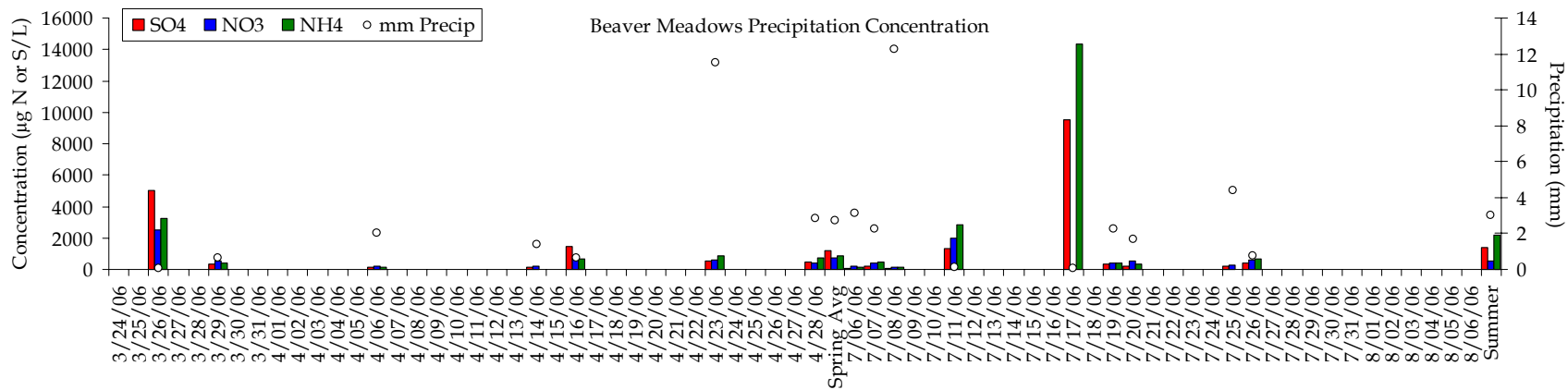


Figure 3.13 Timelines of precipitation concentrations of sulfate (red), nitrate (blue), and ammonium (green) at Beaver Meadows for both the spring and summer studies. The amount of precipitation (mm) received and the campaign averages are also shown.

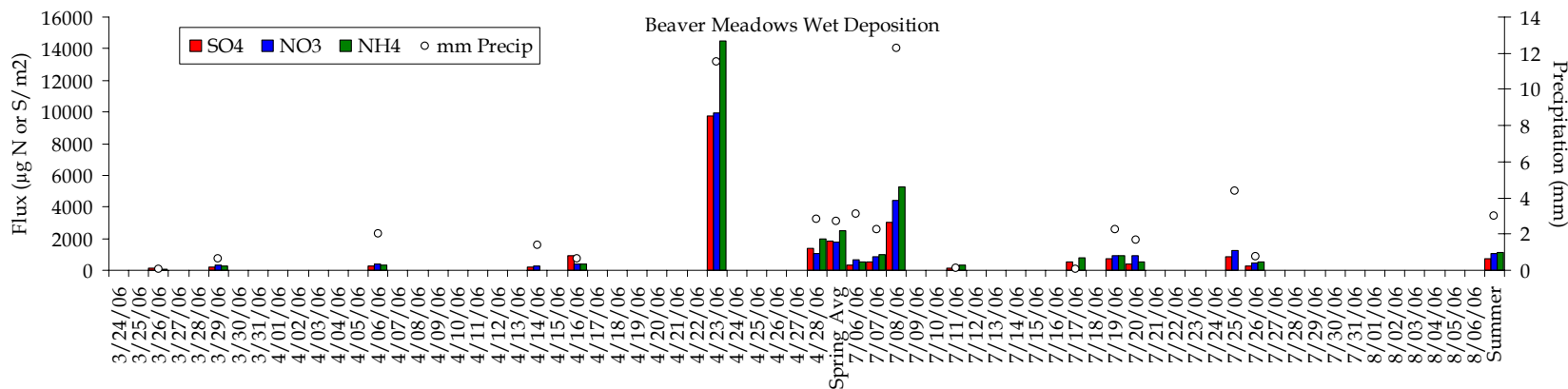


Figure 3.14 Timelines of sulfate (red), nitrate (blue), and ammonium (green) wet-deposited by precipitation at Beaver Meadows for both the spring and summer study periods. The amount of precipitation (mm) received and the campaign averages are also shown.

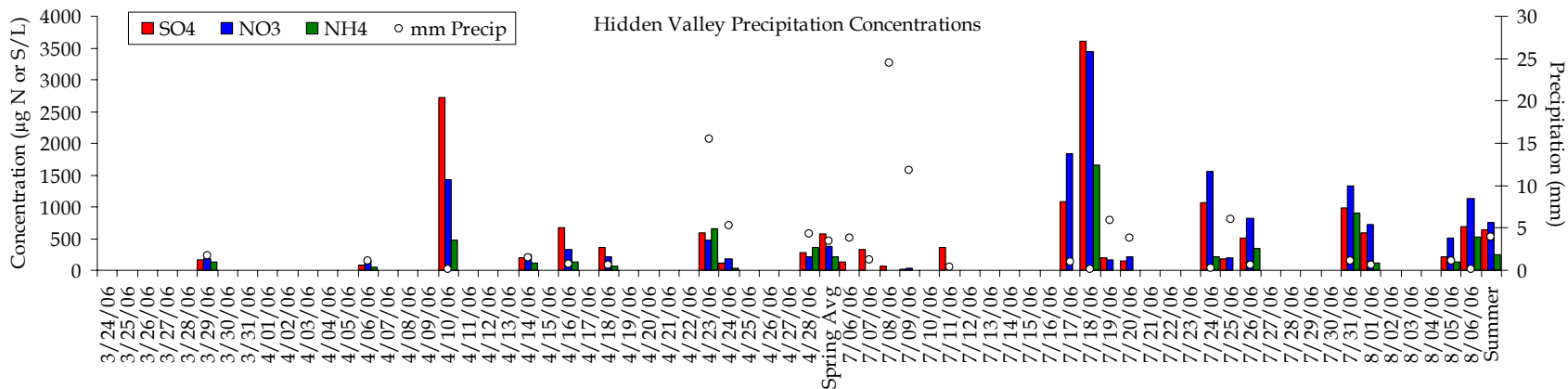


Figure 3.15 Timelines of precipitation concentrations of sulfate (red), nitrate (blue), and ammonium (green) Hidden Valley for both the spring and summer studies. The amount of precipitation (mm) received and the campaign averages are also shown.

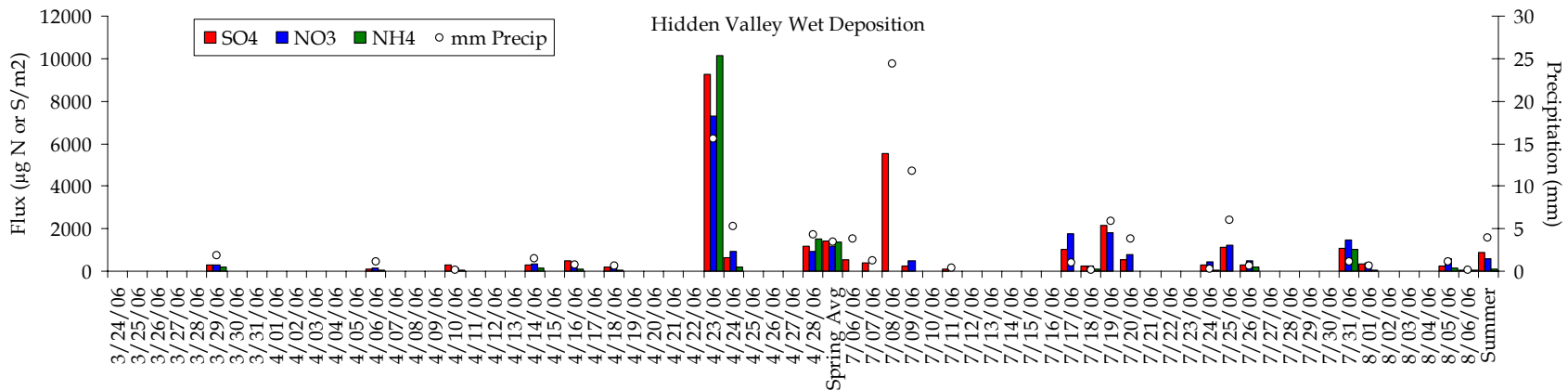


Figure 3.16. Timelines of sulfate (red), nitrate (blue), and ammonium (green) wet-deposited by precipitation at Hidden Valley during both the spring and summer study periods. The amount of precipitation (mm) received and the campaign averages are also shown.

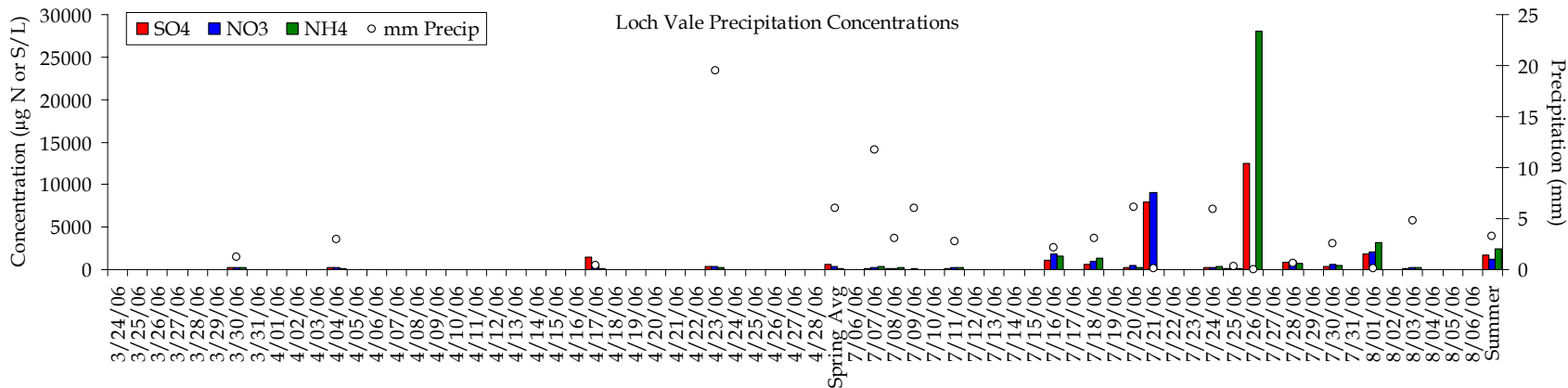


Figure 3.17 Timelines of precipitation concentrations of sulfate (red), nitrate (blue), and ammonium (green) at Loch Vale for both the spring and summer studies. The amount of precipitation (mm) received and the campaign averages are also shown.

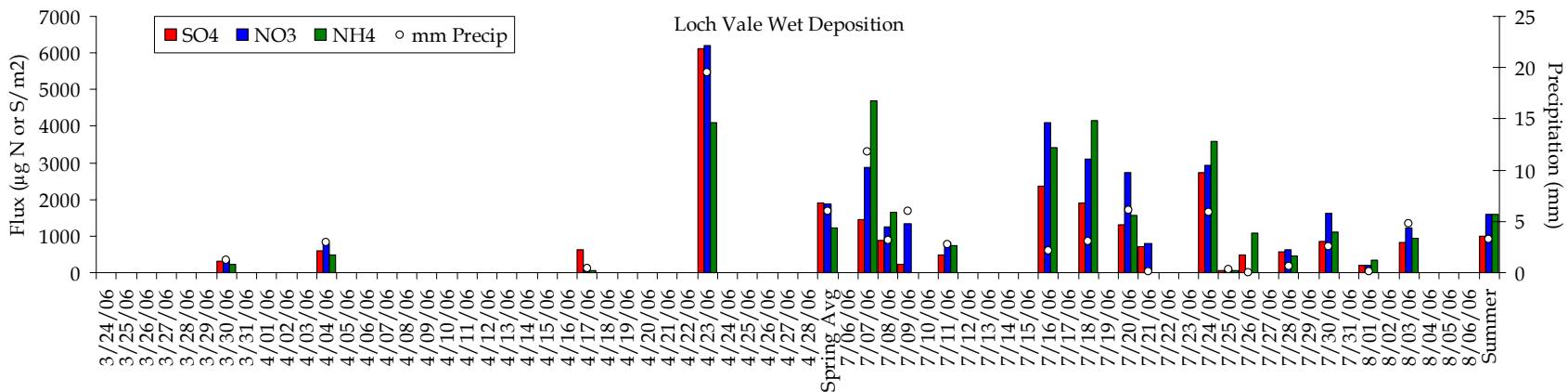


Figure 3.18 Timelines of sulfate (red), nitrate (blue), and ammonium (green) wet-deposited by precipitation at Loch Vale during both the spring and summer study periods. The amount of precipitation (mm) received and the campaign averages are also shown.

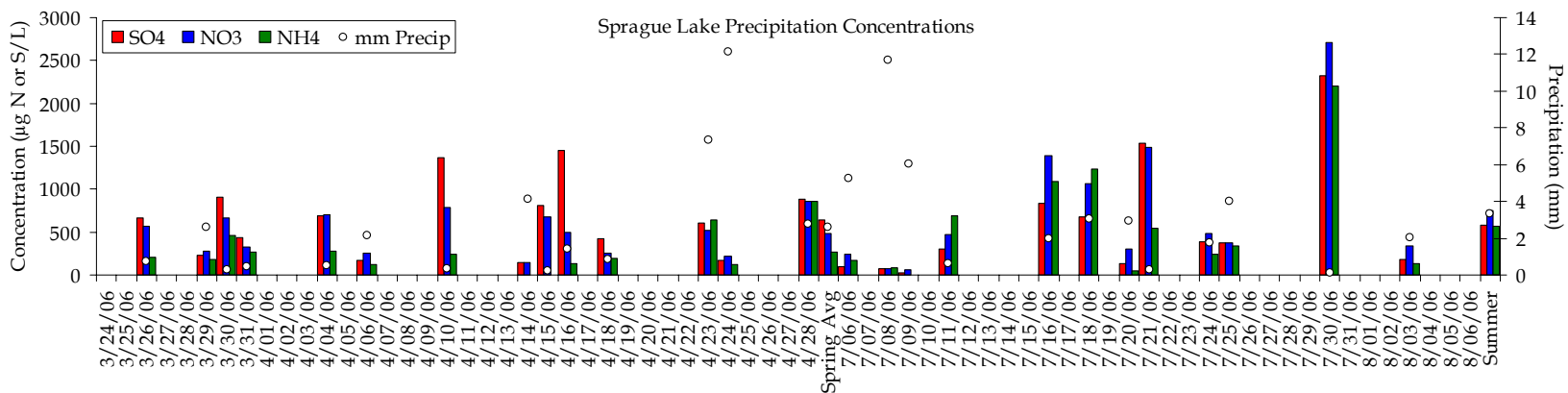


Figure 3.19 Timelines of precipitation concentrations of sulfate (red), nitrate (blue), and ammonium (green) at Sprague Lake for both the spring and summer studies. The amount of precipitation (mm) received and the campaign averages are also shown.

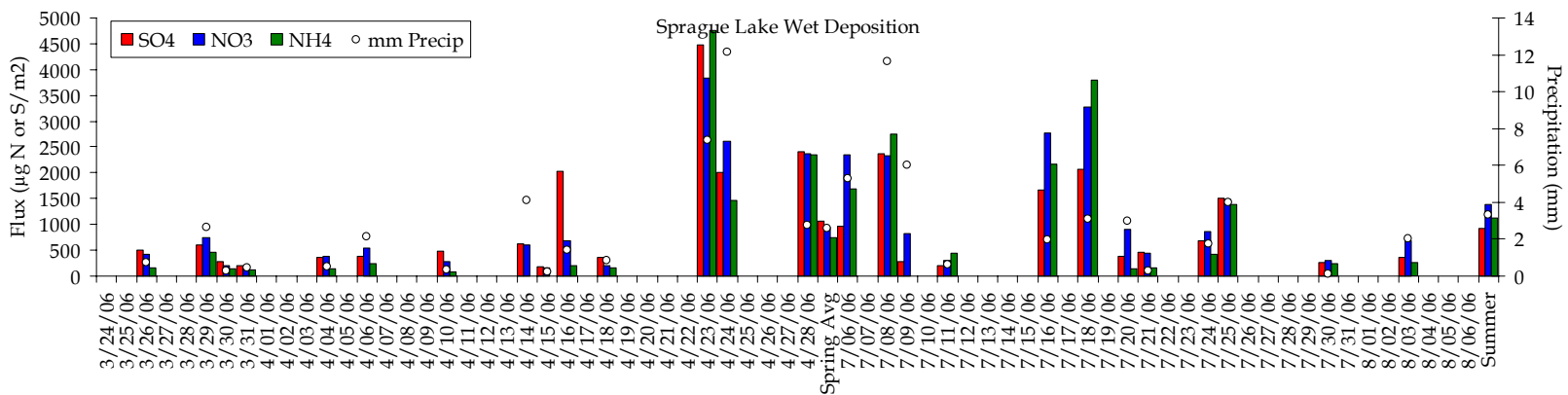


Figure 3.20 Timelines of sulfate (red), nitrate (blue), and ammonium (green) wet-deposited by precipitation at Sprague Lake during both the spring and summer study periods. The amount of precipitation (mm) received and the campaign averages are also shown.

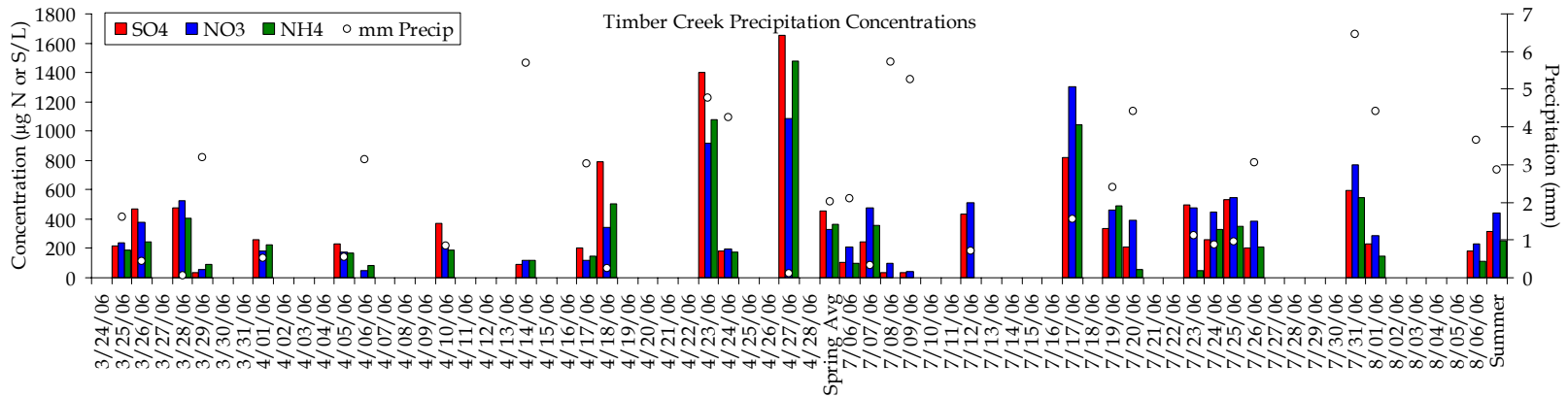


Figure 3.21 Timelines of precipitation concentrations of sulfate (red), nitrate (blue), and ammonium (green) at Timber Creek for both the spring and summer studies. The amount of precipitation (mm) received and the campaign averages are also shown.

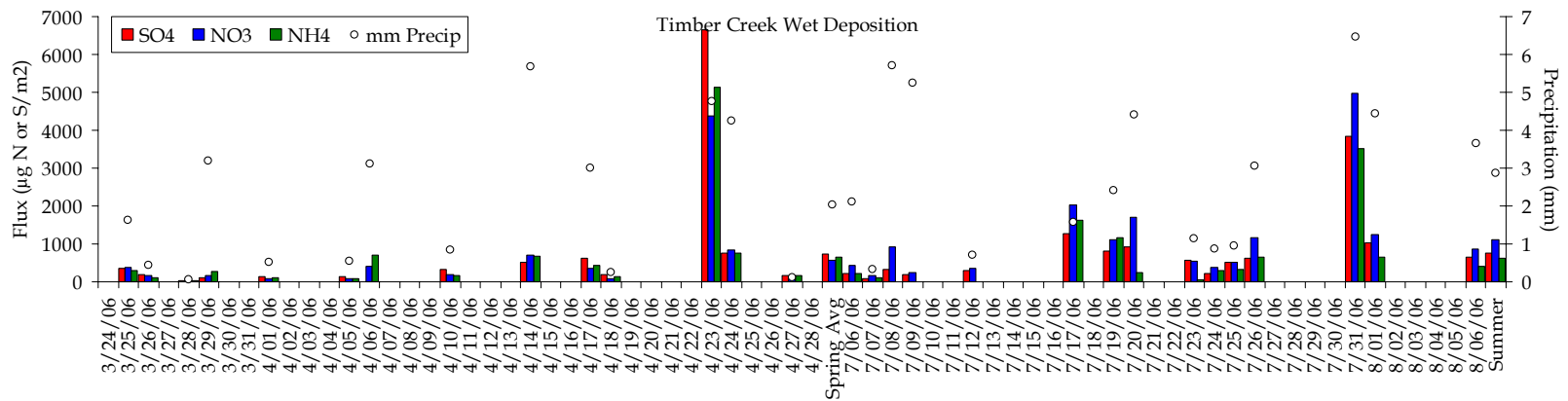


Figure 3.22 Timelines of sulfate (red), nitrate (blue), and ammonium (green) wet-deposited by precipitation at Timber Creek during both the spring and summer study periods. The amount of precipitation (mm) received and the campaign averages are also shown.

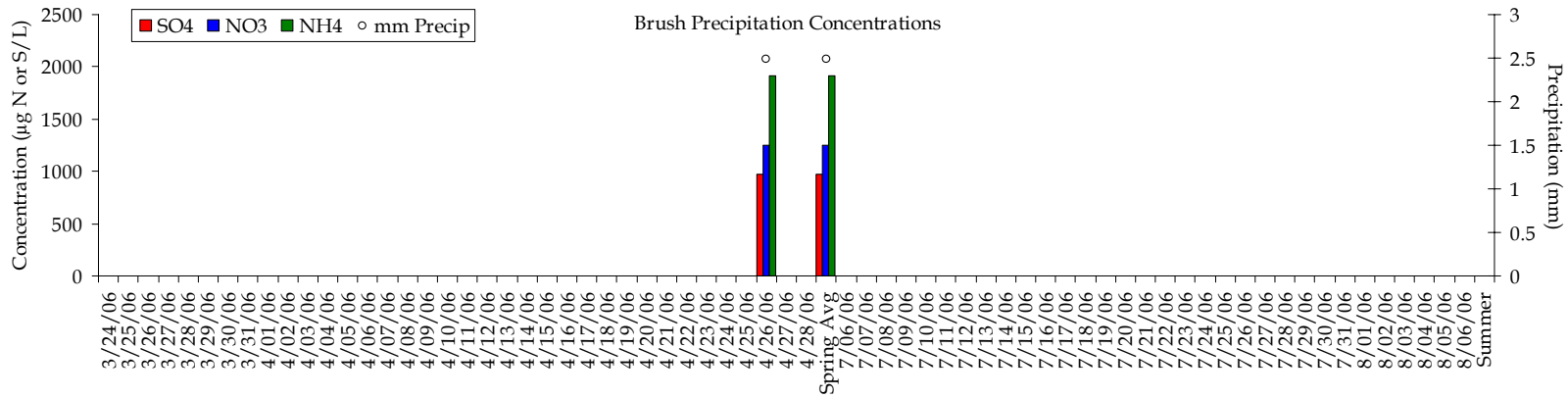


Figure 3.23 Timelines of precipitation concentrations of sulfate (red), nitrate (blue), and ammonium (green) at Brush for the spring study. The amount of precipitation (mm) received and the campaign averages are also shown. Site was not operated during the summer study.

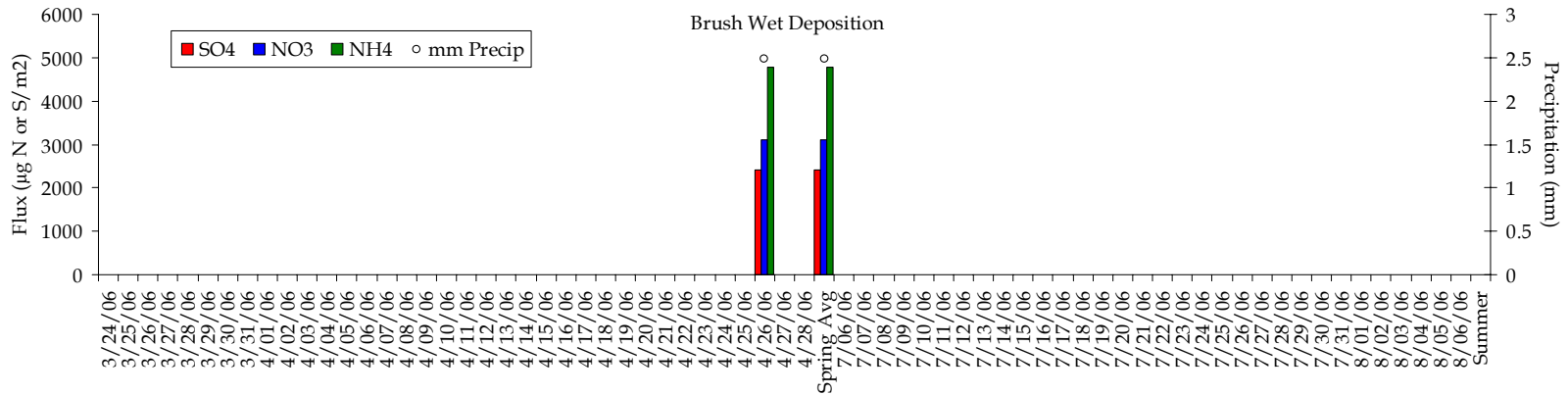


Figure 3.24 Timelines of sulfate (red), nitrate (blue), and ammonium (green) wet-deposited by precipitation at Brush for the spring study period. The amount of precipitation (mm) received and the campaign averages are also shown. Site was not operated during the summer study period.

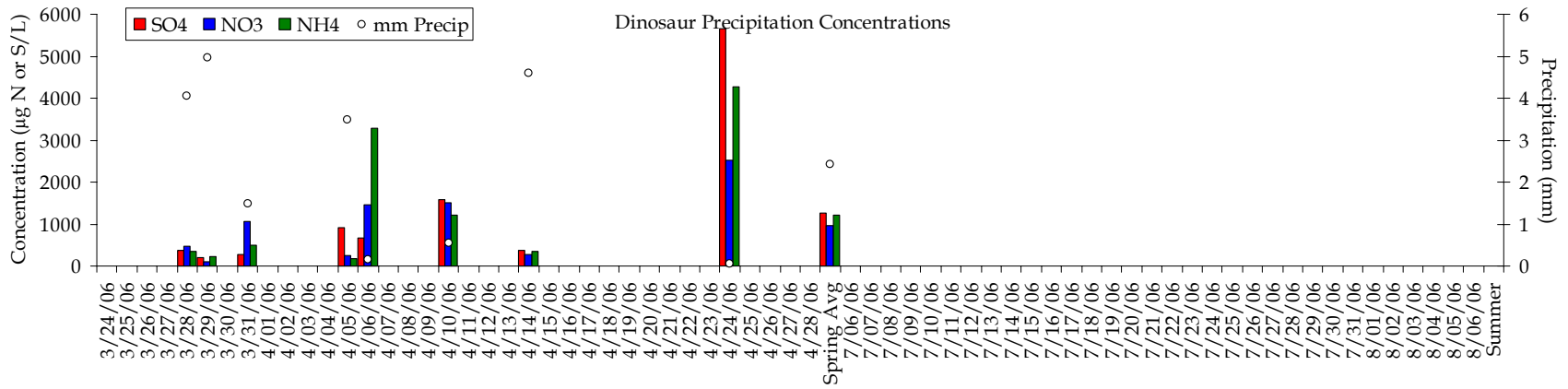


Figure 3.25 Timelines of precipitation concentrations of sulfate (red), nitrate (blue), and ammonium (green) at Dinosaur for the spring study. The amount of precipitation (mm) received and the campaign averages are also shown. Site was not operated during the summer study.

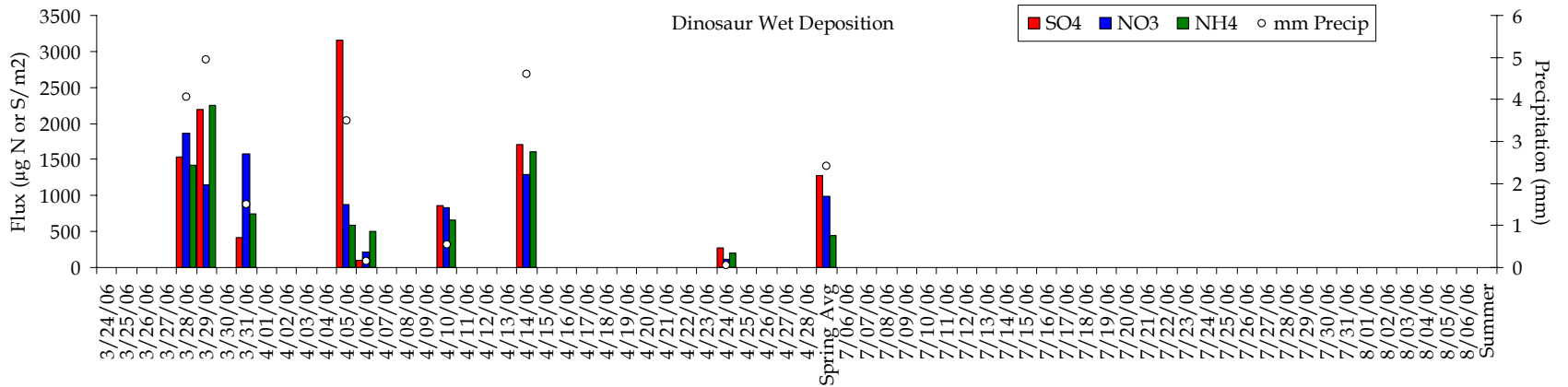


Figure 3.26 Timelines of sulfate (red), nitrate (blue), and ammonium (green) wet-deposited by precipitation at Dinosaur during the spring study period. The amount of precipitation (mm) received and the campaign averages are also shown. Site was not operated during the summer study period.

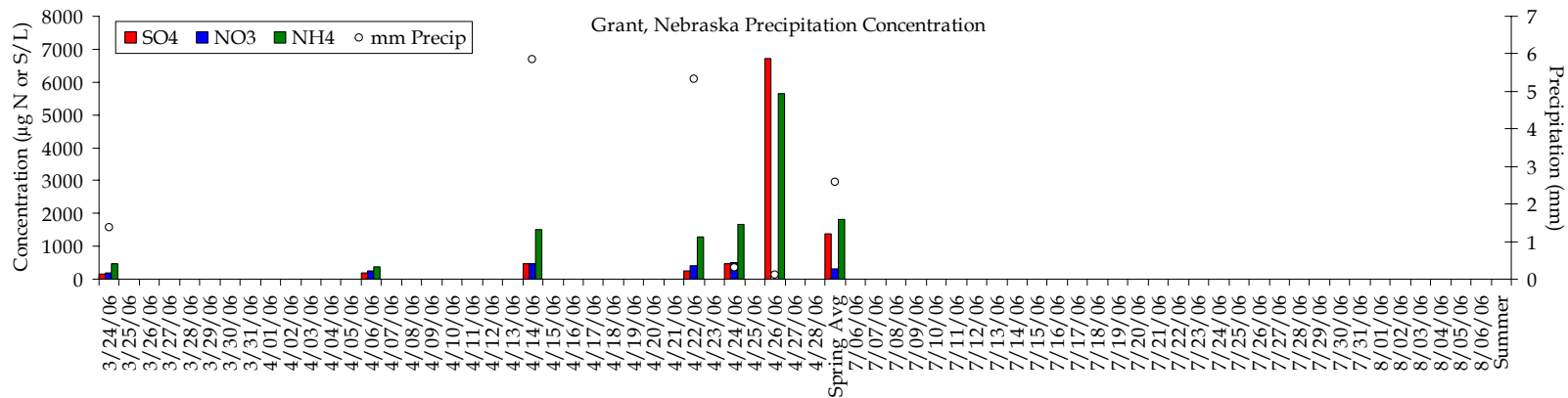


Figure 3.27 Timelines of precipitation concentrations of sulfate (red), nitrate (blue), and ammonium (green) at Grant, Nebraska during the spring study. The amount of precipitation (mm) received and the campaign averages are also shown. Site was not operated during the summer study.

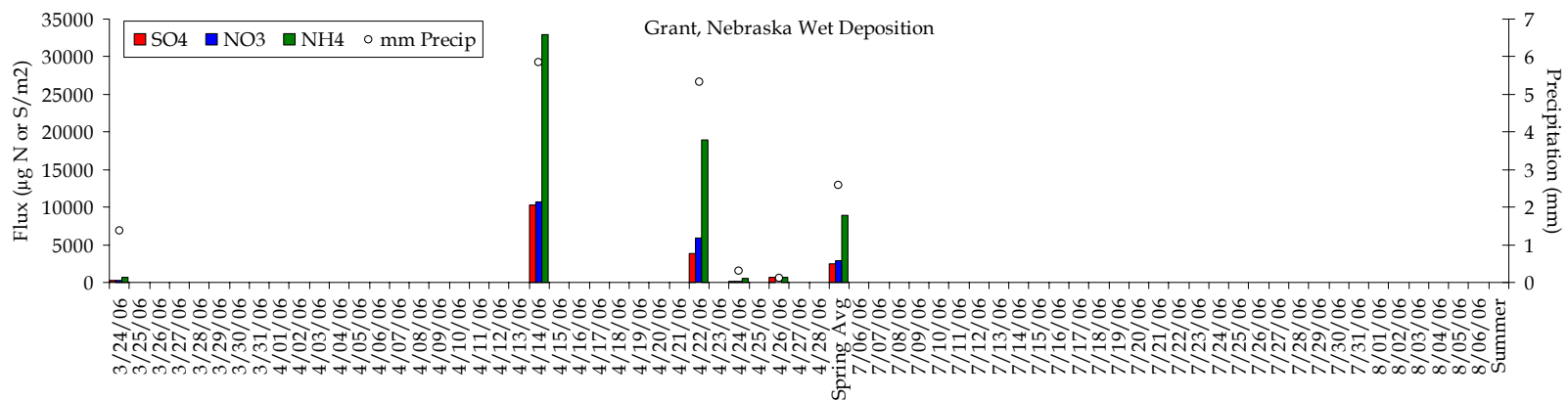


Figure 3.28 Timelines of sulfate (red), nitrate (blue), and ammonium (green) wet-deposited by precipitation at the Grant, Nebraska site during the spring study period. The amount of precipitation (mm) received and the campaign averages are also shown. Site was not operated during the summer study period.

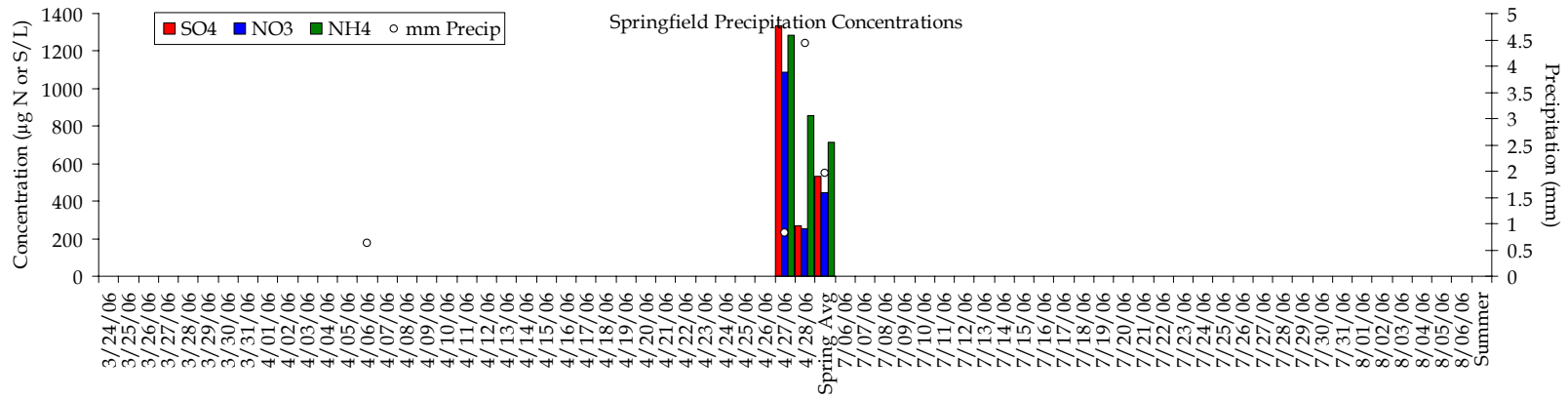


Figure 3.29 Timelines of precipitation concentrations of sulfate (red), nitrate (blue), and ammonium (green) at Springfield for the spring study. The amount of precipitation (mm) received and the campaign averages are also shown. Site was not operated during the summer study.

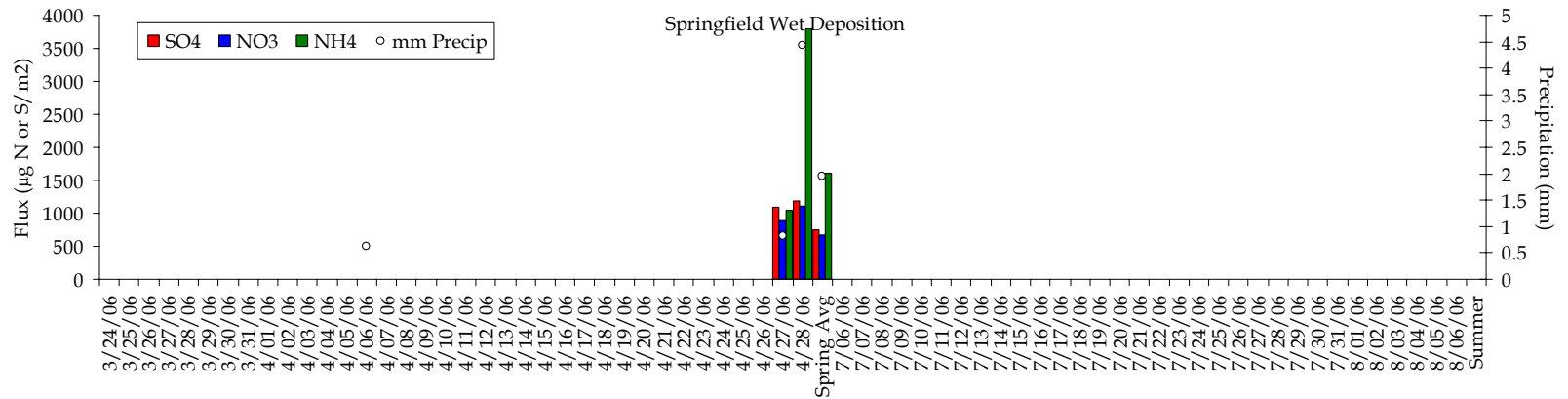


Figure 3.30 Timelines of sulfate (red), nitrate (blue), and ammonium (green) wet-deposited by precipitation Springfield during the spring study period. The amount of precipitation (mm) received and the campaign averages are also shown. Site was not operated during the summer study period.

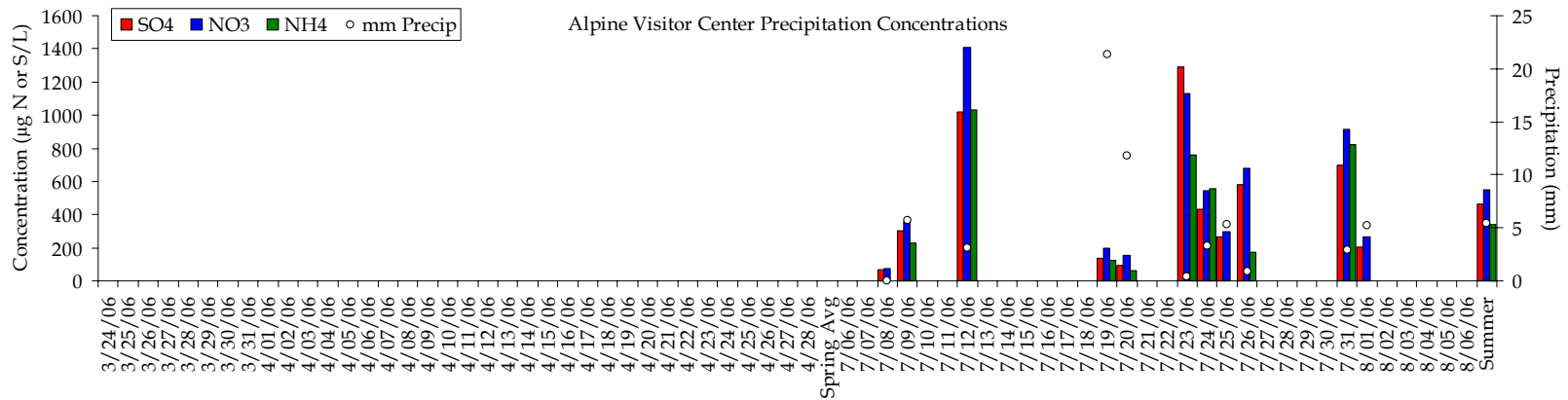


Figure 3.31 Timelines of precipitation concentrations of sulfate (red), nitrate (blue), and ammonium (green) at the Alpine Visitors Center during the summer study. The amount of precipitation (mm) received and the campaign averages are also shown. Site was not operational in the spring study.

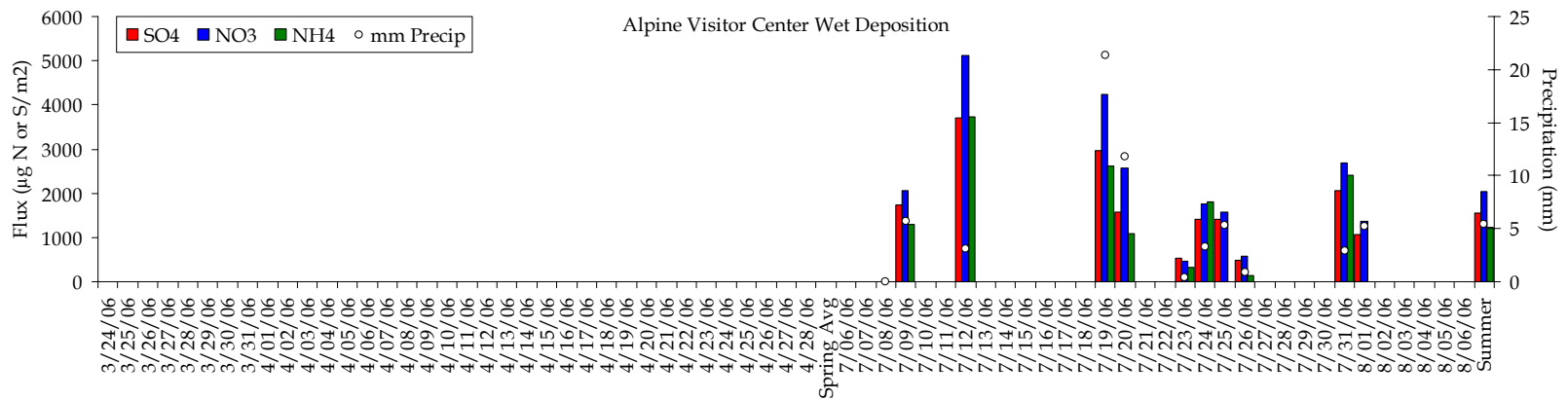


Figure 3.32 Timelines of sulfate (red), nitrate (blue), and ammonium (green) wet-deposited by precipitation at Alpine Visitors Center during the summer study period. The amount of precipitation (mm) received and the campaign averages are also shown. Site was not operational in the spring study period.

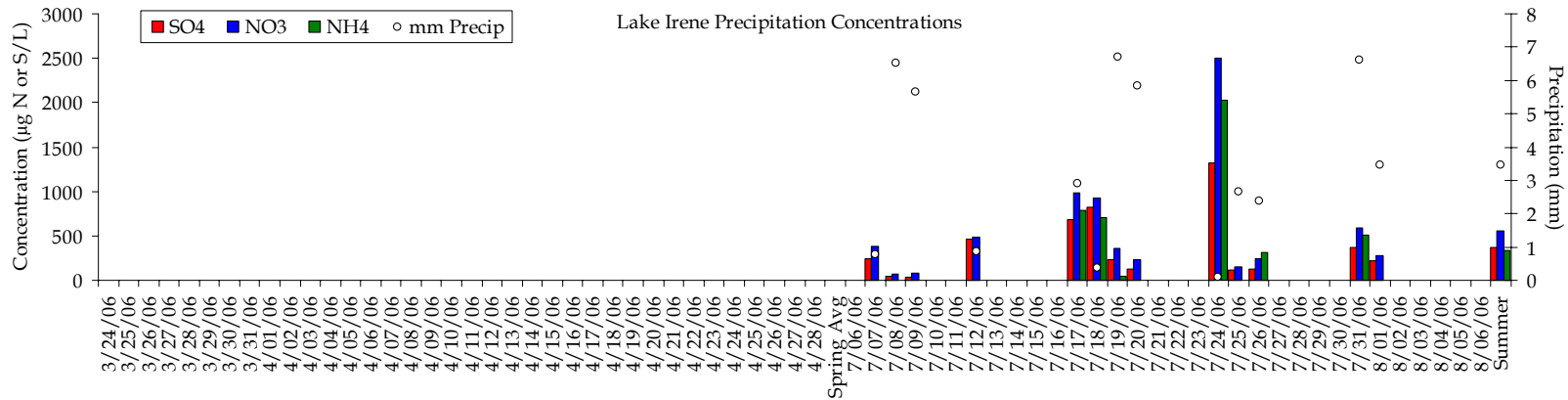


Figure 3.33 Timelines of precipitation concentrations of sulfate (red), nitrate (blue), and ammonium (green) at Lake Irene during the summer study. The amount of precipitation (mm) received and the campaign averages are also shown. Site was not operational in the spring study.

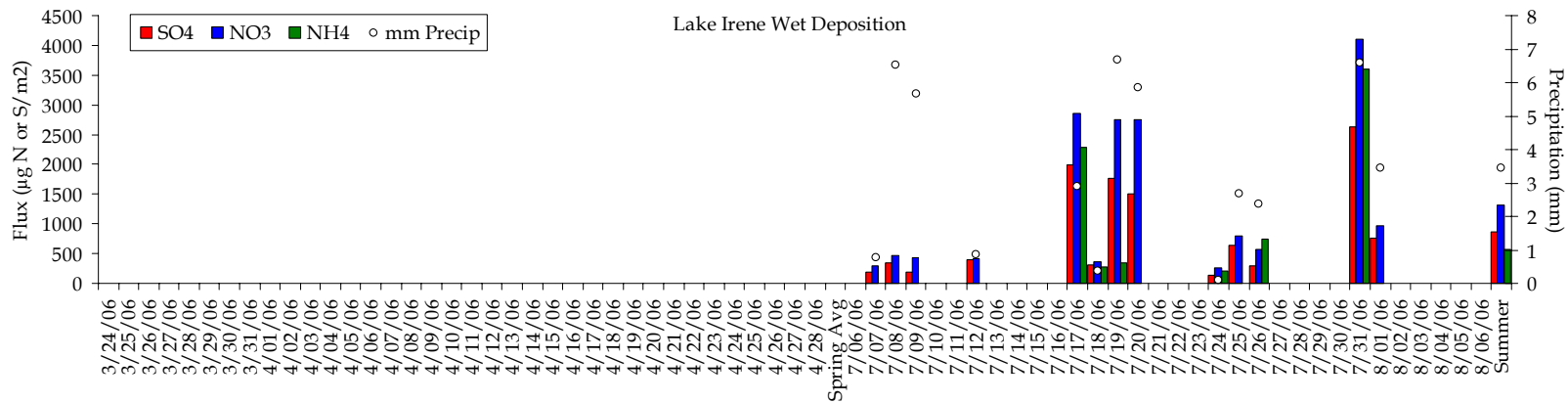


Figure 3.34 Timelines of sulfate (red), nitrate (blue), and ammonium (green) wet-deposited by precipitation at Lake Irene during the summer study period. The amount of precipitation (mm) received and the campaign averages are also shown. Site was not operational in the spring study period.

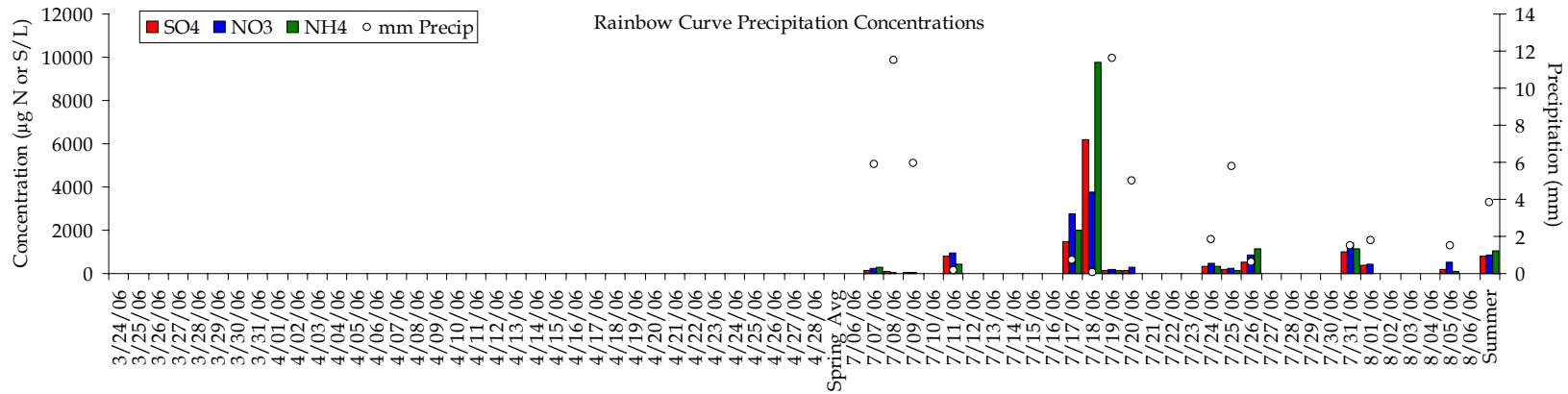


Figure 3.35 Timelines of precipitation concentrations of sulfate (red), nitrate (blue), and ammonium (green) at Rainbow Curve during the summer study. The amount of precipitation (mm) received and the campaign averages are also shown. Site was not operational in the spring study.

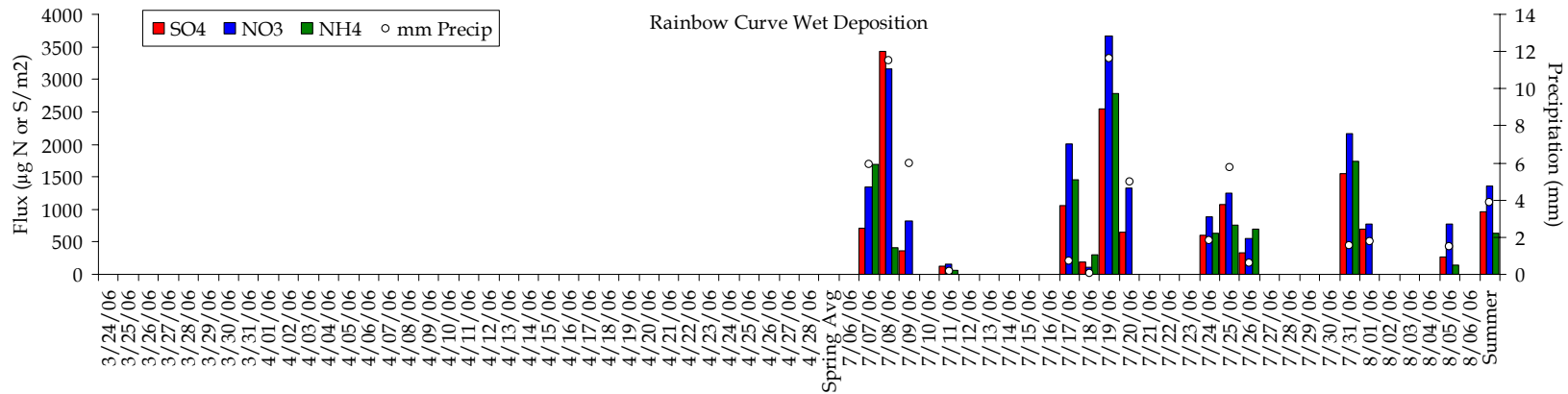


Figure 3.36 Timelines of sulfate (red), nitrate (blue), and ammonium (green) wet-deposited by precipitation at Rainbow Curve during the summer study period. The amount of precipitation (mm) received and the campaign averages are also shown. Site was not operational in the spring period.

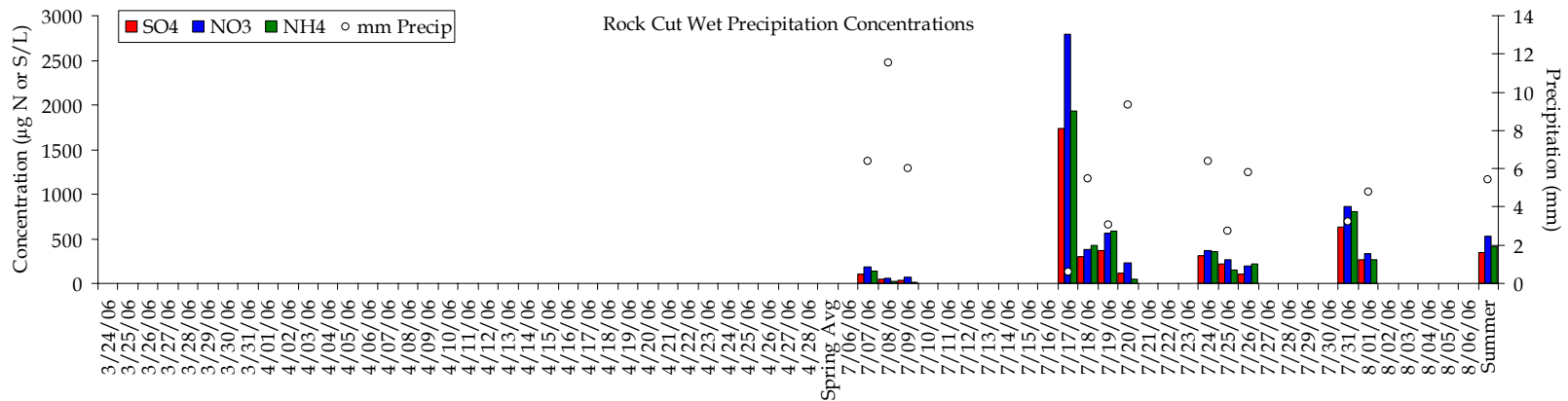


Figure 3.37 Timelines of precipitation concentrations of sulfate (red), nitrate (blue), and ammonium (green) at Rock Cut during the summer study. The amount of precipitation (mm) received and the campaign averages are also shown. Site was not operational in the spring study.

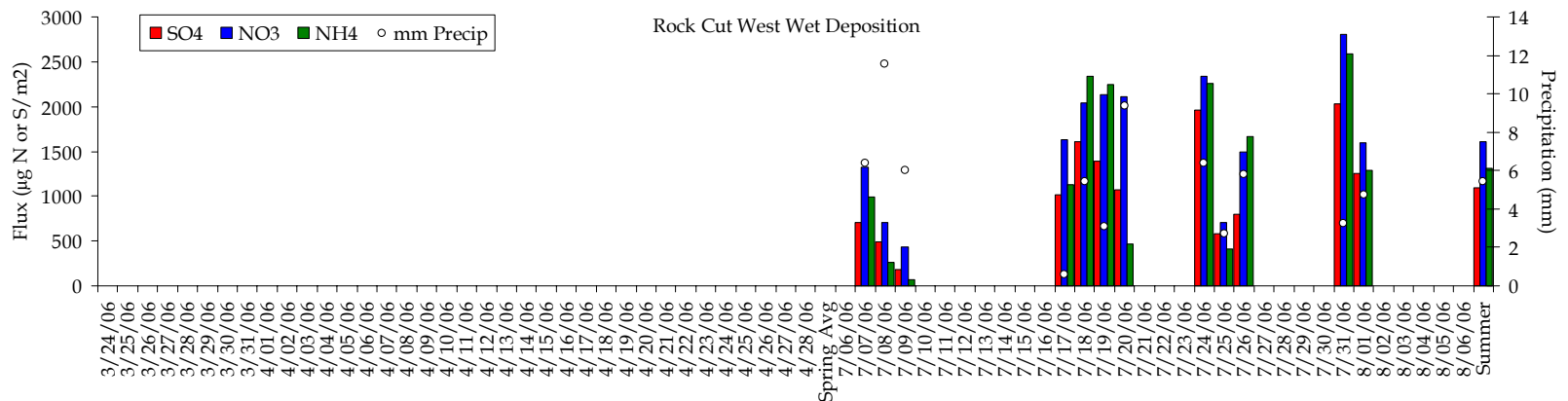


Figure 3.38 Timelines of sulfate (red), nitrate (blue), and ammonium (green) wet-deposited by precipitation at Rock Cut during the summer study period. The amount of precipitation (mm) received and the campaign averages are also shown. Site was not operational in the spring study period.

4 Wet Deposition Discussion

4.1 Precipitation Amount and Deposition Compared with Historical Data

Historically, the largest volume of precipitation is recorded and the largest fluxes of sulfate, nitrate, and ammonium are received (Figure 4.1) in May at the Beaver Meadows (BM) NADP site and in April at the Loch Vale (LV) NADP site. Table 4.1 presents the climatological averages of total precipitation for the same time periods as the RoMANS campaigns and the total precipitation measured at three key RoMANS sites. Spring precipitation received at the Beaver Meadows site during RoMANS was about 74% less than average. At Loch Vale RoMANS spring precipitation was approximately 83% less than climatology (Table 4.1). During the summer campaign, approximately 50% less precipitation than average was received at both the NADP sites. The low amounts of precipitation received in 2006 indicate the wet deposition fluxes calculated for this study may also be smaller than average.

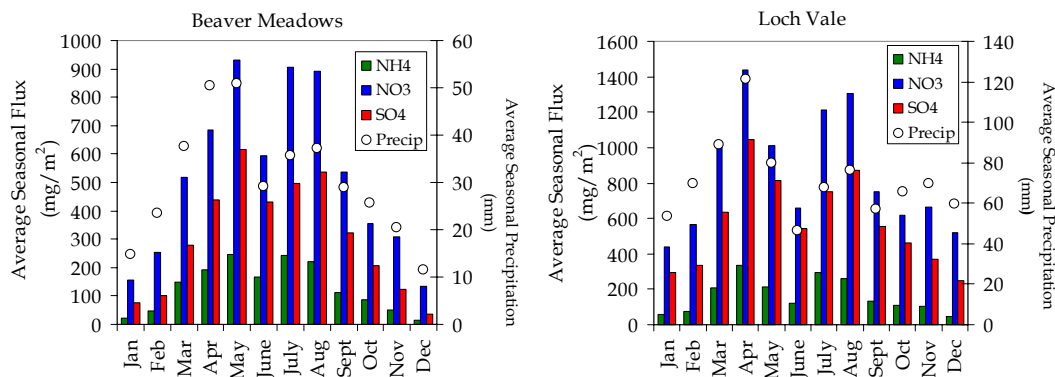


Figure 4.1. Average seasonal wet deposition fluxes and precipitation from January 1998-January 2004 for the Beaver Meadows and Loch Vale NADP sites. Provided by Bret Schichtel.

Table 4.1. Total precipitation for the RoMANS campaign compared with historical data. Historical averages were calculated with NADP data from 1983 - 2004 for the time period overlapping RoMANS.

	Spring		Summer	
	Historical Average	RoMANS Spring 2006	Historical Average	RoMANS Summer 2006
Loch Vale	142.1 mm	24.15 mm	101.6 mm	49.35 mm
Beaver Meadows	73.5 mm	19.01 mm	62.35 mm	26.87 mm
Core Site	no data	23.33 mm	no data	96.03 mm

While the lower than average precipitation indicates that wet deposition could be underrepresented by the data collected during RoMANS, it is important to compare actual deposition amounts to historical values. Wet deposition totals were calculated for the same periods as RoMANS from 1983-2005 for Beaver Meadows and 1984-2005 for Loch Vale. An average was taken to compare with the RoMANS deposition total and these average totals are presented in Table 4.2 for Beaver Meadows and Table 4.3 for Loch Vale. Wet deposition measured during the spring study of RoMANS at Beaver Meadows compares surprisingly well with historical deposition for the same time period. However, summer deposition at Beaver Meadows was less than the historical averages: NH_4^+ deposition was 43% less, NO_3^- was 50% less, and SO_4^{2-} was 61% less than average. The same comparison for Loch Vale is much different. During the spring study period, total wet deposition amounts do not compare well. Spring RoMANS measurements at Loch Vale were lower than average by 576% for NH_4^+ , 66% for NO_3^- , and 68% for SO_4^{2-} . During the summer study period, RoMANS measured above average deposition at Loch Vale for NH_4^+ (39%) and NO_3^- (6%), but 30% less than average deposition for SO_4^{2-} . To gain a greater understanding of how deposition and precipitation amounts vary from year to year, time series of deposition totals for both sites and RoMANS study periods are

presented in Figure 4.2. In addition the RoMANS Core Site data are plotted for comparison. In the spring the Core Site data compares well with the averages at BM. In the summer study period, the measurements at the Core Site were higher than both NADP site averages. From these timelines we can see that measurements made during RoMANS, while differing in some cases from the historical average, do not fall outside of the year-to-year historical variations as measured by the NADP.

In addition, in Figure 4.2 we can see that it is rare for such a low amount of precipitation to fall at either site during the spring. Although the amount of precipitation is unusual, the amount of deposition for all three species of interest does not appear that different from the historical record. A direct comparison of 2006 NADP data to RoMANS data may also provide insight into the measurements and the ability to compare RoMANS data with historical data.

Table 4.2 Comparison of historical wet deposition totals to RoMANS measurements at Beaver Meadows. Units are μg of N or S/ m^2 .

	Beaver Meadows			
	Spring		Summer	
	<i>Historical Average</i>	<i>RoMANS</i>	<i>Historical Average</i>	<i>RoMANS</i>
NH_4^+	15,600	17,500	17,300	9,800
NO_3^-	14,300	12,400	19,300	9,700
SO_4^{2-}	13,800	12,800	17,400	6,700

Table 4.3 Comparison of historical wet deposition totals to RoMANS measurements at Loch Vale. Units are μg of N or S/ m^2 .

	Loch Vale			
	Spring		Summer	
	<i>Historical Average</i>	<i>RoMANS</i>	<i>Historical Average</i>	<i>RoMANS</i>
NH_4^+	20,000	4,900	17,000	23,800
NO_3^-	21,900	7,500	22,300	23,700
SO_4^{2-}	23,900	7,600	21,600	15,000

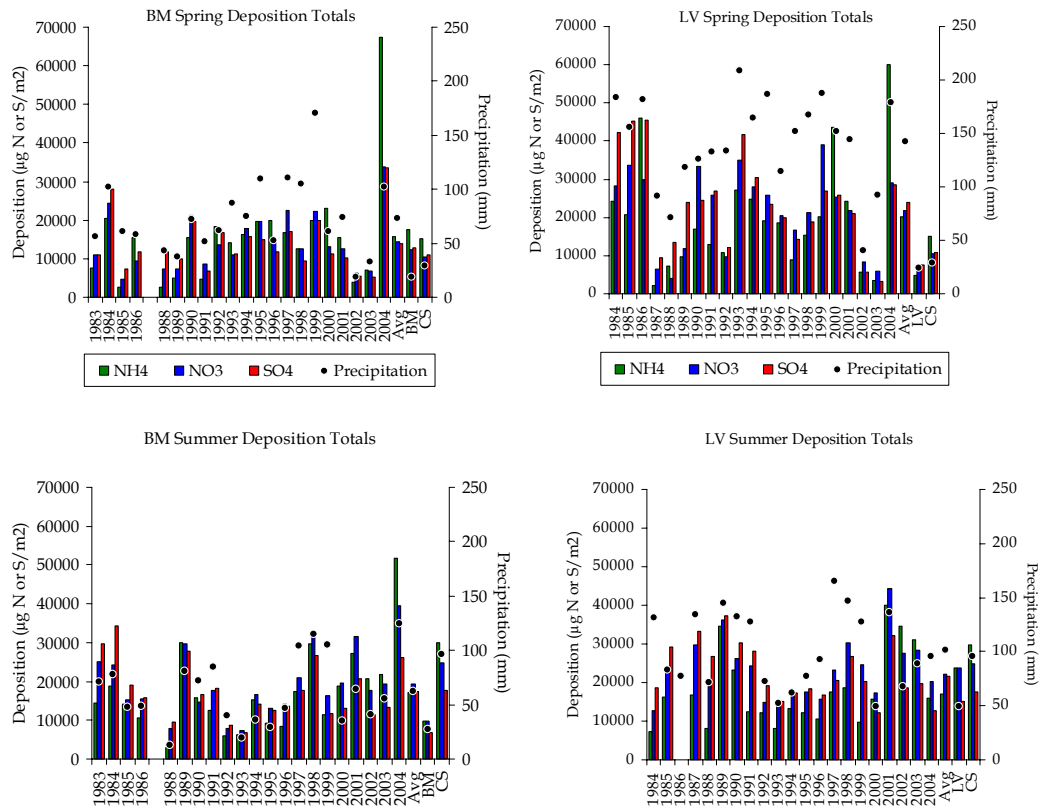


Figure 4.2 Yearly deposition totals for Beaver Meadows and Loch Vale for the weeks overlapping the RoMANS spring and summer study. Values are listed at the right side of each figure for the historical average and for RoMANS measurements at Beaver Meadows (BM) or Loch Vale (LV) and the Core Site (CS).

The 2006 NADP data for the same weeks as RoMANS were also available for comparison. As with the historical averages, the NADP data were selected for the weeks that overlapped RoMANS, 3/28/06-4/3/06 and 7/11/06-8/1/06. The NADP and RoMANS deposition and precipitation totals are presented in Table 4.4. In Figure 4.3 we see that the amount of precipitation in the spring is very similar at all five sampling sites, while in the summer precipitation amounts are not consistent between NADP and RoMANS sites that are co-located. In the spring, RoMANS deposition was greater than that from NADP for all three major species of particular interest. In the summer, the BM NADP site measured higher deposition than the RoMANS BM site, but the Core Site was higher than either of these sites. Deposition was higher at the Loch Vale RoMANS site

compared to both the LV NADP site and the RoMANS Core Site. The low deposition amounts at the LV NADP site during both the spring and summer may be due to a lack of chemistry data for 4/11-4/17 and 7/11-7/17. The precipitation amounts were available and included in the precipitation volume total. The impact of the included versus missing data can be seen in Figure 4.3 where the weekly precipitation totals for all five sets of data for all the weeks are examined. In the spring the majority of the precipitation fell during the week of 4/18-4/24, which overwhelmed the other samples collected during this season. The missing data from LV might not make a large difference to spring deposition totals based on the deposition at the other sites. The week missing from the LV NADP site in the summer had the smallest deposition for any week during the summer at BM, CS, and from measurements made at LV as a part of RoMANS. Based on the relative amounts of deposition at each site, it is likely that the LV NADP deposition total in the summer would be similar to RoMANS if the data weren't missing. If the first week of the summer data is removed from all the totals, agreements are good as seen in Figure 4.4.

Table 4.4 Comparison with measurements made by the NADP during the same weeks RoMANS took place. Total deposition values have units of μg of N (or S)/ m^2 .

Study	Data Set	Precip (mm)	NH_4^+	NO_3^-	SO_4^{2-}
Spring 3/28-4/25	BM NADP 2006	21.1	6446.5	4695.0	5213.2
	BM RoMANS	16.2	15427.3	11300.8	11299.3
	Core Site RoMANS	24.3	12968.7	8725.6	8897.5
	LV RoMANS	24.2	4901.4	7548.3	7654.2
	LV NADP 2006	27.6	3656.0	4407.8	4755.4
Summer 7/11-8/1	BM NADP 2006	14.0	4482.6	5145.7	3472.0
	BM RoMANS	9.2	3084.8	3801.9	2936.9
	Core Site RoMANS	25.6	14712.4	12591.5	9271.2
	LV RoMANS	23.7	16495.4	17022.4	11653.0
	LV NADP 2006	47.9	11363.6	12104.5	9213.9

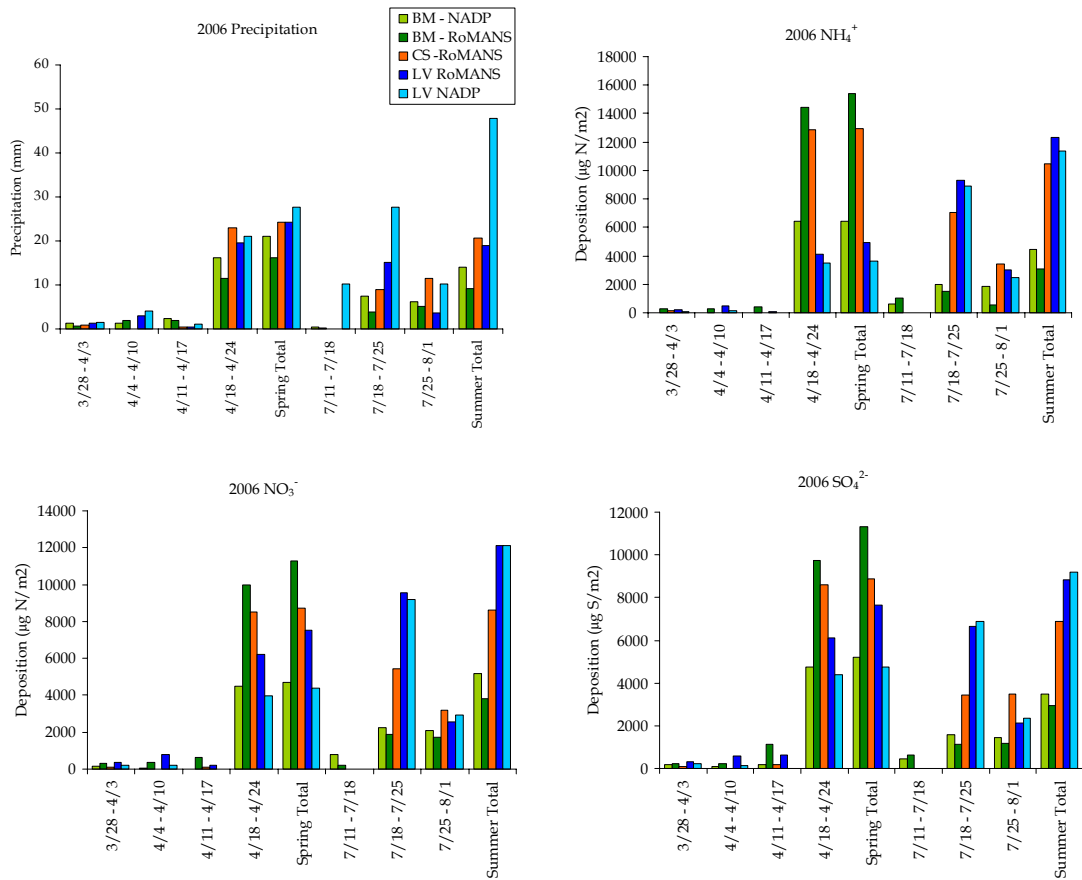


Figure 4.3 Weekly deposition totals for the RoMANS Core Site (CS) and the collocated NADP-RoMANS sites at Beaver Meadows (BM) and Loch Vale (LV).

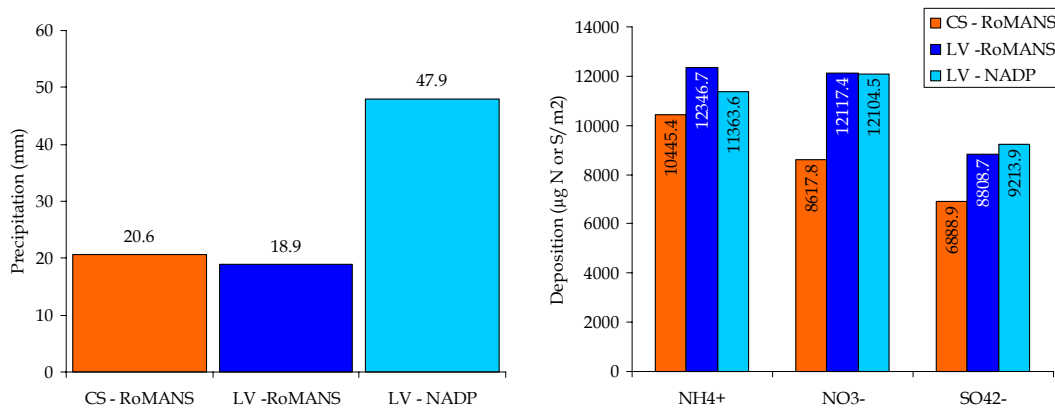


Figure 4.4 Precipitation and deposition totals at Loch Vale (LV) and the Core Site (CS) for 7/18-8/1.

It is interesting to note that even though the deposition amounts are similar for all three species of interest, the precipitation totals are very different. NADP collection

at LV had more than twice as much precipitation as the RoMANS LV or CS sites. Deposition amounts at the Core Site were more similar to LV than BM for both RoMANS and NADP collection. This is true for the deposition total and for most weeks examined here.

4.2 Solute Characteristics

Concentrations are often related to the amount of precipitation that occurred. Higher concentrations may be associated with a smaller amount of precipitation; however, this is not always the case. Other factors like air mass source and concentration of species in the air mass are often more important. By examining the Pearson correlation coefficient (r) between the measured species and the amount of precipitation that fell at a particular site, it is possible to gain some insight into possible sources and processes. For example, correlations between calcium, sodium, magnesium, and chloride may indicate that soil dust is an important source of precipitation solutes. The mixing of air masses and other interactions can make this type of interpretation difficult as several source regions may be contributing and it may become difficult to distinguish between air masses. Further, correlations between species concentrations may not indicate a direct relationship. It is possible that both species are correlated to another parameter. For example, as a precipitating cloud scavenges material from the atmosphere, multiple species concentrations may decrease in concert. Finally, although a correlation between two species may indicate similar sources or factors influencing concentration, the lack of a strong correlation could simply indicate that the relationship is not *linear*.

In Table 4.5, significant correlation coefficients between the concentrations of different species and precipitation amounts for the RoMANS spring campaign are presented for the Core Site. During the spring, few significant correlations exist between species concentrations. A comparatively higher number of significant correlations (with higher correlation coefficients) are noted for deposition fluxes (Table 4.6). While it is possible that some species may be related, the high correlations are likely due to the low number of precipitation events in the spring.

The correlation tables for the summer data are more meaningful, with a larger number of events increasing the sample sizes and the number of statistically significant correlations. In Table 4.7, where the correlations for concentrations at the Core Site for the summer are presented, we see that magnesium and calcium ($r = 0.818$, $a = 3.1$) and magnesium and sodium ($r = 0.918$, $a=3.9$) have fairly high correlations, possibly indicating a common soil or dust source. In addition, higher correlations are also present between ON and nitrite, nitrate, and sulfate. Also, the significant correlations between precipitation amount and each species are all negative (approximately -0.5); as the amount of precipitation increases it is not surprising that the concentration would drop. The corollary table for fluxes is presented in Table 4.8. The significant correlations between species differ for the flux correlations. Interestingly, significant relationships between ammonium and sulfate (slope 0.7) and ammonium and nitrate (slope 0.49) appear when the fluxes are examined, which were not apparent from the concentration correlations.

Table 4.5. Correlation table of Pearson's r-values for concentrations during the spring campaign measured at the Core Site for samples collected with the autosampler.

	Ca ²⁺	K ⁺	Mg ²⁺	Na ⁺	NH ₄ ⁺	Cl ⁻	NO ₂ ⁻	NO ₃ ⁻	SO ₄ ²⁻	ON	[H ⁺]	Precip.
Ca ²⁺		n.s.	0.656	0.645	n.s.	n.s.	b.d.	n.s.	n.s.	n.s.	n.s.	n.s.
K ⁺			n.s.	n.s.	n.s.	0.620	b.d.	n.s.	n.s.	n.s.	n.s.	n.s.
Mg ²⁺				n.s.	n.s.	n.s.	b.d.	n.s.	n.s.	n.s.	n.s.	n.s.
Na ⁺					n.s.	n.s.	b.d.	n.s.	n.s.	n.s.	n.s.	n.s.
NH ₄ ⁺						n.s.	b.d.	n.s.	n.s.	n.s.	n.s.	n.s.
Cl ⁻							b.d.	n.s.	n.s.	n.s.	n.s.	n.s.
NO ₂ ⁻								b.d.	b.d.	b.d.	b.d.	b.d.
NO ₃ ⁻									0.718	n.s.	n.s.	n.s.
SO ₄ ²⁺										n.s.	-0.633	n.s.
ON											n.s.	n.s.
[H ⁺]												n.s.
Precip.												

*n.s – r-values are not significant at the 95% confidence level for a 2-tailed t-test

**b.d – samples below detection

Table 4.6. Correlation table for fluxes during the spring campaign measured at the Core Site for samples collected with the autosampler.

	Ca ²⁺	K ⁺	Mg ²⁺	Na ⁺	NH ₄ ⁺	Cl ⁻	NO ₂ ⁻	NO ₃ ⁻	SO ₄ ²⁻	DON	precip
Ca ²⁺		0.935	0.969	0.989	0.960	0.997	b.d.	0.999	0.995	0.949	0.948
K ⁺			0.849	0.953	0.965	0.951	b.d.	0.928	0.956	0.967	0.816
Mg ²⁺				0.925	0.861	0.957	b.d.	0.977	0.940	0.843	0.996
Na ⁺					0.987	0.991	b.d.	0.983	0.997	0.982	0.894
NH ₄ ⁺						0.967	b.d.	0.949	0.982	0.998	0.821
Cl ⁻							b.d.	0.993	0.994	0.956	0.934
NO ₂ ⁻								b.d.	b.d.	b.d.	b.d.
NO ₃ ⁻									0.991	0.938	0.958
SO ₄ ²⁻										0.976	0.912
DON											0.801
precip											

*n.s – r-values are not significant at the 95% confidence level for a 2-tailed t-test

**b.d – samples below detection

Table 4.7. Correlation table for concentrations during the summer campaign measured at the Core Site for samples collected with the autosampler.

	Ca ²⁺	K ⁺	Mg ²⁺	Na ⁺	NH ₄ ⁺	Cl ⁻	NO ₂ ⁻	NO ₃ ⁻	SO ₄ ²⁻	DON	[H ⁺]	precip
Ca ²⁺		0.552	0.818	0.731	0.761	n.s.	n.s.	0.472	n.s.	n.s.	n.s.	-0.472
K ⁺			0.559	0.616	0.514	n.s.	n.s.	n.s.	n.s.	n.s.	n.s.	n.s.
Mg ²⁺				0.918	0.500	0.553	n.s.	n.s.	n.s.	n.s.	n.s.	n.s.
Na ⁺					0.493	0.622	n.s.	n.s.	n.s.	n.s.	n.s.	-0.463
NH ₄ ⁺						n.s.	n.s.	n.s.	n.s.	n.s.	n.s.	n.s.
Cl ⁻							n.s.	0.733	0.888	0.598	n.s.	-0.539
NO ₂ ⁻								0.630	0.668	0.838	n.s.	n.s.
NO ₃ ⁻									0.914	0.802	n.s.	-0.551
SO ₄ ²⁻										0.846	n.s.	-0.495
DON											n.s.	n.s.
[H ⁺]												n.s.
precip												

*n.s – r-values are not significant at the 95% confidence level for a 2-tailed t-test

Table 4.8. Correlation table for fluxes during the summer campaign measured at the Core Site for samples collected with the autosampler.

	Ca ²⁺	K ⁺	Mg ²⁺	Na ⁺	NH ₄ ⁺	Cl ⁻	NO ₂ ⁻	NO ₃ ⁻	SO ₄ ²⁻	DON	precip
Ca ²⁺		0.612	0.446	0.784	0.842	0.687	n.s.	0.801	0.607	0.604	0.562
K ⁺			n.s.	0.862	0.694	0.631	n.s.	0.565	0.460	0.682	0.661
Mg ²⁺				n.s.	n.s.	n.s.	n.s.	n.s.	n.s.	n.s.	n.s.
Na ⁺					0.668	0.851	n.s.	0.558	n.s.	0.702	0.620
NH ₄ ⁺						0.489	n.s.	0.957	0.837	n.s.	0.772
Cl ⁻							n.s.	n.s.	n.s.	0.790	n.s.
NO ₂ ⁻								n.s.	n.s.	n.s.	n.s.
NO ₃ ⁻									0.922	n.s.	0.808
SO ₄ ²⁻										n.s.	0.858
DON											n.s.
precip											

*n.s – r-values are not significant at the 95% confidence level for a 2-tailed t-test

Ion concentrations in precipitation can provide useful information about the possible sources of the pollutants in an air mass and information about the impact of the precipitation on an ecosystem. During this study we are especially interested in the amount of each species that reaches the ground and the related ecological implications. Events that appear to be important in regards to snow/rain concentrations are not necessarily contributing significant amounts of N or S to the ecosystem because of the small amount of precipitation received, as discussed earlier. We can examine the relationship between precipitation amount and flux to identify events where atypical behavior occurs (Figure 4.5). In the spring, flux and precipitation appear to be well correlated, likely due to the small number of events as seen in Table 4.6. In the summer a similar trend generally exists; however, data from events on 7/08/06 and 7/19/06 have similar magnitudes of ammonium and nitrate flux but the amount of precipitation differed by a factor of about 6 (5 mm on 7/19/06 and 32.67 mm on 7/08/06). This clearly doesn't follow the general trend of increasing flux with increasing precipitation and may indicate that something interesting may be influencing one or both events.

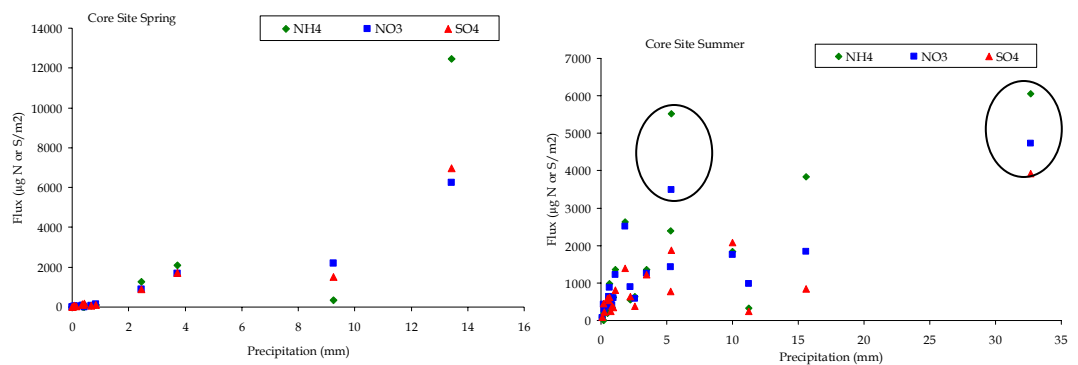


Figure 4.5 Precipitation amount plotted against the flux of N and S species for a)Core Site Spring and b)Core Site Summer.

Radar observations from 7/19 indicate that local convection was the source of rain. During the first 1.5 hours of the event 4.45 mm of rain fell, while in the last hour of the event 0.638 mm of rain fell. This is quite different from the 7/8 event which appeared to be widespread and not initiated by local convection. Initially, the precipitation moved in from the west and then from the south. During the first five hours of the event, 4.1 mm of rain fell, and during the next 1.4 hrs, 4.4 mm fell. The event continued through the next morning for approximately 24 hours of precipitation.

Six samples were collected periodically throughout the 7/8 episode with the sub-event sampler. The concentrations in Figure 4.6 are plotted at the time the sample collection began. These samples show higher concentrations initially and decreasing concentrations 7 hours into the event. In Figure 4.7 the cumulative deposition is plotted for the entire day, and we can see that the largest input of N and S occurred at the end of the event. This is likely due in part from the longer sampling time for the final sample, which was collected from 7/8 18:00 to 7/9 08:00, although as seen in Figure 4.6 solute concentrations also increased during this period.

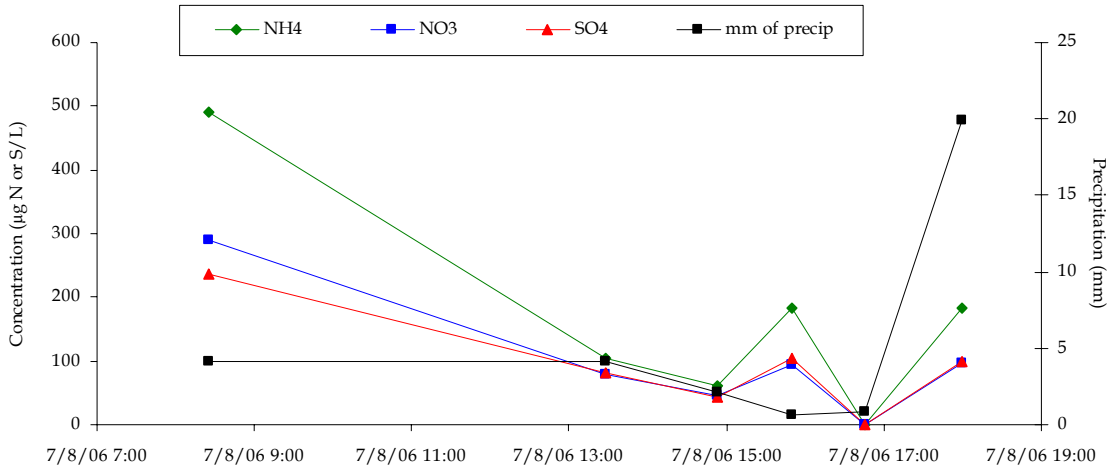


Figure 4.6 Time evolution of precipitation solute concentrations and precipitation amount during rainfall at the RoMANS Core Site during the period 7/08-7/09/06.

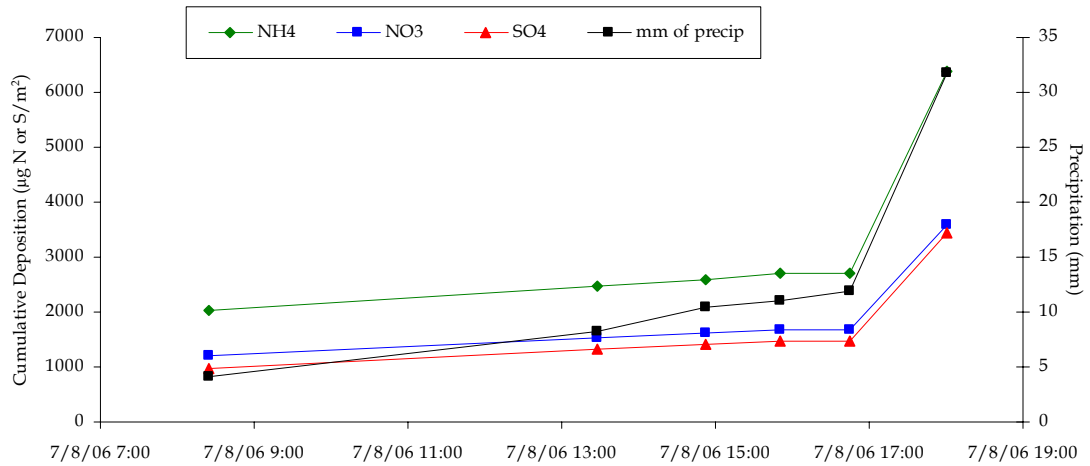


Figure 4.7 Time evolution of cumulative precipitation and wet deposition of major solute species during rainfall at the RoMANS Core Site during the period 7/08-7/09/06.

The event from 7/19 is difficult to compare with data from the sub-event samples since the event only lasted 2.5 hours and only two samples were taken. The data from these samples indicate a high concentration and flux initially and lower concentrations and low fluxes during the second half of the event. The high concentrations paired with the higher precipitation volume resulted in a large flux for this short event compared to the flux from the 24 hour event on 7/8. Investigation into gas

concentrations from continuous gas samplers during these periods did not yield any insight as there were no data available for 7/8.

The localized convective nature of summer precipitation events likely contributed to higher fluxes. Given that most pollution sources influencing deposition in RMNP are located outside the park, conditions where emissions can be transported into the park and then scavenged and deposited by precipitation can produce locally high deposition fluxes, as was the case on 7/19. The 7/19 event began at 14:30, a time when upslope winds were also observed at the Core Site. The upslope winds bring more pollutants into the park, creating conditions that are optimal for high deposition amounts. In addition, spring and summer convective storms in the intermountain west are typically initiated locally in the higher elevations (e.g., RMNP). In cases where precipitation is widespread and extended in duration, it is unlikely that pollutants from distant sources will make it into the park before being scavenged by the precipitation. On 7/8, upslope winds were observed for most of the day; however, the widespread nature of the event indicates that pollutants in the air mass were scavenged away before they reached the park. Larger-scale storms, especially those associated with frontal systems, may also produce lower deposition fluxes if the prevailing wind direction results in pollutants emitted into the regional atmosphere that are advected away and replaced by cleaner air masses.

As seen from the previous example, the changes in solute concentration and deposition flux vary with time and differ between events. A RoMANS spring event

from 4/6 has interesting trends that contrast with the 7/8 event. Ammonium always had the highest concentration during the 7/8 precipitation event, while the species with the highest N concentration changed throughout the 4/6 event. Ammonium, nitrate, and ON all had the highest N concentration at some point during the event (Figure 4.8). Initial changes in concentrations show a decreasing trend with the exception of ON. ON shows a large increase and then decrease over the first three hours of the event. Ammonium, nitrate, and sulfate all follow a similar trend of a slight decrease, followed by a slight increase, but these changes occur before the changes in ON. Such changes are likely the result of more intense precipitation falling during the second sample. During this event, nitrate and sulfate concentrations appear to follow a similar trend and briefly become the largest species. At the end of the event, however, during the morning of 4/7, ammonium and ON were the species with the highest concentrations. Again, as ON increased the concentrations of the other three species decreased, possibly indicating that a different process or source is important for ON wet deposition.

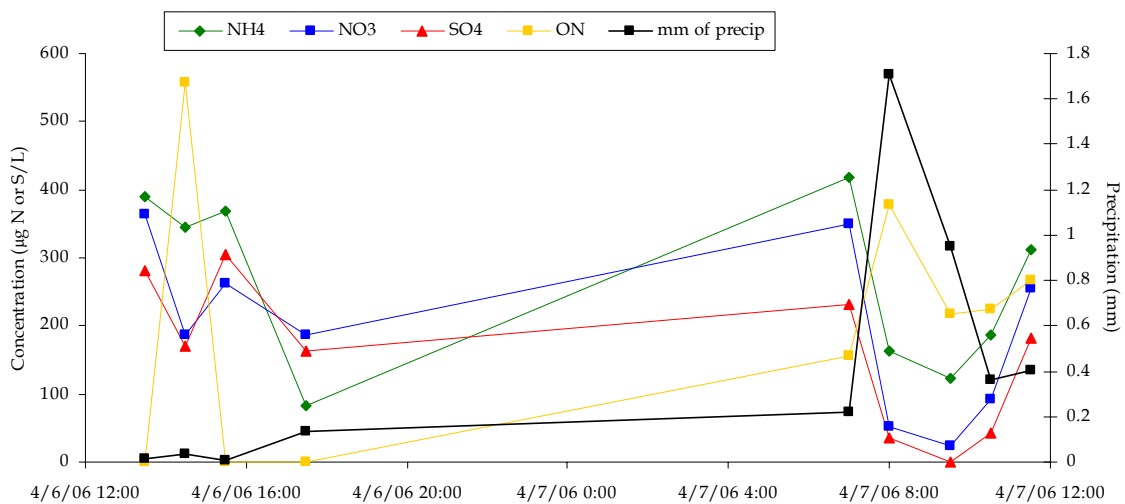


Figure 4.8 Timeline of concentrations from 4/6 13:30 to 4/7 11:30 from sub event sampler at the Core Site.

The cumulative deposition flux for the entire event is shown in Figure 4.9.

Interestingly, ON had the highest cumulative flux even when concentrations of ON were quite low for several periods during the event. Even though the episode lasted almost 24 hours the majority of the deposition occurred in the last four hours, largely due to increased precipitation during this timeframe.

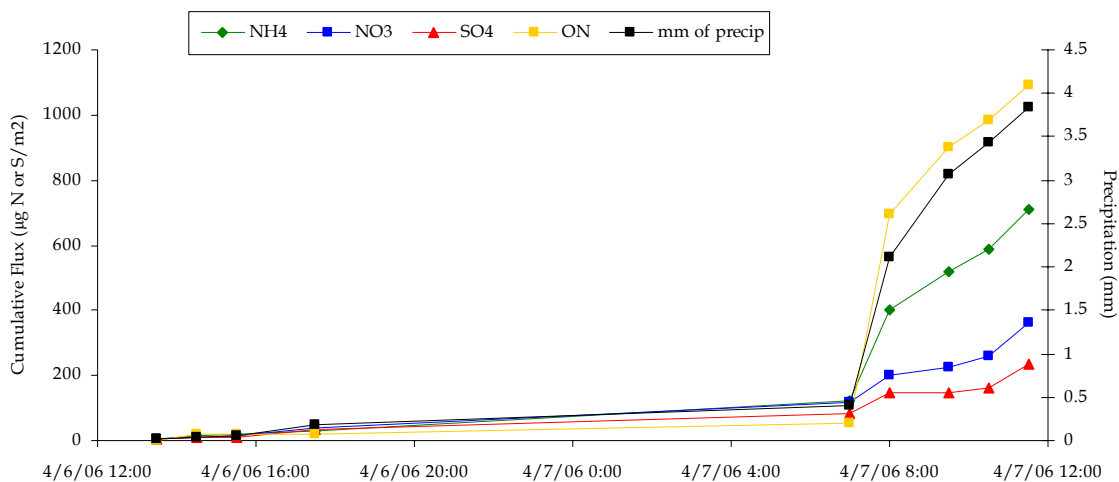


Figure 4.9 Cumulative deposition throughout the event beginning 4/6 13:30 and ending 4/7 11:30 from sub event sampler at the Core Site.

4.3 Seasonal and Spatial Variations of Wet Deposition

The patterns of precipitation during the spring and summer campaigns were very different. In the spring, the majority of the precipitation fell during a single event towards the end of the study, while in the summer there were many more events. This trend generally holds for all RoMANS sites where samples were collected in the spring and summer. Overall precipitation amounts increased for most RoMANS sampling sites from spring to summer. LV and HV are the only sites where precipitation was lower in the summer campaign than in the spring.

The spatial and temporal variability of the amount of precipitation received is shown in Figure 4.10. From this figure it is evident that sampling sites closest to each other often received precipitation from the same event, especially in the summer. During the summer, a precipitation event more often appeared to encompass the majority of sites; however, this is likely a result of the change in sampling site locations from the spring to the summer study. To determine if a relationship exists between the precipitation received at each site, the Pearson correlation coefficient r was calculated. This parameter is used to indicate the strength of the linear relationship between two variables. The r values are presented in Table 4.9 and Table 4.10 for the spring and summer, respectively.

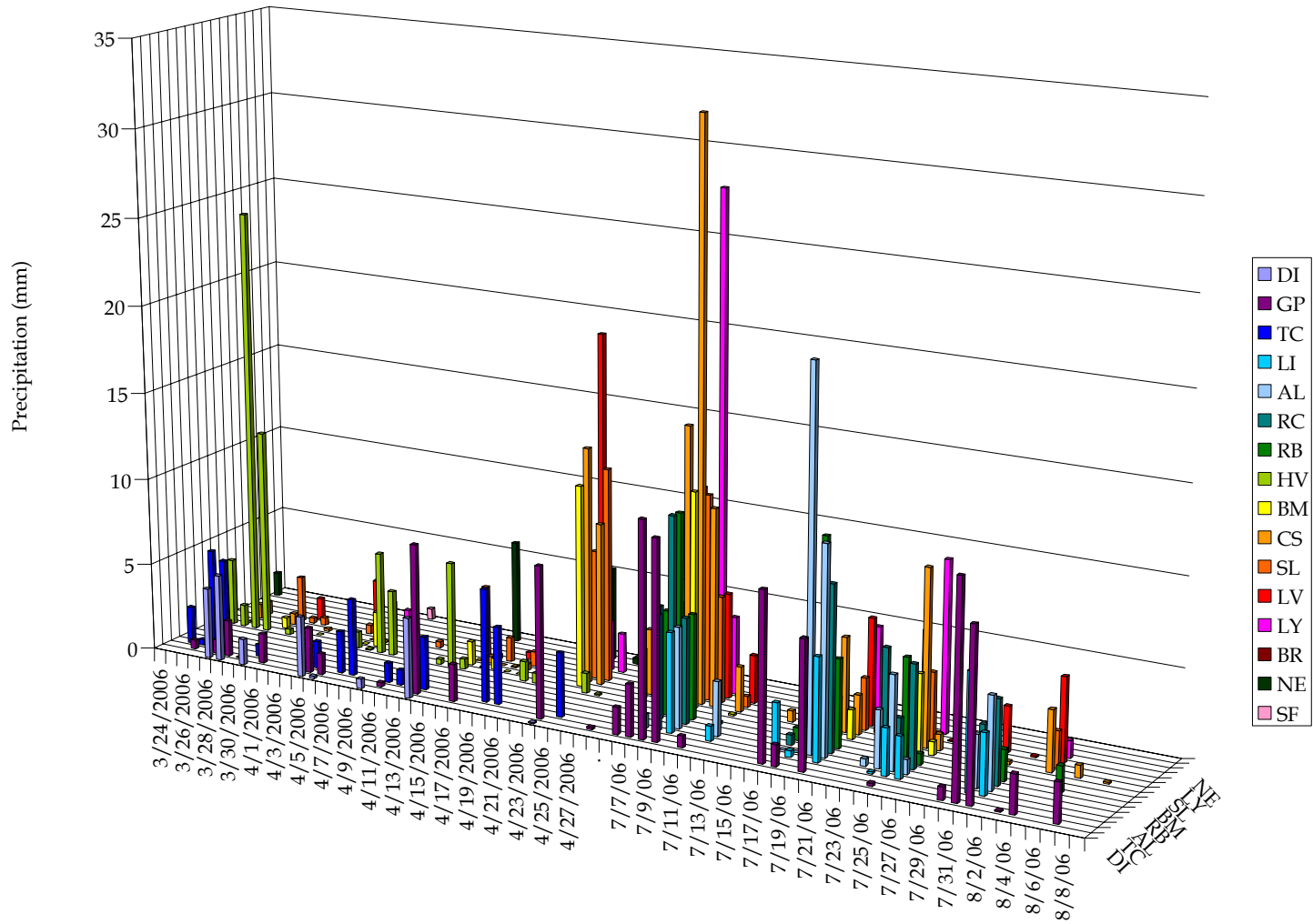


Figure 4.10 Spatial and temporal 3-D plot of the amount of precipitation received during the spring and summer RoMANS study periods.

Table 4.9 Correlation (r) between sites for precipitation amount (mm) during the RoMANS spring study period.

	<i>DI</i>	<i>GP</i>	<i>TC</i>	<i>HV</i>	<i>BM</i>	<i>CS</i>	<i>SL</i>	<i>LV</i>	<i>LY</i>	<i>BR</i>	<i>NE</i>	<i>SF</i>
<i>DI</i>		n.s.	n.s.	n.s.	n.s.	n.s.	n.s.	N/A	n.s.	N/A	n.s.	N/A
<i>GP</i>			0.753	n.s.								
<i>TC</i>				n.s.	n.s.	n.s.	0.743	n.s.	n.s.	N/A	n.s.	n.s.
<i>HV</i>					0.940	0.951	0.741	N/A	n.s.	N/A	n.s.	n.s.
<i>BM</i>						0.800	n.s.	n.s.	n.s.	N/A	N/A	n.s.
<i>CS</i>							0.847	n.s.	n.s.	N/A	n.s.	n.s.
<i>SL</i>								n.s.	n.s.	N/A	n.s.	n.s.
<i>LV</i>									N/A	N/A	N/A	N/A
<i>LY</i>										N/A	N/A	n.s.
<i>BR</i>											N/A	N/A
<i>NE</i>												N/A
<i>SF</i>												

n.s – r-values are not significant at the 95% confidence level for a 2-tailed t-test
 N/A – not enough site pairs were available for analysis

Table 4.10 Correlation (r) between sites for precipitation amount (mm) during the RoMANS summer study period.

	<i>GP</i>	<i>TC</i>	<i>LI</i>	<i>AL</i>	<i>RC</i>	<i>RB</i>	<i>HV</i>	<i>BM</i>	<i>CS</i>	<i>SL</i>	<i>LV</i>	<i>LY</i>
<i>GP</i>		0.824	0.805	n.s.	n.s.	n.s.	n.s.	n.s.	n.s.	0.764	n.s.	n.s.
<i>TC</i>			0.817	n.s.								
<i>LI</i>					n.s.							
<i>AL</i>					n.s.	0.920	n.s.	n.s.	n.s.	n.s.	n.s.	n.s.
<i>RC</i>						n.s.	0.579	n.s.	n.s.	n.s.	n.s.	n.s.
<i>RB</i>							0.767	0.713	0.727	0.911	n.s.	0.952
<i>HV</i>								0.975	0.881	0.954	n.s.	0.900
<i>BM</i>									0.930	0.975	n.s.	0.988
<i>CS</i>										0.940	n.s.	n.s.
<i>SL</i>											n.s.	0.921
<i>LV</i>												n.s.
<i>LY</i>												

n.s – r-values are not significant at the 95% confidence level for a 2-tailed t-test

In both the spring and summer we see that precipitation amounts at Beaver Meadows, the Core Site, and Sprague Lake all had comparatively high correlations with each other. Correlation coefficients between sites ranged from 0.800 to 0.954. This is not unexpected since they are all on the eastern side of the park and are likely to experience similar weather patterns, whether from a large-scale storm system or local convectively-driven storm. Lyons was also highly correlated with most of these sites even though it is located at lower altitude and some distance to the east. Loch Vale, though in a similar region as the other park sites mentioned above, is at a much higher elevation which likely influences the low correlations seen with other sites during the summer. The relationship between precipitation amounts shows some interesting trends indicating that spatial variations may also be observed in deposition.

Documenting spatial variability of deposition is important since long term measurements are only taken at one site. In the 3-D plot of NH_4^+ deposition, Figure 4.11, it is evident the Brush precipitation event on 4/14 had the largest deposition of NH_4^+ for both RoMANS study periods. The Brush site is located in northeast Colorado, a region of high ammonia emissions. During both study periods, sites close together often, but not always, had similar deposition amounts during the same event. In addition, events spread over a multi-day period or when precipitation fell on consecutive days, such as 4/23-4/25 and 7/7-7/9, show some interesting but expected patterns of decreasing deposition as the event continued. These same patterns are also apparent in plots of NO_3^- (Figure 4.12) and SO_4^{2-} (Figure 4.12) deposition.

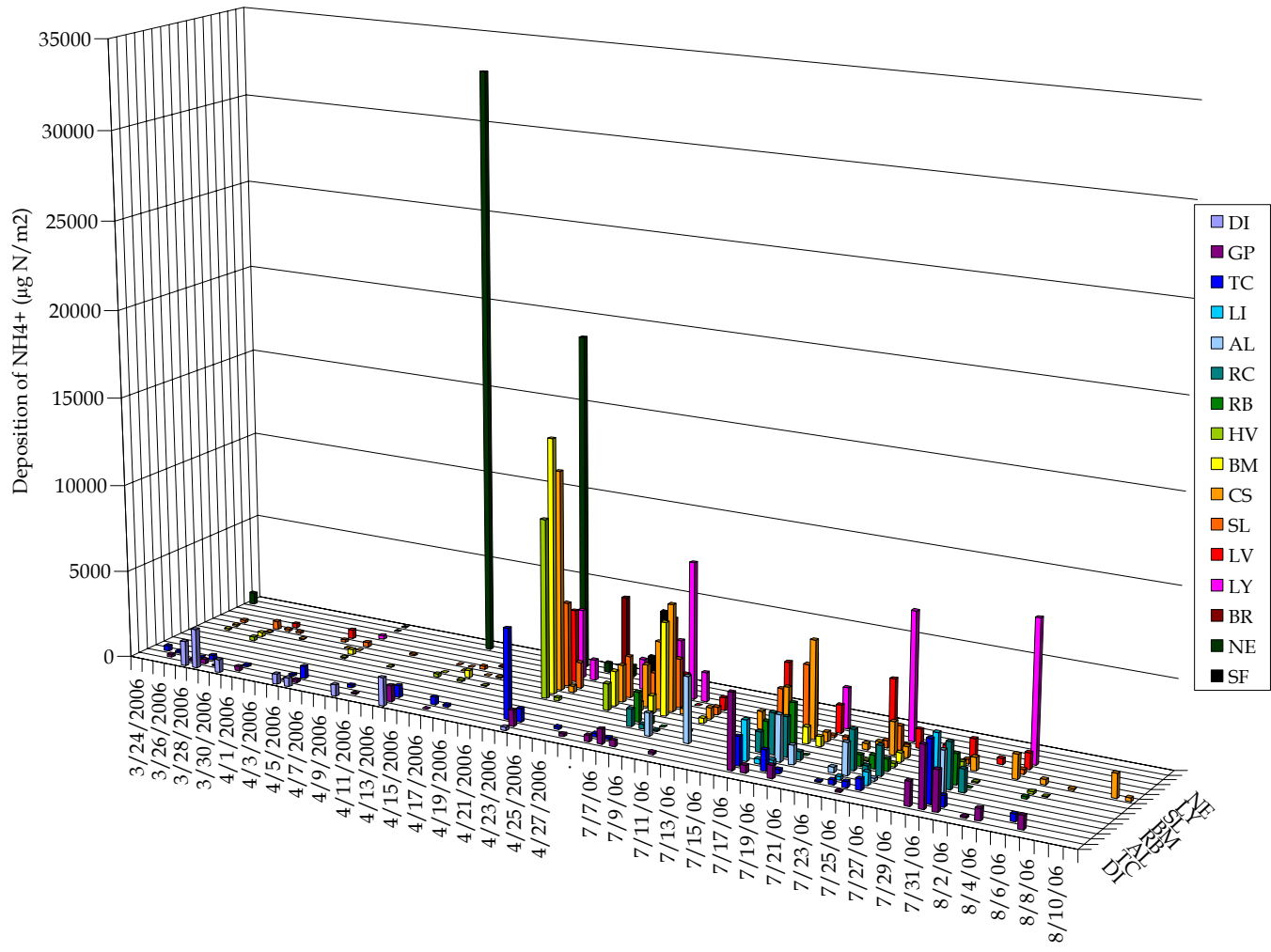


Figure 4.11 Spatial and temporal NH₄⁺ deposition during the spring and summer studies of RoMANS.

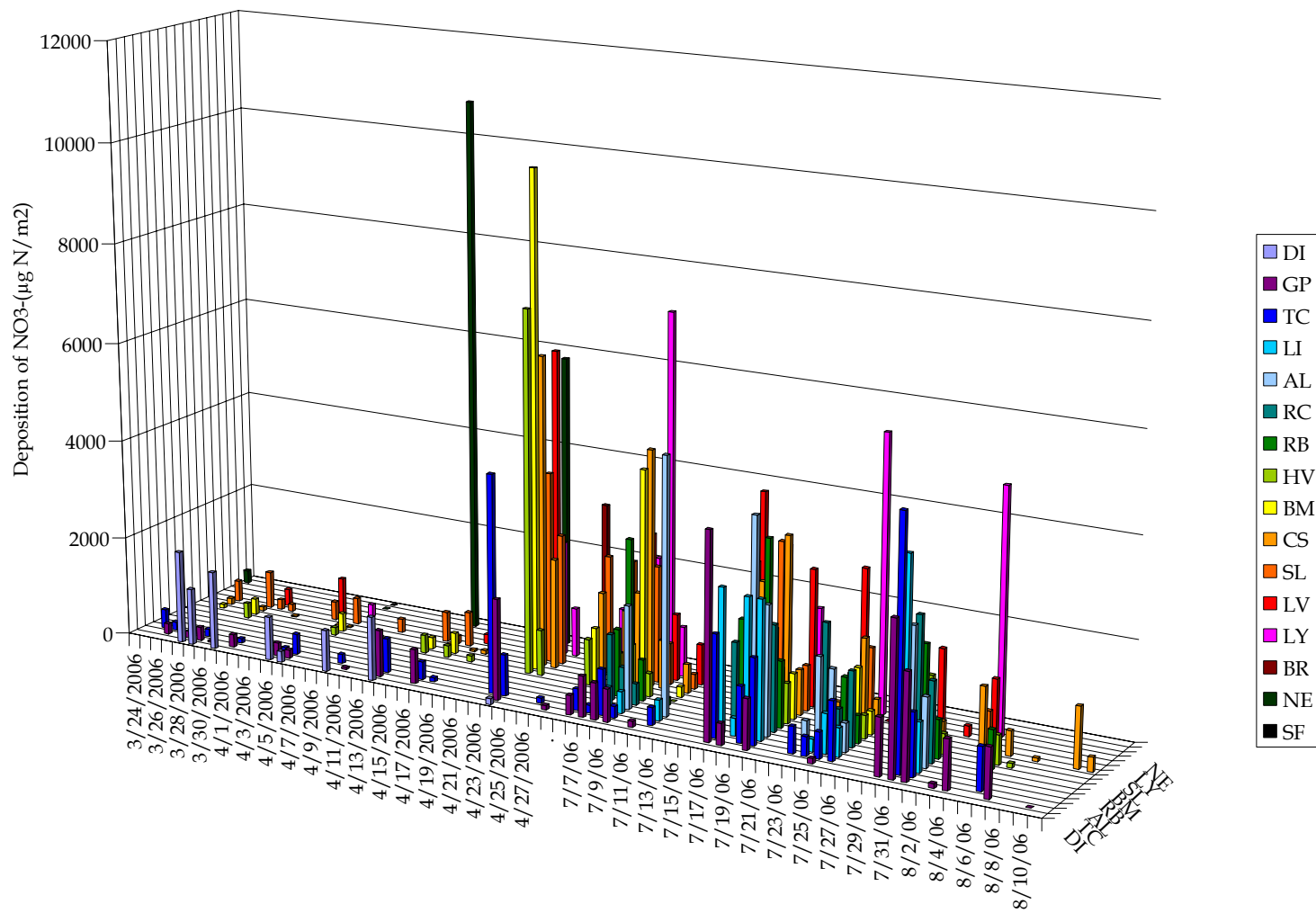


Figure 4.12 Spatial and temporal NO_3^- deposition during the spring and summer studies of RoMANS.

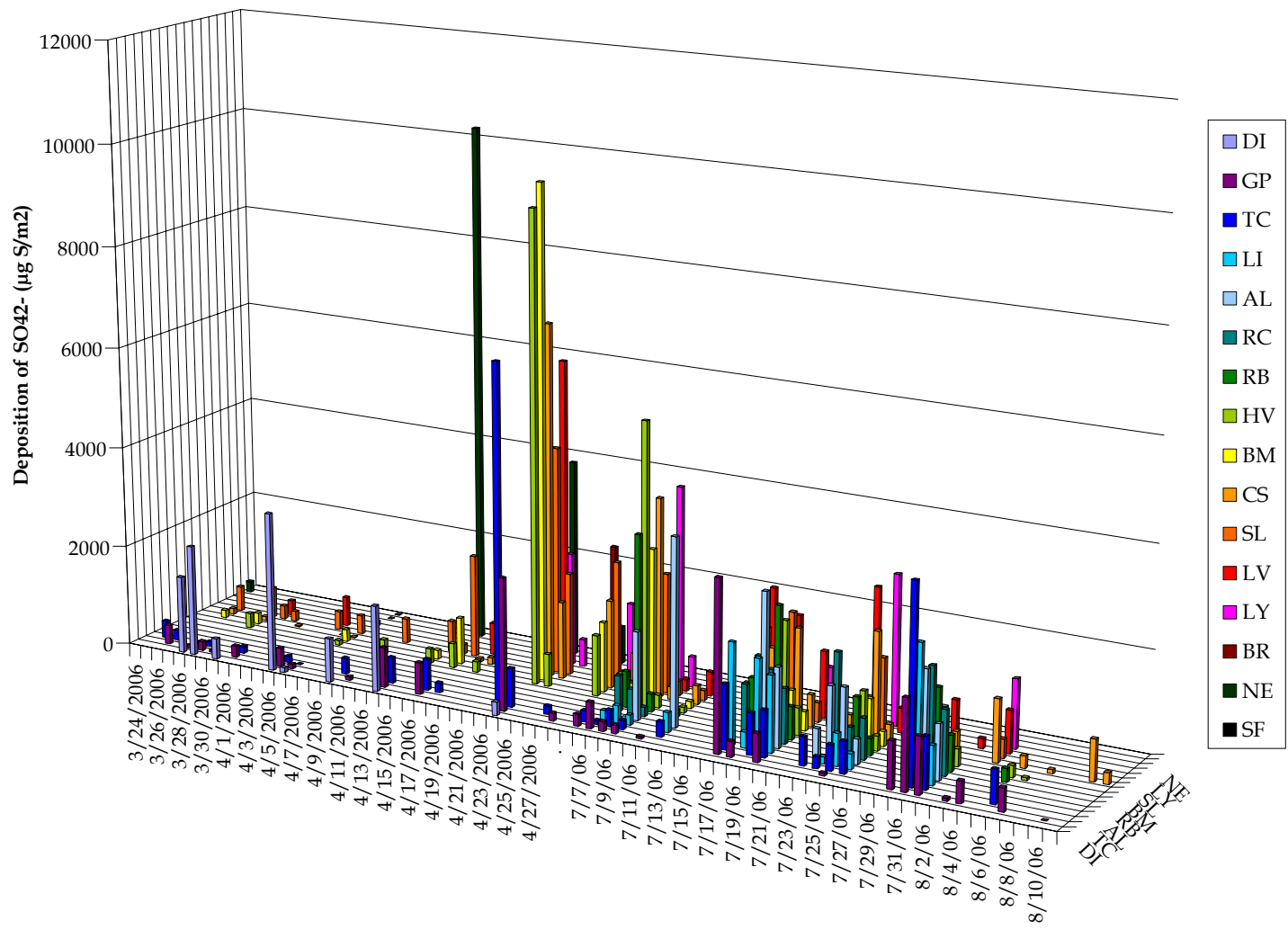


Figure 4.13 Spatial and temporal SO₄²⁻ deposition during the spring and summer studies of RoMANS.

In both Figure 4.12 and Figure 4.13 the spring Brush event still had the largest event deposition, but there are several other events with similar magnitudes of deposition for both NO_3^- and SO_4^{2-} . It is also interesting to observe in all of the 3-D plots that periods of no deposition (no precipitation) are easily observed, and sites are often clustered together for localized precipitation activity. An example of this can be seen in the spring for the westernmost sites (Dinosaur (DI), Gore Pass, and Timber Creek) which show deposition amounts of nitrate and sulfate highest at DI and decreasing to the east. Deposition of ammonium was low at these sites so the trend is not as easily seen. The westernmost sites also appear to display a similar trend during the summer study period.

To examine the spatial relationships for a given event, several profiles were made across the site network for precipitation amounts and NH_4^+ , NO_3^- , and SO_4^{2-} deposition. In Figure 4.14, sites are orientated approximated east to west and we can see that precipitation peaked at Loch Vale but deposition peaked at Beaver Meadows for all three species during the widespread 4/23 event. Ammonium deposition decreased both to the east and west of Beaver Meadows. Nitrate and sulfate follow a similar pattern but have a secondary peak in deposition at Loch Vale. In addition, the difference between deposition at Sprague Lake and the Core Site is greatest for ammonium. Profiles across the sites are also presented for the 7/20 event in Figure 4.15. In these profiles it is again fairly obvious that ammonium deposition follows a different pattern than nitrate or sulfate deposition.

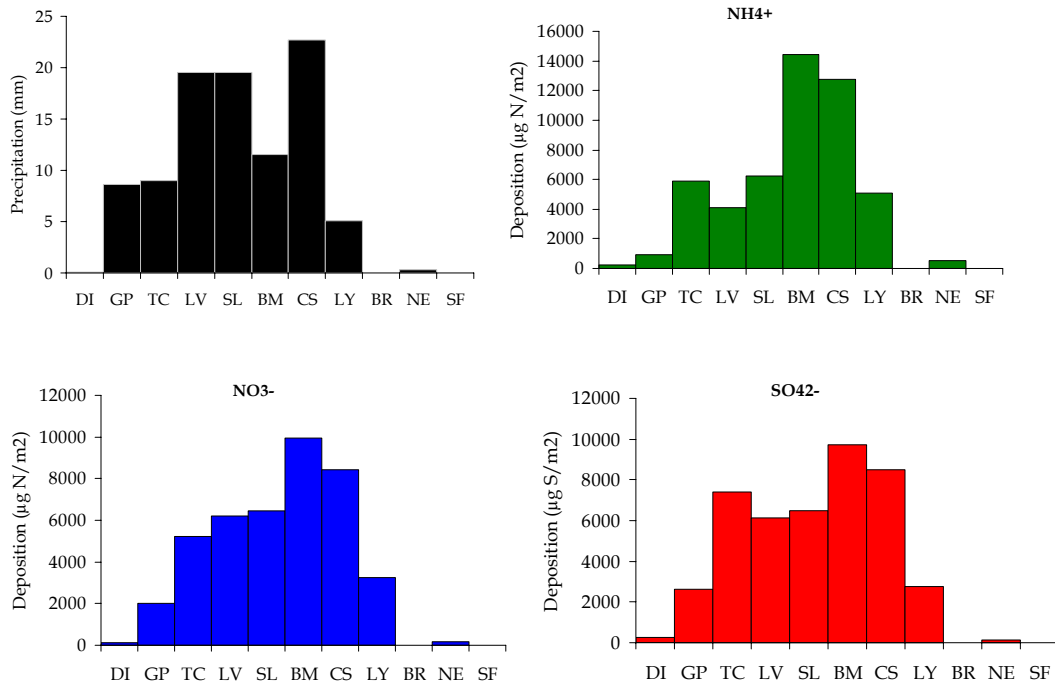


Figure 4.14 Spatial profile of wet deposition from samples collected during the 4/23 event. a) Precipitation amount is shown in black, b) ammonium deposition is shown in green, c) nitrate deposition is shown in blue, and d) sulfate deposition is shown in red.

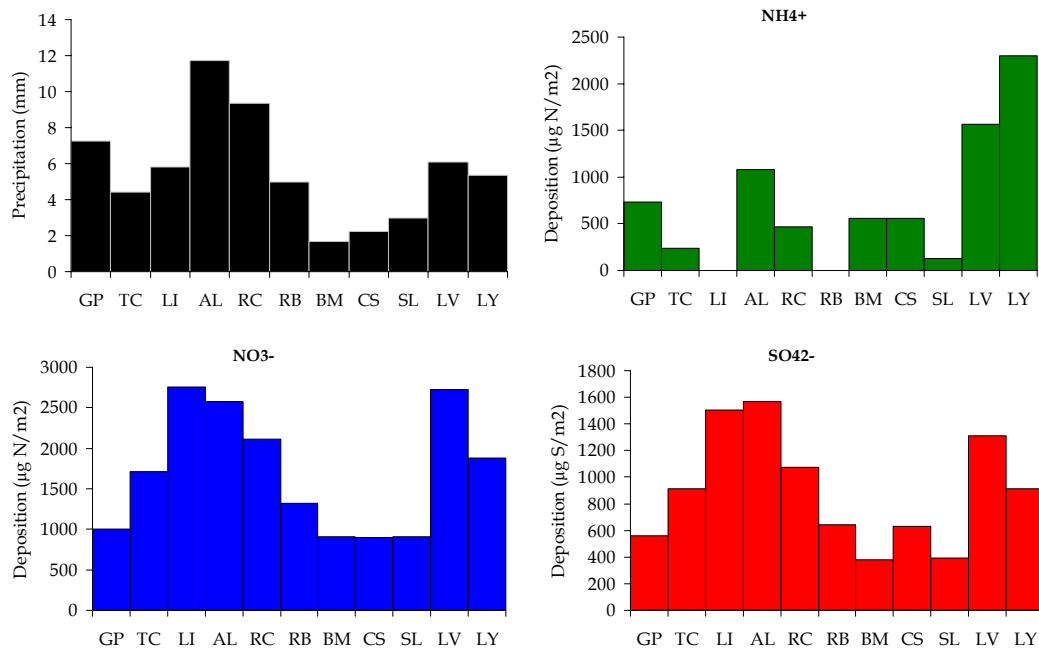


Figure 4.15 Profile of wet deposition from samples collected during the 7/20 event. a) Precipitation amount shown in black, b) ammonium deposition is shown in green, c) nitrate deposition is shown in blue, and d) sulfate deposition is shown in red.

Ammonium deposition is fairly low within the park, with a maximum at Lyons for the 7/20 event. Loch Vale had the second highest amount of NH_4^+ deposition. No ammonium was measured in the sample from Lake Irene (LI) for this event, while wet deposition of both sulfate and nitrate peaked at LI and Alpine VC (AL) and Loch Vale. It is also interesting to note that although there was a large difference in precipitation that fell at LI and AL, similar amounts of nitrate and sulfate were deposited at these sites.

Some of the deposition relationships between sites can be inferred from Figure 4.11 to Figure 4.15; however, as seen above, the relationship can change with event and study period. A more quantitative approach can be used to examine these relationships more closely by calculating the Pearson correlation coefficients as done for precipitation amounts. Table 4.11, Table 4.12, and Table 4.13 give the significant r-values for each site pair for ammonium, nitrate, and sulfate deposition for the summer study period. Significant r-values for the spring can be found in Appendix F. The low number of events during the spring resulted in many site pairs with high correlation coefficients.

Correlations for sulfate are consistently higher between sites in the park than for either NH_4^+ or NO_3^- . Site pairs that had high correlations for the precipitation amount (Table 4.10) were also high for sulfate (Table 4.13). Ammonium wet deposition at SL is well correlated with most of the sites in the park, and the sites farthest west – Gore Pass, Timber Creek, and Lake Irene – are all well correlated. It is interesting to note that correlations are not very consistent between species as we might have inferred from Figure 4.14 and Figure 4.15.

Table 4.11 Correlation coefficient between sites for ammonium deposition during the RoMANS summer study period.

	<i>GP</i>	<i>TC</i>	<i>LI</i>	<i>AL</i>	<i>RC</i>	<i>RB</i>	<i>HV</i>	<i>BM</i>	<i>CS</i>	<i>SL</i>	<i>LV</i>	<i>LY</i>
<i>GP</i>		0.775	0.821	N/A	n.s.	n.s.	0.778	n.s.	n.s.	n.s.	n.s.	-0.909
<i>TC</i>			0.935	0.609	n.s.	n.s.	0.993	n.s.	n.s.	n.s.	n.s.	n.s.
<i>LI</i>					n.s.	n.s.	0.999	n.s.	n.s.	N/A	-0.959	N/A
<i>AL</i>					n.s.	0.729	n.s.	0.945	n.s.	N/A	n.s.	N/A
<i>RC</i>						n.s.						
<i>RB</i>							n.s.	n.s.	0.600	n.s.	n.s.	-0.988
<i>HV</i>								N/A	0.635	N/A	n.s.	N/A
<i>BM</i>									0.694	n.s.	n.s.	0.998
<i>CS</i>										0.941	n.s.	n.s.
<i>SL</i>											n.s.	n.s.
<i>LV</i>												n.s.
<i>LY</i>												

n.s – r-values are not significant at the 95% confidence level for a 2-tailed t-test

N/A – too few pairs were available to calculate an r-value (1 or less)

Table 4.12 Correlation coefficient between sites for nitrate deposition during the RoMANS summer study period.

	<i>GP</i>	<i>TC</i>	<i>LI</i>	<i>AL</i>	<i>RC</i>	<i>RB</i>	<i>HV</i>	<i>BM</i>	<i>CS</i>	<i>SL</i>	<i>LV</i>	<i>LY</i>
<i>GP</i>		0.700	0.742	n.s.	n.s.	n.s.	0.724	n.s.	n.s.	n.s.	n.s.	n.s.
<i>TC</i>			0.852	n.s.	0.644	n.s.						
<i>LI</i>					0.591	n.s.	0.805	n.s.	n.s.	n.s.	n.s.	n.s.
<i>AL</i>					n.s.	n.s.	0.837	n.s.	n.s.	-0.932	n.s.	n.s.
<i>RC</i>						n.s.						
<i>RB</i>							0.536	n.s.	0.823	n.s.	n.s.	n.s.
<i>HV</i>								n.s.	n.s.	n.s.	n.s.	n.s.
<i>BM</i>									0.745	n.s.	n.s.	n.s.
<i>CS</i>										0.753	n.s.	n.s.
<i>SL</i>											n.s.	n.s.
<i>LV</i>												n.s.
<i>LY</i>												

n.s – r-values are not significant at the 95% confidence level for a 2-tailed t-test

Table 4.13 Correlation coefficient between sites for sulfate deposition during the RoMANS summer study period.

	<i>GP</i>	<i>TC</i>	<i>LI</i>	<i>AL</i>	<i>RC</i>	<i>RB</i>	<i>HV</i>	<i>BM</i>	<i>CS</i>	<i>SL</i>	<i>LV</i>	<i>LY</i>
<i>GP</i>		n.s.	0.751	n.s.								
<i>TC</i>			0.835	n.s.	0.608	n.s.						
<i>LI</i>					n.s.							
<i>AL</i>					n.s.	n.s.	n.s.	n.s.	n.s.	-0.898	n.s.	n.s.
<i>RC</i>						n.s.	n.s.	n.s.	n.s.	n.s.	0.754	n.s.
<i>RB</i>							0.937	0.865	0.875	n.s.	n.s.	n.s.
<i>HV</i>								0.973	0.930	0.672	n.s.	n.s.
<i>BM</i>									0.944	0.908	n.s.	n.s.
<i>CS</i>										0.936	n.s.	0.968
<i>SL</i>											n.s.	0.983
<i>LV</i>												n.s.
<i>LY</i>												

n.s – r-values are not significant at the 95% confidence level for a 2-tailed t-test

In the summer, correlation coefficients between Beaver Meadows and the Core Site were relatively high for NH_4^+ (0.694), NO_3^- (0.745) and SO_4^{2-} (0.944). This consistency is not seen for many other site pairs and is likely a result of the proximity of BM to the CS (BM is 10 km NNW of the CS). A closer look at the relationships between these two sites for both the spring and summer provides some interesting results.

During the spring, precipitation occurred at one site (either) more often than it occurs at both sites on the same day. When precipitation is measured at both sites, the agreement is fairly good with points falling on the 1:1 line (Figure 4.16a). Agreement between concentrations and deposition measured during the same event is also good. The outliers in Figure 4.16b coincide with the lowest volume of precipitation measured at BM which would influence the high concentrations measured. The plot of deposition (Figure 4.16c) did not show similar outliers. The summer did not demonstrate the same agreement; precipitation amount is consistently higher at the Core Site as is deposition (Figure 4.17a,c). Even on 7/7, when the automated sampler under-collected precipitation, as discussed in the previous chapter, precipitation amounts were higher at the Core Site. At the Core Site approximately 15 mm of precipitation were collected on 7/7 with the automated sampler and ~26 mm was collected with the sub-event sampler, while approximately 2 mm was collected at Beaver Meadows. The difference in agreement between spring and summer is not surprising given the difference in precipitation activity in these two seasons. While large-scale forcing tends to produce widespread precipitation in spring, localized convective activity produces more isolated precipitation during many summer days.

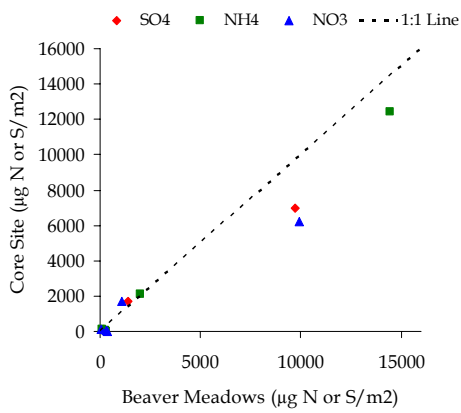
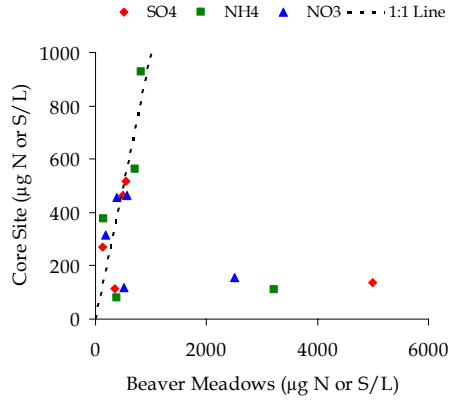
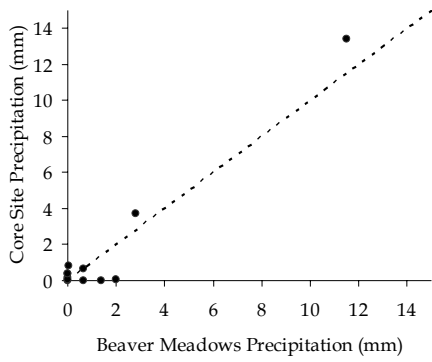


Figure 4.16 Beaver Meadows comparison with the Core Site for the RoMANS spring study. a) precipitation b) concentration c) deposition

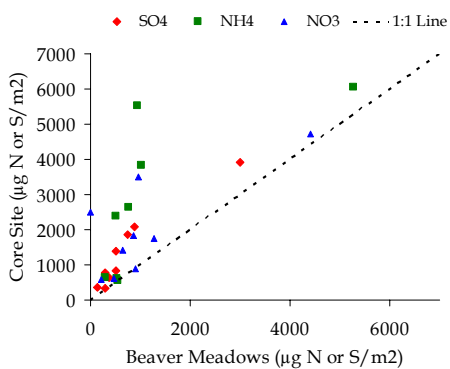
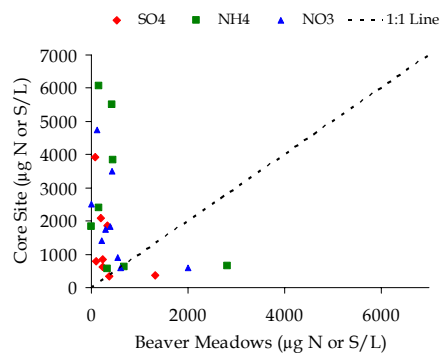
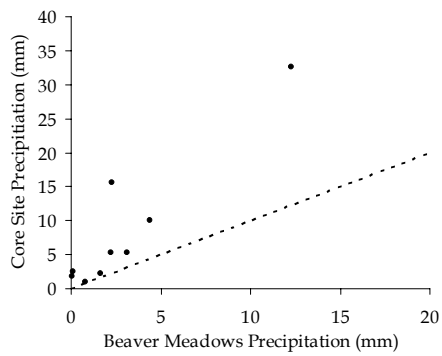


Figure 4.17 Beaver Meadows comparison with the Core Site for the RoMANS summer study. a) precipitation b) concentration c) deposition

The above relationships between sites for specific events but have not yet examined the spatial variations of total deposition. In the historical data there were noticeable differences in total deposition at CS, BM, and LV. Further investigation into the differences at these sites and the other RoMANS sites follows.

In the spring, the spatial pattern of total wet deposition fluxes peaked at Beaver Meadows (BM) and at the easternmost site in Grant, NE (Figure 4.18). The peak in ammonium flux at Grant, NE (NE) is not unexpected since it is near regions where significant amounts of ammonia are emitted from agricultural and livestock operations. In the park the fluxes at BM were not significantly different from the Core Site (CS) or Sprague Lake (SL) to the west. The more interesting observation is that BM received a smaller amount of precipitation than any of those sites. Among RMNP sites, SL actually had the highest amount of sulfate deposition and is the easternmost site where the sulfate flux is larger than both the ammonium and nitrate fluxes. All sites to the west of SL have higher fluxes of sulfate than either N species. The change in species dominance suggests a difference in atmospheric composition during periods of precipitation at sites in the western and eastern portions of the RoMANS measurement network. It is likely that regional transport patterns east and west of the continental divide affect sources influencing the wet deposition in the area. A general trend from ammonium-dominated N deposition in the east to nitrate-dominated N deposition in the west is also observed. The relative decrease in ammonium moving westward is probably a result of the increasing distance from major ammonia source regions located in eastern Colorado and further east.

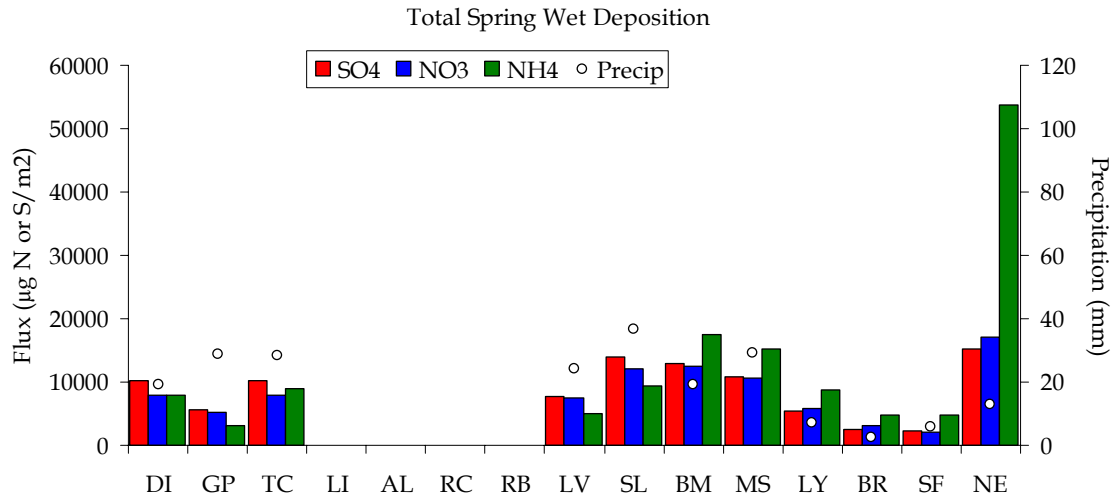


Figure 4.18 Total spring wet deposition of SO_4^{2-} , NO_3^- , and NH_4^+ by site with total amount of precipitation. Sites are ordered by longitude.

In the summer, wet deposition of most species was greater than the spring at most sites (Figure 4.19). This is likely a result, in part, of the increase in precipitation during the summer. However, BM does not follow this trend. At BM the wet deposition flux of all three species (NH_4^+ , NO_3^- , and SO_4^{2+}) decreased in the summer even though the amount of precipitation was higher. The total deposition does not show the same pattern as seen in the spring. Instead, there was fairly consistent deposition across most sites. The CS and Lyons (LY) sites measured maximum N deposition while S deposition was slightly higher at the Core Site and Alpine VC (Figure 4.19).

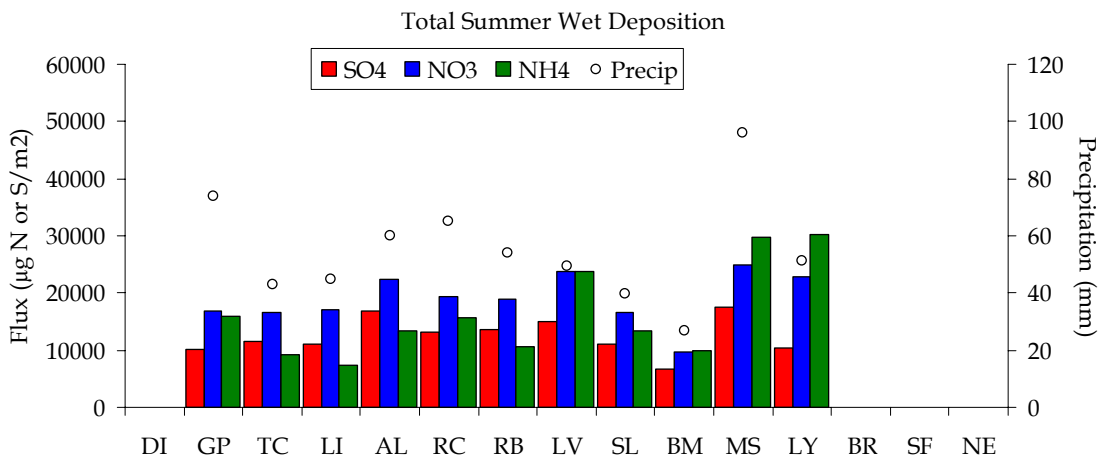


Figure 4.19 Total summer wet deposition of SO₄²⁻, NO₃⁻, and NH₄⁺ by site with total amount of precipitation. Sites are order by longitude.

The relative amounts of nitrate and ammonium are also interesting to compare from site to site and for both campaigns. In Figure 4.20 the ratio of NH₄⁺/NO₃⁻ deposition is plotted by site for both the spring and summer. In the spring there is a strong trend of increasing NH₄⁺/NO₃⁻ ratio from west to east. It is interesting that the ratios for Brush, Lyons, the Core Site, and Beaver Meadows are similar for the spring, considering Brush is located in the plains, Lyons is a foothills site, and Beaver Meadows and the Core Site are located in RMNP. In both the spring and summer at these four sites there is a slight increase in the ratio to the east indicating a greater contribution of NH₄⁺ as one moves east from the continental divide. During the summer only those sites closest to and within the park were in operation. All of the summer sites, with the exception of the three easternmost and Loch Vale, had higher fluxes of nitrate than ammonium. At Beaver Meadows and Loch Vale the wet deposition of each species was very similar, while at the Core Site and Lyons wet deposition of ammonium was slightly higher. Five of the eight sites where samples were taken during both campaigns had higher ratios of ammonium to nitrate in the

spring and eight sites had ratios above one. The other three sites, Gore Pass, Loch Vale, and Sprague Lake all had higher ratios in the summer but wet nitrate deposition was still higher than wet ammonium deposition. The exception was at Loch Vale, where deposition of ammonium and nitrate was about equal.

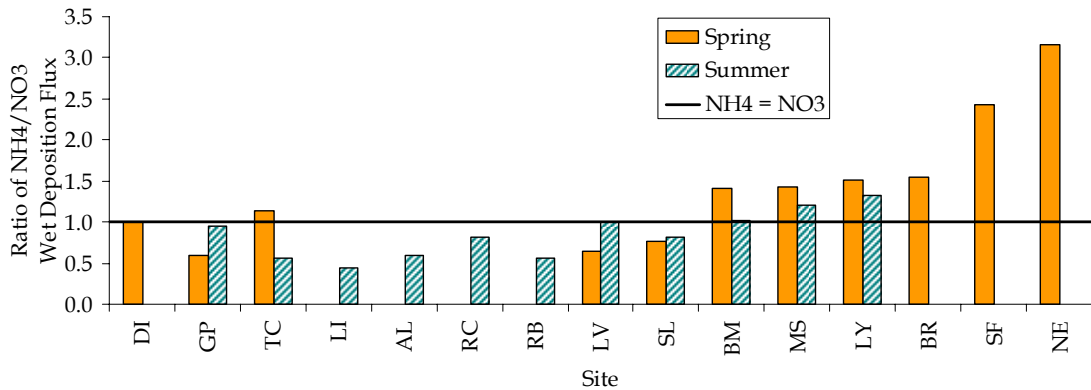


Figure 4.20 Ratio of ammonium wet deposition flux to nitrate wet deposition flux totals by site for both the spring (orange) and summer (green striped).

Changes in total inorganic nitrogen deposited at each site from spring to summer are shown in Figure 4.21. Generally, there was an increase in N deposition in the summer. The exception to this trend was Beaver Meadows. Lyons and Loch Vale had the largest increase of wet deposited inorganic nitrogen in the summer.

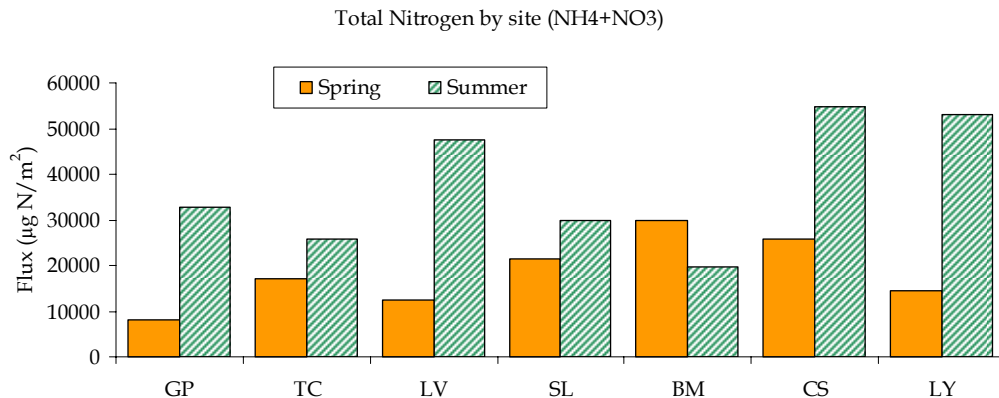


Figure 4.21 Total inorganic nitrogen deposition ($\mu\text{g N}/\text{m}^2$) by site and season for sites where measurements were made in both the spring and summer.

The mass of sulfur deposited during RoMANS was lower than that of N and was less variable across the sites (Figure 4.22). Only Beaver Meadows and Sprague Lake show a decrease in S flux during the summer. All other sites show an increase. The decrease at Beaver Meadows is consistent with the decrease in N observed at this site. Sprague Lake S deposition decreased in summer while N deposition increased.

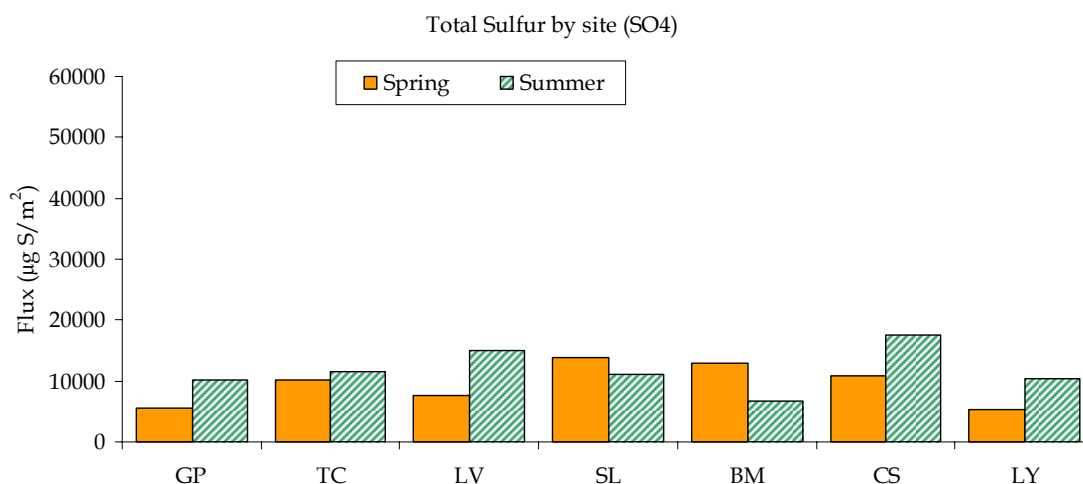


Figure 4.22 Total sulfate deposition ($\mu\text{g S}/\text{m}^2$) by site and season for sites where measurements were made in both the spring and summer.

4.4 Organic Nitrogen

Specific sources of organic nitrogen (ON) measured during RoMANS are unknown. Atmospheric ON can include contributions from biological sources (Jones and Cookson, 1983; Littmann, 1997), oxidation products of combustion emissions (Roberts, 1990), and reduced forms of nitrogen primarily from agricultural sources (Schade and Crutzen, 1995). Other studies have focused on some subsets of organic nitrogen compounds: aliphatic amines (Gronberg et al., 1992), amino compounds (Gorzelska et al., 1992), urea and free amino acids (Mace et al., 2003), and free and combined amino nitrogen (Zhang and Anastasio, 2001). During RoMANS total ON

was measured in precipitation samples to determine its importance to the total N deposition budget.

4.4.1 *Organic Nitrogen Relationships*

ON deposition varies with event just as the other N species do. In general, ON concentrations do not appear to reach the same levels as nitrate or ammonium. In only a few instances during the summer, at the Core Site and Gore Pass, do the concentrations of ON exceed one or both N species. Concentrations of ON were greater during the summer at the Core Site. At Lyons, however, concentrations were greater during the spring. The amount of ON deposited by precipitation typically varied with event intensity and duration; however, concentrations at Gore Pass appeared to be fairly constant from event to event.

Since so little is known about the sources of ON in the study area, we wanted to determine if a relationship exists between fluxes of ON and either of the other N species measured. In the correlation tables above (and those presented in Appendix A) the relationship between ON deposition and deposition of other N species was not consistently significant at the 95% confidence level. The data are shown visually in Figure 4.23 to help determine if a relationship exists and if it would perhaps be significant if the sample size were larger. As seen in this figure the relationship is not particularly strong between deposition fluxes of NH_4^+ and ON or NO_3^- and ON. The weak relationships that do exist for each species are different; generally ON is approximately half the nitrate deposited and a little more than a third of deposited ammonium.

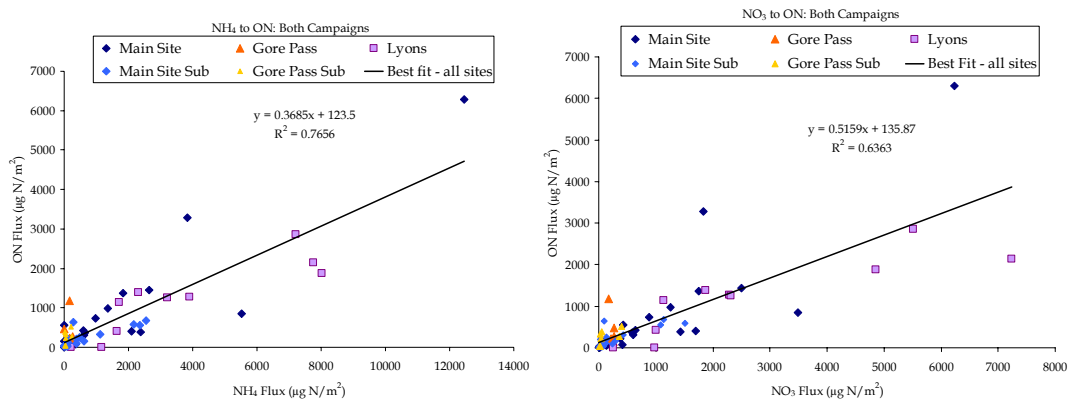


Figure 4.23 Relationship between inorganic N species and organic nitrogen measured during both the spring and summer a) Ammonium and organic nitrogen by site with the best-fit of all data $R^2=0.77$ b) Nitrate and organic nitrogen by site with the best-fit of all data $R^2=0.64$.

4.4.2 Precipitation Amount and Organic Nitrogen Deposition

ON fluxes do not appear to be strongly related to the amount of precipitation received as illustrated in Figure 4.24. In the spring, the maximum ON flux occurs with the maximum amount of precipitation at the Core Site and Lyons, but not at Gore Pass. In summer, Lyons is the only site where the maximum event ON flux occurs with maximum precipitation amount. In Figure 4.24 there isn't a clear trend between the flux and precipitation amount, but the points can be grouped into general trends. The first group is the cluster of points with 5 mm of precipitation or less which have fluxes less than $1500 \mu\text{g N/m}^2$, with the exception of a few points. The second group falls in the range of 10-15 mm of precipitation where the fluxes range from 1500-6500 $\mu\text{g N/m}^2$. There is much more variability in the amount of N received as organic nitrogen per event in this region of the plot. There were few events with more than 15 mm of precipitation so it is difficult to determine how these general trends would change with a larger data set. There is a general trend toward more ON

slight shift between the organic nitrogen and nitrate contribution: ON decreased to 17% and nitrate increased to 37% of total N deposited in the summer. In the spring at Gore Pass, nitrate, ammonium, and ON comprised 49%, 29%, and 22%, respectively, of N wet deposition. In the summer, a shift similar to that at the Core Site occurred in the N breakdown at Gore Pass. However, at Gore Pass a larger shift occurred as the ON contribution increased to 35% and nitrate contribution decreased to 34% of total wet N deposited at the site.

Deposited N budget results from RoMANS (16%-35% organic nitrogen) are fairly comparable to other studies that examined the contribution of organic nitrogen to total nitrogen in precipitation. The amount of ON relative to total N has been found to vary with location. In Southern Quebec it was found that ON was 38% of total nitrogen deposited (Dillon et al., 1991), in the Colorado Front Range 16% of total N was organic (Williams et al., 2001), and in drier areas, like central and western Colorado, 25% of N deposited was thought to be organic (Sickman et al., 2001). While knowing the relative amount of ON is important, very little information can be gathered pertaining to sources and ecosystem availability from a bulk total dissolved organic nitrogen measurement. Further work toward speciation of organic nitrogen compounds would help to determine the sources and likely impacts of organic nitrogen on the ecosystems of concern in RMNP.

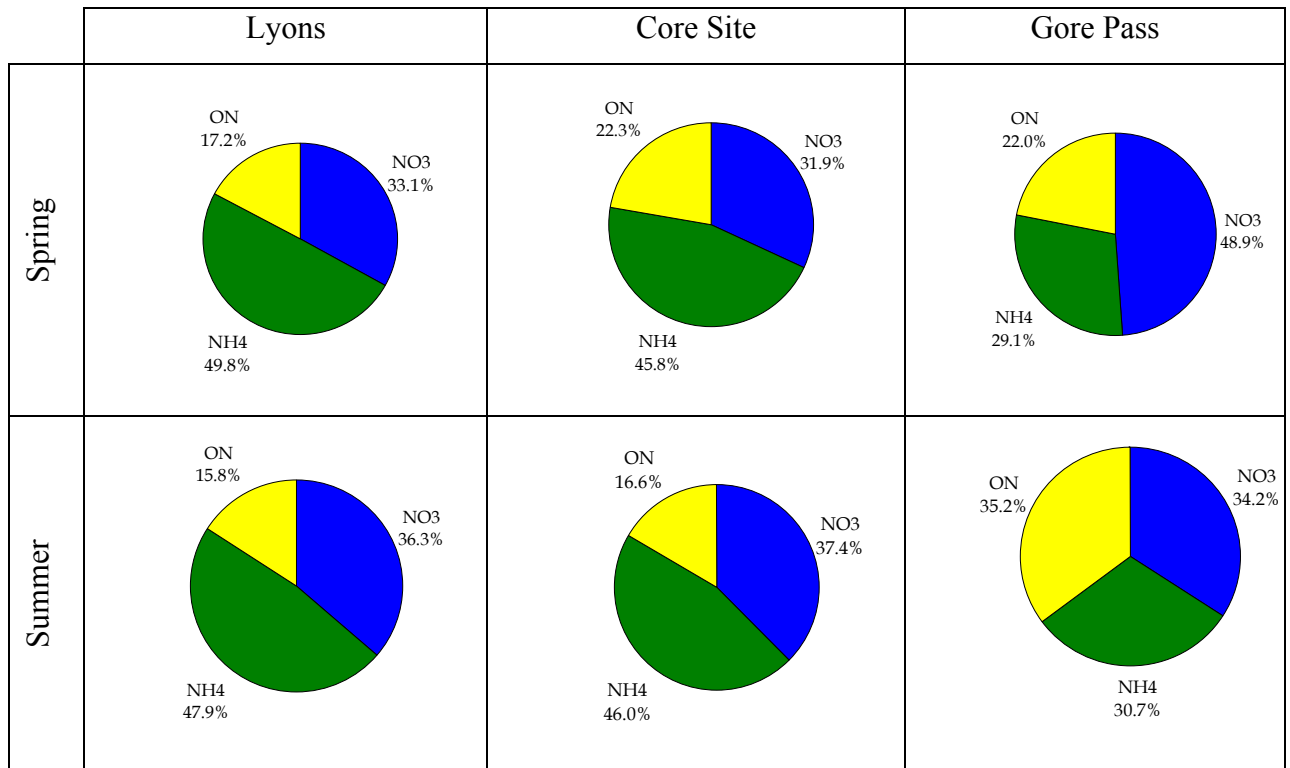


Figure 4.25. Contribution of each N species measured to total N deposition at Lyons, the Core Site, and Gore Pass for both the spring and summer campaign sampling periods.

5 Dry Deposition Discussion

Dry deposition is the removal of atmospheric species, both gaseous and particles, to the surface of the Earth without precipitation. Deposition to all types of surfaces is possible. The rate of deposition is dependent upon the turbulent transport of material to the surface, transport via diffusion (gases) or sedimentation (particles) through the laminar surface sublayer, and the surface reactivity of the species (including, where applicable, stomatal resistance). These parameters are described in terms of an electrical resistance analogy to calculate the deposition velocity which is inversely proportional to the sum of the transport resistances. Dry deposition flux (F_{dry}), the amount of material transferred per unit area and per unit time, is calculated from the deposition velocity (V_d) and concentration (C), parameters that are unique to each species:

$$F_{dry} = V_d C$$

Concentrations were measured during RoMANS while deposition velocities were calculated by CASTNet for sulfur dioxide, nitric acid, and fine particles. The lack of $NH_3(g)$ measurements in the CASTNet network means that CASTNet does not calculate deposition velocities for NH_3 . Since V_d is site specific and the Core Site is the only RoMANS site co-located with a CASTNet site, it is the only site where dry deposition fluxes will be calculated.

5.1 Source of Deposition Velocities

Deposition velocities are modeled with the NOAA Multilayer Deposition Velocity Model (MLM) described by Meyers et al (1998). The model separates the vegetative canopy into 20 layers and only requires input of meteorological data after the inclusion of site survey data. Each CASTNet site is surveyed for input information including type and quantity of vegetation, which includes an estimation of leaf area index (LAI). Finklestein et al. (2000) and Meyers et al. (1998) compared modeled deposition velocities to observations in order to determine if the MLM calculates a representative deposition velocity. Meyers et al. (1998) found that average deposition velocities showed good agreement with little average bias. For specific periods, however, the model under- or over-predicted deposition velocity. Finkelstein et al. (2000) found similar results but also found that the model generally under-predicts higher values of both O₃ and SO₂ deposition velocities during the day and night. It was also found that seasonal and diurnal cycles are reproduced quite well but the times and magnitudes of the average daily peaks are missed. Both of these studies focused on O₃ and SO₂, since HNO₃ observations were only available during the daytime. Meyers et al. (1998) observed that for HNO₃ the model biases the deposition velocity low but the ranges of predicted and observed values are similar.

CASTNet sites measure meteorological conditions for input into the model to calculate deposition velocity. Weekly average concentrations of nitric acid, sulfur dioxide, and fine particles are measured by CASTNet to calculate dry deposition fluxes (Clarke et al., 1997).

Since the focus of the RoMANS project is to determine total N deposition in the park, it is important that dry deposition of ammonia, not currently measured by CASTNet, is taken into account. The deposition velocity for ammonia is not modeled in the MLM because of the bi-directional nature of NH₃ exchange with the environment. Ammonia exchange has been shown to be a result of interaction between physical, chemical, and biological processes (Wyers and Erisman, 1998). In some environments ammonia has been found to be both emitted and deposited depending on atmospheric conditions, concentrations, and the time of day (Langford and Fehsenfeld, 1992; Pryor et al., 2001; Wyers and Erisman, 1998). Flux evaluation in a forest generally shows net deposition unlike agricultural croplands where net emissions are observed (Sutton et al., 1994). The net canopy compensation point, the air concentration below which NH₃ is emitted and above which it is deposited, has been suggested to be near or below 1 µg/m³ for a coniferous forest (Duyzer et al., 1994; Langford and Fehsenfeld, 1992). In semi-natural (not fertilized) and forest ecosystems the compensation point is frequently negligible but exceptions have been observed in very dry conditions (RH<60%) and when an area is subject to large NH₃ concentrations. While NH₃ dry deposition is likely dependent on concentration as well as other factors, there is currently no model available to represent the net flux of NH₃ as ammonia exchange.

The data collected during this study do not allow for calculation of the ammonia deposition velocity based on environmental conditions and properties specifically

important to the ammonia deposition velocity. Instead, to estimate the deposition velocity we examined results from previously published studies that measured deposition velocities of ammonia to see if there was a relationship between the deposition velocities of nitric acid and ammonia or to determine if there was an appropriate fixed value to use. In addition, we compared the CASTNet calculated deposition velocities for HNO₃ to measured values in literature.

Dry deposition velocities have been measured for many species but, since V_d is dependent upon the environmental conditions and changes with location and over time, it is problematic to use a deposition velocity in a time and place other than where it was measured. At one site over the course of a single study (Sievering et al., 2001) a wide range, 0.8 cm·s⁻¹ to 20 cm·s⁻¹, of nitric acid deposition velocities was measured.

Generally, to make a dry deposition calculation, an average deposition velocity is used which is dependent on the time period and timescale of interest. Measurements of V_d provide information about the dependence of V_d on the area, which can be used to test models. However, there is not always good agreement between studies. A consensus on deposition velocities, especially for NH₃, is difficult to find. A literature search revealed some interesting findings regarding measurements of V_d (Table 5.1).

Table 5.1 Deposition velocities of nitric acid and ammonia from a number of studies. Studies where both species were measured are shaded.

Source	Year	Environment	Location	Method	HNO ₃ (cm/s)		NH ₃ (cm/s)	
					Range	Avg	Range	Avg
(Andersen and Hovmand)	1995	forest	Denmark	gradient		1		2
(Zimmermann et al.)	2006	forest	Germany			6.48		3.33
(Pryor and Klemm)	2004	forest - conifer	Germany	REA*		7.5		
(Duyzer et al.)	1994	forest - conifer (Douglas Fir)	The Netherlands	gradient			2-3.0	
(Wyers et al.)	1992	forest - conifer (Douglas Fir)	The Netherlands	gradient				3.2
(Sievering et al.)	2001	forest - conifer (mixed)	Niwot Ridge, CO	gradient	0.8- >20	7.6		
(Sievering et al.)	1994	forest - conifer (mixed)	Southern Germany	gradient		5.5		
(Neiryneck et al.)	2007	forest - conifer (mixed)	Belgium	gradient		4.35		3.0+4.6
(Janson and Granat)	1999	forest – conifer (scots pine)	Northern Sweden	foliar rinse	3-11.0			
(Andersen et al.)	1993	forest - conifer (spruce)	Denmark	gradient				4.5
(Andersen et al.)	1999	forest - conifer (spruce)	Denmark	gradient				4
(Pryor et al.)	2002	forest - deciduous	Midwestern USA	REA		3		
(Meyers et al.)	1989	forest - deciduous (fully leafed)	southeaster n USA	gradient	2.2-6	4		
(Yamulki et al.)	1996	arable	unspecified	unspecified			0.2-2.6	
(Muller et al.)	1993	grassland/ agriculture	UK/ Germany	unspecified	0.4-8.0			
(Nemitz et al.)	2004	heathland	The Netherlands	unspecified		0.424		0.311
(Duyzer)	1994	heathland	The Netherlands	gradient				1.4
(Erisman et al.)	1994	heathland	unspecified	unspecified				0.8
(Goulding et al.)	1998	Winter Wheat	unspecified	unspecified	3.5-13.5			
(Duyzer et al.)	1992	unspecified	unspecified	gradient				3.6
(Ivens et al.)	1988	unspecified	unspecified	unspecified				3.8
(Zimmermann et al.)	2001	unspecified	unspecified	gradient				3.8
(Harrison and Allen)	1991	unspecified	unspecified	unspecified		2.2		2.2

* REA=relaxed eddy accumulation

While the results presented in the table do not provide a clear answer regarding the most appropriate choice for the deposition velocity of ammonia, there is enough evidence to suggest that the deposition velocity of ammonia is typically similar to that of nitric acid. $V_d(\text{NH}_3)$ is certainly at least half and could be equal to $V_d(\text{HNO}_3)$. A conservative estimate that agrees well with Namiesnik et al. (2003) and Nemitz et al. (2004) is $V_d(\text{NH}_3) = 0.7 V_d(\text{HNO}_3)$. This relationship was used to estimate ammonia deposition velocities during RoMANS based on modeled nitric acid deposition velocities.

CASTNet nitric acid deposition velocities during the RoMANS spring campaign period range from 0.859-3.18 $\text{cm}\cdot\text{s}^{-1}$, with an average deposition velocity of 2.01 $\text{cm}\cdot\text{s}^{-1}$. During the summer campaign period, HNO_3 deposition velocities ranged from 1.11-2.31 $\text{cm}\cdot\text{s}^{-1}$, with an average of 1.71 $\text{cm}\cdot\text{s}^{-1}$. These deposition velocities for nitric acid are slightly lower than literature values for similar environments (conifer mixed forest). The highest deposition velocity occurred in the spring while reported values for this type of environment are generally above 4 $\text{cm}\cdot\text{s}^{-1}$. There may be factors unique to the Core Site study area that cause the deposition velocity to be slightly lower or it could be a function of the CASTNet modeling approach. The discrepancy most likely indicates our estimates are conservative for both $V_d(\text{HNO}_3)$ and $V_d(\text{NH}_3)$, which will make our dry deposition estimates conservative as well.

5.2 Variations in Deposition Velocities

Variations in deposition velocity, especially when they co-vary with species concentrations, directly impact dry deposition flux calculations and are important to examine. Average deposition velocities for particles, HNO₃, NH₃, and SO₂ were calculated as a function of time of day for the spring and summer RoMANS field campaign periods. The deposition velocities typically exhibit a regular diurnal variation with maximum values at mid-day and minimum values at night (Figure 5.1). SO₂ doesn't fit this pattern in the spring where a larger V_d occurs during the night. The range of deposition velocities is different for each species, with HNO₃ and NH₃ having the largest range of V_d during both the spring and summer. However, the range of average deposition velocities in the spring is larger compared to the summer, while the average diurnal variability for nitric acid and ammonia deposition velocities is greater during summer.

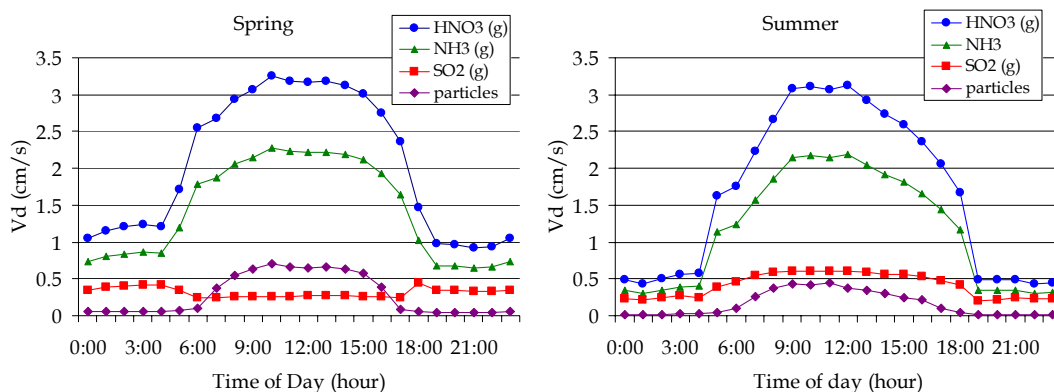


Figure 5.1. Average diurnal variation of deposition velocities for HNO₃, NH₃, SO₂, and particles from continuous gas data and CASTNet deposition velocities.

In addition to the diurnal variations, there are also daily variations which differ between the spring and summer. The daily variations (Figure 5.2, Figure 5.3) don't have a regular pattern but appear to be more a function of the meteorological conditions. The daily maxima and minima during the spring (Figure 5.2) are more extreme compared to the average than in the summer (Figure 5.3). This is likely a function of the drastic changes in temperature and boundary layer stability that occur during the spring in Colorado. Differences between the spring and summer could also be a result of changing environmental conditions (*e.g.*, ground cover, leaf area).

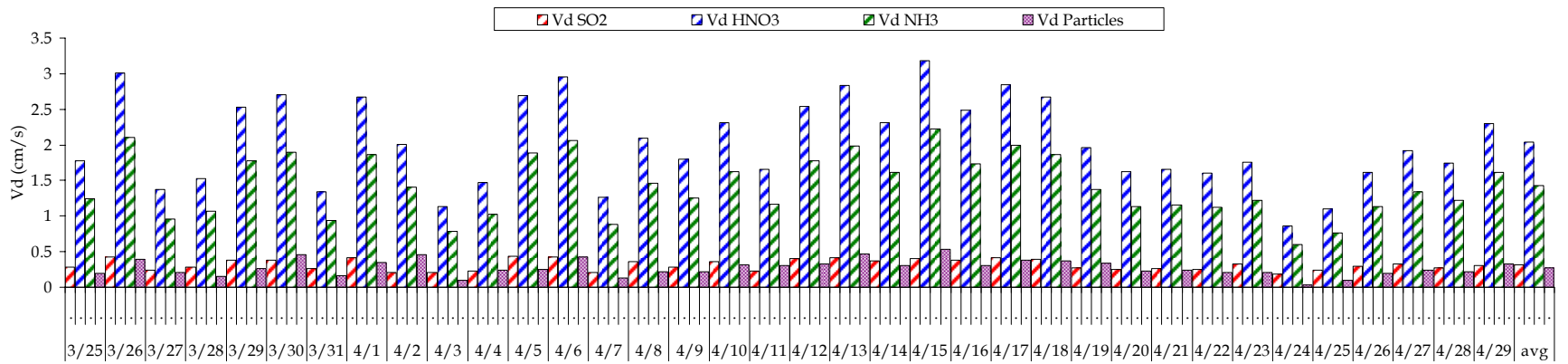


Figure 5.2 Spring deposition velocities for SO₂, HNO₃, NH₃ and particles.

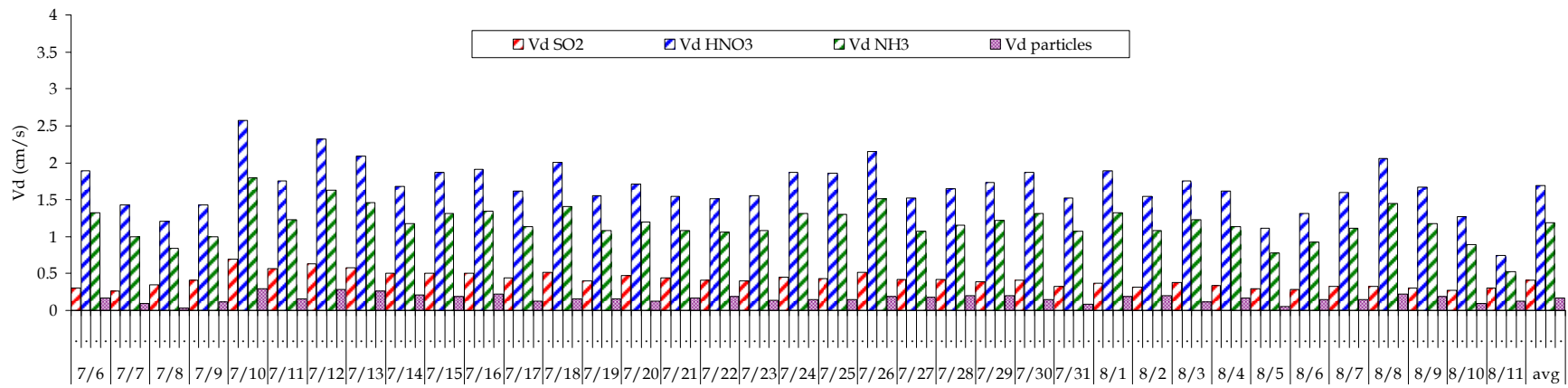


Figure 5.3 Summer deposition velocities for SO₂, HNO₃, NH₃ and particles.

To determine how much the daily deposition velocity changes over the course of a season and from season to season, frequency distributions of deposition velocities for SO₂, HNO₃, and particles were examined. Figure 5.4 shows the distribution of sulfur dioxide daily deposition velocities for the RoMANS spring and summer campaigns. Deposition velocities in the spring are bimodally distributed with values 0.225-0.25 cm·s⁻¹ and 0.40-0.425 cm·s⁻¹ occurring most frequently. In the summer the deposition velocities also have a bimodal distribution but the range of deposition velocities is greater. Nitric acid deposition velocities are plotted in Figure 5.5. In the spring the distribution of nitric acid deposition velocities is bimodal while in the summer there is a high frequency of deposition velocities in the 1.75-2.0 cm·s⁻¹ bin. Unlike for SO₂ the spring has a wider distribution of deposition velocities than the summer for HNO₃ and for particles (Figure 5.6). In the histogram for particle deposition velocities we see that the spring deposition velocities peak slightly higher than the summer. Average daily particle deposition velocities in the summer are skewed lower compared to the spring. Since $V_d(\text{NH}_3)$ was calculated simply as 0.7 times $V_d(\text{HNO}_3)$, the distribution is not shown.

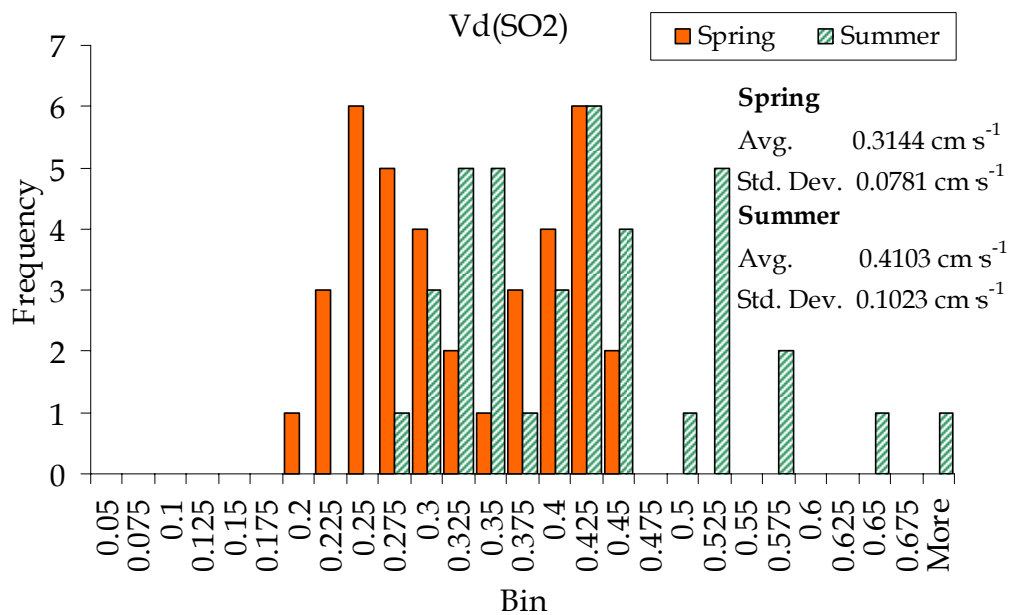


Figure 5.4 Histogram of daily averaged deposition velocities for SO₂ for both the spring (orange) and summer (green stripes) study periods. X-axis bin values are the upper range for the bin in cm·s⁻¹.

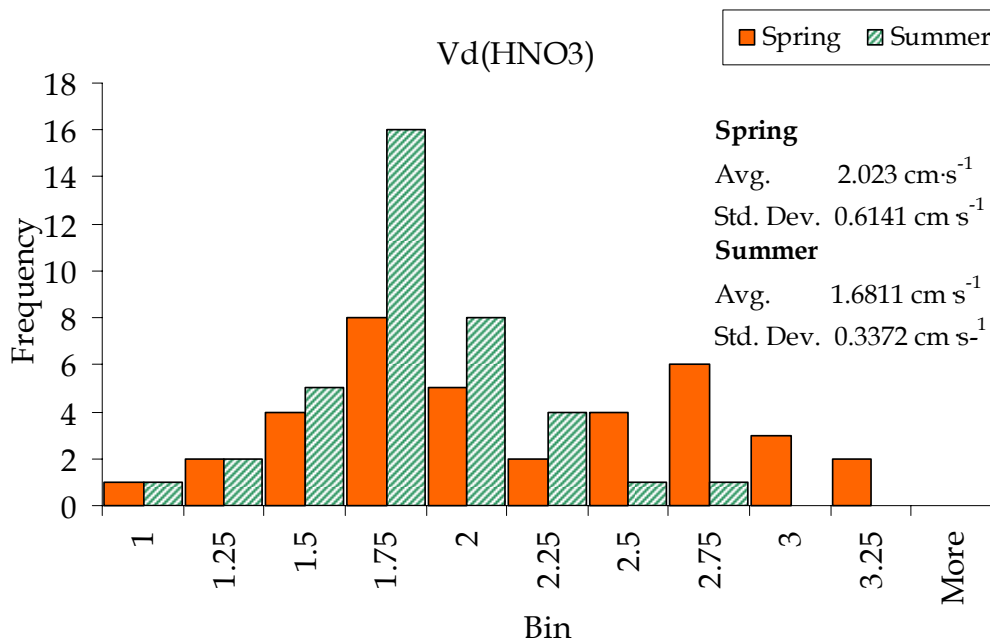


Figure 5.5 Histogram of HNO₃ deposition velocities for both the spring (orange) and summer (green stripes) study periods. X-axis bin values are the upper range for the bin in cm·s⁻¹.

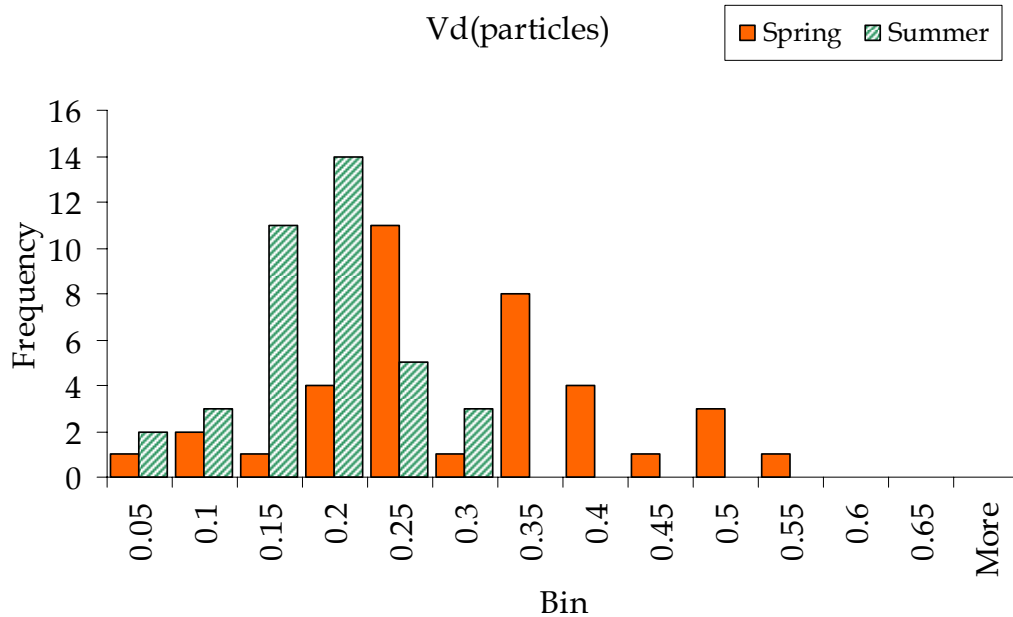


Figure 5.6 Histogram of particle deposition velocities for both the spring (orange) and summer (green stripes) study periods. X-axis bin values are the upper range for the bin in $\text{cm}\cdot\text{s}^{-1}$.

5.3 Averaging Timescales of Concentration and Deposition Velocity

During RoMANS, two methods were used to determine ambient gas concentrations: continuous gas monitors, which collect 1-minute data, and URG denuders, which collect 24-hr integrated samples. Dry deposition fluxes calculated using concentrations measured on different timescales may differ if there is a temporal correlation between a species concentration and its deposition velocity. Positive (negative) correlations between deposition velocity and concentration produce higher (lower) deposition fluxes if calculated at high time resolution compared to calculations made using time-averaged values. If deposition velocities and concentrations vary in time but are independent of each other, deposition fluxes will be unaffected by the choice of averaging timescales. To determine the importance of the averaging time, both daily averages and hourly averages of V_d and concentrations of ammonia were utilized. Daily averages of both deposition velocity and

concentration were used to calculate a daily flux, while hourly averages were used to find hourly fluxes which were then averaged over the same time period as the daily averages to get a daily dry deposition flux. Results from the two calculation methods were then compared for ammonia:

$$F_{24} = \langle V_d \rangle_{24} \langle C \rangle_{24} \text{ compared to } F'_{24} = \langle V_d \cdot C \rangle_{24} \quad \text{where } V_d \text{ and } C \text{ are hourly data}$$

Figure 5.7 compares the deposition fluxes calculated by the two methods for spring and summer. Agreement between these two methods of calculating the dry flux is very good. On most days the fluxes were equivalent. The fluxes varied the most during the summer when concentrations had a greater diurnal variation (Figure 5.8) causing the timescale over which concentration was averaged to have a larger impact.

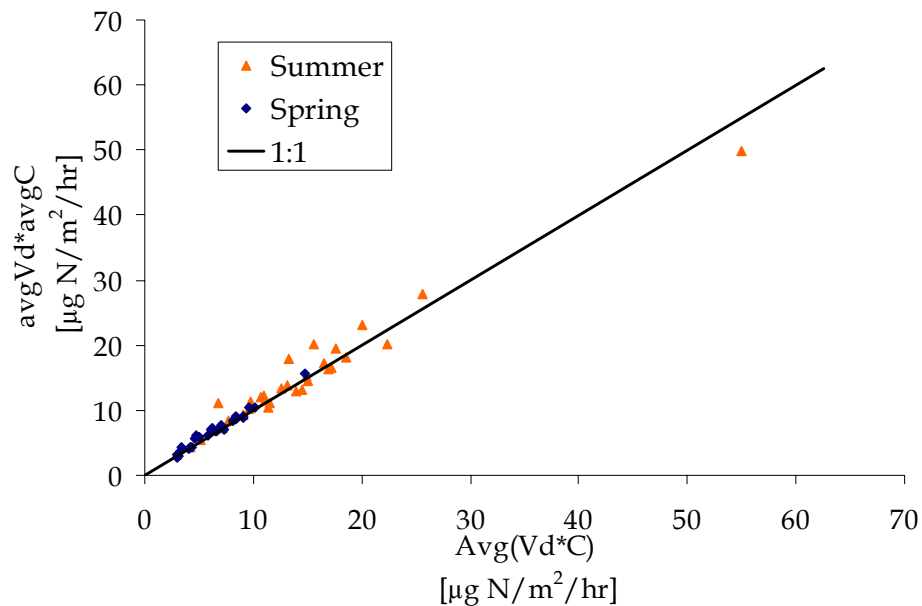


Figure 5.7 Comparison of the dry deposition fluxes calculated by each averaging method of NH₃.

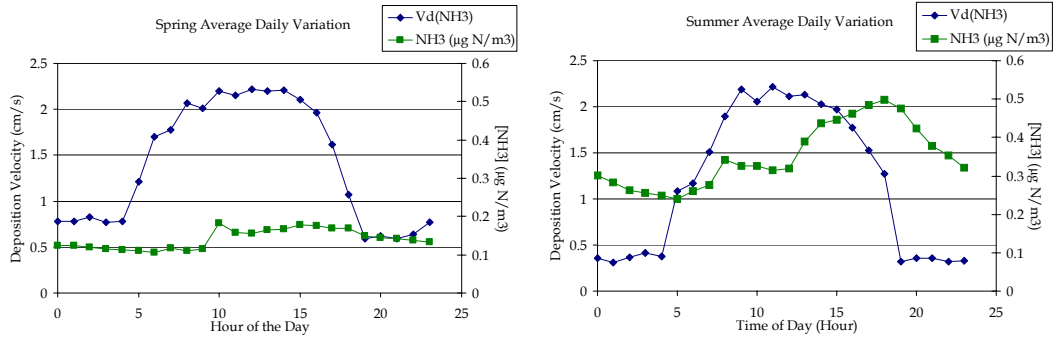


Figure 5.8. Average diurnal variation for each study period of NH₃ concentration (green) and NH₃ deposition velocity (blue).

In both the spring and summer, the peak time of day for the deposition velocity and the concentration do not coincide (Figure 5.8). NH₃ concentrations tend to peak later in the day than do NH₃ deposition velocities. In addition, the range of deposition velocity is greater than concentration especially in the spring where the average concentration oscillates between 0.1 $\mu\text{g N}\cdot\text{m}^{-3}$ and 0.18 $\mu\text{g N}\cdot\text{m}^{-3}$ compared with 0.25 $\mu\text{g N}\cdot\text{m}^{-3}$ and 0.5 $\mu\text{g N}\cdot\text{m}^{-3}$ in the summer. If NH₃ concentrations and deposition velocities co-varied, one would expect dry deposition fluxes calculated from daily average values to differ significantly from fluxes based on higher time resolution data. Because the concentrations and deposition velocities vary independently of each other, the difference is small.

To determine the influence of averaging over a larger timescale, monthly and weekly averages were compared. In Table 5.2 the influence of averaging timescales on total dry deposition for a month is presented. The daily total deposition was calculated using daily averaged deposition velocities and concentrations. Weekly averages were taken from Tuesday to Tuesday during each study period of the RoMANS campaign and resulted in averages for 4 weeks (for both the spring and summer study) for

concentrations and deposition velocities. These weekly averages were used to calculate a weekly average deposition flux. The weekly average depositions were then added together to get a monthly deposition based on weekly averages (column labeled weekly). In addition, monthly averages of concentration and deposition velocity were taken over the same 4-week period to get a monthly deposition based on the monthly average (column labeled monthly).

Table 5.2 Influence of averaging timescale on total deposition. Column titles correspond to the timescale over which averages of deposition velocity and concentration were taken.

		Daily	Weekly	Monthly	Daily to Weekly	Daily to Monthly
		$\mu\text{g N (or S)}/\text{m}^2$	$\mu\text{g N (or S)}/\text{m}^2$	$\mu\text{g N (or S)}/\text{m}^2$	% difference	
NO ₃ ⁻ (p)	Spring	330.84	364.13	478.56	-9.6%	-36.5%
	Summer	151.59	144.19	130.61	5.0%	14.9%
HNO ₃ (g)	Spring	2816.05	2778.87	2666.62	1.3%	5.5%
	Summer	5393.54	5538.40	5096.97	-2.7%	5.7%
SO ₄ ²⁻ (p)	Spring	922.14	931.40	1069.63	-1.0%	-14.8%
	Summer	859.08	874.64	817.32	-1.8%	5.0%
SO ₂ (g)	Spring	621.13	608.38	705.25	2.1%	-12.7%
	Summer	836.95	871.51	757.39	-4.0%	10.0%
NH ₄ ⁺ (p)	Spring	997.73	1053.24	1260.37	-5.4%	-23.3%
	Summer	1064.79	1062.72	942.30	0.2%	12.2%
NH ₃ (g)	Spring	4839.17	4628.18	4931.85	4.5%	-1.9%
	Summer	12356.94	10463.99	9355.47	16.6%	27.6%

The agreement between the deposition fluxes calculated from daily, weekly, and monthly averages is different for each species but they don't compare as well as for the hourly and daily average comparison presented above. There is not a consistent pattern of increasing or decreasing deposition with averages over larger time scales. Even trends for the same species do not stay the same from spring to summer. Differences between daily averaged and weekly average deposition are smaller for all species than between daily averaged and monthly averaged deposition. The largest difference in total flux is 36.5% for nitrate during the spring study period. The smallest difference in total flux is 0.2% for ammonium during the spring. Most differences are less than 20% for all timescale comparisons, suggesting that the value of making high-resolution temporal measurements of parameters needed to calculate deposition velocities is of limited value if a determination of flux budgets is the only objective.

5.4 Dry Deposition

Dry deposition changes daily based on gas concentrations (measured with the URG), so the same factors affecting airborne concentrations of each species will also affect the amount of deposition occurring. As discussed previously, the deposition velocity also plays a role in the amount of material that is deposited. As shown in Figure 5.6 and Figure 5.7, the deposition changes daily, sometimes quite significantly. Note the difference in scales between the two campaigns: the y-axis for the timeline of summer daily dry deposition flux goes up to 1200 $\mu\text{g N or S/m}^2/\text{day}$ compared with the spring where the maximum y-axis value is 700 $\mu\text{g N or S/m}^2/\text{day}$.

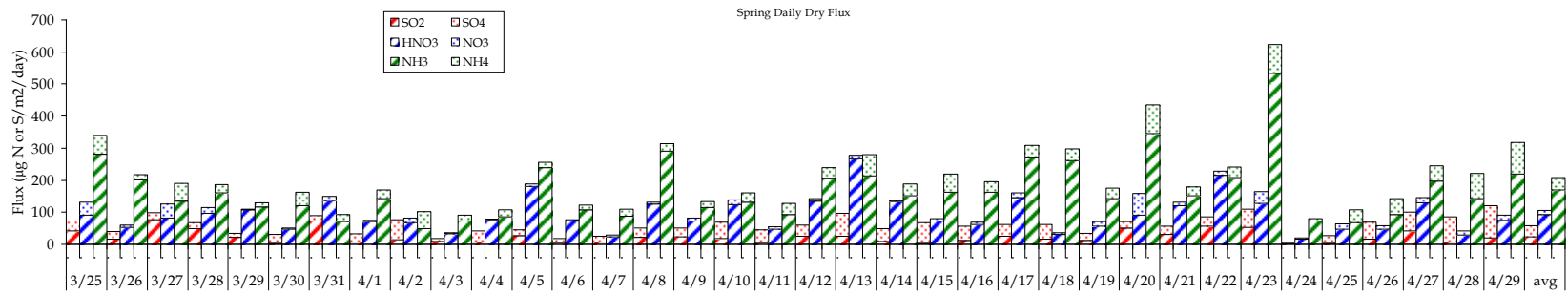


Figure 5.9 Bar chart of spring dry daily deposition of each particulate species (dots) with appropriate gas (stripes) stacked for total of the species group. Red: $\text{SO}_4^{2-}/\text{SO}_2$, Blue: $\text{NO}_3^-/\text{HNO}_3$, and Green: $\text{NH}_4^+/\text{NH}_3$

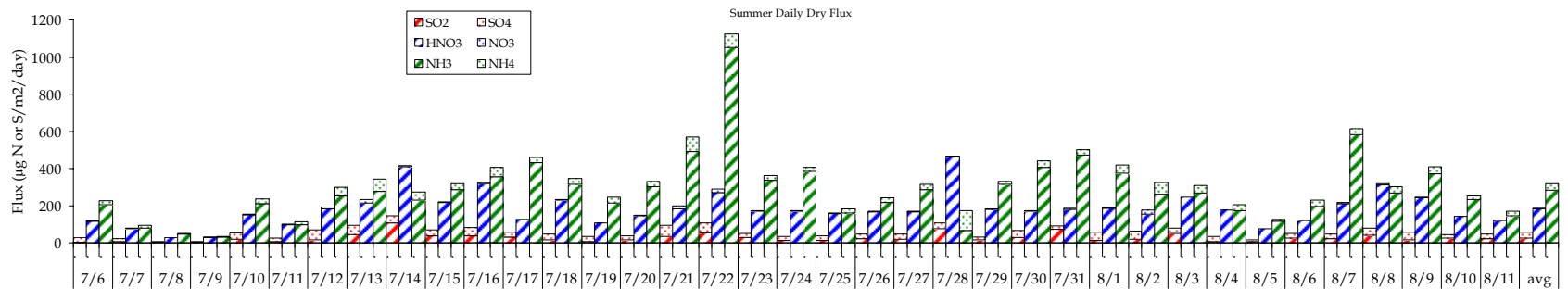


Figure 5.10 Bar chart of summer dry daily deposition of each particulate species (dots) with appropriate gas (stripes) stacked for total of the species group. Red: $\text{SO}_4^{2-}/\text{SO}_2$, Blue: $\text{NO}_3^-/\text{HNO}_3$, and Green: $\text{NH}_4^+/\text{NH}_3$

On most of the sampling days the deposition of ammonium plus ammonia is greater than deposition of nitric acid plus nitrate. The deposition velocity of nitric acid is always greater than ammonia while the deposition velocities of particulate nitrate and ammonium are the same. This indicates that the species concentrations are driving the relative deposition amounts of reduced and oxidized nitrogen. Nitrate/nitric acid deposition exceeded ammonia/ammonium deposition for only four days in the spring campaign and only for three days during the summer.

In summer deposition of the gaseous species was greater than the spring, while particulate species deposition was greater in the spring. Table 5.2 summarizes the total deposition of individual species for spring and summer at the Core Site. These changes are driven by concentrations for the gas phase species and deposition velocities for particles. Higher gas concentrations in the summer increase the deposition of these species while reduced particle deposition velocities and particle concentrations of N species decrease deposition of particulates. In general, the deposition of gases appears to be mainly a function of the concentrations. In Figures 5.11 to 5.13, timelines are shown for the gaseous species concentrations, with deposition velocities and fluxes on the same plot. In these plots we can see that, generally, when the concentration increases the deposition increases similarly. However, there are several occasions when the deposition flux doesn't follow the concentration. These cases are best seen in the particle data; particle nitrate is shown in Figure 5.14, particle ammonium is shown in Figure 5.15, and particle sulfate is shown in Figure 5.16. Data from 4/25 and 7/31 are examples where particle nitrate

concentrations increase but a similar increase is not seen in the deposition flux. This is more evident in the plot of ammonium concentration, deposition velocity, and deposition flux. On 4/15 even though the concentration of ammonium stays fairly consistent, the higher deposition velocity results in a higher flux.

Table 5.3 Dry deposition totals by species for both the summer and spring campaigns at the Core Site. Units are $\mu\text{g N}$ or S/m^2 .

	Spring	Summer
NO_3^- (p)	478.36	181.45
HNO_3 (g)	3325.22	6704.37
NH_4^+ (p)	1401.07	1261.44
NH_3 (g)	6109.74	14723.54
SO_4^{2-} (p)	1294.32	1086.03
SO_2 (g)	840.83	979.98

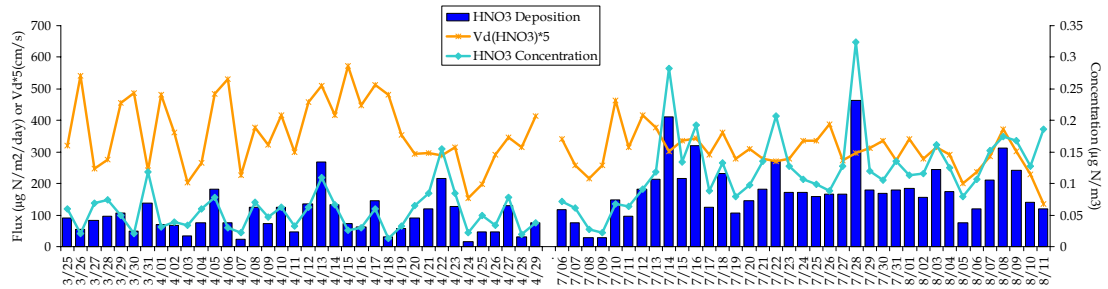


Figure 5.11 Timelines of deposition flux (blue bar), deposition velocity (orange), and concentration (light blue line) for nitric acid. The deposition velocity was multiplied by a factor of 5 so all three parameters could be shown on the same plot.

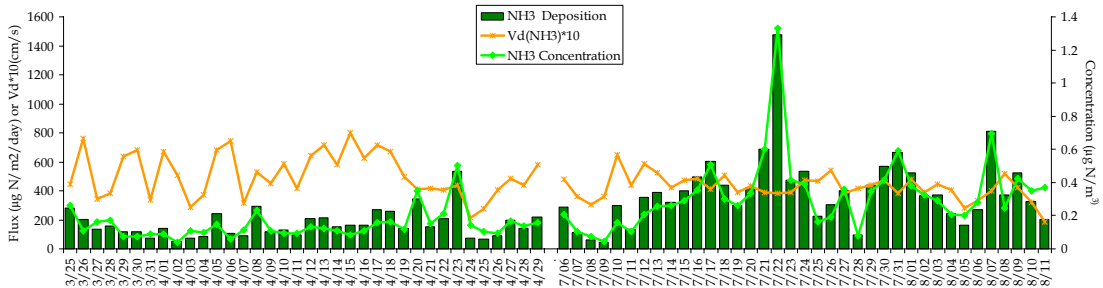


Figure 5.12 Timelines of deposition flux (green bar), deposition velocity (orange), and concentration (light green line) for ammonia. The deposition velocity was multiplied by a factor of 10 so all three parameters could be shown on the same plot.

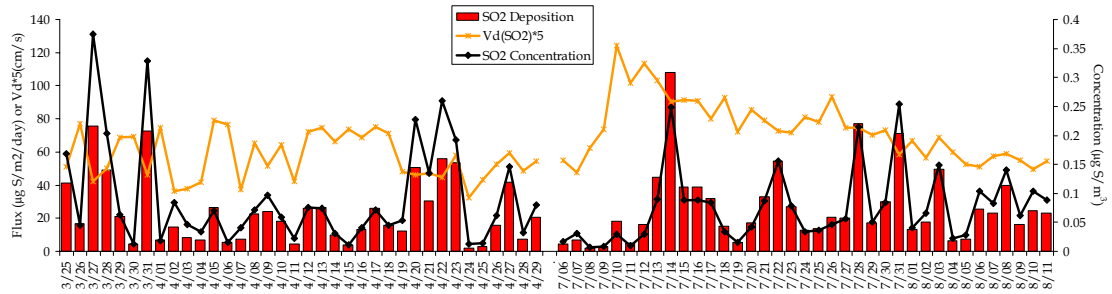


Figure 5.13 Timelines of deposition flux (red bar), deposition velocity (orange), and concentration (black line) for sulfur dioxide. The deposition velocity was multiplied by a factor of 5 so all three parameters could be shown on the same plot.

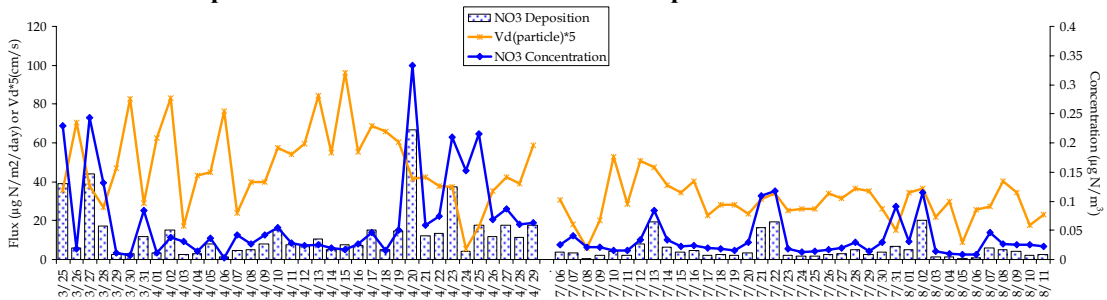


Figure 5.14 Timelines of deposition flux (bar), deposition velocity (orange), and concentration (blue line) for fine particle nitrate. The deposition velocity was multiplied by a factor of 5 so all three parameters could be shown on the same plot.

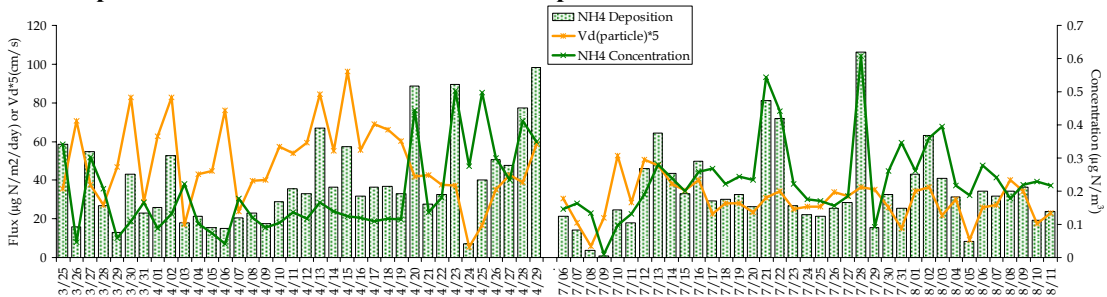


Figure 5.15 Timelines of deposition flux (bar), deposition velocity (orange), and concentration (green line) for fine particle ammonium. The deposition velocity was multiplied by a factor of 5 so all three parameters could be shown on the same plot.

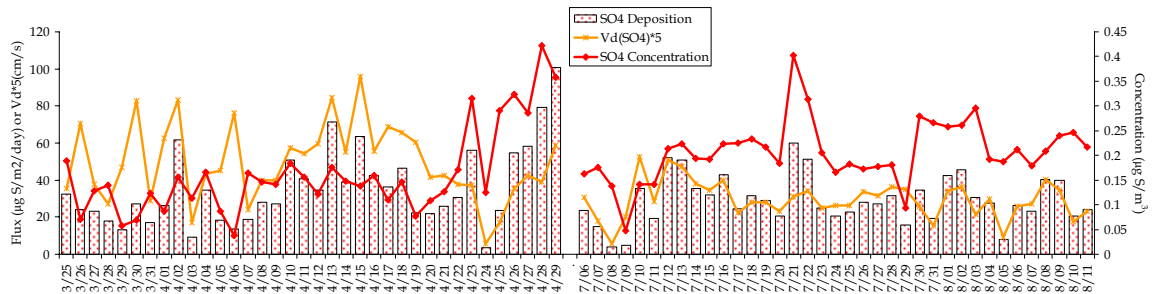


Figure 5.16 Timelines of deposition flux (bar), deposition velocity (orange), and concentration (red) for fine particle sulfate. The deposition velocity was multiplied by a factor of 5 so all three parameters could be shown on the same plot.

5.5 Comparison with Historical Dry Deposition Data

A comparison of dry deposition totals from the RoMANS campaigns with historical averages indicates RoMANS deposition was lower than average for all species measured by CASTNet for both study periods (Table 5.4). The historical average was calculated using weekly data for the weeks overlapping the RoMANS study periods from 1995-2005. Deposition of gases had a much larger difference than particles. Also shown in Table 5.4 are the dry deposition totals for the weeks overlapping RoMANS from CASTNet during 2006. The dry deposition calculations made from data at the RoMANS Core Site in general do not compare well with the CASTNet deposition totals. The RoMANS Core Site dry deposition and CASTNet 2006 dry deposition compare well for nitrate in both the spring (6% difference) and summer (0.4% difference) and for sulfate only in the spring (3% difference). RoMANS dry deposition only compares well with historical data for NH_4 (8% difference) in the spring; in the summer there was a 39% difference. The comparison of CASTNet 2006 data with the historical average was generally better, with the best comparisons in the spring for nitric acid (5% difference) and sulfur dioxide (8% difference) and in the summer for sulfate (9% difference) and sulfur dioxide (9% difference). For all comparisons there was not a data set that was consistently greater or less than any other. The worst comparisons between the RoMANS and CASTNet 2006 data sets occurred for sulfur dioxide (92% difference) and nitric acid (76% difference) for summer dry deposition. In the summer the comparison between the historical data and RoMANS data was generally not good for all species with the difference between dry depositions ranging from 39% to 86%. The comparison

between the summer CASTNet and historical average was generally the best if nitrate is not included.

Table 5.4 Comparison of dry deposition during RoMANS with historical CASTNet data average from 1995-2005 for the same periods as RoMANS as well as measurements made by CASTNet during the period overlapping RoMANS in 2006. Units are in μg of N (or S)/ m^2 .

	Spring			Summer		
	Average	RoMANS	CASTNet 2006	Average	RoMANS	CASTNet 2006
NO ₃	616.18	478.36	451.86	338.90	181.45	180.75
HNO ₃	6053.10	3325.22	5758.02	12823.27	6704.37	14961.96
SO ₄ ²⁻	1787.45	1294.32	1335.28	2036.30	1086.03	1869.39
SO ₂	1251.37	840.83	1351.47	2467.69	979.98	2702.95
NH ₄ ⁺	1517.75	1401.07	1164.78	1871.42	1261.44	1553.04
NH ₃		6109.74			14723.54	

6 Total Fluxes

6.1 *Wet vs. Dry*

The total amount of dry deposition flux was significantly smaller than wet deposition flux for all species measured during both the spring (Figure 6.1) and summer (Figure 6.2) at the Core Site. Dry deposition of all particulate species decreased in the summer, while gaseous dry deposition and wet deposition increased. In the spring the particulate deposition of nitrate and ammonium was smaller than gaseous nitric acid and ammonia deposition. Sulfate dry deposition, however, was greater than sulfur dioxide dry deposition. Wet deposition fluxes of nitrate, ammonium, organic nitrogen, and sulfate all increased from spring to summer. Ammonium increased by 101.9%, nitrate by 189.9%, ON by 32.8%, and sulfate by 38.1%. Dry deposition fluxes of nitric acid, ammonia, and sulfur dioxide also increased in summer by 101.6%, 72.1%, and 14.2%, respectively. By contrast, dry deposition fluxes of particulate nitrate, ammonium, and sulfate decreased by 62.1%, 10.0%, and 19.2%, respectively.

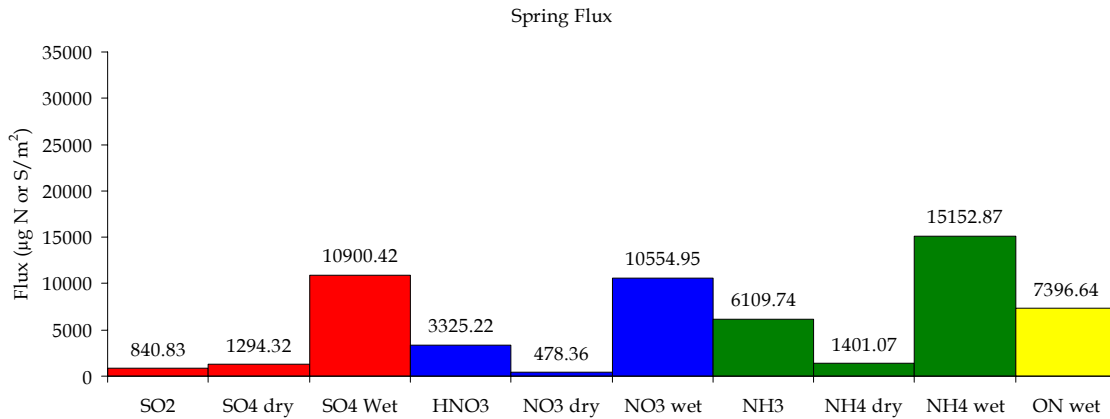


Figure 6.1 Core Site spring deposition fluxes broken down for each species by dry gaseous, dry particle, and wet.

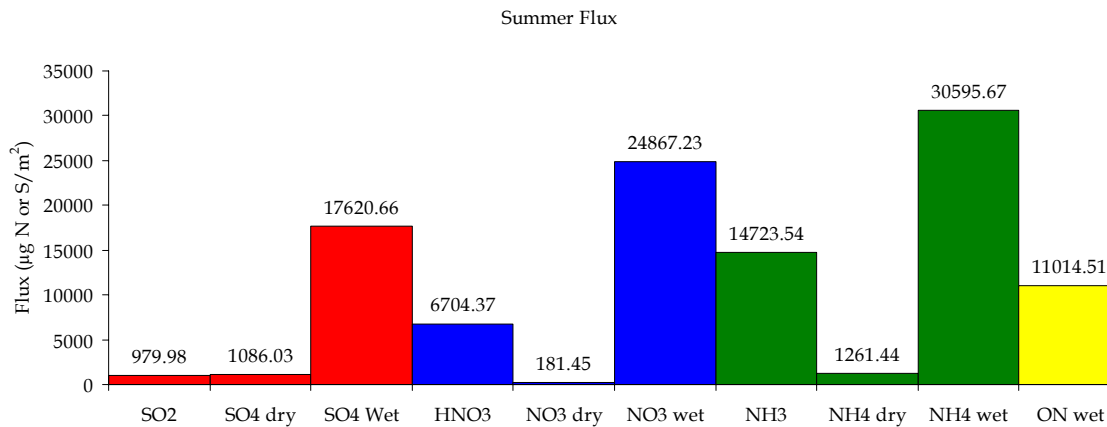


Figure 6.2 Core Site summer deposition fluxes broken down for each species by dry gaseous, dry particle, and wet.

In the spring a total of 45,262 µg/m² of nitrogen was deposited along with 13,036 µg/m² of sulfur. In the summer a total of 95,077 µg/m² of nitrogen and 19,687 µg/m² of sulfur was deposited. There is a much greater difference from the spring to summer for nitrogen compared to sulfur (Figure 6.3).

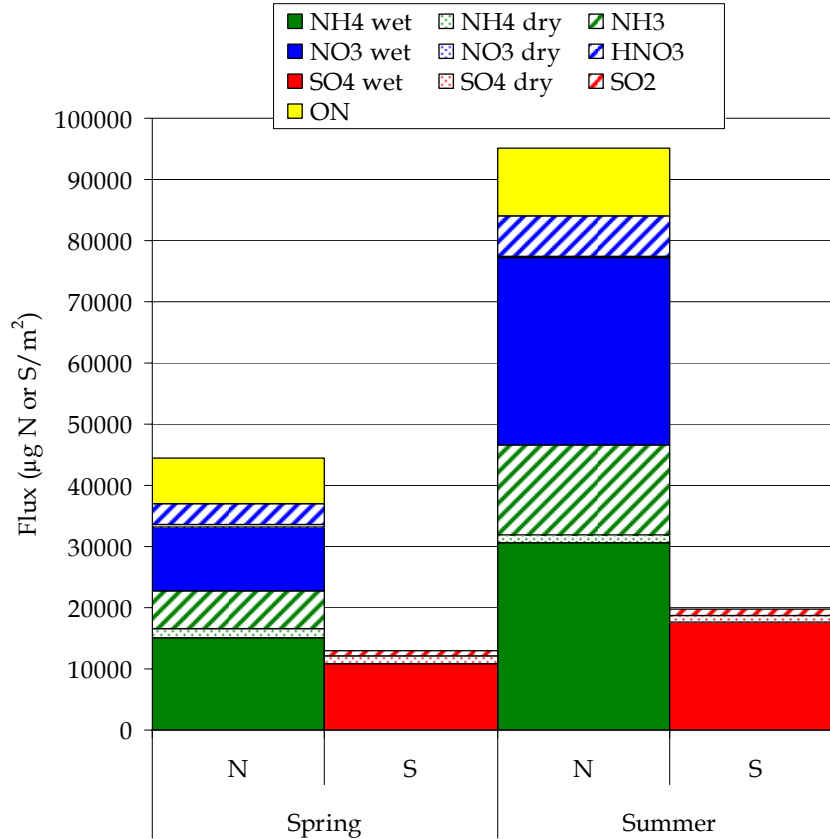


Figure 6.3. Total N and S flux for the Core Site showing the amount of deposition due to each species and process.

6.2 Core Site Nitrogen Deposition Budget

As seen earlier, wet deposition is the major process by which N is deposited. In the spring, only 25.5% of measured N deposition occurred by dry processes (Figure 6.4): 13.8% from NH₃, 7.5% from HNO₃, 3.2% from NH₄⁺(p), and 1% from NO₃⁻(p). NH₄⁺ wet deposition is greater than all the dry processes combined with 34.1% of N, followed by wet NO₃⁻ with 23.8% and wet ON with 16.7%. The summer (Figure 6.5) is very similar to the spring with slightly more wet deposition of NO₃⁻ (27.8%), but wet deposition of NH₄⁺ still is the largest contributor with 34.2% of N deposition. ON still accounts for an important fraction of the total measured N deposited (12.3%)

but is somewhat less than dry deposition of $\text{NH}_3(\text{g})$ which contributes 16.5%. In the summer, approximately 25% of measured N deposition occurs from dry processes, with 16.5% from NH_3 , 7.5% from HNO_3 , 1.4% from $\text{NH}_4^+(\text{p})$, and 0.20% from NO_3^- (p). During both spring and summer, ammonia deposition is about twice nitric acid deposition indicating the important role it plays in the N budget and providing support for expanded measurements to the existing network of gaseous measurements by CASTNet.

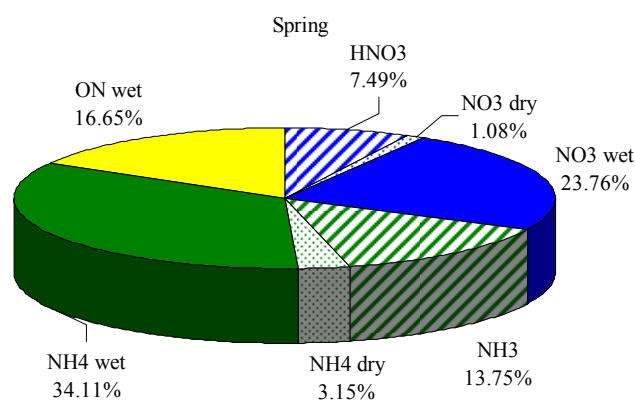


Figure 6.4 Fraction of each nitrogen species that contributes to total N deposition at the Core Site during the spring RoMANS campaign.

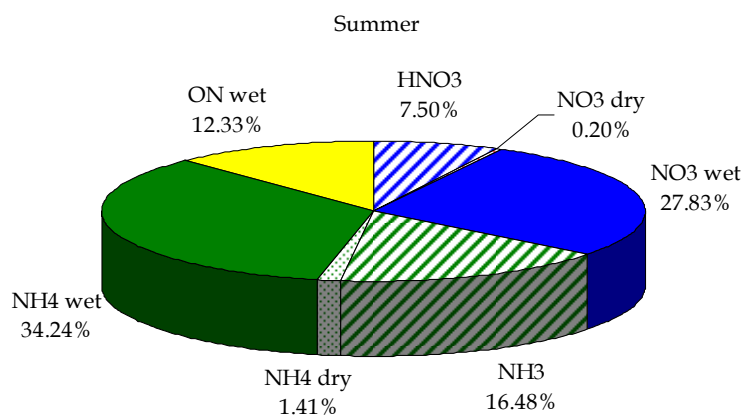


Figure 6.5 Fraction of each nitrogen species that contributes to total N deposition at the Core Site during the summer RoMANS campaign.

Dry NH₃ and wet ON deposition are not routinely measured but are the third and fourth largest contributors to N deposition (Figure 6.6). In both seasons combined they comprise approximately 30% of the total N deposition budget at the Core Site.

Springtime wet ON deposition is 16.7% of total N deposited while NH₃ dry deposition comprises 13.8%. Summertime dry NH₃ deposition is 16.5% and wet ON deposition is 12.3% of total N deposition. It is important to recognize the contribution these species are making to the critical load in the park as steps are taken to reduce N deposition.

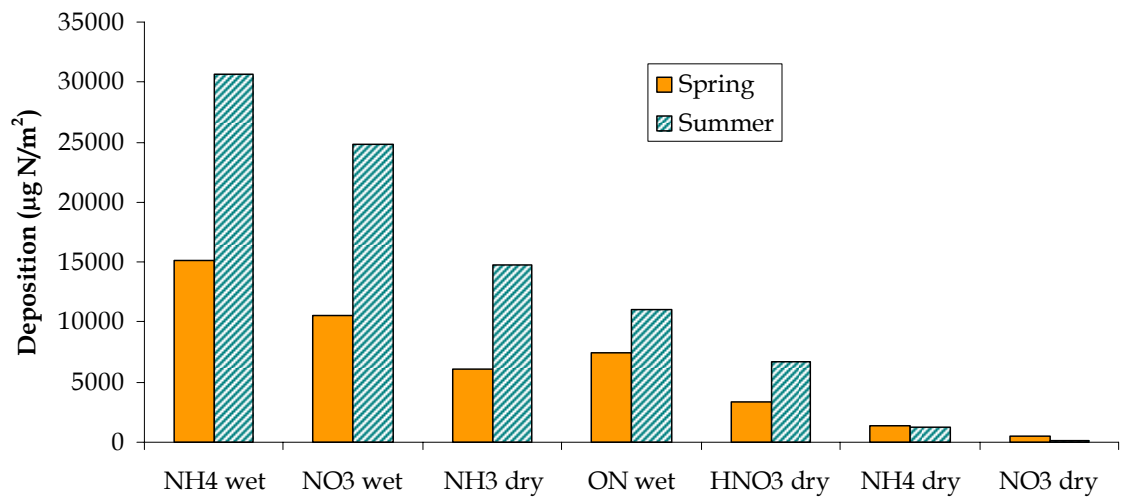


Figure 6.6 Nitrogen deposition totals by species and pathway in order of contribution to total N deposition at the Core Site.

In addition, dry deposition of ON, not measured during RoMANS, is another unknown contributor to N deposition. Little information is known about the composition of ON deposited through wet and dry pathways. As discussed earlier, dry deposition is species-dependent, and the lack of knowledge about the species present, or their concentrations, makes estimating the amount of dry ON deposition flux difficult. In addition, very little is known about the deposition velocities of ON

species. Some work has been done to investigate the deposition of several ON species (Farmer et al., 2006).

Alkyl nitrates and multifunctional alkyl nitrates (RONO_2), peroxy acyl ($\text{RC(O)O}_2\text{NO}_2$), and peroxy nitrates (RO_2NO_2) dry deposition fluxes were measured using eddy covariance along with HNO_3 fluxes (Farmer et al., 2006). Deposition velocities were reported over a range in which 80% of that data was observed. Deposition velocities for HNO_3 were in the range -1.2 to $8.2 \text{ cm}\cdot\text{s}^{-1}$. The alkyl nitrate group had deposition velocities in the range 1.3 to $18 \text{ cm}\cdot\text{s}^{-1}$, while the peroxy acyl and peroxy nitrate deposition velocities were in the range of -0.57 to $6.3 \text{ cm}\cdot\text{s}^{-1}$. These deposition velocities indicate that dry deposition of some organic species may be appreciable and may be an important factor in N deposition.

Using data from the RoMANS study we can compare N deposition inputs with the recently established critical load for N deposition in RMNP. Total N deposition for both RoMANS campaigns was measured to be $133,767 \mu\text{g N/m}^2$ or 1.34 kg N/ha . This total includes both dry deposition and wet deposition of ON which was not included in the critical load estimate. Using just wet deposition of nitrate and ammonium, N deposition during the RoMANS study was found to be 0.81 kg N/ha which is still more than half the annual critical load in only 10 weeks of measurements. Both of these deposition amounts from just 10 weeks of measurements are much closer to the critical load of 1.5 kg N/ha/yr than expected.

This emphasizes the need to measure the full annual cycle of deposition in order to better observe annual N inputs to RMNP ecosystems.

7 Summary and Conclusions

A network of air quality measurement sites stretching across much of Colorado was operated during the 2006 Rocky Mountain Airborne Nitrogen and Sulfur (RoMANS) Study. The highest measurement density and the most sophisticated and temporally-resolved measurements were made at sites in and near Rocky Mountain National Park. The RoMANS study included two major field campaigns, one in spring and one in summer. Precipitation samples were collected during RoMANS to quantify wet deposition of ammonium, nitrate, organic nitrogen, and sulfate. In addition to precipitation measurements, gaseous concentrations of ammonia, nitric acid, and sulfur dioxide and fine particle ($PM_{2.5}$) measurements were made to examine spatial and temporal gradients in pollutant concentrations. These concentration measurements were combined with modeled dry deposition velocities for the RoMANS core study site in order to calculate dry deposition amounts at that location.

Considerable differences in precipitation amount and in deposition fluxes of various N and S species were observed between the spring and summer campaigns and across the RoMANS measurement network. Within RMNP, spring wet deposition was dominated by a single, large upslope snowfall in late April. This event contributed 84% of NH_4^+ , 80% of NO_3^- , and 79% of SO_4^{2-} of the total spring wet deposition at the RoMANS core study site and also dominated wet deposition fluxes at many other

network sites. Wet deposition in summer tended to be more localized. Summer wet deposition in RMNP featured important contributions from many individual rainfall episodes. Total wet deposition measured during summer was substantially higher than during spring, with an increase of approximately 114% in N deposition and 46% in S deposition.

The relative contributions of oxidized and reduced nitrogen to total N wet deposition changed across the RoMANS network. Higher ratios of ammonium deposition compared to nitrate deposition were measured at eastern network sites.

Organic nitrogen contributed from 16%-35% of wet N deposition measured at the RoMANS core study site in RMNP. The average contribution during the spring (summer) campaign was 20.5% (22.5%). The RoMANS dataset illustrates the importance of organic nitrogen deposition within the park. The high contributions observed suggest that more routine monitoring of this parameter is warranted.

Meteorological measurements made by the CASTNet program at the RoMANS core study site were used to model dry deposition velocities of nitric acid and fine particles. The dry deposition velocity for gaseous ammonia was assumed to equal 70% of the nitric acid velocity based on a review of past studies where both values were measured. By combining daily concentrations of gas and particle species measured during RoMANS with modeled dry deposition velocities, we were able to estimate dry deposition fluxes for key species. Dry deposition of ammonia +

ammonium was generally determined to be greater than nitric acid + nitrate deposition. The dry deposition of particles decreased in the summer while dry deposition of gases increased. This reflected, in part, a change in phase partitioning of N species observed between spring and summer. Warmer conditions in summer tended to push the partitioning of oxidized and reduced inorganic nitrogen toward the gas phase species ammonia and nitric acid. The higher deposition velocities of these gases produced summer dry deposition estimates higher than those determined for spring.

Dry deposition fluxes of NH_3 were much larger than dry deposition fluxes for any other species during both the summer and winter study periods. As in the case of wet organic nitrogen deposition, the RoMANS study provided a first look at this important and previously unquantified piece of the N deposition budget. Gaseous nitric acid deposition was second in importance among dry deposition pathways. Much smaller inputs were provided by dry deposition of fine particle ammonium and nitrate.

Dry deposition velocities vary over the course of a day, from day to day, and from season to season. The CASTNet program currently collects high time resolution meteorological data in order to calculate temporal changes in modeled species deposition velocities. Unlike RoMANS, the CASTNet routine monitoring network collects species averaged over weekly time intervals. During RoMANS, measurements of species concentrations on timescales ranging from once per minute

to once daily were undertaken. In order to determine whether correlations between species concentrations and their deposition velocities result in biased estimates of dry deposition fluxes, we compared deposition fluxes determined for different averaging timescales. Variations in averaging time from hourly to daily did not appear to significantly change estimated fluxes. Changes start to appear when concentrations and deposition velocities are averaged over a longer time scale such as weekly or monthly.

At the RoMANS Core Site, dry deposition was a much smaller contributor than wet deposition to total inputs of N and S. During both spring and summer, wet deposition of ammonium represented the largest N input followed by wet deposition of nitrate. The third and fourth largest inputs were wet deposition of organic nitrogen and dry deposition of ammonia. Dry deposition of nitric acid was 5th in importance during both seasons, followed by small contributions from dry deposition of fine particle nitrate and ammonium. Neither gaseous ammonia nor the organic nitrogen content of precipitation are routinely measured in Rocky Mountain National Park. The importance of these inputs to determining the total input of nitrogen to park ecosystems, as documented during RoMANS, suggests that these species should not be overlooked during future measurements in the park and elsewhere in the region.

8 Future Work

Recommendations for further study include:

Additional measurement across a similar monitoring network, based around the Core Site, would provide information about variability from year to year. In addition, measurements could be focused on the areas where the least information is known, specifically measurements of wet organic nitrogen deposition and gas and particle measurements of organic nitrogen. RoMANS focused on the spring and summer which had historically high periods of deposition but investigations into deposition during the fall and winter may provide further insight.

To gain a better understanding of organic nitrogen deposition, additional work should be done to determine the speciation and sources of organic nitrogen.

Additional work should also be done related to the stability of samples to be analyzed for organic nitrogen.

Expanding measurements to other sites would provide additional information about the processes and important sources. Choosing sites where the significance and contribution of organic nitrogen is unknown would be interesting. This might aid in the determination of sources of ON when compared with the data presented here.

Additional investigation of ammonia deposition velocities specific to the RoMANS sites would aid in the quantification of dry deposition. This could be done either by direct measurements or applying the CASTNet model to the other sites in order to calculate deposition velocities. The spatial variability of dry deposition would be interesting to consider and compare with wet deposition.

References

- Andersen, H.V., Hovmand, M.F., Hummelshoj, P. and Jensen, N.O., 1993. Measurements of ammonia flux to a spruce stand in Denmark. *Atmospheric Environment Part a-General Topics* 27, 189-202.
- Andersen, H.V. and Hovmand, M.F., 1995. Ammonia and nitric acid dry deposition and throughfall. *Water Air and Soil Pollution* 85, 2211-2216.
- Andersen, H.V. and Hovmand, M.F., 1999. Review of dry deposition measurements of ammonia and nitric acid to forest. *Forest Ecology and Management* 114, 5-18.
- Andersen, H.V., Hovmand, M.F., Hummelshoj, P. and Jensen, N.O., 1999. Measurements of ammonia concentrations, fluxes and dry deposition velocities to a spruce forest 1991-1995. *Atmospheric Environment* 33, 1367-1383.
- Baron, J.S., Rueth, H.M., Wolfe, A.M., Nydick, K.R., Allstott, E.J., Minear, J.T. and Moraska, B., 2000. Ecosystem responses to nitrogen deposition in the Colorado Front Range. *Ecosystems* 3, 352-368.
- Baron, J.S., Del Grosso, S., Ojima, D.S., Theobald, D.M. and Parton, W.J. (2004). Nitrogen Emissions Along the Colorado Front Range: Response to Population Growth, Land and Water Use Change, and Agriculture, pp. 117-127 In: R. DeFries, Asner, G., and Houghton R., ed., *Ecosystems and Land Use Change*. Geophysical Monograph Series 153, American Geophysical Union, Washington, D.C.
- Baron, J.S., 2006. Hindcasting Nitrogen Deposition To Determine An Ecological Critical Load. *Ecological Applications* 16, 433-439.
- Brazel, A. and Brazel, P., 1983. Summer diurnal wind patterns at Niwot Ridge, CO. *Physical Geography* 4, 53-61.
- Burns, D.A., 2003. Atmospheric nitrogen deposition in the Rocky Mountains of Colorado and southern Wyoming - a review and new analysis of past study results. *Atmospheric Environment* 37, 921-932.
- Clarke, J.F., Edgerton, E.S. and Martin, B.E., 1997. Dry deposition calculations for the clean air status and trends network. *Atmospheric Environment* 31, 3667-3678.
- Cornell, S.E. and Jickells, T.D., 1999. Water-soluble organic nitrogen in atmospheric aerosol: a comparison of UV and persulfate oxidation methods. *Atmospheric Environment* 33, 833-840.
- Cornell, S.E., Jickells, T.D., Cape, J.N., Rowland, A.P. and Duce, R.A., 2003. Organic nitrogen deposition on land and coastal environments: a review of methods and data. *Atmospheric Environment* 37, 2173-2191.
- Craig, B.W. and Friedland, A.J., 1991. Spatial patterns in forest composition and standing dead red spruce in montane forests of the Adirondacks and northern Appalachians. *Environmental Monitoring and Assessment* 18, 129-143.
- Dillon, P.J., Molot, L.A. and Scheider, W.A., 1991. Phosphorus and nitrogen export from forested stream catchments in Central Ontario. *Journal of Environmental Quality* 20, 857-864.
- Duyzer, J., 1994. Dry deposition of ammonia and ammonium aerosols over heathland. *Journal of Geophysical Research-Atmospheres* 99, 18757-18763.

- Duyzer, J.H., Verhagen, H.L.M., Weststrate, J.H. and Bosveld, F.C., 1992. Measurement of the dry deposition flux of NH₃ on to coniferous forest. *Environmental Pollution* 75, 3-13.
- Duyzer, J.H., Verhagen, H.L.M., Weststrate, J.H., Bosveld, F.C. and Vermetten, A.W.M., 1994. The dry deposition of ammonia onto a douglas-fir forest in the Netherlands. *Atmospheric Environment* 28, 1241-1253.
- Erismann, J.W., Otjes, R., Hensen, A., Jongejan, P., van den Bulk, P., Khlystov, A., Mols, H. and Slanina, S., 2001. Instrument development and application in studies and monitoring of ambient ammonia. *Atmospheric Environment* 35, 1913-1922.
- Farmer, D.K., Wooldridge, P.J. and Cohen, R.C., 2006. Application of thermal-dissociation laser induced fluorescence (TD-LIF) to measurement of HNO₃, Sigma alkyl nitrates, Sigma peroxy nitrates, and NO₂ fluxes using eddy covariance. *Atmospheric Chemistry and Physics* 6, 3471-3486.
- Fenn, M.E., Poth, M.A., Aber, J.D., Baron, J.S., Bormann, B.T., Johnson, D.W., Lemly, A.D., McNulty, S.G., Ryan, D.E. and Stottlemyer, R., 1998. Nitrogen excess in North American ecosystems: Predisposing factors, ecosystem responses, and management strategies. *Ecological Applications* 8, 706-733.
- Finkelstein, P.L., Ellestad, T.G., Clarke, J.F., Meyers, T.P., Schwede, D.B., Hebert, E.O. and Neal, J.A., 2000. Ozone and sulfur dioxide dry deposition to forests: Observations and model evaluation. *Journal of Geophysical Research-Atmospheres* 105, 15365-15377.
- Gorzelska, K., Galloway, J.N., Watterson, K. and Keene, W.C., 1992. Water-soluble primary amine compounds in rural continental precipitation. *Atmospheric Environment Part a-General Topics* 26, 1005-1018.
- Goulding, K.W.T., Bailey, N.J., Bradbury, N.J., Hargreaves, P., Howe, M., Murphy, D.V., Poulton, P.R. and Willison, T.W., 1998. Nitrogen deposition and its contribution to nitrogen cycling and associated soil processes. *New Phytologist* 139, 49-58.
- Gronberg, L., Lovkvist, P. and Jonsson, J.A., 1992. Measurement of aliphatic amines in ambient air and rainwater. *Chemosphere* 24, 1533-1540.
- Harrison, R.M. and Allen, A.G., 1991. SCAVENGING RATIOS AND DEPOSITION OF SULFUR, NITROGEN AND CHLORINE SPECIES IN EASTERN ENGLAND. *Atmospheric Environment Part a-General Topics* 25, 1719-1723.
- Ivens, W., Draaijers, G.P.J., Bleuten, W. and Bos, M.M., 1989. THE IMPACT OF AIR-BORNE AMMONIA FROM AGRICULTURAL SOURCES ON FLUXES OF NITROGEN AND SULFUR TOWARDS FOREST SOILS. *Catena* 16, 535-544.
- Janson, R. and Granat, L., 1999. A foliar rinse study of the dry deposition of nitric acid to a coniferous forest. *Agricultural and Forest Meteorology* 98-9, 683-696.
- Jones, B.L. and Cookson, J.T., 1983. Natural atmospheric microbial conditions in a typical suburban area. *Applied and Environmental Microbiology* 45, 919-934.
- Langford, A.O. and Fehsenfeld, F.C., 1992. Natural Vegetation as a Source or Sink for Atmospheric Ammonia - A Case Study *Science* 255, 581-583.
- Littmann, T., 1997. Atmospheric input of dust and nitrogen into the Nizzana sand dune ecosystem, north-western Negev, Israel. *Journal of Arid Environments* 36, 433-457.

- Lovett, G.M., 1994. Atmospheric deposition of nutrients and pollutants in North America - An ecological perspective. *Ecological Applications* 4, 629-650.
- Mace, K.A., Kubilay, N. and Duce, R.A., 2003. Organic nitrogen in rain and aerosol in the eastern Mediterranean atmosphere: An association with atmospheric dust. *Journal of Geophysical Research-Atmospheres* 108.
- Meyers, T.P., Huebert, B. and Hicks, B.B., 1989. HNO₃ Deposition to a deciduous forest. *Boundary-Layer Meteorology* 49, 395-410.
- Meyers, T.P., Finkelstein, P., Clarke, J., Ellestad, T.G. and Sims, P.F., 1998. A multilayer model for inferring dry deposition using standard meteorological measurements. *Journal of Geophysical Research-Atmospheres* 103, 22645-22661.
- Muller, H., Kramm, G., Meixner, F., Dollard, G.J., Fowler, D. and Possanzini, M., 1993. Determination of HNO₃ dry deposition by modified bowen ratio and aerodynamic profile techniques. *Tellus Series B-Chemical and Physical Meteorology* 45, 346-367.
- Namiesnik, J., Jastrzebska, A. and Zygmunt, B., 2003. Determination of volatile aliphatic amines in air by solid-phase microextraction coupled with gas chromatography with flame ionization detection. *Journal of Chromatography A* 1016, 1-9.
- Neirynek, J., Kowalski, A.S., Carrara, A., Genouw, G., Berghmans, P. and Ceulemans, R., 2007. Fluxes of oxidised and reduced nitrogen above a mixed coniferous forest exposed to various nitrogen emission sources. *Environmental Pollution* 149, 31-43.
- Nemitz, E., Sutton, M.A., Wyers, G.P. and Jongejan, P.A.C., 2004. Gas-particle interactions above a Dutch heathland: I. Surface exchange fluxes of NH₃, SO₂, HNO₃ and HCl. *Atmospheric Chemistry and Physics* 4, 989-1005.
- Petersen, W.A., Carey, L.D., Rutledge, S.A., Knievel, J.C., Doesken, N.J., Johnson, R.H., McKee, T.B., Vonder Haar, T. and Weaver, J.F., 1999. Mesoscale and radar observations of the Fort Collins flash flood of 28 July 1997. *Bulletin of the American Meteorological Society* 80, 191-216.
- Pryor, S.C., Barthelmie, R.J., Sorensen, L.L. and Jensen, B., 2001. Ammonia concentrations and fluxes over a forest in the midwestern USA. *Atmospheric Environment* 35, 5645-5656.
- Pryor, S.C., Barthelmie, R.J., Jensen, B., Jensen, N.O. and Sorensen, L.L., 2002. HNO₃ fluxes to a deciduous forest derived using gradient and REA methods. *Atmospheric Environment* 36, 5993-5999.
- Pryor, S.C. and Klemm, O., 2004. Experimentally derived estimates of nitric acid dry deposition velocity and viscous sub-layer resistance at a conifer forest. *Atmospheric Environment* 38, 2769-2777.
- Roberts, J.M., 1990. The Atmospheric Chemistry of Organic Nitrates. *Atmospheric Environment Part a-General Topics* 24, 243-287.
- Russell, K.M., Galloway, J.N., Macko, S.A., Moody, J.L. and Scudlark, J.R., 1998. Sources of nitrogen in wet deposition to the Chesapeake Bay region. *Atmospheric Environment* 32, 2453-2465.
- Schade, G.W. and Crutzen, P.J., 1995. Emission of aliphatic amines from animal husbandry and their reactions - potential source of N₂O and HCN. *Journal of Atmospheric Chemistry* 22, 319-346.

- Scudlark, J.R., Russell, K.M., Galloway, J.N., Church, T.M. and Keene, W.C., 1998. Organic nitrogen in precipitation at the mid-Atlantic US coast - Methods evaluation and preliminary measurements. *Atmospheric Environment* 32, 1719-1728.
- Sickman, J.O., Leydecker, A. and Melack, J.M., 2001. Nitrogen mass balances and abiotic controls on N retention and yield in high-elevation catchments of the Sierra Nevada, California, United States. *Water Resources Research* 37, 1445-1461.
- Sievering, H., Enders, G., Kins, L., Kramm, G., Ruoss, K., Roeder, G., Zelger, M., Anderson, L. and Dlugi, R., 1994. Nitric acid, Particulate Nitrate and Ammonium Profiles at the Bayerischer Wald - Evidence for Large Deposition Rates of Total Nitrate. *Atmospheric Environment* 28, 311-315.
- Sievering, H., Rusch, D. and Marquez, L., 1996. Nitric acid, particulate nitrate and ammonium in the continental free troposphere: Nitrogen deposition to an alpine tundra ecosystem. *Atmospheric Environment* 30, 2527-2537.
- Sievering, H., Kelly, T., McConville, G., Seibold, C. and Turnipseed, A., 2001. Nitric acid dry deposition to conifer forests: Niwot Ridge spruce-fir-pine study. *Atmospheric Environment* 35, 3851-3859.
- Sutton, M.A., Asman, W.A.H. and Schjorring, J.K., 1994. Dry deposition of reduced nitrogen. *Tellus Series B-Chemical and Physical Meteorology* 46, 255-273.
- Williams, M.W., Brown, A.D. and Melack, J.M., 1993. Geochemical and hydrologic controls on the composition of surface water in a high elevation basin, Sierra-Nevada, California. *Limnology and Oceanography* 38, 775-797.
- Williams, M.W., Baron, J.S., Caine, N., Sommerfeld, R. and Sanford, R., 1996. Nitrogen saturation in the Rocky Mountains. *Environmental Science & Technology* 30, 640-646.
- Williams, M.W. and Tonnessen, K.A., 2000. Critical loads for inorganic nitrogen deposition in the Colorado Front Range, USA. *Ecological Applications* 10, 1648-1665.
- Williams, M.W., Hood, E. and Caine, N., 2001. Role of organic nitrogen in the nitrogen cycle of a high-elevation catchment, Colorado Front Range. *Water Resources Research* 37, 2569-2581.
- Wyers, G.P., Vermeulen, A.T. and Slanina, J., 1992. Measurement of dry deposition of ammonia on a forest. *Environmental Pollution* 75, 25-28.
- Wyers, G.P. and Erisman, J.W., 1998. Ammonia exchange over coniferous forest. *Atmospheric Environment* 32, 441-451.
- Yamulki, S., Harrison, R.M. and Goulding, K.W.T., 1996. Ammonia surface-exchange above an agricultural field in southeast England. *Atmospheric Environment* 30, 109-118.
- Yu, X.Y., Taehyoung, L., Ayres, B., Kreidenweis, S.M., Collett, J.L. and Maim, W., 2005. Particulate nitrate measurement using nylon filters. *Journal of the Air & Waste Management Association* 55, 1100-1110.
- Zhang, Q. and Anastasio, C., 2001. Chemistry of fog waters in California's Central Valley - Part 3: concentrations and speciation of organic and inorganic nitrogen. *Atmospheric Environment* 35, 5629-5643.

Zimmermann, F., Plessow, K., Queck, R., Bernhofer, C. and Matschullat, J., 2006.
Atmospheric N- and S-fluxes to a spruce forest - Comparison of inferential
modeling and the throughfall method. *Atmospheric Environment* 40, 4782-4796.

Appendix A Autosampler and sub-event histograms of blanks and samples for both the spring and summer at all sites.

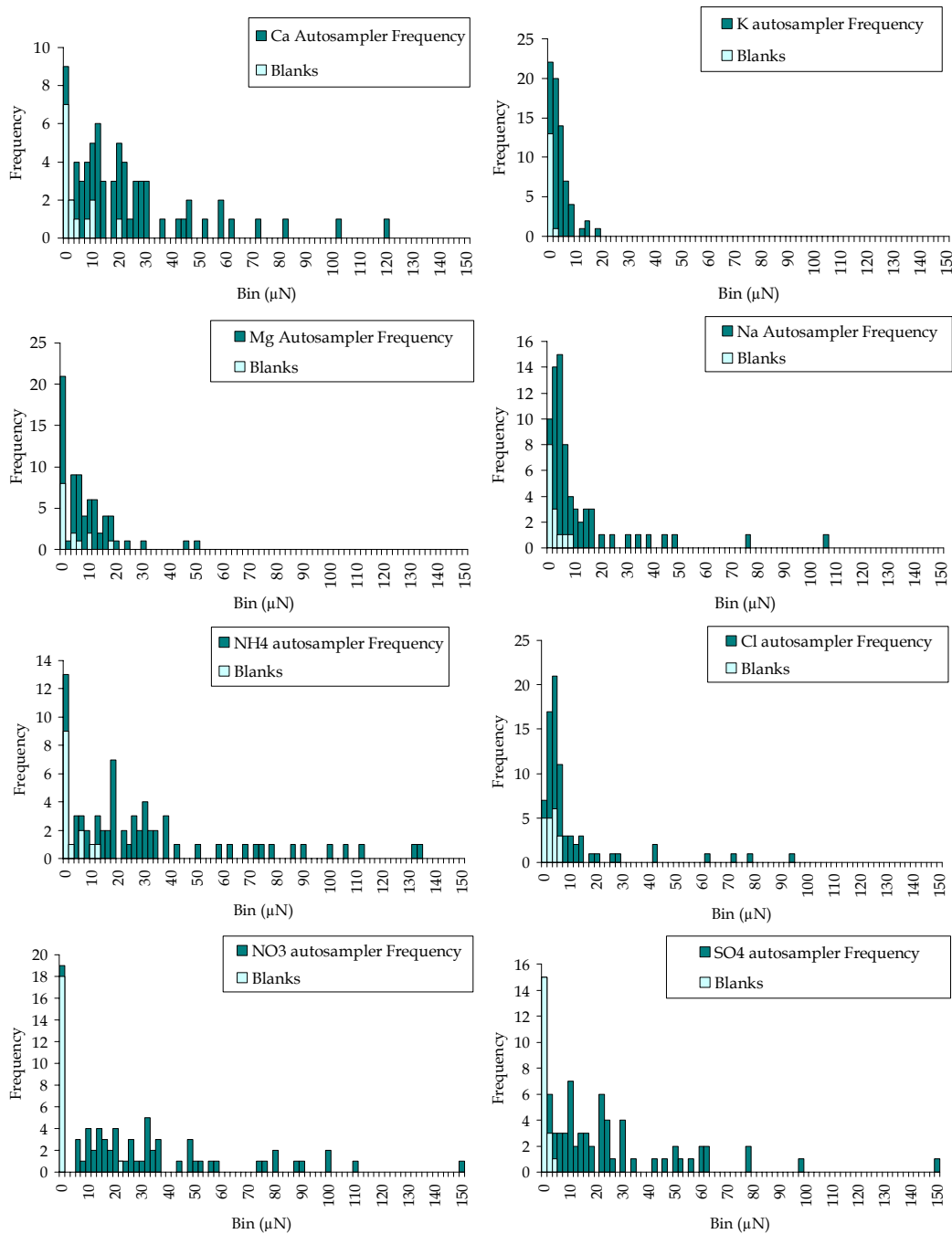


Figure A.1 Histograms for each ionic species measured by IC. All autosampler samples including blanks are shown in dark green with just the blanks in light green plotted on top. The difference between the two bars is the number of samples with concentrations in that bin

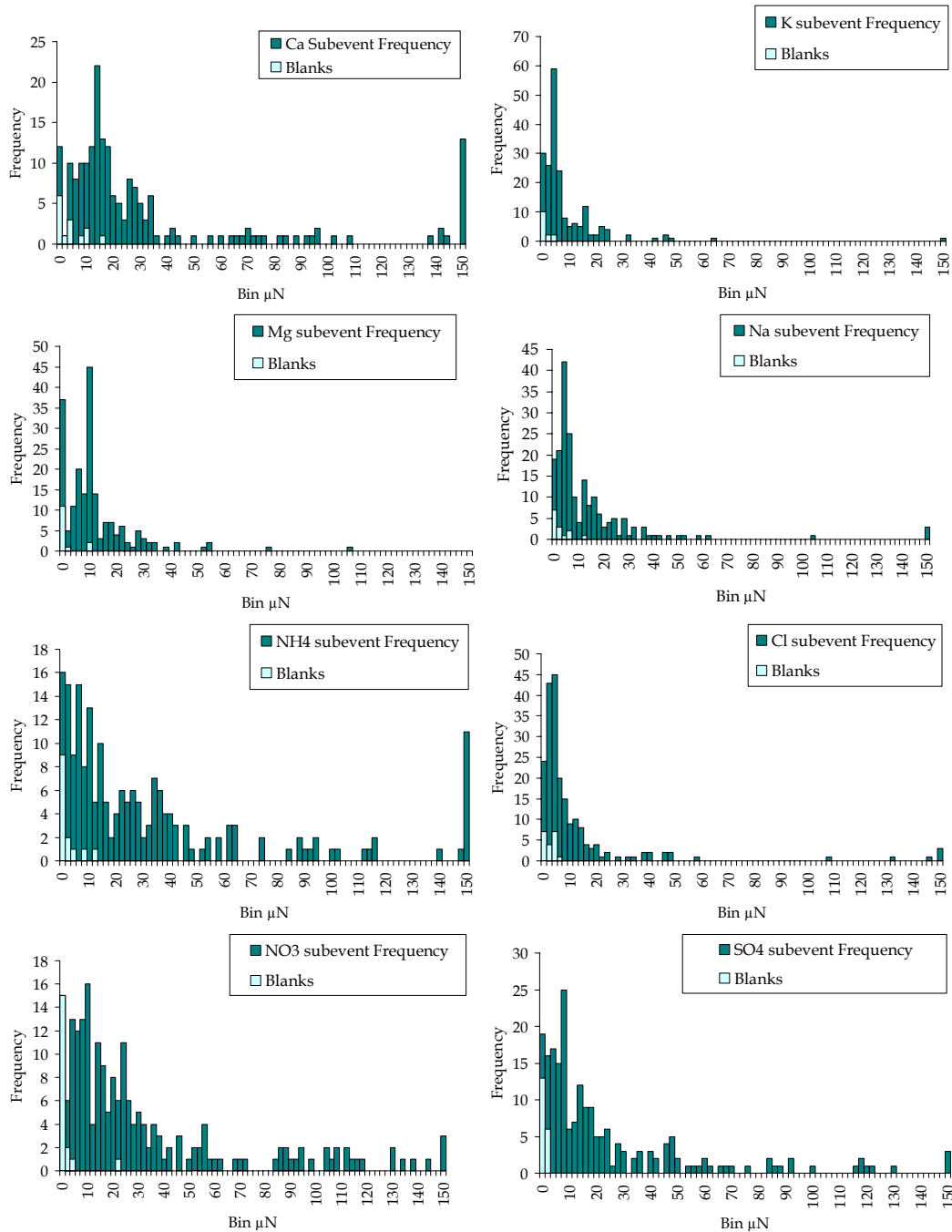


Figure A.2 Histograms for each ionic species measured by IC. All subevent samples including blanks are shown in dark green with just the blanks in light green plotted on top. The difference between the two bars is the number of samples with concentrations in that bin

Appendix B Correlation Coefficient Tables

Table B.1 Correlation coefficients for concentrations from the spring campaign at Gore Pass for precipitation collected with a bucket.

	Ca ²⁺	K ⁺	Mg ²⁺	Na ⁺	NH ₄ ⁺	Cl ⁻	NO ₂ ⁻	NO ₃ ⁻	SO ₄ ²⁻	DON	[H ⁺]	precip
Ca ²⁺		0.770	0.853	0.909	0.619	n.s	n.s	0.644	0.745	n.s	n.s	n.s
K ⁺			0.673	0.854	n.s	0.766	n.s	n.s	n.s	n.s	n.s	n.s
Mg ²⁺				0.737	n.s	n.s	n.s	n.s	0.635	n.s	n.s	n.s
Na ⁺					n.s	0.580	n.s	n.s	n.s	n.s	n.s	n.s
NH ₄ ⁺						n.s	n.s	0.939	0.940	n.s	n.s	n.s
Cl ⁻							n.s	n.s	n.s	n.s	-0.578	n.s
NO ₂ ⁻								n.s	n.s	n.s	n.s	n.s
NO ₃ ⁻									0.983	n.s	n.s	n.s
SO ₄ ²⁻										n.s	n.s	n.s
DON											n.s	n.s
[H ⁺]												n.s
precip												

*n.s – r-values are not significant at the 95% confidence level for a 2-tailed t-test

Table B.2. Correlation coefficients for fluxes from the spring campaign at Gore Pass for precipitation collected with a bucket.

	Ca ²⁺	K ⁺	Mg ²⁺	Na ⁺	NH ₄ ⁺	Cl ⁻	NO ₂ ⁻	NO ₃ ⁻	SO ₄ ²⁻	DON	precip
Ca ²⁺		0.659	0.979	0.796	0.961	n.s	n.s	0.815	0.791	-0.670	0.948
K ⁺			0.694	0.714	n.s	0.667	n.s	n.s	n.s	n.s	0.638
Mg ²⁺				0.714	0.951	n.s	n.s	0.741	0.699	-0.707	0.929
Na ⁺					0.627	0.844	n.s	0.809	0.868	n.s	0.795
NH ₄ ⁺						n.s	n.s	0.748	0.705	n.s	0.887
Cl ⁻							n.s	0.704	0.750	n.s	0.631
NO ₂ ⁻								n.s	n.s	n.s	n.s
NO ₃ ⁻									0.984	-0.761	0.915
SO ₄ ²⁻										-0.607	0.870
DON											n.s
precip											

*n.s – r-values are not significant at the 95% confidence level for a 2-tailed t-test

Table B.3. Correlation coefficients for concentrations from the summer campaign at Gore Pass for precipitation collected with the autosampler.

	Ca ²⁺	K ⁺	Mg ²⁺	Na ⁺	NH ₄ ⁺	Cl ⁻	NO ₂ ⁻	NO ₃ ⁻	SO ₄ ²⁻	[H ⁺]	precip
Ca ²⁺		0.864	0.970	0.676	0.932	0.792	b.d	0.938	0.961	n.s	-0.525
K ⁺			0.892	0.730	0.958	0.859	b.d	0.963	0.931	n.s	-0.555
Mg ²⁺				0.737	0.933	0.834	b.d	0.960	0.944	n.s	-0.590
Na ⁺					0.630	0.937	b.d	0.729	0.629	n.s	-0.494
NH ₄ ⁺						0.780	b.d	0.983	0.991	n.s	-0.499
Cl ⁻							b.d	0.857	0.774	n.s	-0.569
NO ₂ ⁻								b.d	b.d	b.d	b.d
NO ₃ ⁻									0.975	n.s	-0.559
SO ₄ ²⁻										n.s	n.s
[H ⁺]											n.s
precip											

*n.s – r-values are not significant at the 95% confidence level for a 2-tailed t-test

Table B.4. Correlation coefficients for fluxes from the summer campaign at Gore Pass for precipitation collected with the autosampler.

	Ca ²⁺	K ⁺	Mg ²⁺	Na ⁺	NH ₄ ⁺	Cl ⁻	NO ₂ ⁻	NO ₃ ⁻	SO ₄ ²⁻	precip
Ca ²⁺		0.873	0.944	0.790	0.948	0.780	n.s	0.951	0.978	n.s
K ⁺			0.955	0.746	0.968	0.530	n.s	0.935	0.892	n.s
Mg ²⁺				0.773	0.978	0.597	n.s	0.966	0.940	n.s
Na ⁺					0.796	0.667	n.s	0.863	0.752	0.734
NH ₄ ⁺						0.658	n.s	0.982	0.965	n.s
Cl ⁻							n.s	0.733	0.797	0.506
NO ₂ ⁻								n.s	n.s	n.s
NO ₃ ⁻									0.965	0.486
SO ₄ ²⁻										n.s
precip										

*n.s – r-values are not significant at the 95% confidence level for a 2-tailed t-test

Table B.5. Correlation coefficients for concentrations from the summer campaign at Gore Pass for precipitation collected with a bucket.

	Ca ²⁺	K ⁺	Mg ²⁺	Na ⁺	NH ₄ ⁺	Cl ⁻	NO ₂ ⁻	NO ₃ ⁻	SO ₄ ²⁻	[H ⁺]	precip
Ca ²⁺		0.694	0.788	0.844	0.864	0.703	n.s	0.979	0.969	n.s	-0.507
K ⁺			0.989	0.782	0.934	0.999	n.s	0.788	0.787	0.669	n.s
Mg ²⁺				0.818	0.968	0.990	n.s	0.864	0.861	0.644	n.s
Na ⁺					0.851	0.796	n.s	0.867	0.876	n.s	n.s
NH ₄ ⁺						0.939	n.s	0.932	0.944	0.604	n.s
Cl ⁻							n.s	0.798	0.797	0.669	n.s
NO ₂ ⁻								n.s	n.s	n.s	n.s
NO ₃ ⁻									0.988	n.s	-0.515
SO ₄ ²⁻										n.s	n.s
[H ⁺]											n.s
precip											

*n.s – r-values are not significant at the 95% confidence level for a 2-tailed t-test

Table B.6. Correlation coefficients for fluxes from the summer campaign at Gore Pass for precipitation collected with a bucket.

	Ca ²⁺	K ⁺	Mg ²⁺	Na ⁺	NH ₄ ⁺	Cl ⁻	NO ₂ ⁻	NO ₃ ⁻	SO ₄ ²⁻	precip
Ca ²⁺		0.530	0.977	n.s	0.773	n.s	n.s	0.910	0.919	0.602
K ⁺			0.630	0.896	n.s	0.892	n.s	n.s	n.s	n.s
Mg ²⁺				n.s	0.724	n.s	n.s	0.873	0.888	0.688
Na ⁺					n.s	0.993	n.s	n.s	n.s	n.s
NH ₄ ⁺						n.s	n.s	0.951	0.932	0.590
Cl ⁻							n.s	n.s	n.s	n.s
NO ₂ ⁻								n.s	n.s	n.s
NO ₃ ⁻									0.980	0.675
SO ₄ ²⁻										0.629
precip										

*n.s – r-values are not significant at the 95% confidence level for a 2-tailed t-test

Table B.7. Correlation coefficients for concentrations from the spring campaign at Lyons for precipitation collected with the autosampler.

	Ca ²⁺	K ⁺	Mg ²⁺	Na ⁺	NH ₄ ⁺	Cl ⁻	NO ₂ ⁻	NO ₃ ⁻	SO ₄ ²⁻	DON	[H ⁺]	precip
Ca ²⁺		n.s.	n.s.	0.985	n.s.	0.980	n.s.	0.955	0.974	0.974	n.s.	n.s.
K ⁺			0.959	n.s.	n.s.	n.s.	n.s.	n.s.	n.s.	0.985	n.s.	n.s.
Mg ²⁺				n.s.	0.993	n.s.	n.s.	0.995	0.972	0.985	n.s.	n.s.
Na ⁺					n.s.	0.996	n.s.	n.s.	n.s.	n.s.	n.s.	n.s.
NH ₄ ⁺						n.s.	n.s.	0.990	0.970	0.951	n.s.	n.s.
Cl ⁻							n.s.	n.s.	n.s.	n.s.	n.s.	n.s.
NO ₂ ⁻								n.s.	n.s.	n.s.	n.s.	n.s.
NO ₃ ⁻									0.990	0.994	n.s.	n.s.
SO ₄ ²⁻										0.999	n.s.	n.s.
DON											n.s.	n.s.
[H ⁺]												n.s.
precip												

*n.s – r-values are not significant at the 95% confidence level for a 2-tailed t-test

Table B.8. Correlation coefficients for fluxes from the spring campaign at Lyons for precipitation collected with the autosampler

	Ca ²⁺	K ⁺	Mg ²⁺	Na ⁺	NH ₄ ⁺	Cl ⁻	NO ₂ ⁻	NO ₃ ⁻	SO ₄ ²⁻	DON	precip
Ca ²⁺		n.s.	0.968	0.969	n.s.	n.s.	n.s.	0.954	n.s.	n.s.	n.s.
K ⁺			n.s.	n.s.	n.s.	0.987	n.s.	0.955	n.s.	n.s.	n.s.
Mg ²⁺				n.s.	0.992	n.s.	n.s.	0.998	0.966	n.s.	n.s.
Na ⁺					n.s.	n.s.	n.s.	n.s.	n.s.	1.000	n.s.
NH ₄ ⁺						n.s.	0.968	0.994	0.962	n.s.	n.s.
Cl ⁻							n.s.	n.s.	n.s.	n.s.	n.s.
NO ₂ ⁻								n.s.	n.s.	n.s.	n.s.
NO ₃ ⁻									n.s.	n.s.	n.s.
SO ₄ ²⁻										n.s.	n.s.
DON											n.s.
precip											

*n.s – r-values are not significant at the 95% confidence level for a 2-tailed t-test

Table B.9. Correlation table for concentrations during the summer campaign measured at Lyons for samples collected with the bucket.

	Ca ²⁺	K ⁺	Mg ²⁺	Na ⁺	NH ₄ ⁺	Cl ⁻	NO ₂ ⁻	NO ₃ ⁻	SO ₄ ²⁻	DON	[H ⁺]	precip
Ca ²⁺		0.901	b.d.	0.992	0.998	0.964	0.975	0.998	0.997	0.993	n.s.	n.s.
K ⁺			b.d.	0.863	0.882	0.851	n.s.	0.891	0.899	0.925	n.s.	n.s.
Mg ²⁺				b.d.	b.d.	b.d.	b.d.	b.d.	b.d.	b.d.	b.d.	b.d.
Na ⁺					0.996	0.980	0.973	0.996	0.988	0.989	n.s.	n.s.
NH ₄ ⁺						0.977	0.979	1.000	0.997	0.993	n.s.	n.s.
Cl ⁻							0.946	0.977	0.963	0.978	n.s.	n.s.
NO ₂ ⁻								0.973	0.971	0.953	n.s.	n.s.
NO ₃ ⁻									0.997	0.995	n.s.	n.s.
SO ₄ ²⁻										0.991	n.s.	n.s.
DON											n.s.	n.s.
[H ⁺]												n.s.
precip												

*n.s – r-values are not significant at the 95% confidence level for a 2-tailed t-test

**b.d. - at least one value of all the pairs was below detection.

Table B.10. Correlation table for fluxes during the summer campaign measured at Lyons for samples collected with the bucket.

	Ca ²⁺	K ⁺	Mg ²⁺	Na ⁺	NH ₄ ⁺	Cl ⁻	NO ₂ ⁻	NO ₃ ⁻	SO ₄ ²⁻	DON	precip
Ca ²⁺		n.s.	b.d.	n.s.	n.s.	n.s.	n.s.	n.s.	n.s.	n.s.	n.s.
K ⁺			b.d.	n.s.	n.s.	n.s.	n.s.	n.s.	n.s.	n.s.	n.s.
Mg ²⁺				b.d.	b.d.	b.d.	b.d.	b.d.	b.d.	b.d.	b.d.
Na ⁺					n.s.	n.s.	n.s.	0.731	n.s.	0.423	n.s.
NH ₄ ⁺						n.s.	n.s.	n.s.	0.764	n.s.	0.454
Cl ⁻							n.s.	n.s.	n.s.	n.s.	n.s.
NO ₂ ⁻								n.s.	-0.355	-0.277	n.s.
NO ₃ ⁻									n.s.	n.s.	0.719
SO ₄ ²⁻										n.s.	n.s.
DON											n.s.
precip											

*n.s – r-values are not significant at the 95% confidence level for a 2-tailed t-test

**b.d. - at least one value of all the pairs was below detection.

Table B.11. Correlation coefficients for concentrations from the spring campaign at the Core Site for precipitation collected with a bucket.

	Ca ²⁺	K ⁺	Mg ²⁺	Na ⁺	NH ₄ ⁺	Cl ⁻	NO ₂ ⁻	NO ₃ ⁻	SO ₄ ²⁻	DON	[H ⁺]	precip
Ca ²⁺		0.901	0.999	0.813	n.s.	n.s.	b.d.	n.s.	0.904	n.s.	n.s.	n.s.
K ⁺			0.905	0.793	n.s.	n.s.	b.d.	0.657	0.882	n.s.	n.s.	n.s.
Mg ²⁺				0.826	n.s.	n.s.	b.d.	n.s.	0.902	n.s.	n.s.	n.s.
Na ⁺					n.s.	0.668	b.d.	n.s.	0.793	n.s.	n.s.	n.s.
NH ₄ ⁺						n.s.	b.d.	0.679	n.s.	n.s.	n.s.	n.s.
Cl ⁻							b.d.	n.s.	n.s.	n.s.	n.s.	n.s.
NO ₂ ⁻								b.d.	b.d.	b.d.	b.d.	b.d.
NO ₃ ⁻									0.802	n.s.	n.s.	n.s.
SO ₄ ²⁻										n.s.	-0.611	n.s.
DON											n.s.	n.s.
[H ⁺]												n.s.
precip												

*n.s – r-values are not significant at the 95% confidence level for a 2-tailed t-test

Table B.12. Correlation coefficients for fluxes from the spring campaign at the Core Site for precipitation collected with a bucket.

	Ca ²⁺	K ⁺	Mg ²⁺	Na ⁺	NH ₄ ⁺	Cl ⁻	NO ₂ ⁻	NO ₃ ⁻	SO ₄ ²⁻	DON	precip
Ca ²⁺		0.995	0.985	0.986	0.945	0.946	n.s.	0.989	0.966	n.s.	0.966
K ⁺			0.981	0.986	0.933	0.960	n.s.	0.986	0.958	n.s.	0.963
Mg ²⁺				0.960	0.879	0.919	n.s.	0.956	0.912	n.s.	0.996
Na ⁺					0.959	0.982	n.s.	0.987	0.975	n.s.	0.935
NH ₄ ⁺						0.918	n.s.	0.973	0.996	n.s.	0.838
Cl ⁻							n.s.	0.955	0.939	n.s.	0.893
NO ₂ ⁻								n.s.	n.s.	n.s.	n.s.
NO ₃ ⁻									0.990	n.s.	0.928
SO ₄ ²⁻										n.s.	0.874
DON											n.s.
precip											

*n.s – r-values are not significant at the 95% confidence level for a 2-tailed t-test

Appendix C Slopes for the significant r-values in Appendix B

Table C.1 Significant slopes for concentrations from the Core Site during the summer campaign for samples collected with the autosampler. Slopes were calculated with the rows as y values and columns as x values.

	Ca ²⁺	K ⁺	Mg ²⁺	Na ⁺	NH ₄ ⁺	Cl ⁻	NO ₂ ⁻	NO ₃ ⁻	SO ₄ ²⁻	DON	[H ⁺]	precip
Ca ²⁺		4.073	3.081	0.766	0.835	n.s.	n.s.	0.122	n.s.	n.s.	n.s.	-78.169
K ⁺			0.286	0.087	0.076	n.s.	n.s.	n.s.	n.s.	n.s.	n.s.	n.s.
Mg ²⁺				0.256	0.145	0.096	n.s.	n.s.	n.s.	n.s.	n.s.	n.s.
Na ⁺					0.515	0.389	n.s.	n.s.	n.s.	n.s.	n.s.	-73.016
NH ₄ ⁺						n.s.	n.s.	n.s.	n.s.	n.s.	n.s.	n.s.
Cl ⁻							n.s.	0.289	0.514	0.851	n.s.	-135.802
NO ₂ ⁻								0.006	0.009	0.029	n.s.	n.s.
NO ₃ ⁻									1.344	2.894	n.s.	-352.715
SO ₄ ²⁻										2.077	n.s.	-215.444
DON											n.s.	n.s.
[H ⁺]												n.s.
precip												

Table C.2 Significant slopes for fluxes from the Core Site during the summer campaign for samples collected with the autosampler. Slopes were calculated with the rows as y values and columns as x values.

	Ca ²⁺	K ⁺	Mg ²⁺	Na ⁺	NH ₄ ⁺	Cl ⁻	NO ₂ ⁻	NO ₃ ⁻	SO ₄ ²⁻	DON	precip
Ca ²⁺		0.644	1.965	1.001	0.283	0.642	n.s.	0.119	0.173	0.588	108.725
K ⁺			n.s.	1.046	0.222	0.561	n.s.	0.080	0.125	0.631	121.603
Mg ²⁺				n.s.	n.s.	n.s.	n.s.	n.s.	n.s.	n.s.	n.s.
Na ⁺					0.176	0.623	n.s.	0.065	n.s.	0.535	94.037
NH ₄ ⁺						1.362	n.s.	0.422	0.711	n.s.	445.047
Cl ⁻							n.s.	n.s.	n.s.	0.822	n.s.
NO ₂ ⁻								n.s.	n.s.	n.s.	n.s.
NO ₃ ⁻									1.776	n.s.	1056.428
SO ₄ ²⁻										n.s.	582.514
DON											n.s.
precip											

Table C.3 Significant slopes for concentrations from the Core Site during the spring campaign for samples collected with the autosampler. Slopes were calculated with the rows as y values and columns as x values.

	Ca ²⁺	K ⁺	Mg ²⁺	Na ⁺	NH ₄ ⁺	Cl ⁻	NO ₂ ⁻	NO ₃ ⁻	SO ₄ ²⁻	DON	[H ⁺]	precip
Ca ²⁺		n.s	1.327	1.023	n.s	n.s	b.d	n.s	n.s	n.s	n.s	n.s
K ⁺			n.s	n.s	n.s	3.191	b.d	n.s	n.s	n.s	n.s	n.s
Mg ²⁺				n.s	n.s	n.s	b.d	n.s	n.s	n.s	n.s	n.s
Na ⁺					n.s	n.s	b.d	n.s	n.s	n.s	n.s	n.s
NH ₄ ⁺						n.s	b.d	n.s	n.s	n.s	n.s	n.s
Cl ⁻							b.d	n.s	n.s	n.s	n.s	n.s
NO ₂ ⁻								b.d	b.d	b.d	b.d	b.d
NO ₃ ⁻									0.716	n.s	n.s	n.s
SO ₄ ²⁻										n.s	-184979626.250	n.s
DON											n.s	n.s
[H ⁺]												n.s
precip												

Table C.4 Significant slopes for fluxes from the Core Site during the spring campaign for samples collected with the autosampler. Slopes were calculated with the rows as y values and columns as x values.

	Ca ²⁺	K ⁺	Mg ²⁺	Na ⁺	NH ₄ ⁺	Cl ⁻	NO ₂ ⁻	NO ₃ ⁻	SO ₄ ²⁻	DON	precip
Ca ²⁺		0.014	1.327	1.023	0.213	0.854	n.s.	0.072	0.099	-0.300	-0.014
K ⁺			-0.446	0.533	-0.013	3.191	n.s.	0.030	-0.018	0.350	0.006
Mg ²⁺				-0.062	-0.013	0.280	n.s.	0.025	0.080	-0.028	-0.006
Na ⁺					0.131	0.483	n.s.	-0.001	-0.042	-0.264	-0.094
NH ₄ ⁺						-0.519	n.s.	0.288	0.076	1.025	0.946
Cl ⁻							n.s.	0.019	0.027	0.044	0.016
NO ₂ ⁻								n.s.	n.s.	n.s.	n.s.
NO ₃ ⁻									0.716	0.763	1.009
SO ₄ ²⁻										0.436	0.472
DON											0.492
precip											

Table C.5 Significant slopes for concentrations from the Core Site during the spring campaign for samples collected with the bucket. Slopes were calculated with the rows as y values and columns as x values.

	Ca ²⁺	K ⁺	Mg ²⁺	Na ⁺	NH ₄ ⁺	Cl ⁻	NO ₂ ⁻	NO ₃ ⁻	SO ₄ ²⁻	DON	[H ⁺]	precip
Ca ²⁺		11.392	9.089	6.403	n.s.	n.s.	n.s.	n.s.	1.565	n.s.	n.s.	n.s.
K ⁺			0.651	0.494	n.s.	n.s.	n.s.	0.120	0.121	n.s.	n.s.	n.s.
Mg ²⁺				0.715	n.s.	n.s.	n.s.	n.s.	0.172	n.s.	n.s.	n.s.
Na ⁺					n.s.	0.795	n.s.	n.s.	0.174	n.s.	n.s.	n.s.
NH ₄ ⁺						n.s.	n.s.	0.254	n.s.	n.s.	n.s.	n.s.
Cl ⁻							n.s.	n.s.	n.s.	n.s.	n.s.	n.s.
NO ₂ ⁻								n.s.	n.s.	n.s.	n.s.	n.s.
NO ₃ ⁻									0.603	n.s.	n.s.	n.s.
SO ₄ ²⁻										n.s.	-261738749.093	n.s.
DON											n.s.	n.s.
[H ⁺]												n.s.
precip												

Table C.6 Significant slopes for fluxes from the Core Site during the spring campaign for samples collected with the bucket. Slopes were calculated with the rows as y values and columns as x values.

	Ca ²⁺	K ⁺	Mg ²⁺	Na ⁺	NH ₄ ⁺	Cl ⁻	NO ₂ ⁻	NO ₃ ⁻	SO ₄ ²⁻	DON	precip
Ca ²⁺		3.244	3.576	4.300	0.497	5.632	n.s.	0.261	0.362	n.s.	438.696
K ⁺			1.093	1.318	0.150	1.753	n.s.	0.080	0.110	n.s.	134.044
Mg ²⁺				1.153	0.127	1.508	n.s.	0.069	0.094	n.s.	124.596
Na ⁺					0.116	1.341	n.s.	0.060	0.084	n.s.	97.401
NH ₄ ⁺						10.392	n.s.	0.487	0.708	n.s.	723.120
Cl ⁻							n.s.	0.042	0.059	n.s.	68.121
NO ₂ ⁻								n.s.	n.s.	n.s.	n.s.
NO ₃ ⁻									1.405	n.s.	1597.907
SO ₄ ²⁻										n.s.	1060.444
DON											n.s.
precip											

Table C.7 Significant slopes for concentrations from the Gore Pass during the spring campaign for samples collected with the bucket. Slopes were calculated with the rows as y values and columns as x values.

	Ca ²⁺	K ⁺	Mg ²⁺	Na ⁺	NH ₄ ⁺	Cl ⁻	NO ₂ ⁻	NO ₃ ⁻	SO ₄ ²⁻	DON	[H ⁺]	precip
Ca ²⁺		1.827	4.040	1.496	0.269	n.s	n.s	0.153	0.140	n.s	n.s	n.s
K ⁺			1.344	0.593	n.s	0.994	n.s	n.s	n.s	n.s	n.s	n.s
Mg ²⁺				0.256	n.s	n.s	n.s	n.s	0.025	n.s	n.s	n.s
Na ⁺					n.s	1.084	n.s	n.s	n.s	n.s	n.s	n.s
NH ₄ ⁺						n.s	n.s	0.513	0.405	n.s	n.s	n.s
Cl ⁻							n.s	n.s	n.s	n.s	-10492603.617	n.s
NO ₂ ⁻								n.s	n.s	n.s	n.s	n.s
NO ₃ ⁻									0.775	n.s	n.s	n.s
SO ₄ ²⁻										n.s	n.s	n.s
DON											n.s	n.s
[H ⁺]												n.s
precip												

Table C.8 Significant slopes for fluxes from the Gore Pass during the spring campaign for samples collected with the bucket. Slopes were calculated with the rows as y values and columns as x values.

	Ca ²⁺	K ⁺	Mg ²⁺	Na ⁺	NH ₄ ⁺	Cl ⁻	NO ₂ ⁻	NO ₃ ⁻	SO ₄ ²⁻	DON	precip
Ca ²⁺		1.904	2.459	2.442	1.601	n.s	n.s	0.230	0.256	-0.148	251.169
K ⁺			0.603	0.759	n.s	0.562	n.s	n.s	n.s	n.s	58.569
Mg ²⁺				0.872	0.630	n.s	n.s	0.083	0.090	-0.146	98.055
Na ⁺					0.340	0.669	n.s	0.074	0.092	n.s	68.657
NH ₄ ⁺						n.s	n.s	0.127	0.137	n.s	141.170
Cl ⁻							n.s	0.082	0.100	n.s	68.796
NO ₂ ⁻								n.s	n.s	n.s	n.s
NO ₃ ⁻									1.127	-0.359	858.557
SO ₄ ²⁻										-0.544	712.730
DON											n.s
precip											

Table C.9 Significant slopes for concentrations from the Gore Pass during the summer campaign for samples collected with the autosampler. Slopes were calculated with the rows as y values and columns as x values.

	Ca ²⁺	K ⁺	Mg ²⁺	Na ⁺	NH ₄ ⁺	Cl ⁻	NO ₂ ⁻	NO ₃ ⁻	SO ₄ ²⁻	[H ⁺]	precip
Ca ²⁺		3.436	7.870	4.094	0.716	2.717	n.s	0.241	0.447	n.s	-55.563
K ⁺			1.819	1.112	0.185	0.741	n.s	0.062	0.109	n.s	-14.771
Mg ²⁺				0.551	0.088	0.353	n.s	0.030	0.054	n.s	-7.705
Na ⁺					0.080	0.530	n.s	0.031	0.048	n.s	-8.627
NH ₄ ⁺						3.483	n.s	0.329	0.599	n.s	-68.786
Cl ⁻							n.s	0.064	0.105	n.s	-17.572
NO ₂ ⁻								n.s	n.s	n.s	n.s
NO ₃ ⁻									1.763	n.s	-230.373
SO ₄ ²⁻										n.s	n.s
[H ⁺]											n.s
precip											

Table C.10 Significant slopes for fluxes from the Gore Pass during the summer campaign for samples collected with the autosampler. Slopes were calculated with the rows as y values and columns as x values.

	Ca ²⁺	K ⁺	Mg ²⁺	Na ⁺	NH ₄ ⁺	Cl ⁻	NO ₂ ⁻	NO ₃ ⁻	SO ₄ ²⁻	precip
Ca ²⁺		3.144	5.881	4.876	0.637	2.982	n.s	0.208	0.421	n.s
K ⁺			1.652	1.279	0.180	0.562	n.s	0.057	0.107	n.s
Mg ²⁺				0.766	0.105	0.366	n.s	0.034	0.065	n.s
Na ⁺					0.087	0.413	n.s	0.031	0.053	28.188
NH ₄ ⁺						3.743	n.s	0.320	0.619	n.s
Cl ⁻							n.s	0.042	0.090	31.376
NO ₂ ⁻								n.s	n.s	n.s
NO ₃ ⁻									1.901	526.766
SO ₄ ²⁻										n.s
precip										

Table C.11 Significant slopes for concentrations from the Gore Pass during the summer campaign for samples collected with the bucket. Slopes were calculated with the rows as y values and columns as x values.

	Ca ²⁺	K ⁺	Mg ²⁺	Na ⁺	NH ₄ ⁺	Cl ⁻	NO ₂ ⁻	NO ₃ ⁻	SO ₄ ²⁻	[H ⁺]	precip
Ca ²⁺		0.159	1.629	5.899	0.490	0.236	n.s	0.281	0.534	n.s	-142.848
K ⁺			8.924	23.831	2.312	1.461	n.s	0.987	1.892	9198.670	n.s
Mg ²⁺				2.764	0.265	0.160	n.s	0.120	0.229	982.277	n.s
Na ⁺					0.069	0.038	n.s	0.036	0.069	n.s	n.s
NH ₄ ⁺						0.555	n.s	0.472	0.917	3355.270	n.s
Cl ⁻							n.s	0.684	1.310	6290.628	n.s
NO ₂ ⁻								n.s	n.s	n.s	n.s
NO ₃ ⁻									1.896	n.s	-505.020
SO ₄ ²⁻										n.s	n.s
[H ⁺]											n.s
precip											

Table C.12 Significant slopes for fluxes from the Gore Pass during the summer campaign for samples collected with the bucket. Slopes were calculated with the rows as y values and columns as x values.

	Ca ²⁺	K ⁺	Mg ²⁺	Na ⁺	NH ₄ ⁺	Cl ⁻	NO ₂ ⁻	NO ₃ ⁻	SO ₄ ²⁻	precip
Ca ²⁺		0.490	5.201	n.s	0.974	n.s	n.s	0.352	0.707	293.238
K ⁺			3.624	2.737	n.s	1.195	n.s	n.s	n.s	n.s
Mg ²⁺				n.s	0.172	n.s	n.s	0.063	0.128	63.057
Na ⁺					n.s	0.436	n.s	n.s	n.s	n.s
NH ₄ ⁺						n.s	n.s	0.292	0.568	228.016
Cl ⁻							n.s	n.s	n.s	n.s
NO ₂ ⁻								n.s	n.s	n.s
NO ₃ ⁻									1.950	850.999
SO ₄ ²⁻										398.271
precip										

Table C.13 Significant slopes for concentrations from the Lyons during the spring campaign for samples collected with the autosampler. Slopes were calculated with the rows as y values and columns as x values.

	Ca ²⁺	K ⁺	Mg ²⁺	Na ⁺	NH ₄ ⁺	Cl ⁻	NO ₂ ⁻	NO ₃ ⁻	SO ₄ ²⁻	DON	[H ⁺]	precip
Ca ²⁺		n.s.	n.s.	3.080	n.s.	6.904	n.s.	0.193	0.196	0.634	n.s.	n.s.
K ⁺			1.100	n.s.	n.s.	n.s.	n.s.	n.s.	n.s.	0.080	n.s.	n.s.
Mg ²⁺				n.s.	0.085	0.000	n.s.	0.043	0.042	0.110	n.s.	n.s.
Na ⁺					n.s.	2.243	n.s.	n.s.	n.s.	n.s.	n.s.	n.s.
NH ₄ ⁺						n.s.	n.s.	0.498	0.486	1.344	n.s.	n.s.
Cl ⁻							n.s.	n.s.	n.s.	n.s.	n.s.	n.s.
NO ₂ ⁻								n.s.	n.s.	n.s.	n.s.	n.s.
NO ₃ ⁻									0.986	2.825	n.s.	n.s.
SO ₄ ²⁻										3.189	n.s.	n.s.
DON											n.s.	n.s.
[H ⁺]												n.s.
precip												

Table C.14 Significant slopes for fluxes from the Lyons during the spring campaign for samples collected with the autosampler. Slopes were calculated with the rows as y values and columns as x values.

	Ca ²⁺	K ⁺	Mg ²⁺	Na ⁺	NH ₄ ⁺	Cl ⁻	NO ₂ ⁻	NO ₃ ⁻	SO ₄ ²⁻	DON	precip
Ca ²⁺		n.s.	3.014	4.115	n.s.	n.s.	n.s.	0.122	n.s.	n.s.	n.s.
K ⁺			n.s.	n.s.	n.s.	2.545	n.s.	0.061	n.s.	n.s.	n.s.
Mg ²⁺				n.s.	0.075	n.s.	n.s.	0.041	0.052	n.s.	n.s.
Na ⁺					n.s.	n.s.	n.s.	n.s.	n.s.	0.082	n.s.
NH ₄ ⁺						n.s.	22.008	0.540	0.684	n.s.	n.s.
Cl ⁻							n.s.	n.s.	n.s.	n.s.	n.s.
NO ₂ ⁻								n.s.	n.s.	n.s.	n.s.
NO ₃ ⁻									n.s.	n.s.	n.s.
SO ₄ ²⁻										n.s.	n.s.
DON											n.s.
precip											

Table C.15 Significant slopes for concentrations from the Lyons during the summer campaign for samples collected with the bucket. Slopes were calculated with the rows as y values and columns as x values.

	Ca ²⁺	K ⁺	Mg ²⁺	Na ⁺	NH ₄ ⁺	Cl ⁻	NO ₂ ⁻	NO ₃ ⁻	SO ₄ ²⁻	DON	[H ⁺]	precip
Ca ²⁺		9.729	n.s.	48.336	0.430	8.250	17.813	0.210	1.184	2.442	n.s.	n.s.
K ⁺			n.s.	3.895	0.035	0.675	0.000	0.017	0.099	0.211	n.s.	n.s.
Mg ²⁺				n.s.	n.s.	n.s.	n.s.	n.s.	n.s.	n.s.	n.s.	n.s.
Na ⁺					0.009	0.172	0.365	0.004	0.024	0.050	n.s.	n.s.
NH ₄ ⁺						19.374	41.478	0.488	2.743	5.659	n.s.	n.s.
Cl ⁻							2.021	0.024	0.134	0.281	n.s.	n.s.
NO ₂ ⁻								0.011	0.063	0.128	n.s.	n.s.
NO ₃ ⁻									5.625	11.628	n.s.	n.s.
SO ₄ ²⁻										2.053	n.s.	n.s.
DON											n.s.	n.s.
[H ⁺]												n.s.
precip												

Table C.16 Significant slopes for fluxes from the Lyons during the summer campaign for samples collected with the bucket. Slopes were calculated with the rows as y values and columns as x values.

	Ca ²⁺	K ⁺	Mg ²⁺	Na ⁺	NH ₄ ⁺	Cl ⁻	NO ₂ ⁻	NO ₃ ⁻	SO ₄ ²⁻	DON	precip
Ca ²⁺		n.s.	n.s.	n.s.	n.s.	n.s.	n.s.	n.s.	n.s.	n.s.	n.s.
K ⁺			n.s.	n.s.	n.s.	n.s.	n.s.	n.s.	n.s.	n.s.	n.s.
Mg ²⁺				n.s.	n.s.	n.s.	n.s.	n.s.	n.s.	n.s.	n.s.
Na ⁺					n.s.	n.s.	n.s.	0.087	n.s.	0.649	n.s.
NH ₄ ⁺						n.s.	n.s.	n.s.	0.703	n.s.	170.254
Cl ⁻							n.s.	n.s.	n.s.	n.s.	n.s.
NO ₂ ⁻								n.s.	-0.009	-0.033	n.s.
NO ₃ ⁻									n.s.	n.s.	766.008
SO ₄ ²⁻										n.s.	n.s.
DON											n.s.
precip											

Table C.17 Significant slopes for spring sulfate concentrations by site. Slopes were calculated with the rows as y values and columns as x values.

	<i>DI</i>	<i>GP</i>	<i>TC</i>	<i>HV</i>	<i>BM</i>	<i>CS</i>	<i>SL</i>	<i>LV</i>	<i>LY</i>	<i>BR</i>	<i>NE</i>	<i>SF</i>
<i>DI</i>		23.283	n.s.	n.s.	n.s.	n.s.	n.s.	N/A	N/A	N/A	n.s.	N/A
<i>GP</i>			n.s.	n.s.	n.s.	n.s.	1.555	N/A	0.845	N/A	n.s.	N/A
<i>TC</i>				n.s.	n.s.	n.s.	n.s.	N/A	n.s.	N/A	n.s.	N/A
<i>HV</i>					0.410	0.946	1.125	N/A	n.s.	N/A	n.s.	N/A
<i>BM</i>						n.s.	n.s.	N/A	n.s.	N/A	N/A	N/A
<i>CS</i>							n.s.	N/A	n.s.	N/A	N/A	N/A
<i>SL</i>								n.s.	0.516	N/A	n.s.	N/A
<i>LV</i>									N/A	N/A	N/A	N/A
<i>LY</i>										N/A	N/A	N/A
<i>BR</i>											N/A	N/A
<i>NE</i>												N/A
<i>SF</i>												

Table C.18 Significant slopes for spring sulfate fluxes by site. Slopes were calculated with the rows as y values and columns as x values.

	<i>DI</i>	<i>GP</i>	<i>TC</i>	<i>HV</i>	<i>BM</i>	<i>CS</i>	<i>SL</i>	<i>LV</i>	<i>LY</i>	<i>BR</i>	<i>NE</i>	<i>SF</i>
<i>DI</i>		n.s.	n.s.	n.s.	n.s.	n.s.	n.s.	N/A	N/A	N/A	n.s.	N/A
<i>GP</i>			2.354	n.s.	n.s.	n.s.	n.s.	N/A	n.s.	N/A	n.s.	N/A
<i>TC</i>				0.709	0.678	0.925	1.502	N/A	n.s.	N/A	n.s.	N/A
<i>HV</i>					0.960	1.325	1.834	N/A	n.s.	N/A	n.s.	N/A
<i>BM</i>						1.380	2.099	N/A	n.s.	N/A	N/A	N/A
<i>CS</i>							1.512	N/A	n.s.	N/A	N/A	N/A
<i>SL</i>								0.731	1.693	N/A	n.s.	N/A
<i>LV</i>									N/A	N/A	N/A	N/A
<i>LY</i>										N/A	N/A	N/A
<i>BR</i>											N/A	N/A
<i>NE</i>												N/A
<i>SF</i>												

Table C.19 Significant slopes for spring nitrate concentrations by site. Slopes were calculated with the rows as y values and columns as x values.

	<i>DI</i>	<i>GP</i>	<i>TC</i>	<i>HV</i>	<i>BM</i>	<i>CS</i>	<i>SL</i>	<i>LV</i>	<i>LY</i>	<i>BR</i>	<i>NE</i>	<i>SF</i>
<i>DI</i>		16.113	n.s.	n.s.	n.s.	n.s.	n.s.	N/A	N/A	N/A	n.s.	N/A
<i>GP</i>			n.s.	n.s.	n.s.	n.s.	1.033	N/A	0.633	N/A	n.s.	N/A
<i>TC</i>				n.s.	n.s.	n.s.	n.s.	N/A	n.s.	N/A	n.s.	N/A
<i>HV</i>					n.s.	n.s.	n.s.	N/A	n.s.	N/A	n.s.	N/A
<i>BM</i>						n.s.	n.s.	N/A	n.s.	N/A	N/A	N/A
<i>CS</i>							n.s.	N/A	n.s.	N/A	N/A	N/A
<i>SL</i>								-3.537	0.642	N/A	n.s.	N/A
<i>LV</i>									N/A	N/A	N/A	N/A
<i>LY</i>										N/A	N/A	N/A
<i>BR</i>											N/A	N/A
<i>NE</i>												N/A
<i>SF</i>												

Table C.20 Significant slopes for spring nitrate fluxes by site. Slopes were calculated with the rows as y values and columns as x values.

	<i>DI</i>	<i>GP</i>	<i>TC</i>	<i>HV</i>	<i>BM</i>	<i>CS</i>	<i>SL</i>	<i>LV</i>	<i>LY</i>	<i>BR</i>	<i>NE</i>	<i>SF</i>
<i>DI</i>		n.s.	n.s.	n.s.	n.s.	n.s.	n.s.	N/A	N/A	N/A	n.s.	N/A
<i>GP</i>			1.868	0.000	n.s.	0.000	n.s.	N/A	n.s.	N/A	n.s.	N/A
<i>TC</i>				0.575	0.414	0.646	0.959	N/A	n.s.	N/A	n.s.	N/A
<i>HV</i>					0.728	1.118	1.468	N/A	n.s.	N/A	n.s.	N/A
<i>BM</i>						1.567	2.509	N/A	n.s.	N/A	N/A	N/A
<i>CS</i>							1.459	N/A	3.076	N/A	N/A	N/A
<i>SL</i>								0.627	1.534	N/A	n.s.	N/A
<i>LV</i>									N/A	N/A	N/A	N/A
<i>LY</i>										N/A	N/A	N/A
<i>BR</i>											N/A	N/A
<i>NE</i>												N/A
<i>SF</i>												

Table C.21 Significant slopes for spring ammonium concentrations by site. Slopes were calculated with the rows as y values and columns as x values.

	<i>DI</i>	<i>GP</i>	<i>TC</i>	<i>HV</i>	<i>BM</i>	<i>CS</i>	<i>SL</i>	<i>LV</i>	<i>LY</i>	<i>BR</i>	<i>NE</i>	<i>SF</i>
<i>DI</i>		n.s.	n.s.	n.s.	n.s.	n.s.	n.s.	N/A	N/A	N/A	n.s.	N/A
<i>GP</i>			n.s.	3.746	n.s.	n.s.	1.687	N/A	n.s.	N/A	n.s.	N/A
<i>TC</i>				n.s.	n.s.	0.871	1.609	N/A	n.s.	N/A	n.s.	N/A
<i>HV</i>					n.s.	0.667	0.552	N/A	n.s.	N/A	n.s.	N/A
<i>BM</i>						n.s.	0.000	N/A	n.s.	N/A	N/A	N/A
<i>CS</i>							0.872	N/A	n.s.	N/A	N/A	N/A
<i>SL</i>								8.353	0.477	N/A	n.s.	N/A
<i>LV</i>									N/A	N/A	N/A	N/A
<i>LY</i>										N/A	N/A	N/A
<i>BR</i>											N/A	N/A
<i>NE</i>												N/A
<i>SF</i>												

Table C.22 Significant slopes for spring ammonium fluxes by site. Slopes were calculated with the rows as y values and columns as x values.

	<i>DI</i>	<i>GP</i>	<i>TC</i>	<i>HV</i>	<i>BM</i>	<i>CS</i>	<i>SL</i>	<i>LV</i>	<i>LY</i>	<i>BR</i>	<i>NE</i>	<i>SF</i>
<i>DI</i>		n.s.	n.s.	-3.689	n.s.	0.000	n.s.	N/A	N/A	N/A	n.s.	N/A
<i>GP</i>			0.808	n.s.	n.s.	n.s.	n.s.	N/A	n.s.	N/A	n.s.	N/A
<i>TC</i>				0.468	0.329	0.389	1.012	N/A	n.s.	N/A	n.s.	N/A
<i>HV</i>					0.702	0.812	1.921	N/A	2.923	N/A	n.s.	N/A
<i>BM</i>						1.153	2.809	N/A	n.s.	N/A	N/A	N/A
<i>CS</i>							2.435	N/A	3.593	N/A	N/A	N/A
<i>SL</i>								1.229	1.209	N/A	n.s.	N/A
<i>LV</i>									N/A	N/A	N/A	N/A
<i>LY</i>										N/A	N/A	N/A
<i>BR</i>											N/A	N/A
<i>NE</i>												N/A
<i>SF</i>												

Table C.23 Significant slopes for spring precipitation amounts by site. Slopes were calculated with the rows as y values and columns as x values.

	<i>DI</i>	<i>GP</i>	<i>TC</i>	<i>HV</i>	<i>BM</i>	<i>CS</i>	<i>SL</i>	<i>LV</i>	<i>LY</i>	<i>BR</i>	<i>NE</i>	<i>SF</i>
<i>DI</i>		n.s.	n.s.	n.s.	n.s.	n.s.	n.s.	N/A	n.s.	N/A	n.s.	N/A
<i>GP</i>			1.230	n.s.								
<i>TC</i>				0.000	n.s.	n.s.	0.347	n.s.	n.s.	N/A	n.s.	n.s.
<i>HV</i>					1.334	0.911	0.783	N/A	n.s.	N/A	n.s.	n.s.
<i>BM</i>						0.822	n.s.	n.s.	n.s.	N/A	N/A	n.s.
<i>CS</i>							1.020	n.s.	n.s.	N/A	n.s.	n.s.
<i>SL</i>								n.s.	n.s.	N/A	n.s.	n.s.
<i>LV</i>									N/A	N/A	N/A	N/A
<i>LY</i>										N/A	N/A	n.s.
<i>BR</i>											N/A	N/A
<i>NE</i>												N/A
<i>SF</i>												

Table C.24 Significant slopes for summer sulfate concentrations by site. Slopes were calculated with the rows as y values and columns as x values.

	<i>GP</i>	<i>TC</i>	<i>LI</i>	<i>AL</i>	<i>RC</i>	<i>RB</i>	<i>HV</i>	<i>BM</i>	<i>CS</i>	<i>SL</i>	<i>LV</i>	<i>LY</i>
<i>GP</i>		0.372	n.s.	0.481	n.s.	0.485						
<i>TC</i>			n.s.	n.s.	0.416	0.434	0.362	0.063	n.s.	0.999	n.s.	n.s.
<i>LI</i>				n.s.	n.s.	n.s.	0.248	0.058	n.s.	n.s.	n.s.	n.s.
<i>AL</i>					n.s.	0.600	0.404	n.s.	n.s.	n.s.	n.s.	n.s.
<i>RC</i>						n.s.	n.s.	0.171	n.s.	0.453	n.s.	n.s.
<i>RB</i>							1.669	0.136	n.s.	7.953	n.s.	n.s.
<i>HV</i>								0.093	n.s.	4.792	n.s.	n.s.
<i>BM</i>									n.s.	n.s.	n.s.	n.s.
<i>CS</i>										n.s.	n.s.	n.s.
<i>SL</i>											n.s.	n.s.
<i>LV</i>												n.s.
<i>LY</i>												

Table C.25 Significant slopes for summer fluxes by site. Slopes were calculated with the rows as y values and columns as x values.

	<i>GP</i>	<i>TC</i>	<i>LI</i>	<i>AL</i>	<i>RC</i>	<i>RB</i>	<i>HV</i>	<i>BM</i>	<i>CS</i>	<i>SL</i>	<i>LV</i>	<i>LY</i>
<i>GP</i>		n.s.	0.912	n.s.								
<i>TC</i>			1.002	n.s.	1.090	n.s.						
<i>LI</i>				n.s.								
<i>AL</i>					n.s.	n.s.	n.s.	n.s.	n.s.	-0.718	n.s.	n.s.
<i>RC</i>						n.s.	n.s.	n.s.	n.s.	n.s.	0.474	n.s.
<i>RB</i>							0.626	1.084	0.802	n.s.	n.s.	n.s.
<i>HV</i>								1.902	1.295	1.482	n.s.	n.s.
<i>BM</i>									0.720	1.223	n.s.	n.s.
<i>CS</i>										1.512	n.s.	0.946
<i>SL</i>											n.s.	0.633
<i>LV</i>												n.s.
<i>LY</i>												

Table C.26 Significant slopes for summer nitrate concentrations by site. Slopes were calculated with the rows as y values and columns as x values.

	<i>GP</i>	<i>TC</i>	<i>LI</i>	<i>AL</i>	<i>RC</i>	<i>RB</i>	<i>HV</i>	<i>BM</i>	<i>CS</i>	<i>SL</i>	<i>LV</i>	<i>LY</i>
<i>GP</i>		n.s.	0.477	n.s.	0.184							
<i>TC</i>			n.s.	n.s.	0.398	0.376	0.325	n.s.	n.s.	1.095	n.s.	n.s.
<i>LI</i>				n.s.	0.391							
<i>AL</i>					n.s.	0.559	0.372	n.s.	-0.162	n.s.	n.s.	n.s.
<i>RC</i>						0.000	0.000	n.s.	n.s.	0.316	n.s.	n.s.
<i>RB</i>							1.002	n.s.	n.s.	3.646	n.s.	n.s.
<i>HV</i>								n.s.	n.s.	3.478	n.s.	n.s.
<i>BM</i>									n.s.	n.s.	n.s.	n.s.
<i>CS</i>										n.s.	n.s.	n.s.
<i>SL</i>											n.s.	n.s.
<i>LV</i>												n.s.
<i>LY</i>												

Table C.27 Significant slopes for summer nitrate fluxes by site. Slopes were calculated with the rows as y values and columns as x values.

	<i>GP</i>	<i>TC</i>	<i>LI</i>	<i>AL</i>	<i>RC</i>	<i>RB</i>	<i>HV</i>	<i>BM</i>	<i>CS</i>	<i>SL</i>	<i>LV</i>	<i>LY</i>
<i>GP</i>		0.631	0.713	n.s.	n.s.	n.s.	1.460	n.s.	n.s.	n.s.	n.s.	n.s.
<i>TC</i>			0.841	n.s.	1.169	n.s.						
<i>LI</i>				n.s.	1.094	n.s.	1.654	n.s.	n.s.	n.s.	n.s.	n.s.
<i>AL</i>					n.s.	n.s.	1.756	n.s.	n.s.	-1.399	n.s.	n.s.
<i>RC</i>						n.s.						
<i>RB</i>							0.894	n.s.	0.635	n.s.	n.s.	n.s.
<i>HV</i>								n.s.	n.s.	n.s.	n.s.	n.s.
<i>BM</i>									0.699	n.s.	n.s.	n.s.
<i>CS</i>										1.278	n.s.	n.s.
<i>SL</i>											n.s.	n.s.
<i>LV</i>												n.s.
<i>LY</i>												

Table C.28 Significant slopes for summer ammonium concentrations by site. Slopes were calculated with the rows as y values and columns as x values.

	<i>GP</i>	<i>TC</i>	<i>LI</i>	<i>AL</i>	<i>RC</i>	<i>RB</i>	<i>HV</i>	<i>BM</i>	<i>CS</i>	<i>SL</i>	<i>LV</i>	<i>LY</i>
<i>GP</i>		0.384	n.s.	0.598	n.s.	0.121						
<i>TC</i>			n.s.	n.s.	0.508	0.338	n.s.	0.059	n.s.	1.149	n.s.	0.390
<i>LI</i>				n.s.	n.s.	n.s.	n.s.	0.053	n.s.	n.s.	n.s.	#DIV/0!
<i>AL</i>					0.739	n.s.	0.801	0.282	n.s.	n.s.	n.s.	n.s.
<i>RC</i>						n.s.	n.s.	0.124	n.s.	n.s.	n.s.	n.s.
<i>RB</i>							4.469	0.125	n.s.	7.061	n.s.	0.296
<i>HV</i>								n.s.	n.s.	1.164	n.s.	#DIV/0!
<i>BM</i>									n.s.	n.s.	n.s.	n.s.
<i>CS</i>										n.s.	n.s.	n.s.
<i>SL</i>											n.s.	n.s.
<i>LV</i>												n.s.
<i>LY</i>												

Table C.29 Significant slopes for summer ammonium fluxes by site. Slopes were calculated with the rows as y values and columns as x values.

	<i>GP</i>	<i>TC</i>	<i>LI</i>	<i>AL</i>	<i>RC</i>	<i>RB</i>	<i>HV</i>	<i>BM</i>	<i>CS</i>	<i>SL</i>	<i>LV</i>	<i>LY</i>
<i>GP</i>		1.023	0.984	N/A	n.s.	n.s.	2.184	n.s.	n.s.	n.s.	n.s.	-0.119
<i>TC</i>			0.804	0.755	n.s.	n.s.	3.216	n.s.	n.s.	n.s.	n.s.	n.s.
<i>LI</i>				n.s.	n.s.	n.s.	3.573	n.s.	n.s.	N/A	-0.173	N/A
<i>AL</i>					n.s.	0.752	n.s.	5.116	n.s.	N/A	n.s.	N/A
<i>RC</i>						n.s.						
<i>RB</i>							n.s.	n.s.	0.235	n.s.	n.s.	-0.263
<i>HV</i>								#DIV/0!	1.386	N/A	n.s.	N/A
<i>BM</i>									0.523	n.s.	n.s.	0.890
<i>CS</i>										1.913	n.s.	n.s.
<i>SL</i>											n.s.	n.s.
<i>LV</i>												n.s.
<i>LY</i>												

Table C.30 Significant slopes for summer precipitation amounts by site. Slopes were calculated with the rows as y values and columns as x values.

	<i>GP</i>	<i>TC</i>	<i>LI</i>	<i>AL</i>	<i>RC</i>	<i>RB</i>	<i>HV</i>	<i>BM</i>	<i>CS</i>	<i>SL</i>	<i>LV</i>	<i>LY</i>
<i>GP</i>		1.719	1.598	n.s.	n.s.	n.s.	n.s.	n.s.	n.s.	1.091	n.s.	n.s.
<i>TC</i>			0.721	n.s.								
<i>LI</i>				n.s.								
<i>AL</i>					n.s.	1.671	n.s.	n.s.	n.s.	n.s.	n.s.	n.s.
<i>RC</i>						n.s.	0.241	n.s.	n.s.	n.s.	n.s.	n.s.
<i>RB</i>							0.448	0.816	0.307	1.009	n.s.	0.239
<i>HV</i>								1.956	0.654	2.325	n.s.	0.790
<i>BM</i>									0.342	1.113	n.s.	0.417
<i>CS</i>										2.693	n.s.	n.s.
<i>SL</i>											n.s.	0.327
<i>LV</i>												n.s.
<i>LY</i>												

Appendix D Core Site Sub-event Timelines: concentrations, fluxes, and cumulative deposition

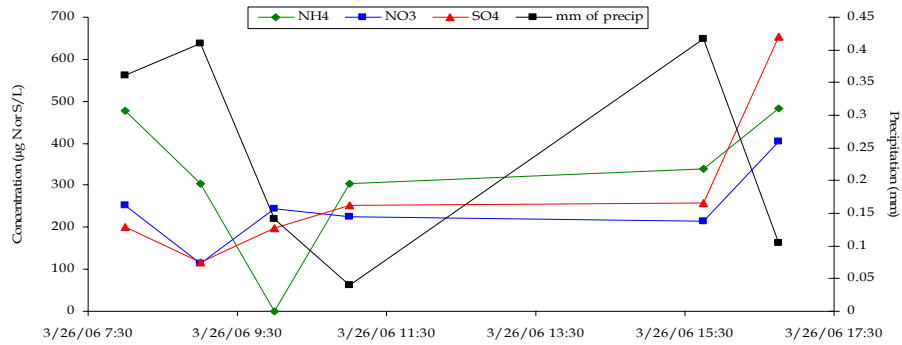


Figure D.1 Concentrations of ammonium (green), nitrate (blue), and sulfate (red) in precipitation samples collected throughout the 3/26/06 event at the Core Site.

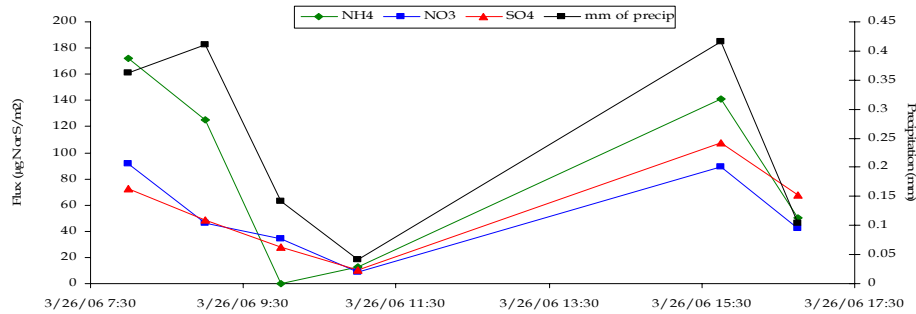


Figure D.2 Deposition of ammonium (green), nitrate (blue), and sulfate (red) throughout the 3/26/06 event at the Core Site.

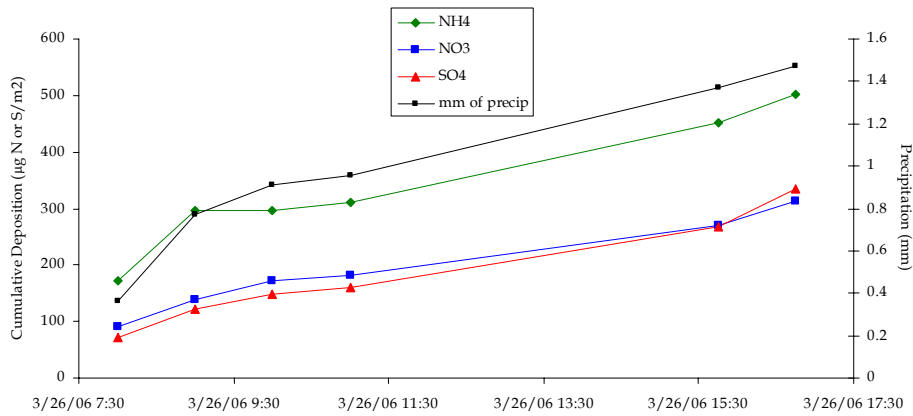


Figure D.3 Cumulative deposition of ammonium (green), nitrate (blue), and sulfate (red) throughout the 3/26/06 event at the Core Site.

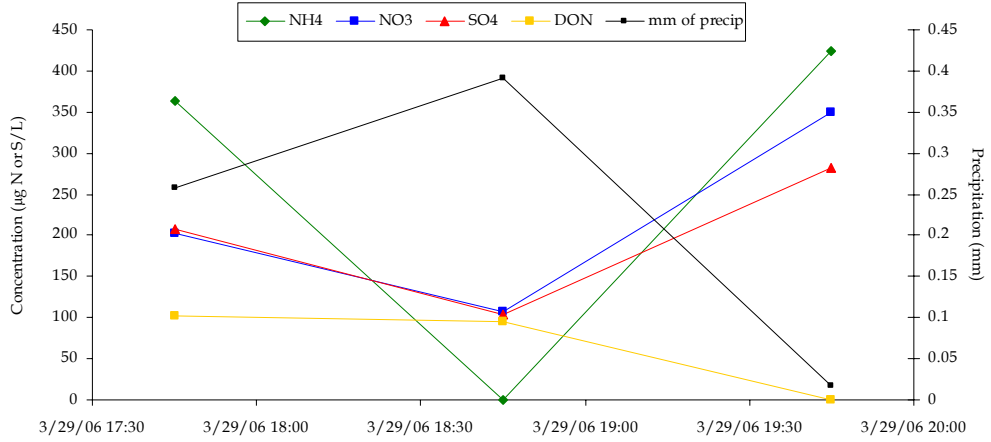


Figure D.4 Timeline of concentrations from 17:45 through 20:45 on 3/29 from sub event sampler at the Core Site.

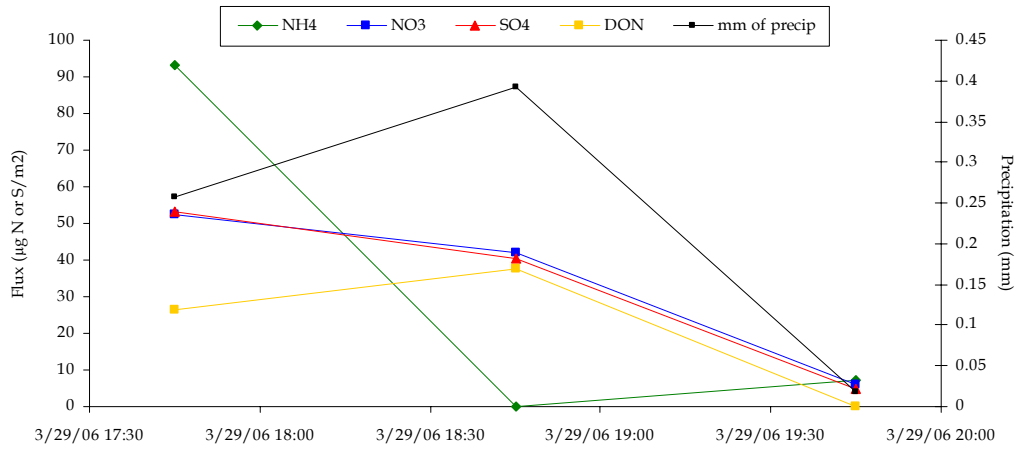


Figure D.5 Deposition of ammonium (green), nitrate (blue), sulfate (red), and organic nitrogen (yellow) throughout the 3/29 event at the Core Site.

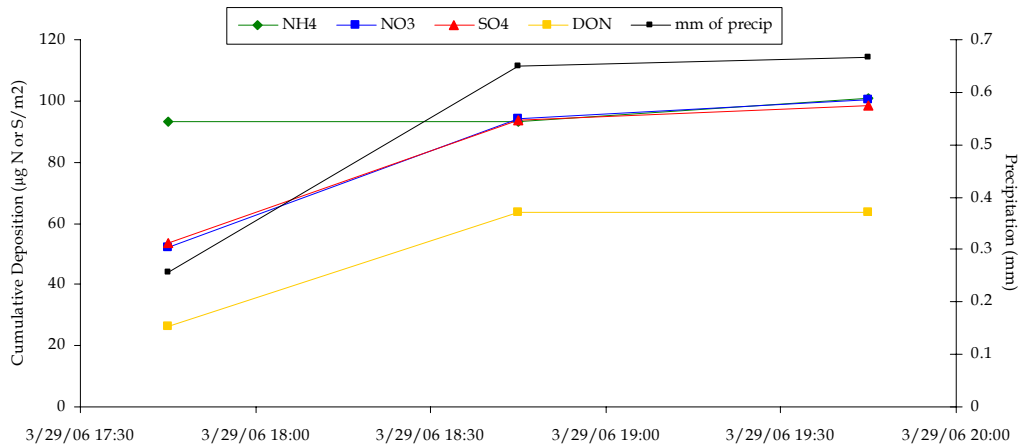


Figure D.6 Cumulative deposition of ammonium (green), nitrate (blue), sulfate (red), organic nitrogen (yellow) throughout the 3/29 event at the Core Site.

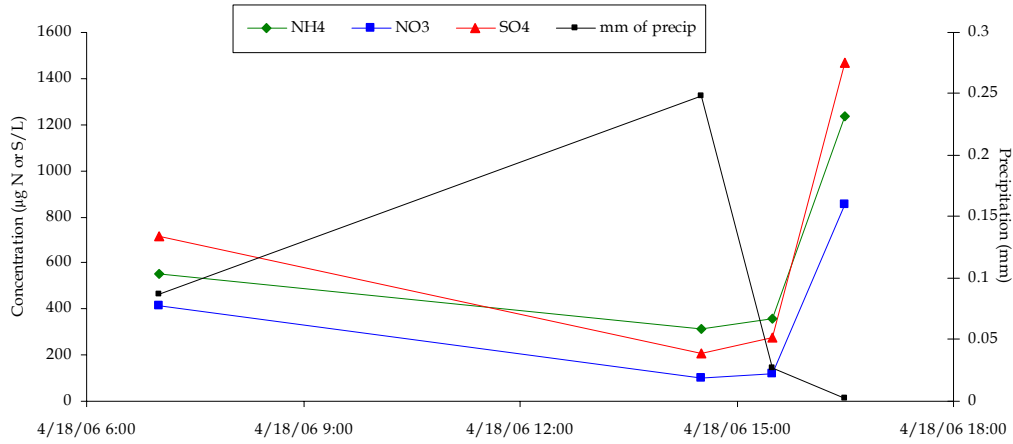


Figure D.7 Concentrations of ammonium (green), nitrate (blue), and sulfate (red) in precipitation samples collected throughout the 4/18 event at the Core Site.

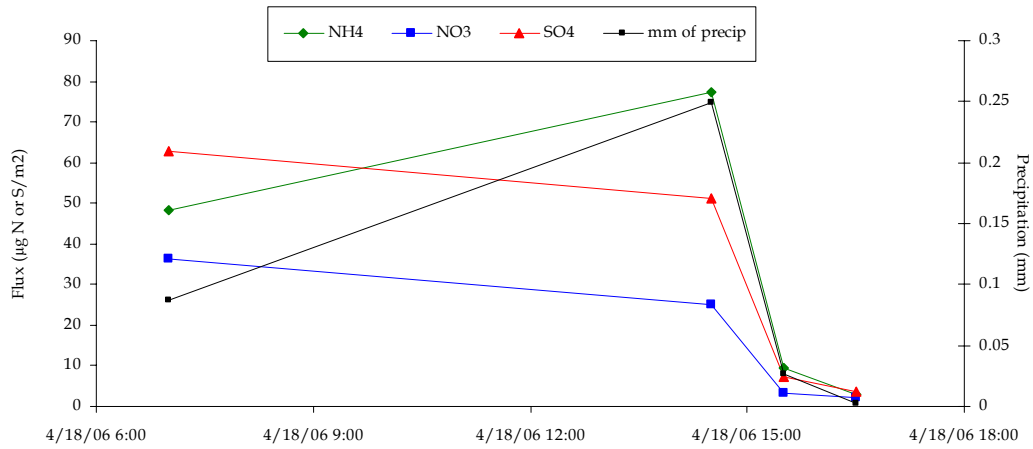


Figure D.8 Deposition of ammonium (green), nitrate (blue), and sulfate (red) throughout the 4/18 event at the Core Site.

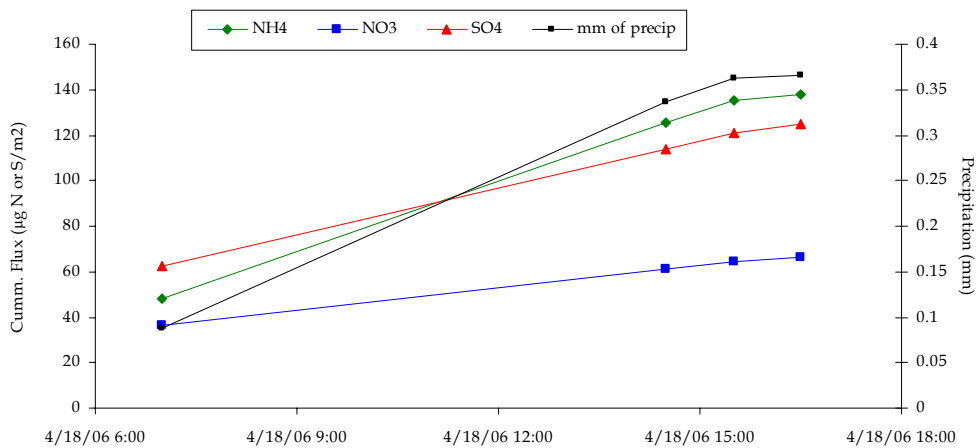


Figure D.9 Cumulative deposition of ammonium (green), nitrate (blue), and sulfate (red) throughout the 4/18 event at the Core Site.

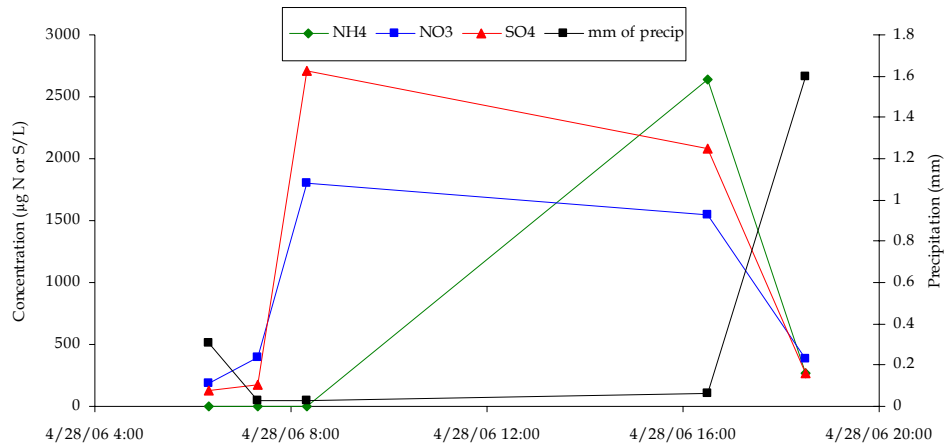


Figure D.10 Concentrations of ammonium (green), nitrate (blue), and sulfate (red) in precipitation samples collected throughout the 4/28 event at the Core Site.

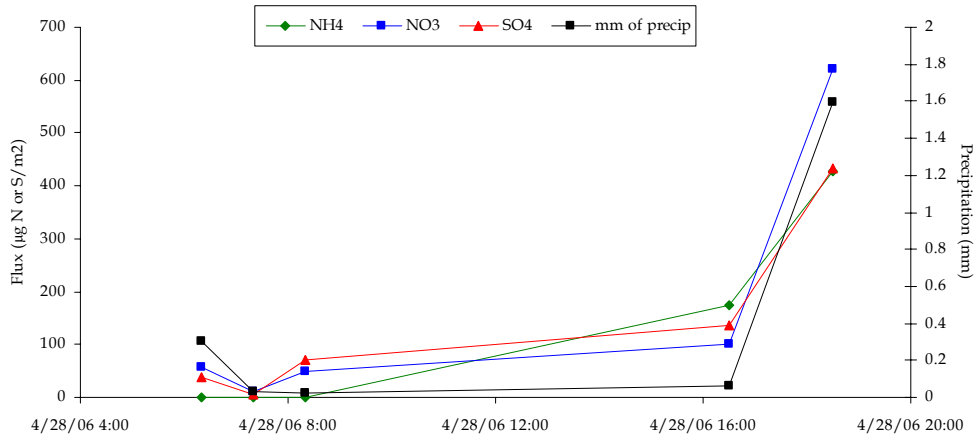


Figure D.11 Deposition of ammonium (green), nitrate (blue), and sulfate (red) throughout the 4/28 event at the Core Site.

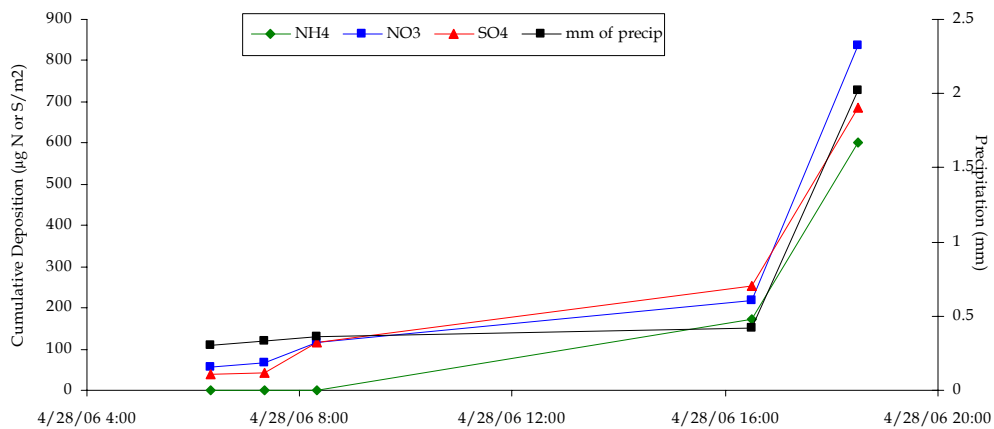


Figure D.12 Cumulative deposition of ammonium (green), nitrate (blue), and sulfate (red) throughout the 4/28 event at the Core Site.

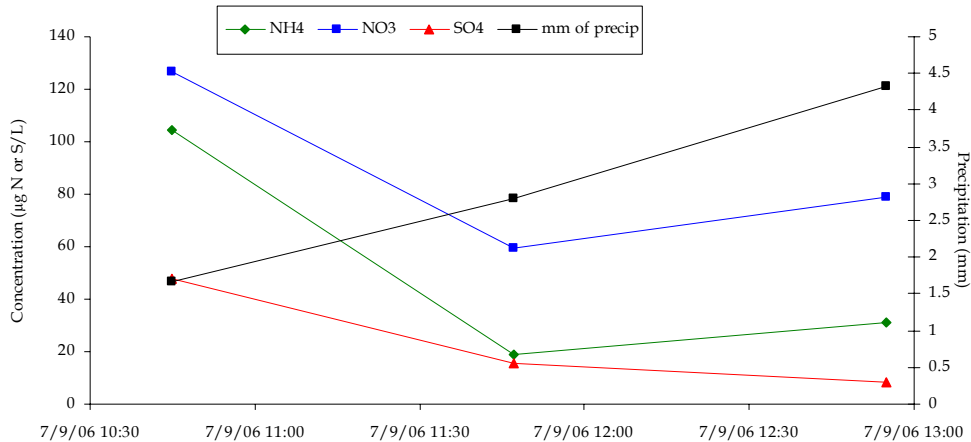


Figure D.13 Concentrations of ammonium (green), nitrate (blue), and sulfate (red) in precipitation samples collected throughout the 7/9 event at the Core Site.

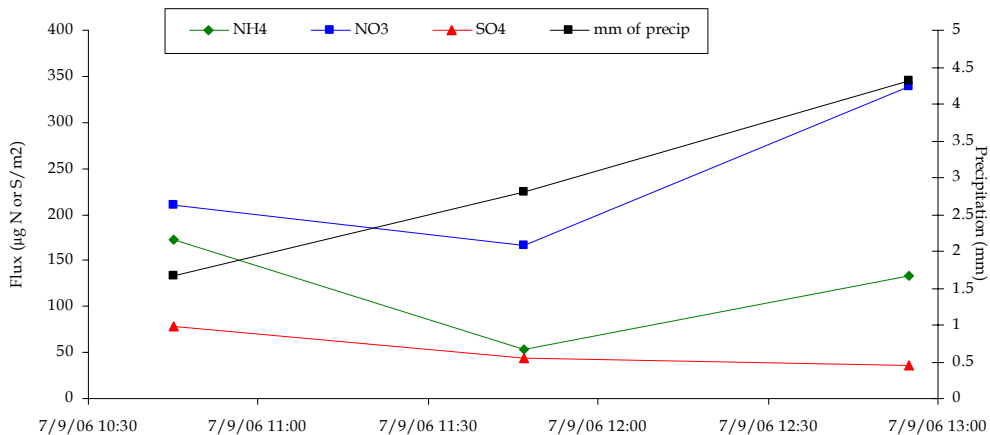


Figure D.14 Deposition of ammonium (green), nitrate (blue), and sulfate (red) throughout the 7/9 event at the Core Site.

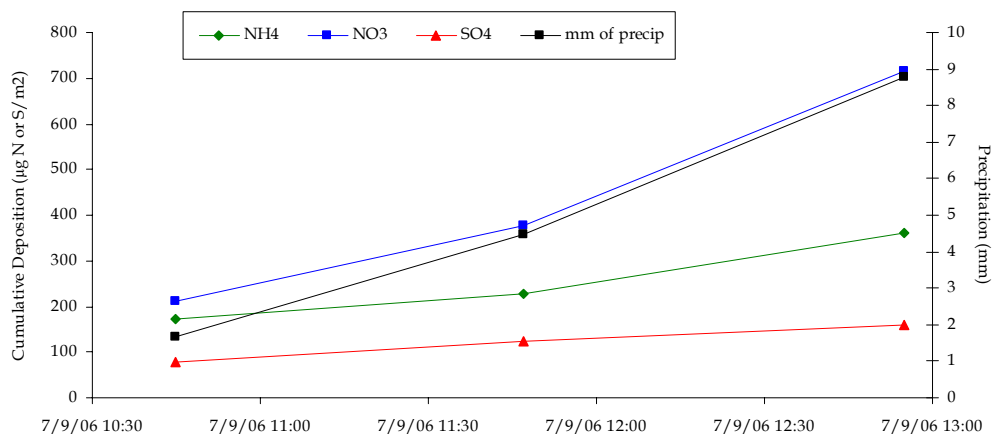


Figure D.15 Cumulative deposition of ammonium (green), nitrate (blue), and sulfate (red) throughout the 7/9 event at the Core Site.

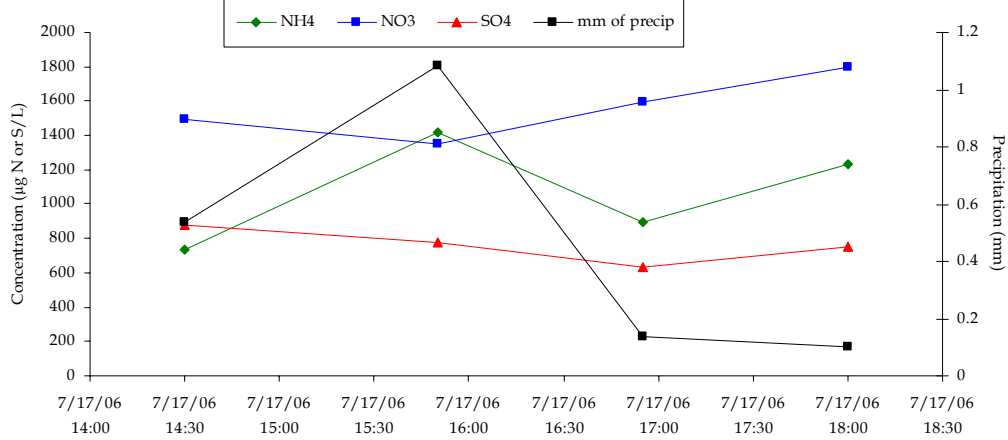


Figure D.16 Concentrations of ammonium (green), nitrate (blue), and sulfate (red) in precipitation samples collected throughout the 7/17 event at the Core Site.

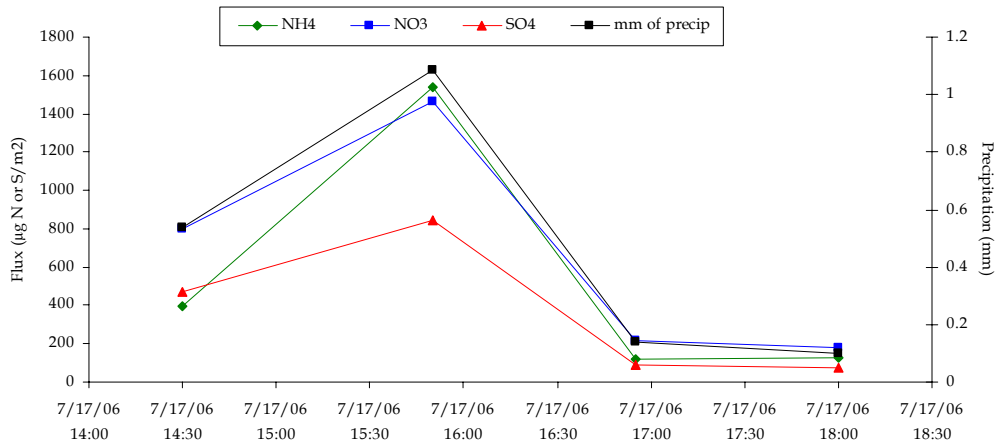


Figure D.17 Deposition of ammonium (green), nitrate (blue), and sulfate (red) throughout the 7/17 event at the Core Site.

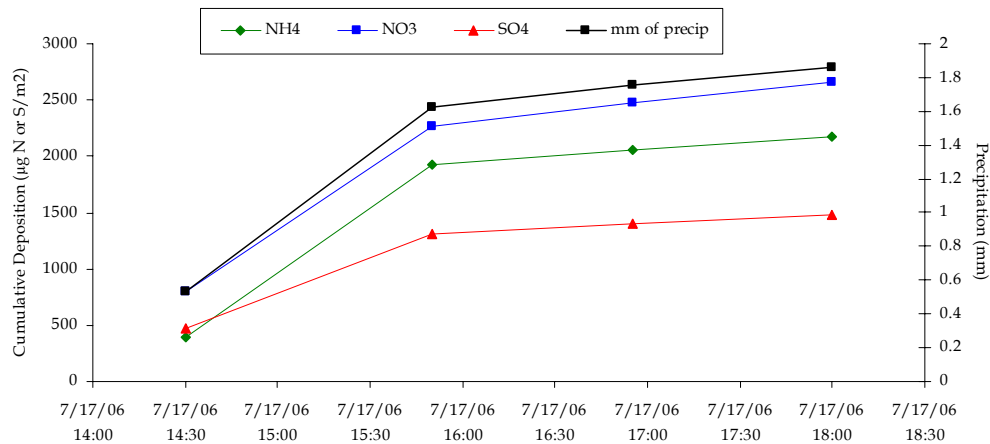


Figure D.18 Cumulative deposition of ammonium (green), nitrate (blue), and sulfate (red) throughout the 7/17 event at the Core Site.

Appendix E Lyons Subevent Timelines: concentrations, fluxes, and cumulative deposition

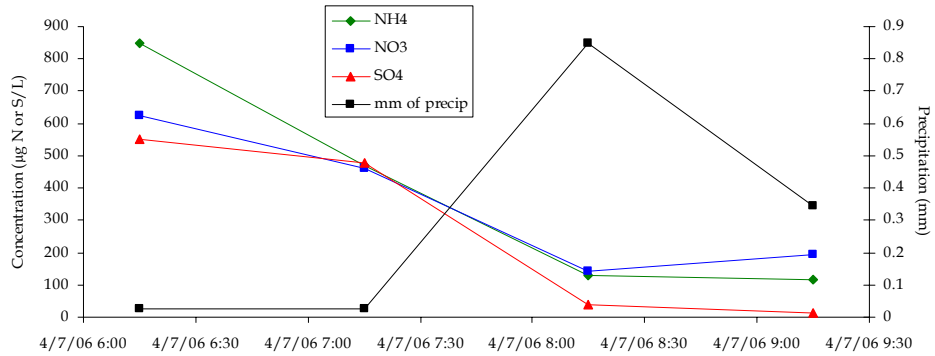


Figure E.1 Timeline of concentrations from sub event sampler at the Lyons site on 4/7.

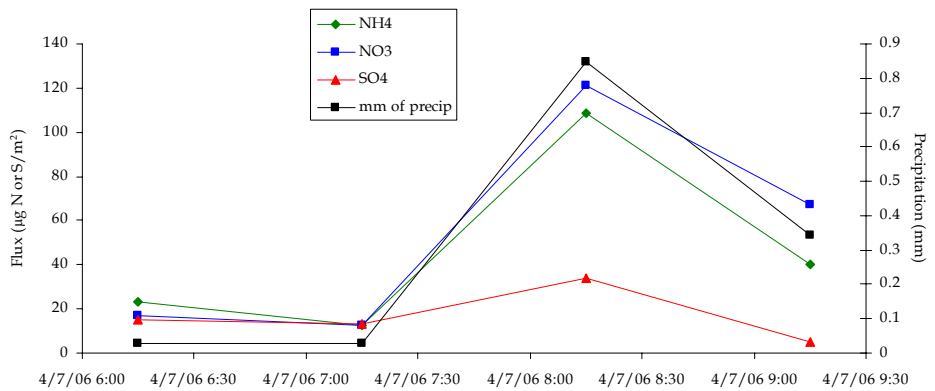


Figure E.2 Deposition of ammonium (green), nitrate (blue), and sulfate (red) throughout the 4/7 event at the Lyons site.

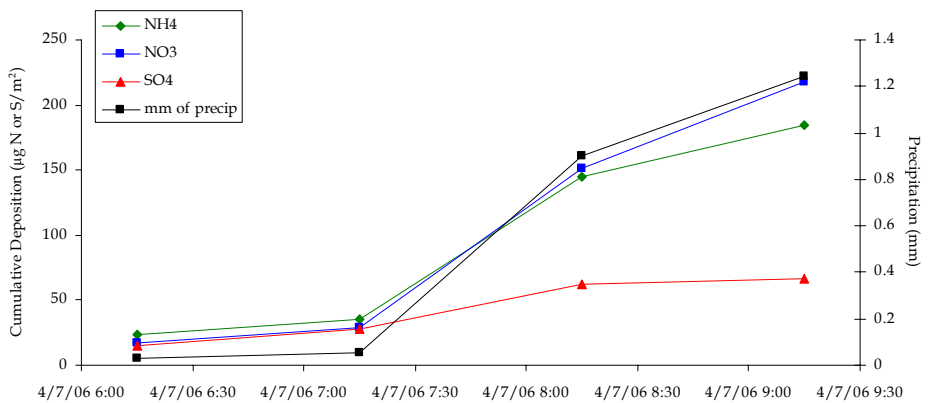


Figure E.3 Cumulative deposition of ammonium (green), nitrate (blue), and sulfate (red) throughout the 4/7 event at the Lyons site.

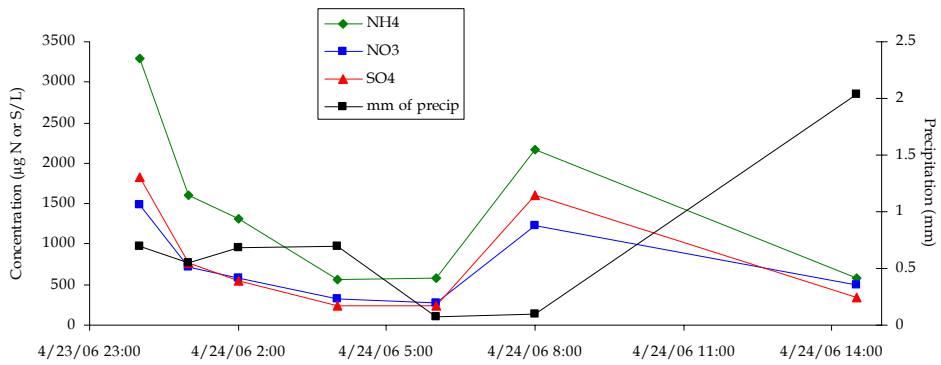


Figure E.4 Timeline of concentrations from sub event sampler at the Lyons site throughout the 4/23-4/24.

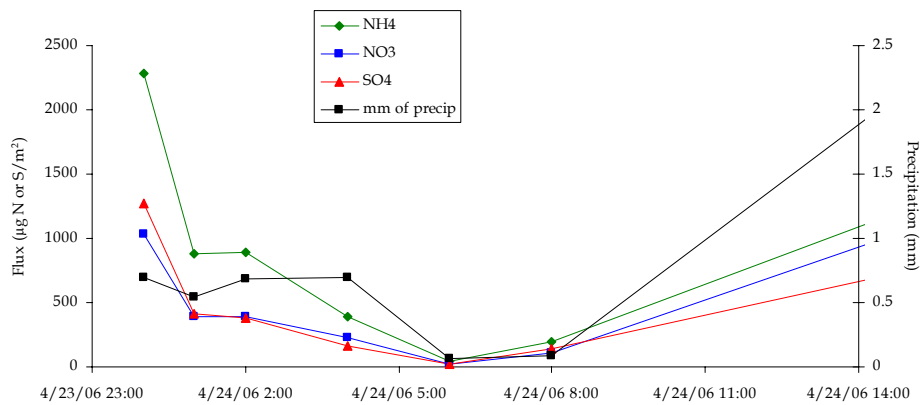


Figure E.5 Deposition of ammonium (green), nitrate (blue), and sulfate (red) throughout the 4/23-4/24 event at the Lyons site.

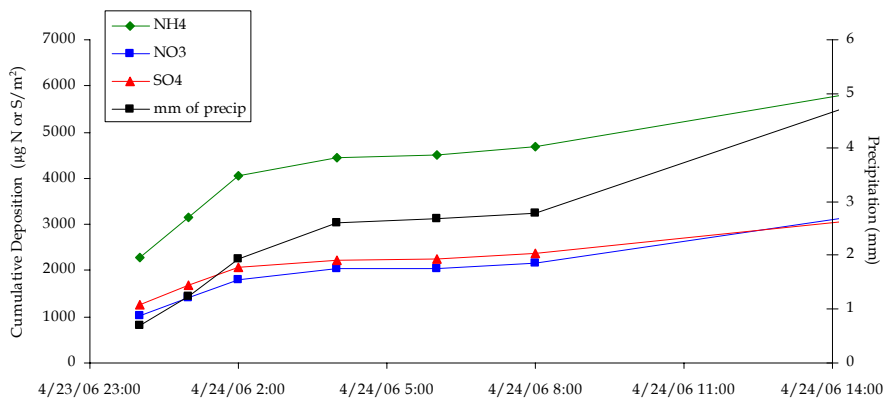


Figure E.6 Cumulative deposition of ammonium (green), nitrate (blue), and sulfate (red) throughout the 4/23-4/24 event at the Lyons site.

Appendix F Gore Pass Subevent Timelines: concentrations, fluxes, and cumulative deposition

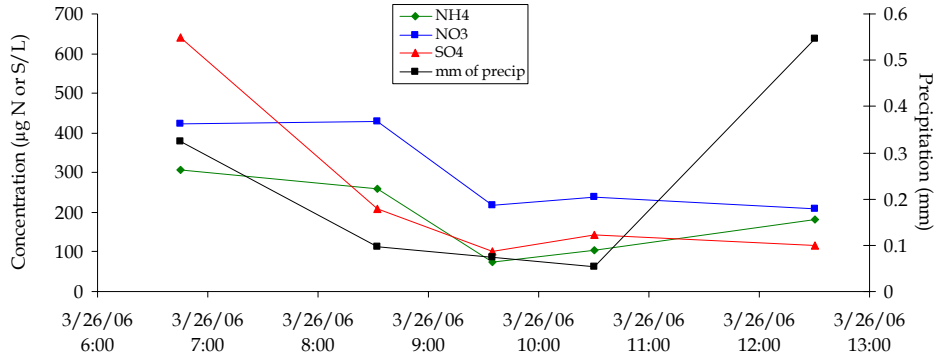


Figure F.1 Timeline of concentrations from sub event sampler at the Gore Pass site for 3/26.

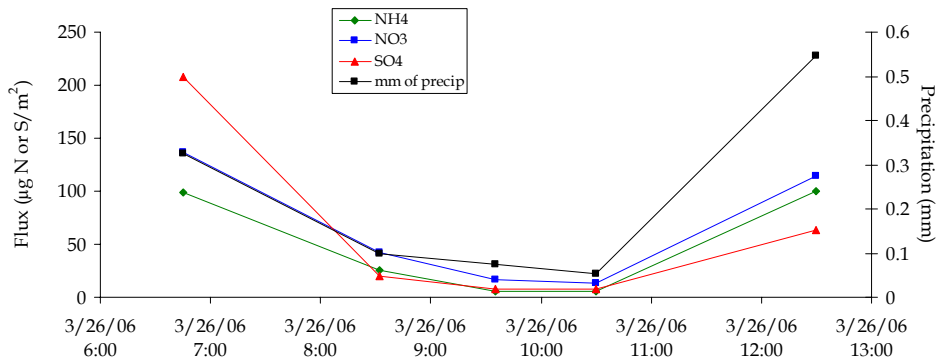


Figure F.2 Deposition of ammonium (green), nitrate (blue), and sulfate (red) throughout the 3/26 event at the Gore Pass site.

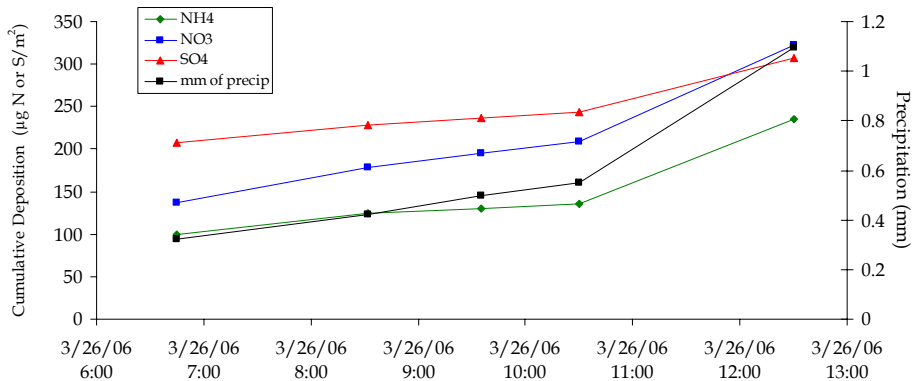


Figure F.3 Cumulative deposition of ammonium (green), nitrate (blue), and sulfate (red) throughout the 3/26 event at the Gore Pass site.

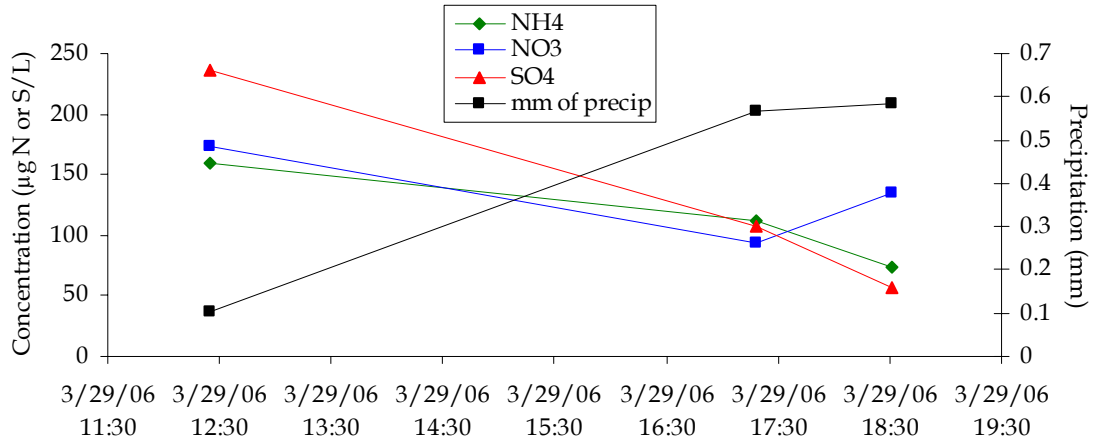


Figure F.4 Timeline of concentrations from the sub event sampler at the Gore Pass site for 3/29.

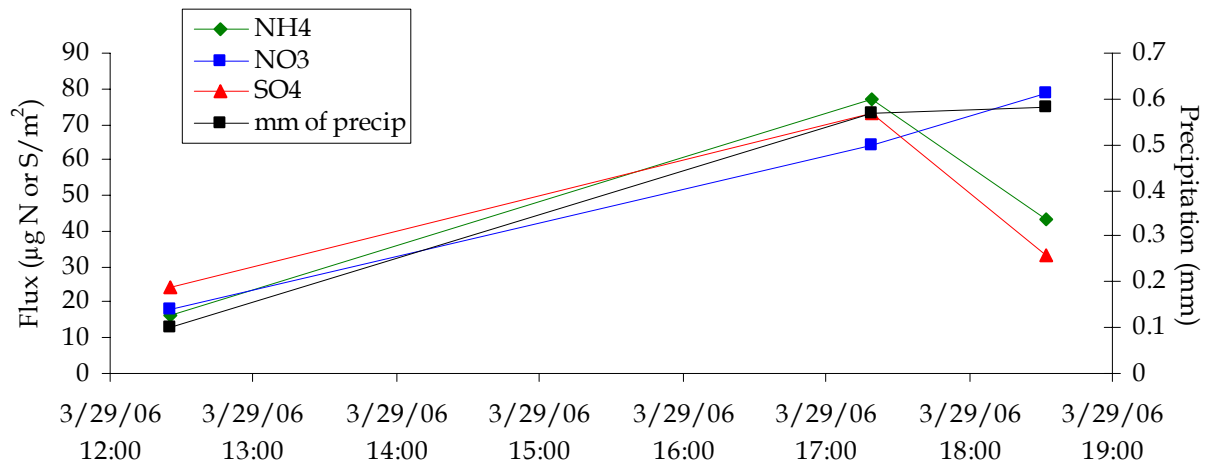


Figure F.5 Deposition of ammonium (green), nitrate (blue), and sulfate (red) throughout the 3/29 event at the Gore Pass site.

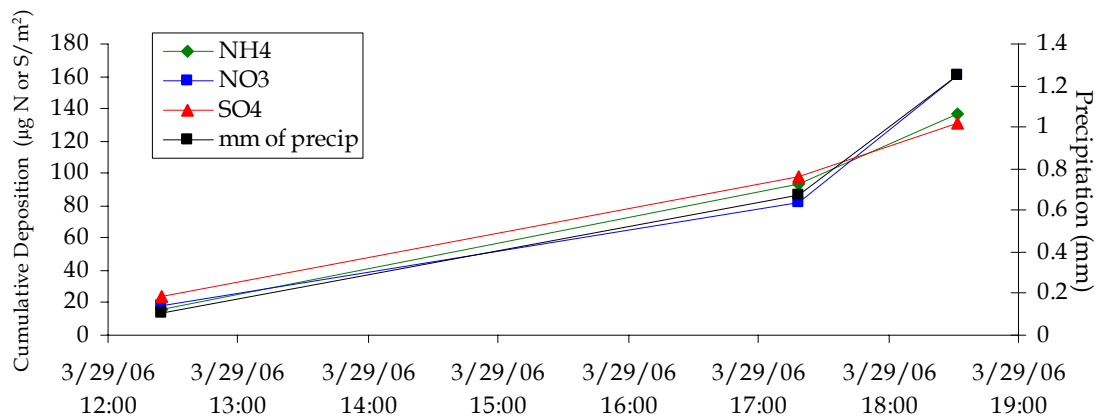


Figure F.6 Cumulative deposition of ammonium (green), nitrate (blue), and sulfate (red) throughout the 3/29 event at the Gore Pass site.

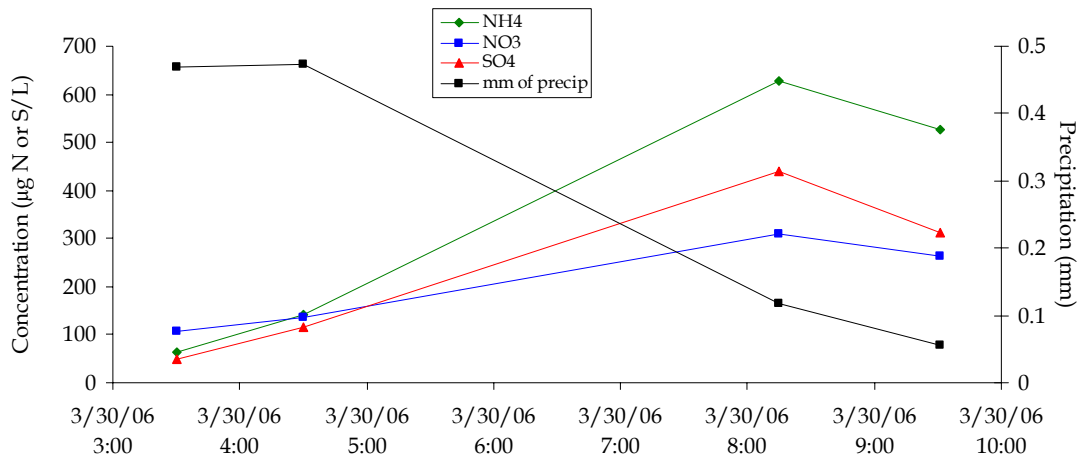


Figure F.7 Timeline of concentrations from the sub event sampler at the Gore Pass site for 3/30.

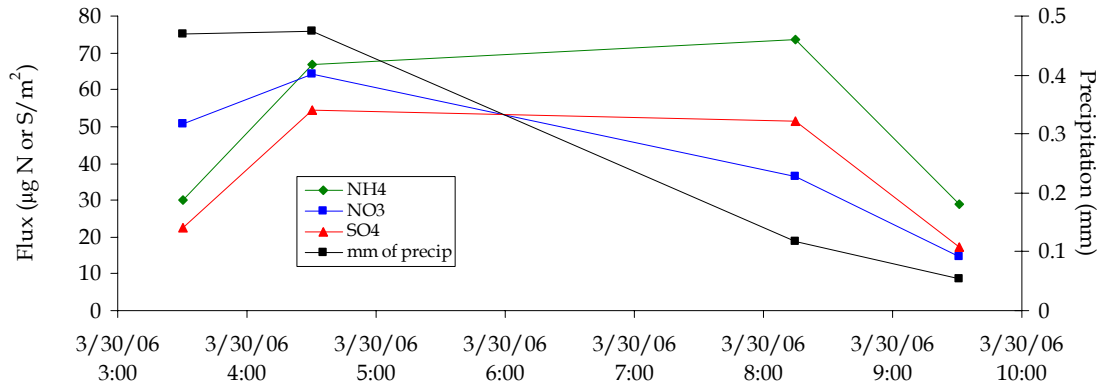


Figure F.8 Deposition of ammonium (green), nitrate (blue), and sulfate (red) throughout the 3/30 event at the Gore Pass site.

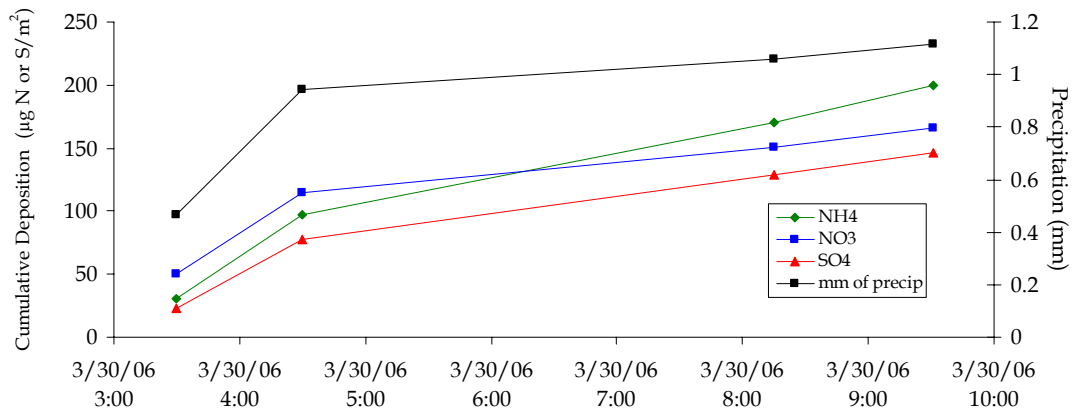


Figure F.9 Cumulative deposition of ammonium (green), nitrate (blue), and sulfate (red) throughout the 3/30 event at the Gore Pass site.

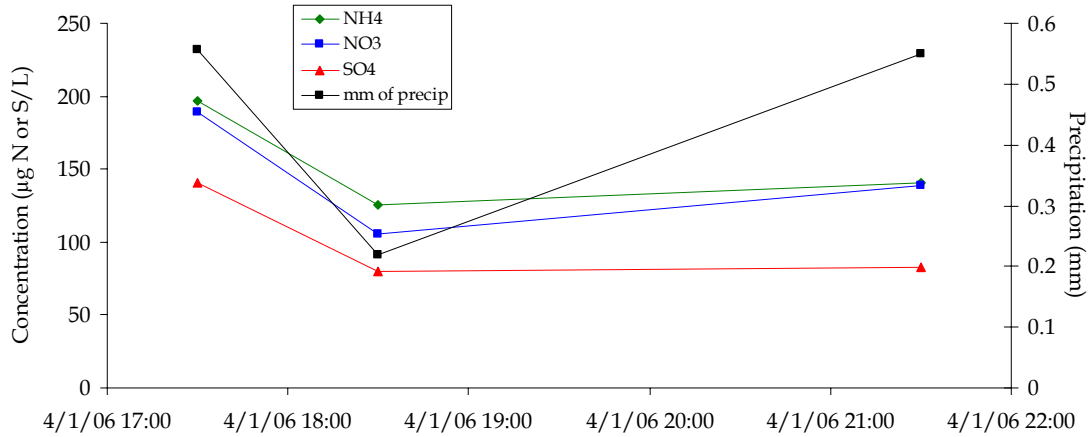


Figure F.10 Timeline of concentrations from the sub event sampler at the Gore Pass site for 4/1.

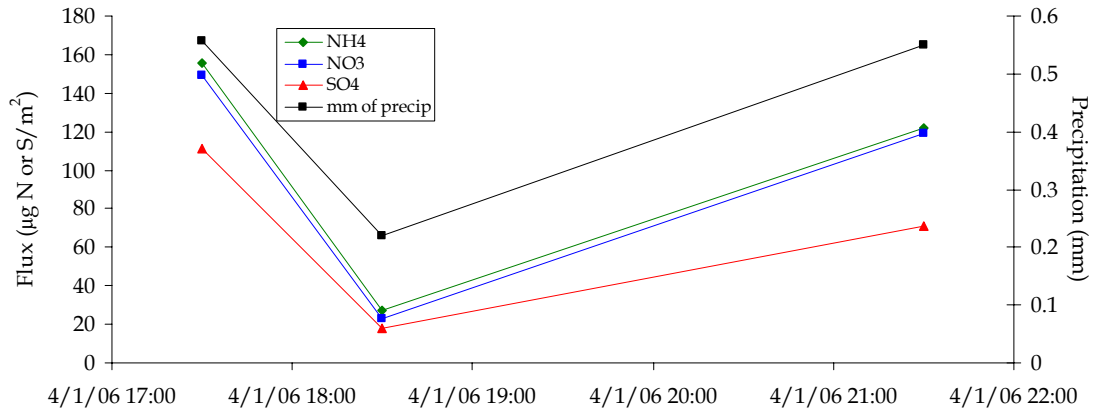


Figure F.11 Deposition of ammonium (green), nitrate (blue), and sulfate (red) throughout the 4/1 event at the Gore Pass site.

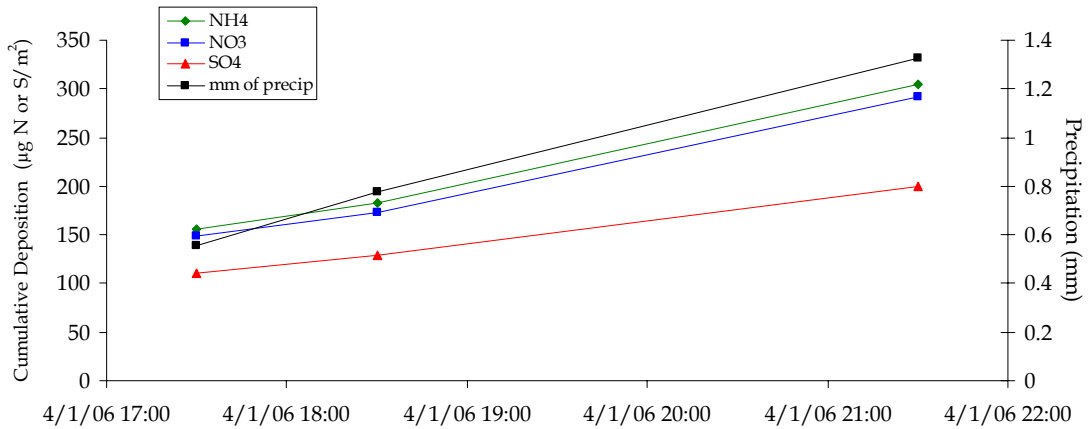


Figure F.12 Cumulative deposition of ammonium (green), nitrate (blue), and sulfate (red) throughout the 4/1 event at the Gore Pass site.

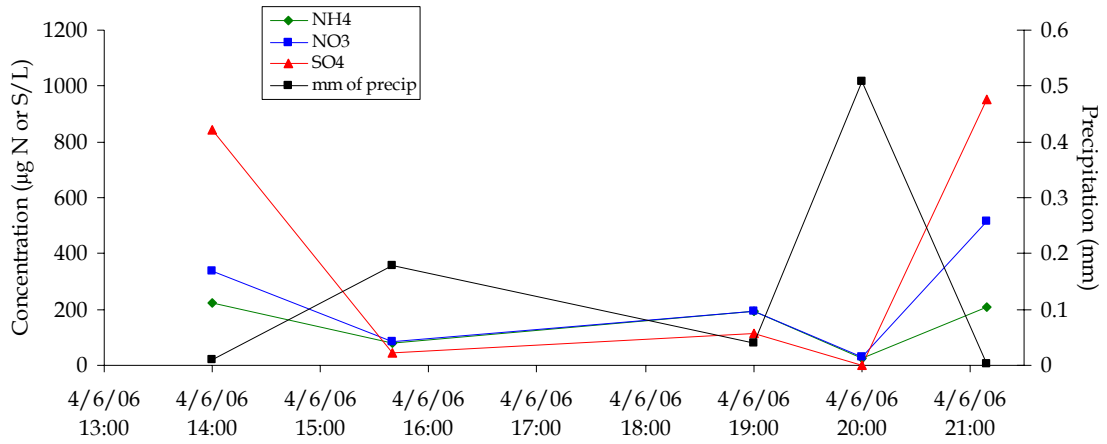


Figure F.13 Timeline of concentrations from the sub event sampler at the Gore Pass site for 4/6.

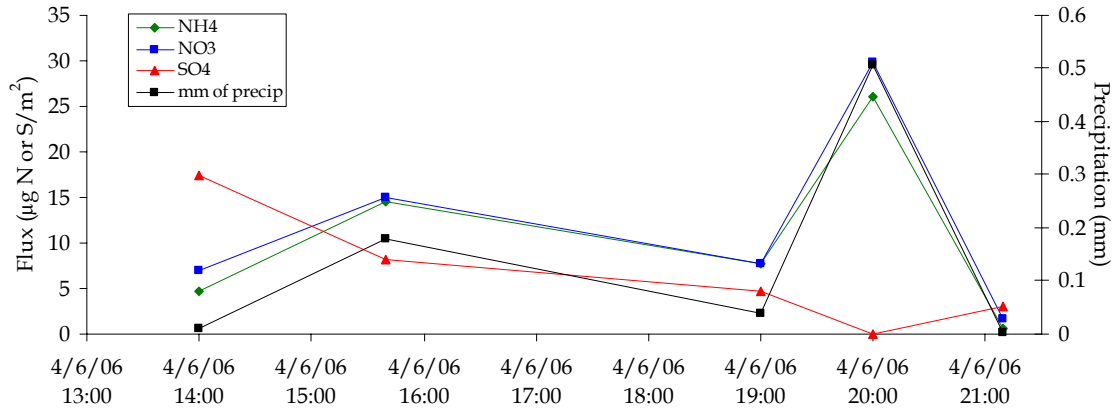


Figure F.14 Deposition of ammonium (green), nitrate (blue), and sulfate (red) throughout the 4/6 event at the Gore Pass site.

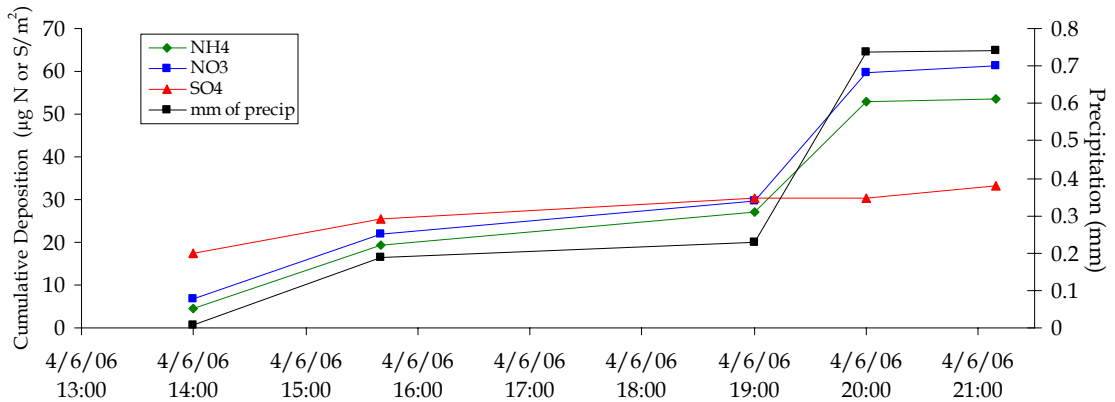


Figure F.15 Cumulative deposition of ammonium (green), nitrate (blue), and sulfate (red) throughout the 4/6 event at the Gore Pass site.

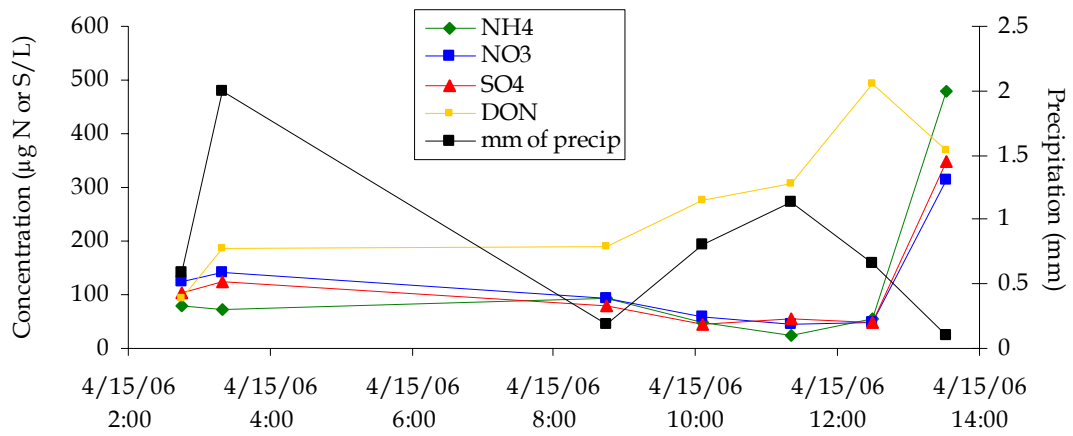


Figure F.16 Timeline of concentrations from the sub event sampler at the Gore Pass site for 4/15.

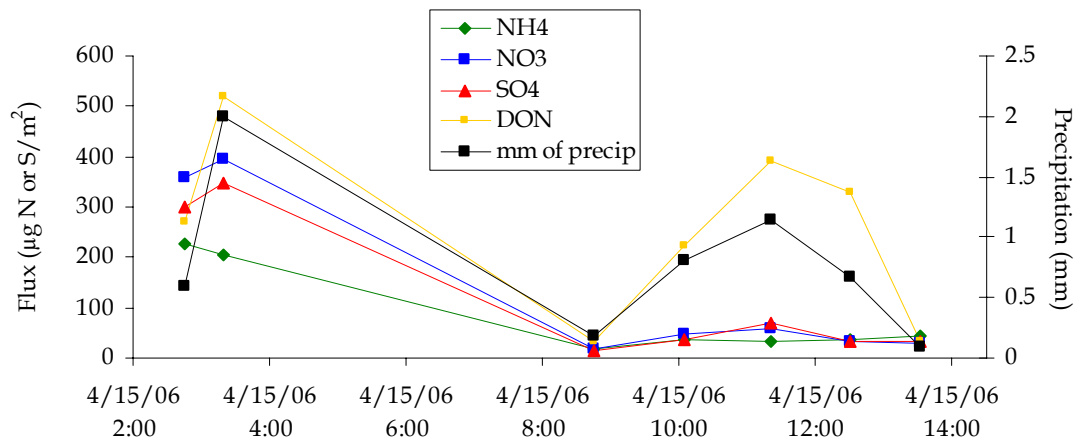


Figure F.17 Deposition of ammonium (green), nitrate (blue), and sulfate (red) throughout the 4/15 event at the Gore Pass site.

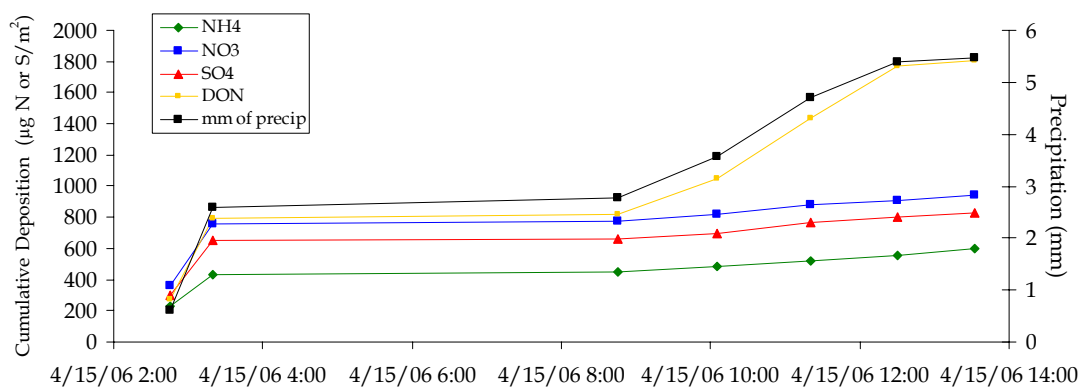


Figure F.18 Cumulative deposition of ammonium (green), nitrate (blue), and sulfate (red) throughout the 4/15 event at the Gore Pass site.

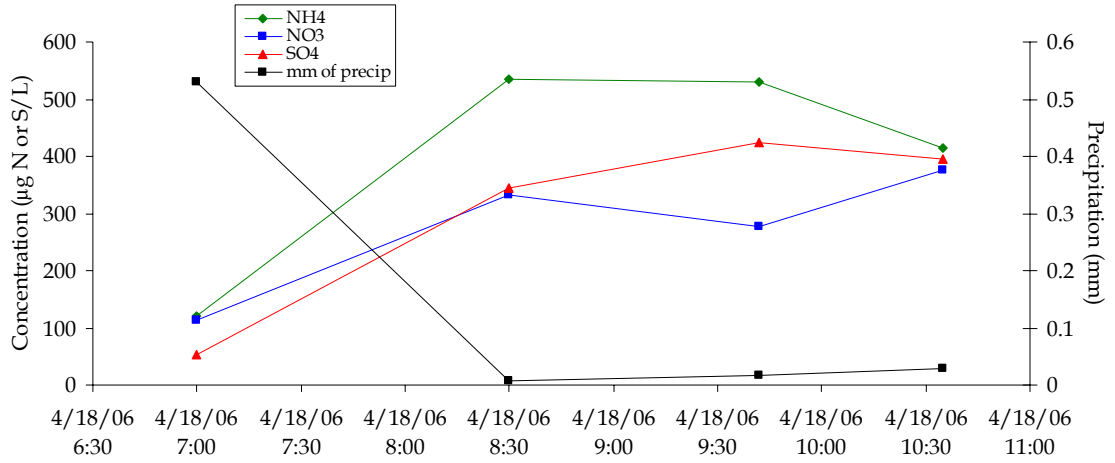


Figure F.19 Timeline of concentrations from the sub event sampler at the Gore Pass site for 4/18.

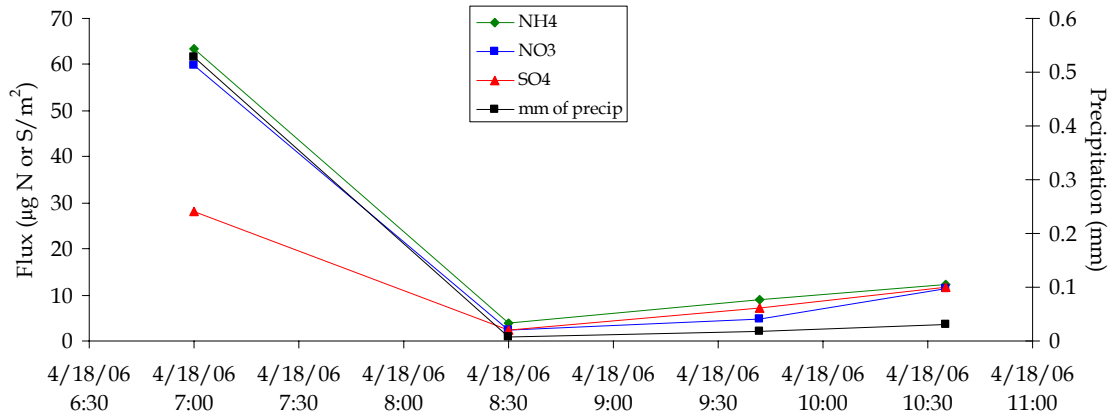


Figure F.20 Deposition of ammonium (green), nitrate (blue), and sulfate (red) throughout the 4/18 event at the Gore Pass site.

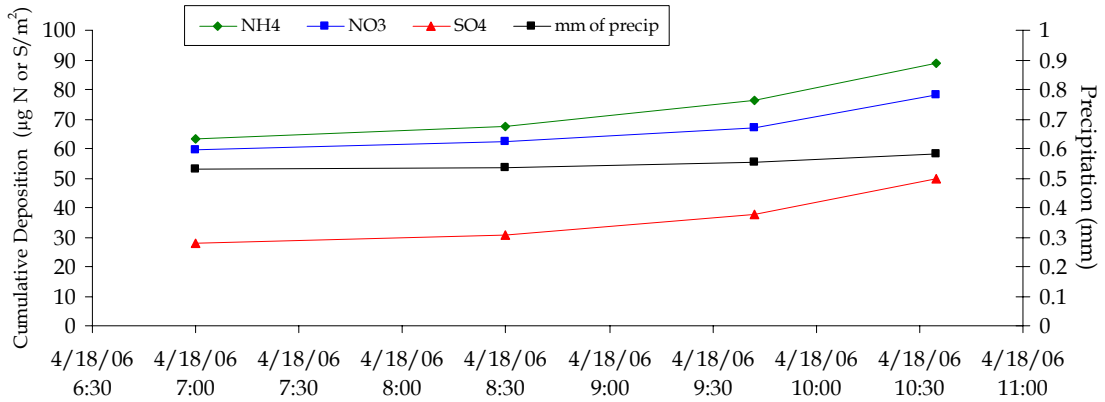


Figure F.21 Cumulative deposition of ammonium (green), nitrate (blue), and sulfate (red) throughout the 4/18 event at the Gore Pass site.

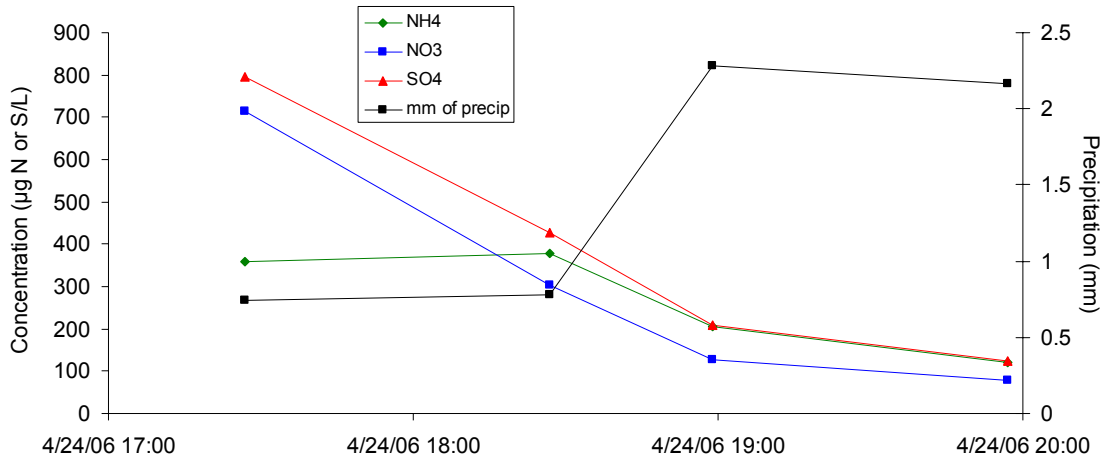


Figure F.22 Timeline of concentrations from the sub event sampler at the Gore Pass site for 4/24.

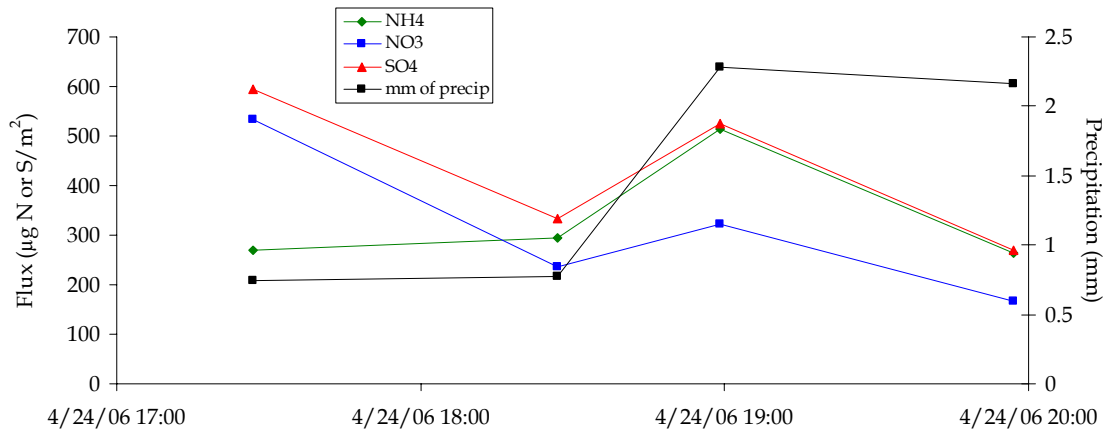


Figure F.23 Deposition of ammonium (green), nitrate (blue), and sulfate (red) throughout the 4/24 event at the Gore Pass site.

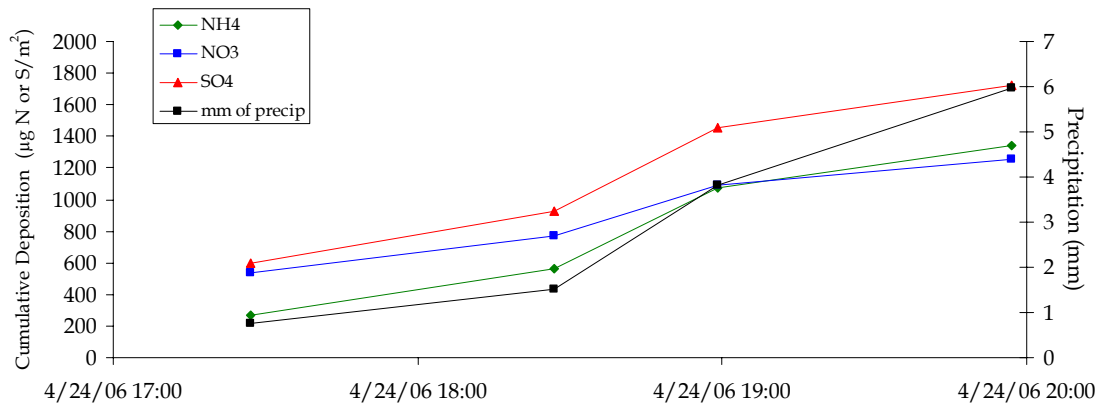


Figure F.24 Cumulative deposition of ammonium (green), nitrate (blue), and sulfate (red) throughout the 4/24 event at the Gore Pass site.

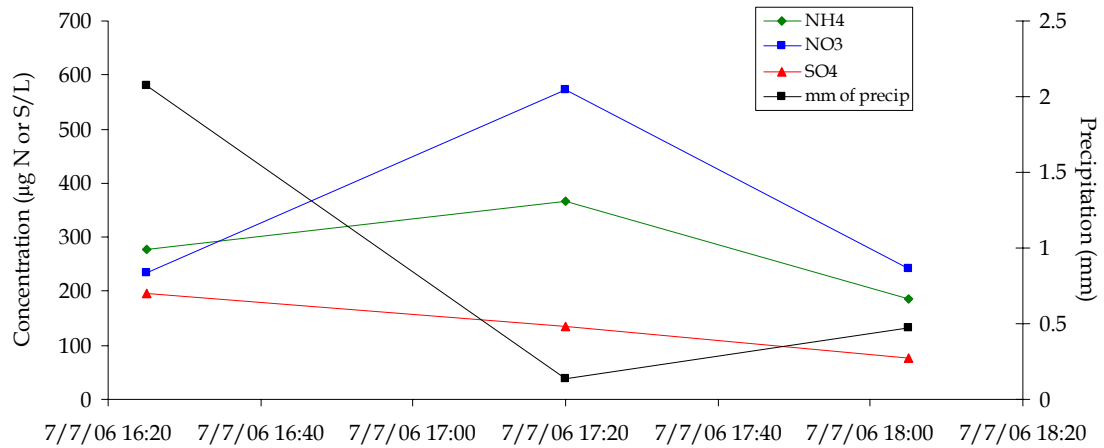


Figure F.25 Timeline of concentrations from the sub event sampler at the Gore Pass site on 7/7.

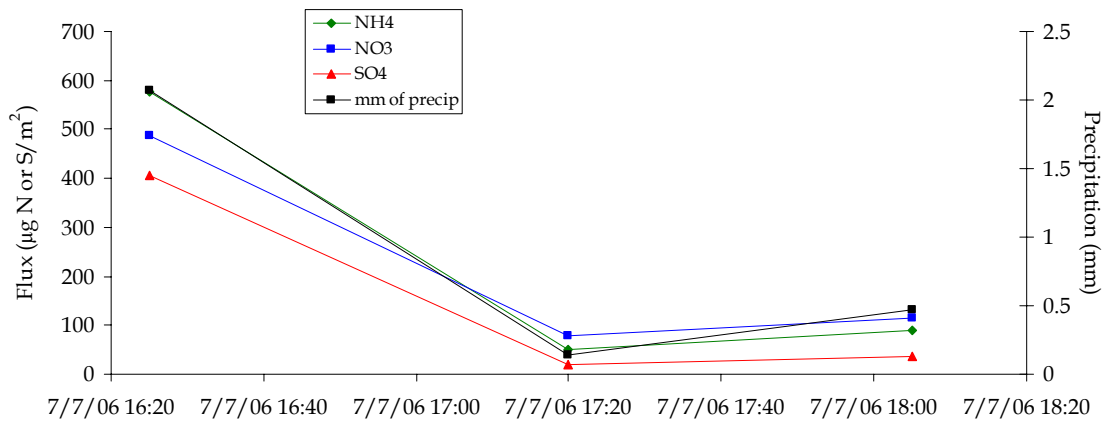


Figure F.26 Deposition of ammonium (green), nitrate (blue), and sulfate (red) throughout the 7/7 event at the Gore Pass site.

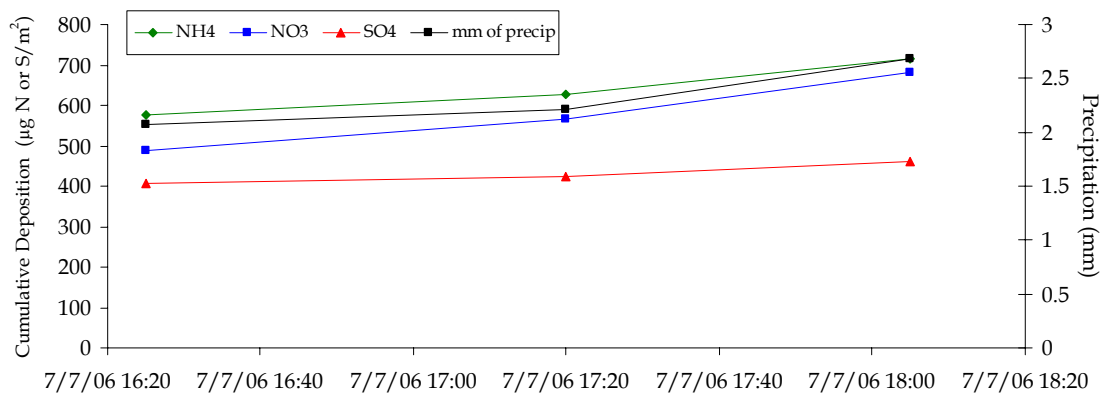


Figure F.27 Cumulative deposition of ammonium (green), nitrate (blue), and sulfate (red) throughout the 7/7 event at the Gore Pass site.

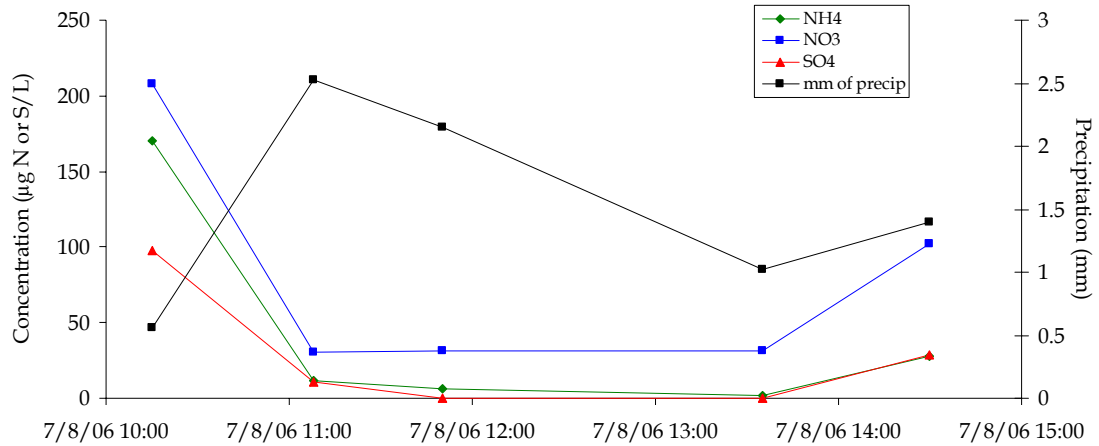


Figure F.28 Timeline of concentrations from the sub event sampler at Gore Pass site for 7/8.

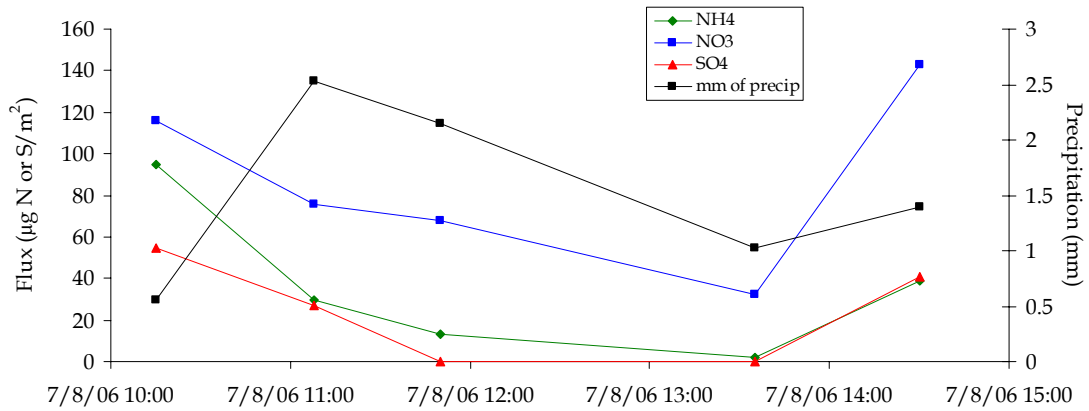


Figure F.29 Deposition of ammonium (green), nitrate (blue), and sulfate (red) throughout the 7/8 event at the Gore Pass site.

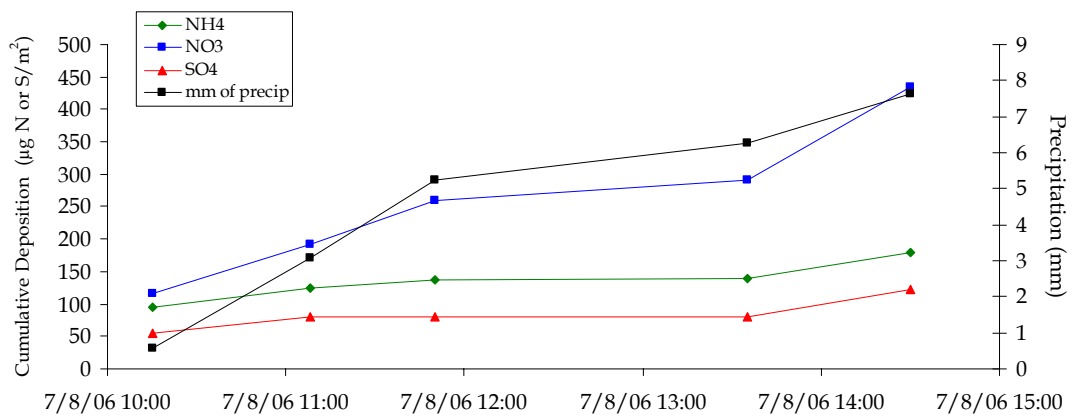


Figure F.30 Cumulative deposition of ammonium (green), nitrate (blue), and sulfate (red) throughout the 7/8 event at the Gore Pass site.

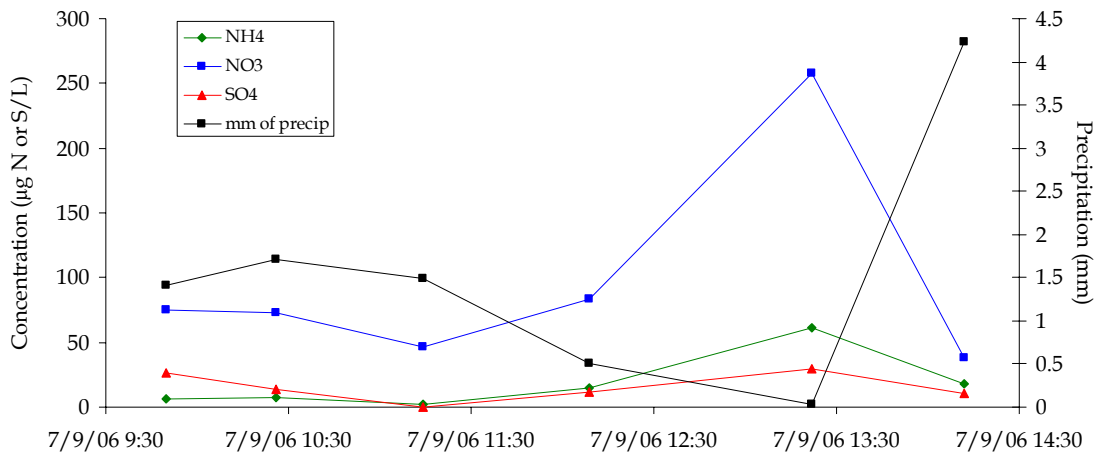


Figure F.31 Timeline of concentrations from the sub event sampler at the Gore Pass site for 7/9.

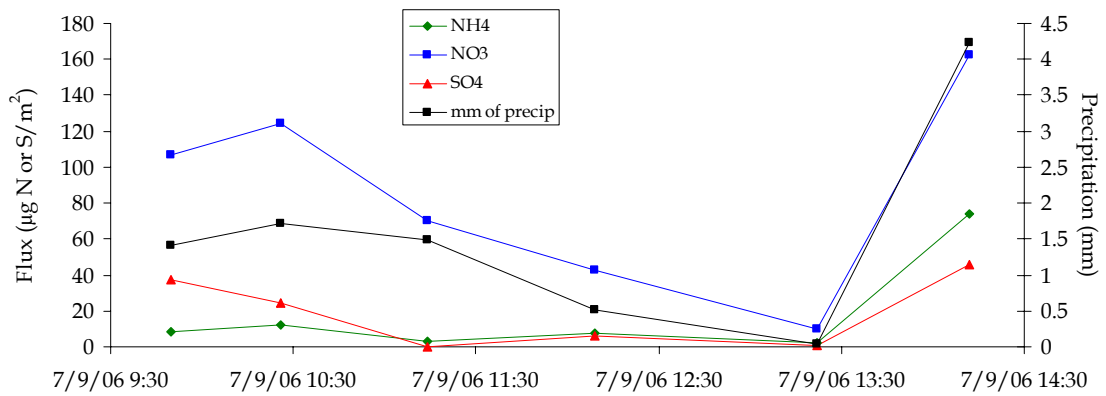


Figure F.32 Deposition of ammonium (green), nitrate (blue), and sulfate (red) throughout the 7/9 event at the Gore Pass site.

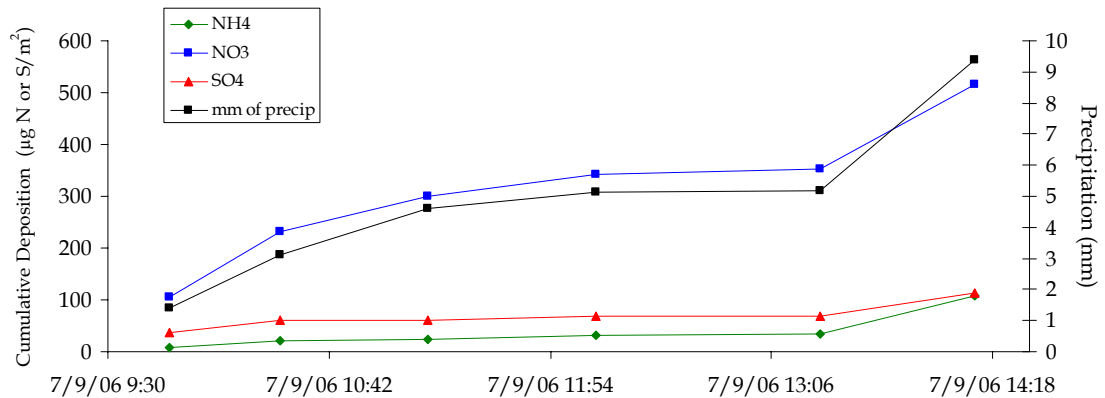


Figure F.33 Cumulative deposition of ammonium (green), nitrate (blue), and sulfate (red) throughout the 7/9 event at the Gore Pass site.

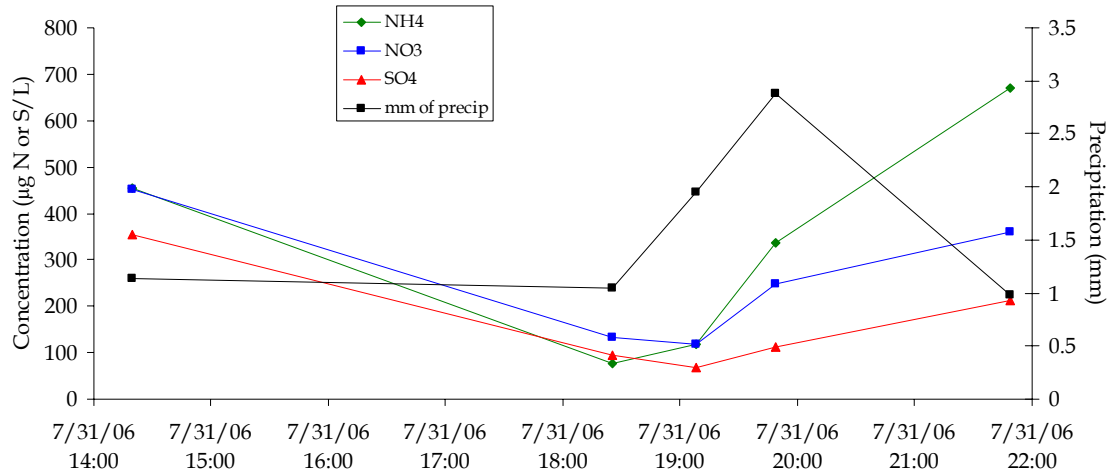


Figure F.34 Timeline of concentrations from the sub event sampler at the Gore Pass site for 7/31.

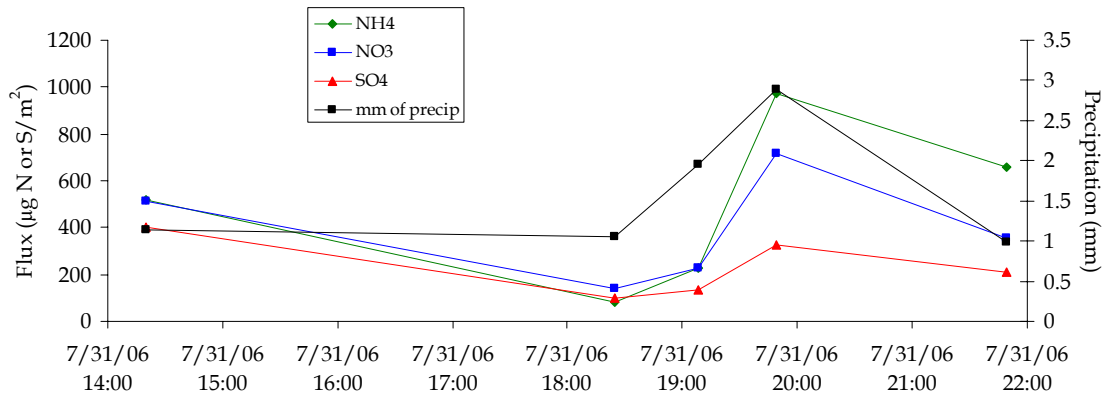


Figure F.35 Deposition of ammonium (green), nitrate (blue), and sulfate (red) throughout the 7/31 event at the Gore Pass site.

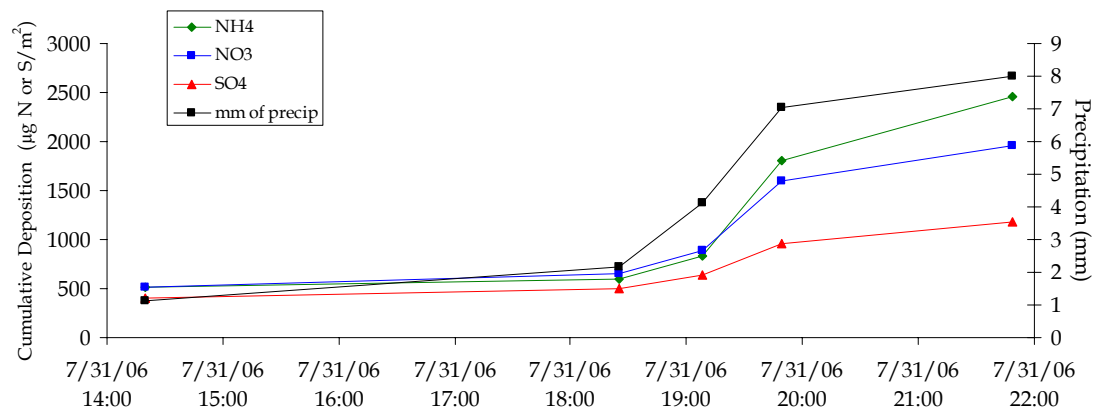


Figure F.36 Cumulative deposition of ammonium (green), nitrate (blue), and sulfate (red) throughout the 7/31 event at the Gore Pass site.

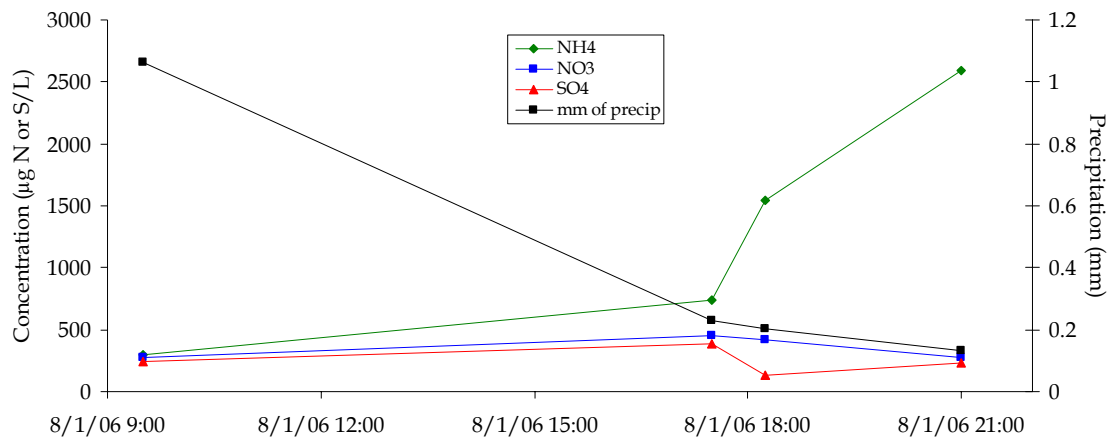


Figure F.37 Timeline of concentrations from the sub event sampler at the Gore Pass site for 8/1.

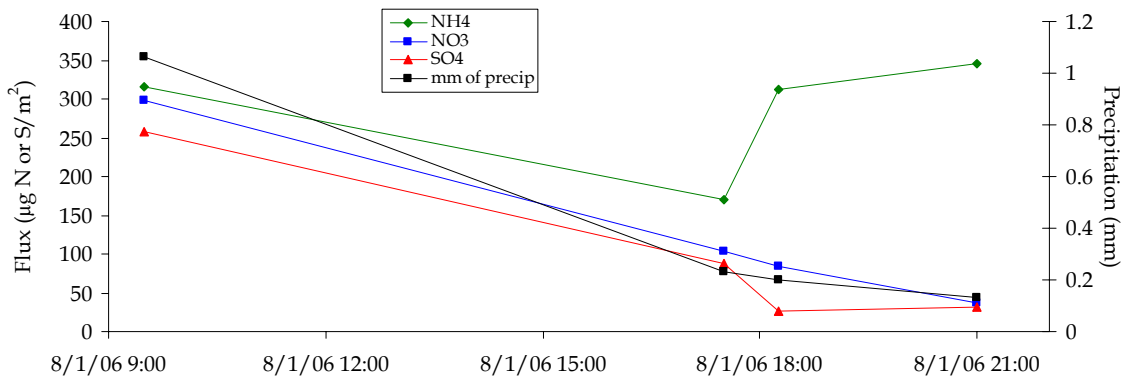


Figure F.38 Deposition of ammonium (green), nitrate (blue), and sulfate (red) throughout the 8/1 event at the Gore Pass site.

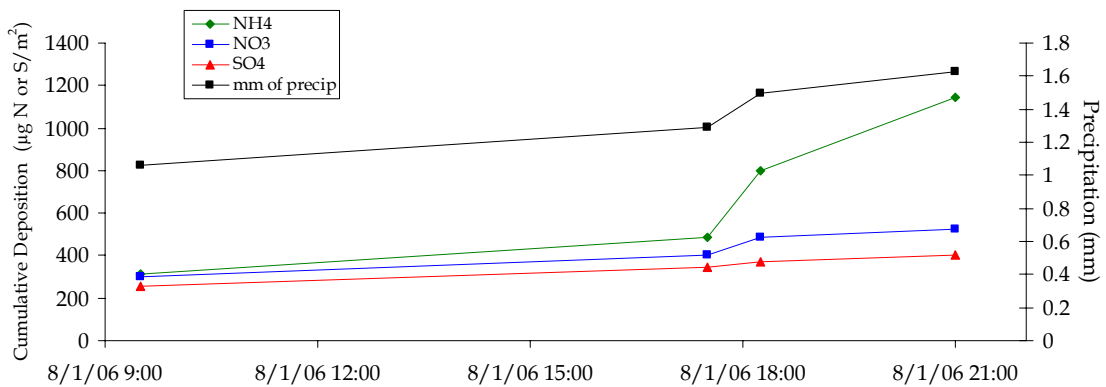


Figure F.39 Cumulative deposition of ammonium (green), nitrate (blue), and sulfate (red) throughout the 8/1 event at the Gore Pass site.

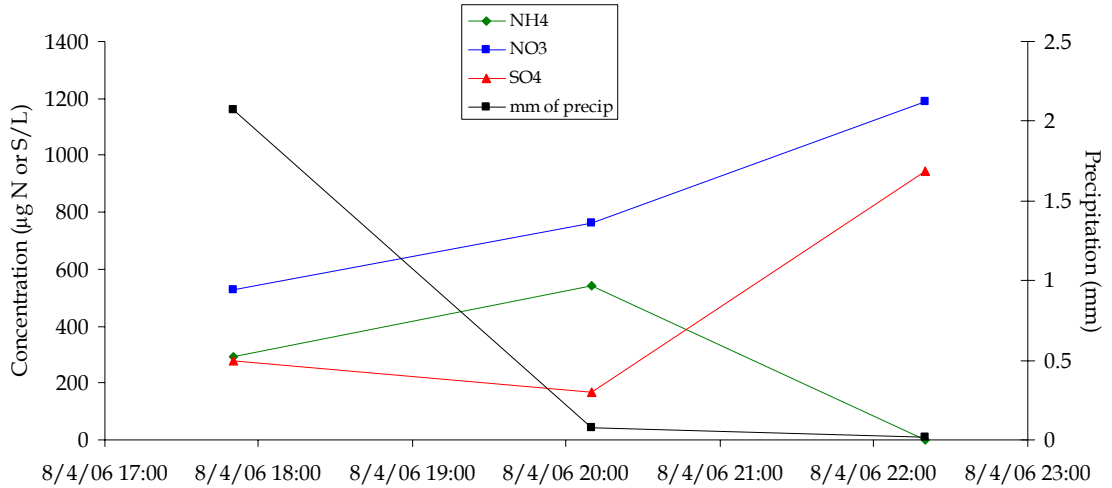


Figure F.40 Timeline of concentrations from the sub event sampler at the Gore Pass site for 8/4.

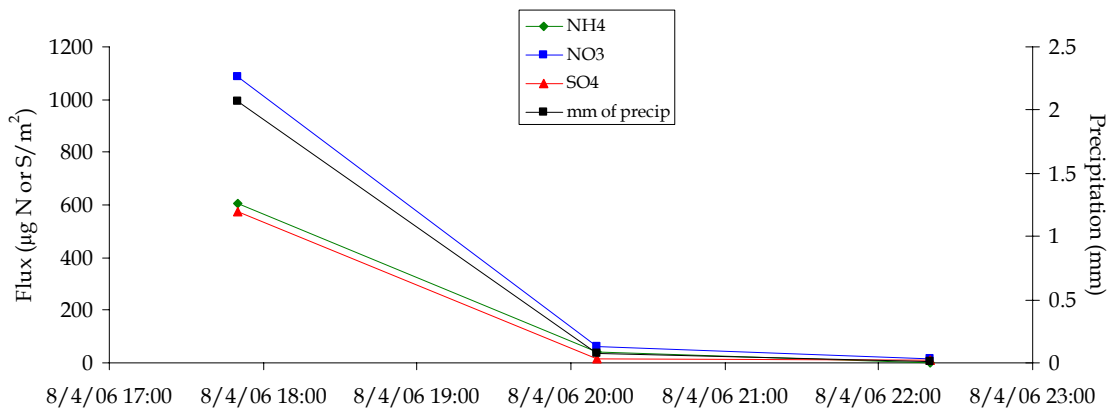


Figure F.41 Deposition of ammonium (green), nitrate (blue), and sulfate (red) throughout the 8/4 event at the Gore Pass site

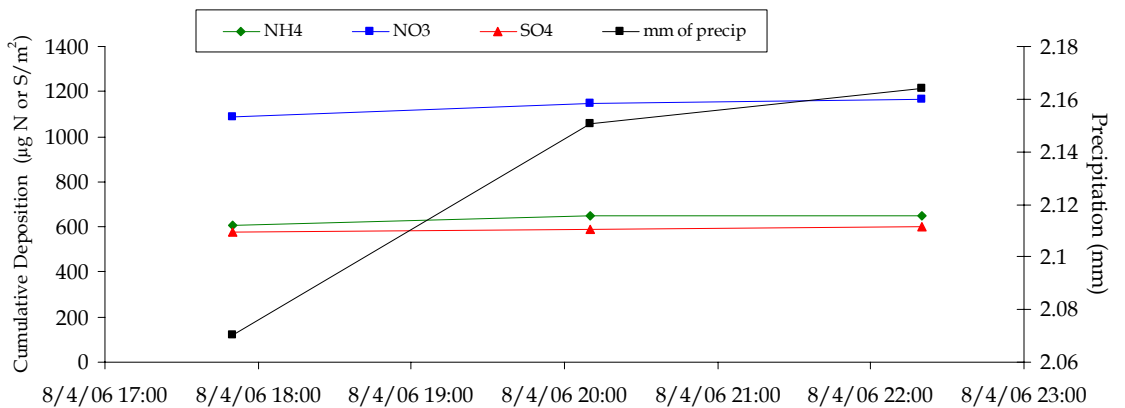


Figure F.42 Cumulative deposition of ammonium (green), nitrate (blue), and sulfate (red) throughout the 8/4 event at the Gore Pass site.

**Appendix G Spatial Variability – Spring deposition correlation tables,
spring and summer concentration correlation tables and 3D plots of
concentration in space and time**

Spring Deposition Correlations

Table G.1 Correlation coefficient between sites for ammonium deposition during the RoMANS spring study period

	DI	GP	TC	HV	BM	CS	SL	LV	LY	BR	NE	SF
DI	1.000	-0.347	-0.423	-0.935	0.637	0.037	-0.296	N/A	-1.000	N/A	-0.821	N/A
GP		1.000	0.670	-0.429	-0.401	0.030	0.048	1.000	0.137	N/A	0.501	-1.000
TC			1.000	0.990	0.992	0.989	0.967	1.000	0.971	N/A	-0.700	-1.000
HV				1.000	0.999	1.000	0.920	N/A	0.954	N/A	0.418	1.000
BM					1.000	0.999	0.940	N/A	0.952	N/A	-1.000	1.000
CS						1.000	0.930	1.000	0.959	N/A	1.000	1.000
SL							1.000	0.998	0.998	N/A	-0.620	1.000
LV								1.000	N/A	N/A	N/A	N/A
LY									1.000	N/A	1.000	1.000
BR										1.000	N/A	N/A
NE											1.000	N/A
SF												1.000

Table G.2 Correlation coefficient between sites for nitrate deposition during the RoMANS spring study period

	DI	GP	TC	HV	BM	CS	SL	LV	LY	BR	NE	SF
DI	1.000	-0.489	-0.552	-0.411	-0.846	-0.613	-0.651	N/A	-1.000	N/A	0.996	N/A
GP		1.000	0.869	0.456	-0.411	0.652	0.576	-1.000	0.308	N/A	-0.084	-1.000
TC			1.000	0.993	0.993	0.977	0.883	1.000	0.966	N/A	0.200	-1.000
HV				1.000	0.999	0.962	0.816	N/A	0.933	N/A	-0.240	1.000
BM					1.000	0.982	0.898	N/A	0.927	N/A	-1.000	1.000
CS						1.000	0.931	1.000	0.981	N/A	1.000	1.000
SL							1.000	1.000	0.950	N/A	-0.466	1.000
LV								1.000	N/A	N/A	N/A	N/A
LY									1.000	N/A	1.000	1.000
BR										1.000	N/A	N/A
NE											1.000	N/A
SF												1.000

Table G.3 Correlation coefficient between sites for sulfate deposition during the RoMANS spring study period

	DI	GP	TC	HV	BM	CS	SL	LV	LY	BR	NE	SF
DI	N/A	-0.423	-0.312	-0.109	-0.537	-0.512	-0.182	N/A	1.000	N/A	0.996	N/A
GP		1.000	0.833	0.121	-0.349	0.537	0.491	1.000	-0.167	N/A	-0.235	1.000
TC			1.000	0.998	0.997	0.989	0.954	1.000	0.996	N/A	0.210	1.000
HV				1.000	0.999	0.981	0.859	N/A	0.864	N/A	-0.149	1.000
BM					1.000	0.993	0.906	N/A	0.846	N/A	-1.000	1.000
CS						1.000	0.956	1.000	0.904	N/A	1.000	1.000
SL							1.000	1.000	0.955	N/A	-0.365	1.000
LV								1.000	N/A	N/A	N/A	N/A
LY									1.000	N/A	1.000	1.000
BR										1.000	N/A	N/A
NE											1.000	N/A
SF												1.000

Spring Concentration Correlations

Table G.4 Correlation between sites for ammonium concentration during the RoMANS spring study period

	DI	GP	TC	HV	BM	CS	SL	LV	LY	BR	NE	SF
DI	1.000	0.241	-0.175	-0.355	-0.147	-0.166	-0.114	N/A	1.000	N/A	-0.177	N/A
GP		1.000	0.344	0.959	0.084	0.631	0.881	1.000	0.976	N/A	-0.990	1.000
TC			1.000	0.703	0.107	0.787	0.909	1.000	0.979	N/A	0.851	1.000
HV				1.000	0.758	0.926	0.710	N/A	0.753	N/A	0.095	1.000
BM					1.000	-0.328	0.078	N/A	0.899	N/A	-1.000	1.000
CS						1.000	0.809	1.000	0.621	N/A	-1.000	1.000
SL							1.000	0.999	0.983	N/A	-0.358	1.000
LV								1.000	N/A	N/A	N/A	N/A
LY									1.000	N/A	1.000	1.000
BR										1.000	N/A	N/A
NE											1.000	N/A
SF												1.000

Table G.5 Correlation between sites for nitrate concentration during the RoMANS spring study period

	DI	GP	TC	HV	BM	CS	SL	LV	LY	BR	NE	SF
DI	1.000	0.818	-0.047	0.162	-0.562	0.069	0.192	N/A	1.000	N/A	0.003	N/A
GP		1.000	0.350	0.329	0.213	0.446	0.938	-1.000	0.997	N/A	0.337	1.000
TC			1.000	0.144	0.233	0.330	0.403	-1.000	0.972	N/A	0.877	1.000
HV				1.000	0.619	0.607	0.585	N/A	0.389	N/A	0.718	1.000
BM					1.000	-0.496	0.312	N/A	0.579	N/A	-1.000	1.000
CS						1.000	0.426	1.000	0.785	N/A	-1.000	1.000
SL							1.000	-1.000	0.962	N/A	-0.746	1.000
LV								1.000	N/A	N/A	N/A	N/A
LY									1.000	N/A	1.000	1.000
BR										1.000	N/A	N/A
NE											1.000	N/A
SF												1.000

Table G.6 Correlation between sites for sulfate concentration during the RoMANS spring study period

	DI	GP	TC	HV	BM	CS	SL	LV	LY	BR	NE	SF
DI	1.000	0.975	0.051	-0.041	-0.814	-0.275	-0.050	N/A	1.000	N/A	0.496	N/A
GP		1.000	0.531	0.812	0.301	0.140	0.973	-1.000	0.998	N/A	0.601	1.000
TC			1.000	0.150	0.137	0.223	0.348	-1.000	0.994	N/A	0.888	1.000
HV				1.000	0.846	0.806	0.702	N/A	0.471	N/A	0.706	1.000
BM					1.000	-0.446	0.304	N/A	0.769	N/A	1.000	1.000
CS						1.000	0.475	1.000	0.748	N/A	-1.000	1.000
SL							1.000	-0.395	0.979	N/A	-0.745	1.000
LV								1.000	N/A	N/A	N/A	N/A
LY									1.000	N/A	1.000	1.000
BR										1.000	N/A	N/A
NE											1.000	N/A
SF												1.000

Spring Concentrations

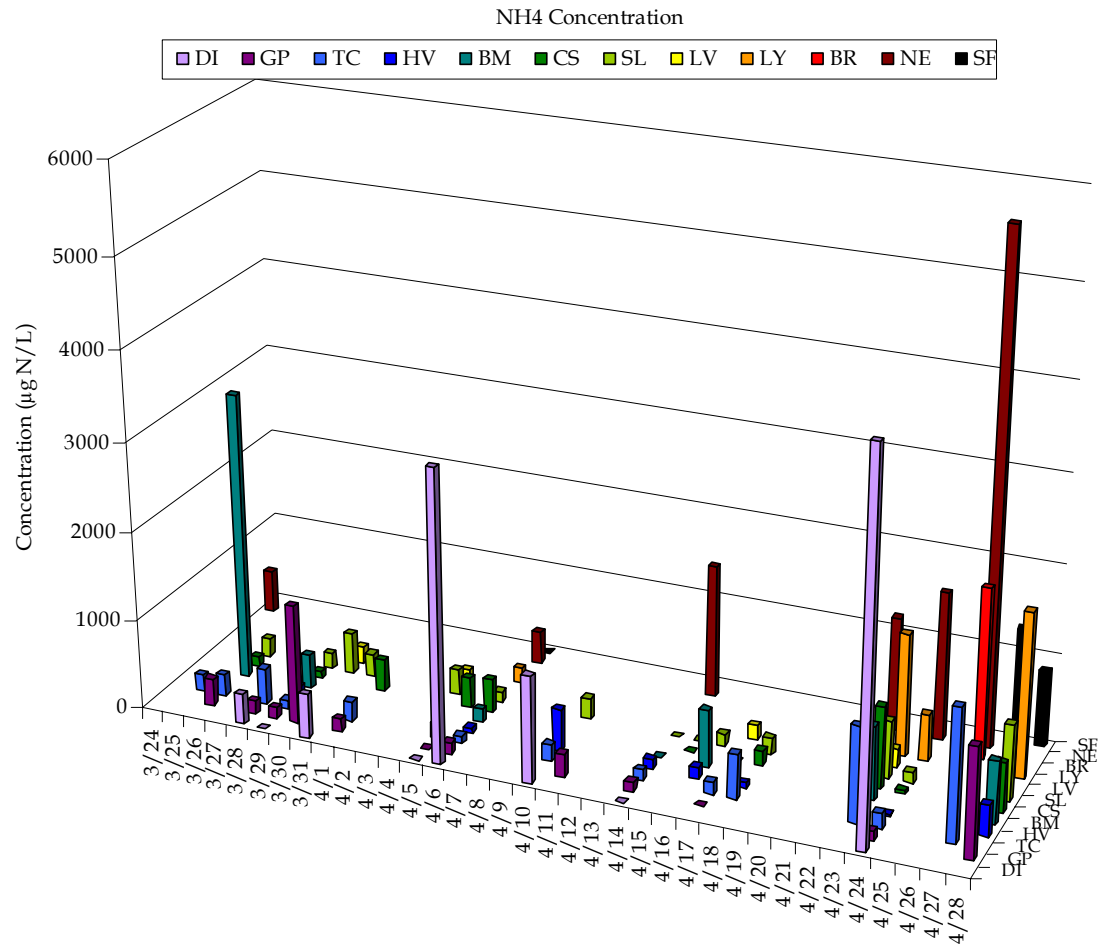


Figure G.1 Wet deposition of NH₄⁺ at all sites during the spring study period.

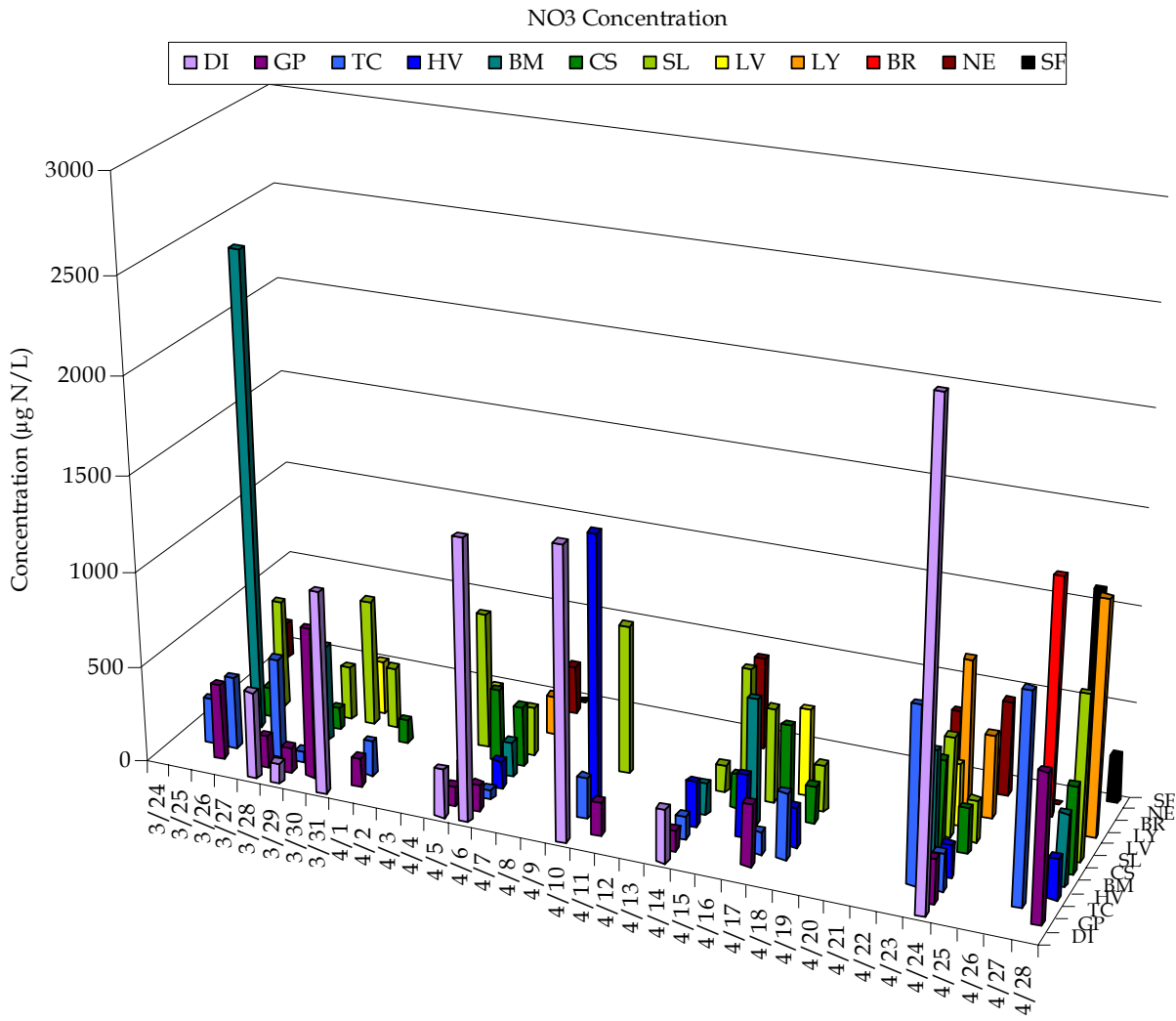


Figure G.2 Wet deposition of NO₃⁻ at all sites during the spring study period.

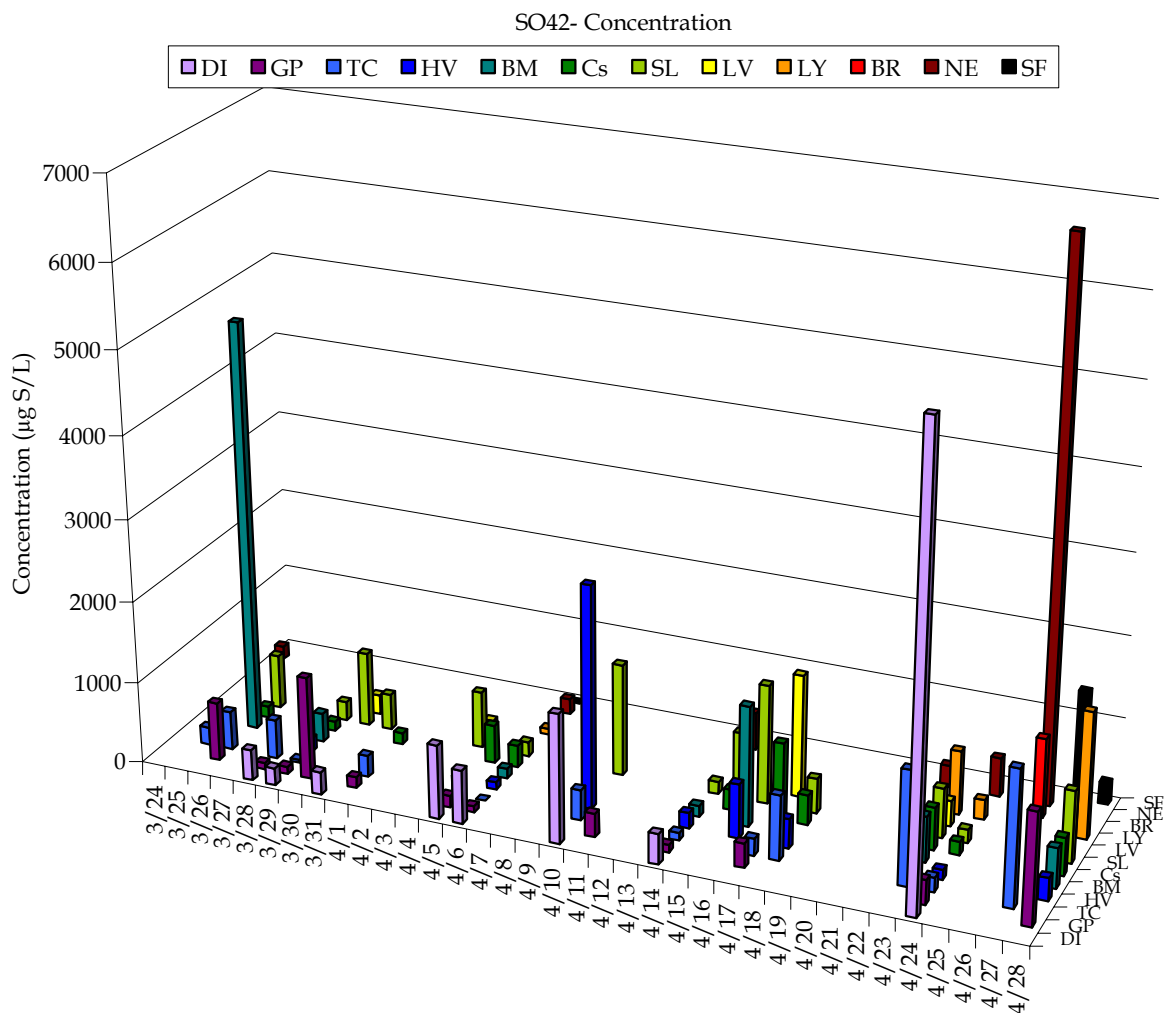


Figure G.3 Wet deposition of SO₄²⁻ at all sites during the spring study period.

Summer Concentrations

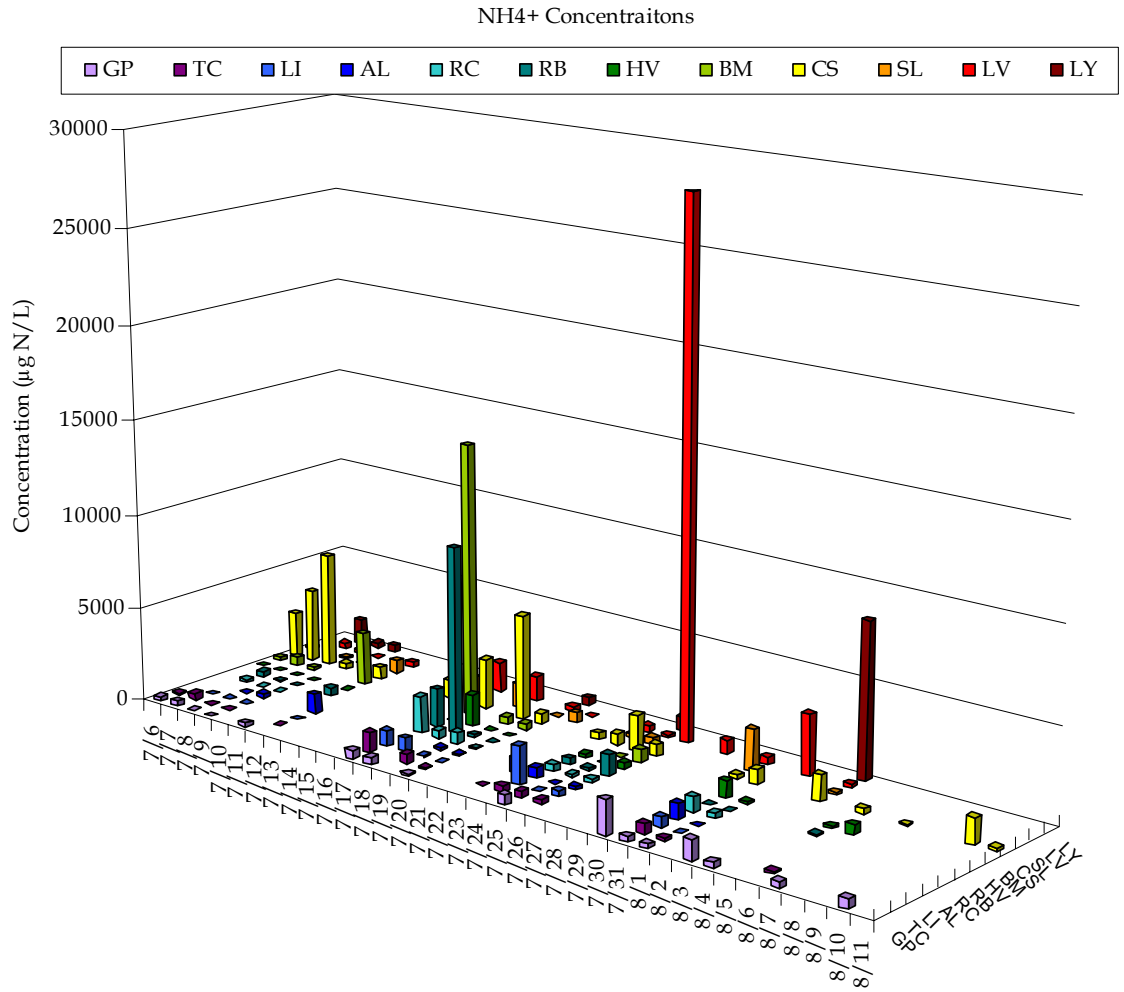


Figure G.4 Wet deposition of NH₄⁺ at all sites during the summer study period.

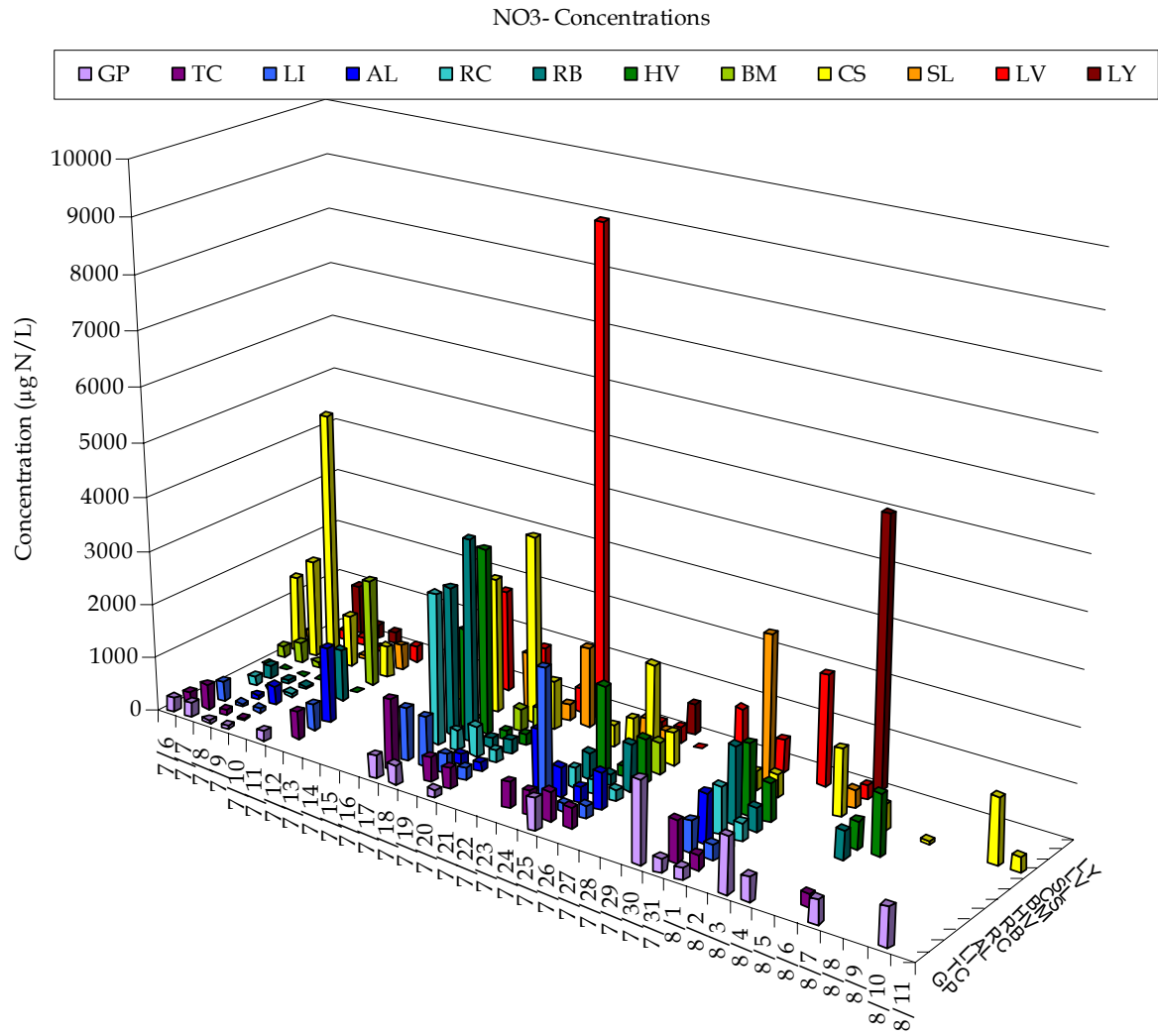


Figure G.5 Wet deposition of NO₃⁻ at all sites during the summer study period.

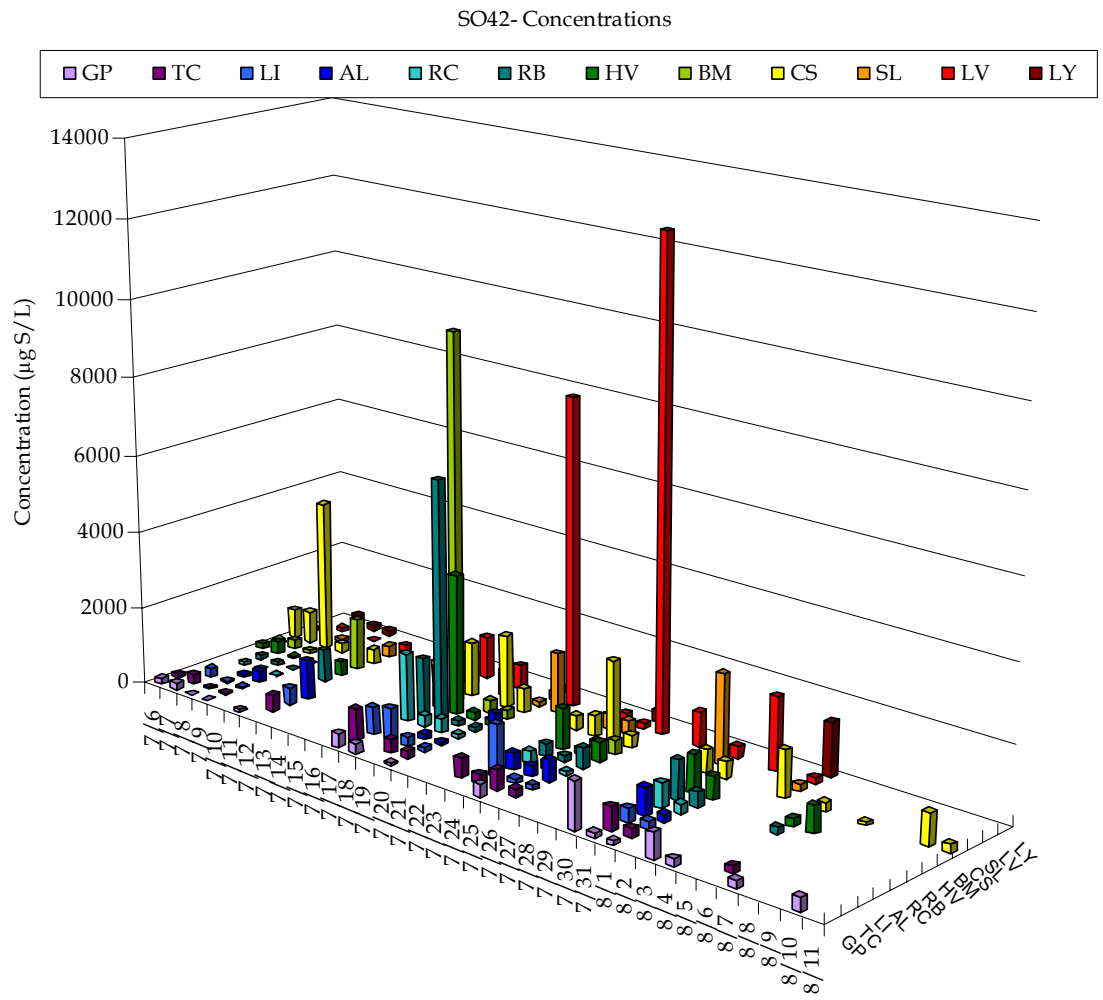


Figure G.6 Wet deposition of SO₄²⁻ at all sites during the summer study period.